Trinity College Dublin

Neuroimaging features of Amyotrophic Lateral Sclerosis

Doctor in Philosophy, Clinical Medicine
Full Time – Research, 2024

Student:	Rangariroyashe Hannah Chipika MB BCh BAO. MSc.
Supervisor:	Professor Peter Bede MD. PhD.

DECLARATION AND PERMISSION:

I have read and understood the College / University statement on plagiarism. I declare that the attached dissertation is my own, original work undertaken in fulfilment of my degree. I have made no use of sources, materials or assistance other than those which have been openly and fully acknowledged in the text. Any direct quotation or source of ideas has been identified in the text by author, date and page number(s) immediately after such an item, and full details are provided in a reference list at the end of the text.

This thesis has not been submitted as an exercise for a degree at this or any other University.

I agree to deposit this thesis in the University's open access institutional repository or allow the library to do so on my behalf, subject to Irish Copyright Legislation and Trinity College Library conditions of use and acknowledgement. I agree that the Library may lend or copy the thesis upon request.

Signature:  Date: 29/08/23

TABLE OF CONTENTS

ACKNOWLEDGEMENTS vi
FIRST-AUTHOR PUBLICATIONS ARISING FROM THIS WORK vii
PRESENTATIONS IN ASSOCIATION WITH THIS WORK x
LIST OF FIGURES xii
LIST OF TABLES xiii
SUMMARY xv
GLOSSARY xx
CHAPTER 1: Presymptomatic and symptomatic findings in ALS 1
Introduction 1
Methods 4
Results 6
Neuroimaging studies of asymptomatic mutation carriers 8
The clinical profile of mutation carriers 17
Clinical findings in presymptomatic cohorts 18
Electrophysiology studies of asymptomatic mutation carriers 19
Biofluid studies of asymptomatic mutation carriers 22
Lessons from other neurodegenerative conditions 26
Discussion 27
Conclusions 35
Corpus Callosum degeneration in ALS 35
CHAPTER 2: Review of sensory findings in ALS 39
Introduction 39
Methods 40
Results 41
Clinical 41
Electrophysiology 47
Post-mortem, biopsy and animal models 53
Imaging 58
PLS, PMA, SBMA, PPS 64
Discussion 65
Conclusions 72

CHAPTER 3: Alterations in somatosensory, visual and auditory pathways in amyotrophic lateral sclerosis 73
1. Introduction 73
1.1 Background 73
1.2 Objectives, aims and hypotheses 75
2. Methods 79
2.1 Participants 79
2.2 Sensory assessment 79
2.3 Screening for sensory symptoms 80
2.4 Magnetic resonance imaging 80
2.5 Grey matter metrics 81
2.6 White matter metrics 82
2.7 Statistics 83
3. Results 83
3.1 Demographic profiles 83
3.2 Clinical signs and symptoms 84
3.3 Cortical alterations 87
3.4 Subcortical nuclear degeneration 87
3.5 White matter alterations 88
4. Discussion 99
5. Conclusions 104
CHAPTER 4: Review of cerebellar pathology in ALS 105
Introduction 105
Functional anatomy 106
Search strategy and selection criteria 110
Results 110
I. Imaging 110
1. Grey matter alterations 111
2. White matter changes 112
3. Functional and metabolic studies 112
II. Post-mortem findings 124
III. Animal models 124
Discussion 126
Neuroimaging and post-mortem infratentorial pathology in ALS 126

Cerebellar findings in related neurodegenerative conditions 129
Clinical relevance 131
Future directions 132
Conclusions 134
CHAPTER 5: Genotype associated cerebellar profiles in ALS 135
Introduction 135
Methods 137
Participants 137
Magnetic resonance imaging 137
Cortical thickness and volume analyses 138
Morphometry 139
White matter analyses 140
Segmentation for superior cerebellar peduncle volumetry 140
Cerebro-cerebellar connectivity 141
Statistical analyses 144
Genotyping 145
Results 145
Discussion 178
Conclusions 181
CHAPTER 6: Selective pathology of thalamic nuclei in ALS and PLS 182
Introduction 182
Methods 185
Ethics statement 185
Participants 186
Neuroimaging methods 186
TIV volumes 187
Thalamic segmentation 187
Vertex analyses 190
Region of interest morphometry 190
Genetics 191
Statistical analysis 191
Results 192
Vertex analyses 201
Morphometric alterations 203

Correlation analyses 205
Discussion 205
Histopathological considerations 210
Study limitations 211
Conclusions 212
Chapter 7: Amygdala pathology in ALS and PLS 213
Introduction 213
Methods 215
Ethics statement 215
Participants 215
Neuroimaging methods 216
TIV volumes 216
Amygdala segmentation 217
Vertex analyses 219
Genetics 219
Statistical analysis 220
Results 221
Volumetric profile 224
Vertex changes 229
Discussion 231
Conclusions 240
REFERENCES 241

ACKNOWLEDGEMENTS

I am immensely grateful to my supervisor, Professor Peter Bede, for his unwavering support, guidance and enthusiasm. He has generously invested time and effort into assisting me to develop invaluable research skills and has made undertaking this PhD a wonderful experience. I also thank the members of the computational neuroimaging group (CNG) in the Academic Unit of Neurology, Dr Eoin Finegan and Dr Stacey Li Hi Shing for their friendship and collaboration.

I am incredibly thankful for the generous financial support of The Andrew Lydon Scholarship, and I also acknowledge the research grants of my supervisor including the Health Research Board (HRB–Ireland; HRB EIA-2017-019 & JPND-Cofund-2-2019-1), the Irish Institute of Clinical Neuroscience (IICN), the EU Joint Programme – Neurodegenerative Disease Research (JPND), The Hayes Family Charitable Fund, the Iris O'Brien Foundation and The Research Motor Neuron (RMN–Ireland) Foundation.

Finally, I wholeheartedly thank all of the patients and caregivers who have supported my research by selflessly and courageously offering their time, effort and resources, even over the course of the pandemic, in order to participate in the research study. Without their generosity this work could not have been undertaken.

FIRST-AUTHOR PUBLICATIONS ARISING FROM THIS WORK

1. **Chipika RH**, Mulkerrin G, Pradat PF, Murad A, Ango F, Raoul C, Bede P. Cerebellar pathology in motor neuron disease: neuroplasticity and neurodegeneration. Neural Regen Res. 2022 Nov;17(11):2335-2341. doi: 10.4103/1673-5374.336139. PMID: 35535867; PMCID: PMC9120698.

2. **Chipika RH**, Mulkerrin G, Murad A, Lope J, Hardiman O, Bede P. Alterations in somatosensory, visual and auditory pathways in amyotrophic lateral sclerosis: an under-recognised facet of ALS. J Integr Neurosci. 2022 Apr 27;21(3):88. doi: 10.31083/j.jin2103088. PMID: 35633169.

3. Bede P*, **Chipika RH***, Christidi F, Hengeveld JC, Karavasilis E, Argyropoulos GD, Lope J, Li Hi Shing S, Velonakis G, Dupuis L, Doherty MA, Vajda A, McLaughlin RL, Hardiman O. Genotype-associated cerebellar profiles in ALS: focal cerebellar pathology and cerebro-cerebellar connectivity alterations. J Neurol Neurosurg Psychiatry. 2021 Jun 24:jnnp-2021-326854. doi: 10.1136/jnnp-2021-326854. *PB and RHC are joint first authors

4. **Chipika RH**, Finegan E, Li Hi Shing S, McKenna MC, Christidi F, Chang KM, Doherty MA, Hengeveld JC, Vajda A, Pender N, Hutchinson S, Donaghy C, McLaughlin RL, Hardiman O, Bede P. "Switchboard" malfunction in motor

neuron diseases: Selective pathology of thalamic nuclei in amyotrophic lateral sclerosis and primary lateral sclerosis. Neuroimage Clin. 2020;27:102300. doi: 10.1016/j.nicl.2020.102300.

5. **Chipika RH**, Christidi F, Finegan E, Li Hi Shing S, McKenna MC, Chang KM, Karavasilis E, Doherty MA, Hengeveld JC, Vajda A, Pender N, Hutchinson S, Donaghy C, McLaughlin RL, Hardiman O, Bede P. Amygdala pathology in amyotrophic lateral sclerosis and primary lateral sclerosis. J Neurol Sci. 2020 Oct 15;417:117039. doi: 10.1016/j.jns.2020.117039.

6. **Chipika RH**, Siah WF, Shing SLH, Finegan E, McKenna MC, Christidi F, Chang KM, Karavasilis E, Vajda A, Hengeveld JC, Doherty MA, Donaghy C, Hutchinson S, McLaughlin RL, Hardiman O, Bede P. MRI data confirm the selective involvement of thalamic and amygdalar nuclei in amyotrophic lateral sclerosis and primary lateral sclerosis. Data Brief. 2020 Sep 1;32:106246. doi: 10.1016/j.dib.2020.106246.

7. **Chipika RH**, Siah WF, McKenna MC, Li Hi Shing S, Hardiman O, Bede P. The presymptomatic phase of amyotrophic lateral sclerosis: are we merely scratching the surface? J Neurol. 2020 Oct 31. doi: 10.1007/s00415-020-10289-5.

8. **Chipika, R. H.**, Finegan, E., Li Hi Shing, S., Hardiman, O., & Bede, P. (2019). Tracking a Fast-Moving Disease: Longitudinal Markers, Monitoring, and Clinical Trial Endpoints in ALS. *Frontiers in neurology*, *10*, 229. doi:10.3389/fneur.2019.00229

PRESENTATIONS IN ASSOCIATION WITH THIS WORK

1. **Chipika RH.** Amygdala Pathology in ALS-FTD, Platform Presentation, 2nd International Meeting on Frontotemporal Dysfunction (IMFTD), 30 September 2022. Part of the organising committee.

2. **Chipika RH.** The preferential involvement of thalamic nuclei in ALS: a multimodal neuroimaging study, Poster presentation, International ALS/MND Symposium 2020, Virtual, 9-11 December 2020

3. **Chipika RH.** Extramotor changes in PLS: a prospective MRI study, Platform Presentation, Neuroimaging Society of ALS, NISALS, Oxford, UK, 12-13 November 2019

4. **Chipika RH.** Li Hi Shing S, Finegan E, Hardiman O, Bede. Parieto-occipital pathology in ALS: The quest for a "posterior" phenotype. Poster presentation European Network for the Cure of ALS (ENCALS) meeting, Tours, France, 15-17 May 2019

5. **Chipika HR**. P. Posterior pathology in ALS: the spectrum of occipital changes, Platform Presentation, Neuroimaging Society of ALS, NISALS, Edinburgh, UK, 5-6 December 2018

6. **Chipika RH**,. Characterising occipital lobe pathology in ALS using individual patient analyses: the quest for a “posterior” phenotype. Poster presentation International ALS/MND Symposium 2018, Glasgow, UK, 7-9 December 2018

7. **Chipika RH**. Neuroimaging in ALS. Platform – The Andrew Lydon Award Scholarship Event, Trinity College Dublin, 21 September 2018

8. **Chipika RH**, Finegan E, Iyer P, Omer T,. Doherty M, Vajda A, Pender N, L. McLaughlin RL, Hutchinson S, Hardiman O, Bede P. Distinctive subcortical grey matter signatures along the ALS-FTD spectrum: a multimodal neuroimaging study. Poster Presentation European Network for the Cure of ALS (ENCALS) meeting, Oxford, UK, 20-22 June 2018

LIST OF FIGURES

Figure 1: Number of ALS studies identified by core search criteria..... 7
Figure 2: Sensory cortical thickness profile in C9+ ALS, C9- ALS patients and HC 92
Figure 3: Radar plots of integrity measures in regions of interest associated with sensory processing..... 98
Figure 4: Gross anatomy of the cerebellum..... 109
Figure 5: Tractography methods and anatomical targets for cerebellar tracts..... 143
Figure 6: Profile of ATXN2 repeat expansions in Irish patients with ALS and population-matched healthy controls..... 147
Figure 7: Cerebellar grey matter alterations as indicated by focal partial volume reductions at p<0.05 FWE TFCE. 161
Figure 8: Cerebellar tract-based white matter changes in ALS as identified by FA, AD and RD alterations at p<0.01 TFCE 162
Figure 9: Atlas-based segmentation of the thalamus..... 189
Figure 10: The volumetric profile of thalamic nuclei in HC, PLS, C9+ ALS, and C9- ALS 196
Figure 11: Boxplot of the volumetric profile of thalamic nuclei 197
Figure 12. Radar plot of the segmental thalamus profile of C9+ ALS, C9- ALS, and PLS with reference to HC. 198
Figure 13: Thalamic shape deformations in C9+ ALS in comparison to HC, C9- ALS compared to HC, C9+ ALS compared to C9- ALS, PLS compared to C9- ALS, and PLS in contrast to HC..... 202
Figure 14: Patterns of thalamic atrophy in C9- ALS in comparison to HC, in C9- ALS versus PLS and in PLS compared to HC..... 204
Figure 15: Atlas-based segmentation of the amygdala 218
Figure 16: Volumetric profile of the amygdala in HC, PLS, C9+ ALS, C9- ALS. 226
Figure 17: Raw volumetric profile of amygdalar nuclei in C9+ ALS, C9- ALS, PLS and HC. 227
Figure 18. Segmental amygdala profile of C9+ ALS, C9- ALS, and PLS with reference to HC.. 228
Figure 19: Amygdala shape deformation in C9+ ALS compared to HC based on vertex analyses at p < 0.05. 230

LIST OF TABLES

Table 1: Selection of presymptomatic neuroimaging studies in ALS/FTD.....13
Table 2: Selection of presymptomatic electrophysiology studies in ALS 21
Table 3: Selection of presymptomatic biofluid studies.....24
Table 4: Lessons of existing presymptomatic studies in ALS, learning points for future study designs 34
Table 5: Selection of clinical studies ALS 44
Table 6: Selection of electrophysiology studies in ALS 50
Table 7: Selection of postmortem, biopsy and animal studies 55
Table 8: Selection of imaging studies in ALS 60
Table 9: Shortcomings of current study design and desirable design.....71
Table 10: Panel of anatomical regions evaluated; key functions and connections. ...76
Table 11: Demographic and clinical profile of study participants in sensory study....84
Table 12: Clinical sensory assessment scores in C9- ALS.....86
Table 13: Sensory cortical grey matter volumes and cortical thickness in C9+ ALS patients, C9- ALS and HC.....89
Table 14: Thalamic and amygdalar nuclear volumes in C9+ ALS patients, C9- ALS patients and HC.....93
Table 15: Axial diffusivity, fractional Anisotropy, mean diffusivity and radial diffusivity in C9+ ALS, C9- ALS and HC in sensory regions.....96
Table 16: Selection of grey and white matter studies investigating cerebellar pathology in MND 114
Table 17: Selection of functional MR studies evaluating cerebellar pathology in ALS: fMRI & spectroscopy 118
Table 18: Selection of PET studies commenting on cerebellar pathology in ALS 121
Table 19: Selection of post mortem studies describing cerebellar pathology in ALS 125
Table 20: Comparative demographic and clinical profile of patient cohorts in cerebellar study 148
Table 21: Cerebellar cortical thickness in healthy controls and ALS-NEG and ALS-C9 150
Table 22: Cerebellar grey matter volumes in healthy controls and ALS-NEG and ALS-C9 151
Table 23: Cerebellar cortical thickness in healthy controls and ALS-ATXi.....152
Table 24: Cerebellar grey matter volumes in healthy controls and ALS-ATXi 154
Table 25: Cerebellar white matter volume profiles in healthy controls and ALS-NEG and ALS-C9.....156
Table 26: Cerebellar white matter volume profiles in healthy controls and ALS-ATXi 158
Table 27: Superior cerebellar peduncle volumes in healthy controls, ALS-NEG and ALS-C9 163

Table 28: Superior cerebellar peduncle volumes in healthy controls and ALS-ATXi 163
Table 29. FA values for the cerebro-cerebellar tracts in healthy controls and ALS-NEG and ALS-C9..... 165
Table 30: Radial diffusivity in cerebro-cerebellar tractography in healthy controls and ALS-NEG and ALS-C9 166
Table 31: Axial Diffusivity in cerebro-cerebellar tractography in healthy controls and ALS-NEG and ALS-C9 168
Table 32: Fractional anisotropy values for the cerebro-cerebellar tracts in healthy controls and ALS-ATXi 170
Table 33: Axial Diffusivity in cerebro-cerebellar tractography in healthy controls and ALS-ATXi 172
Table 34: Radial diffusivity in cerebro-cerebellar tractography in healthy controls and ALS-ATXi 174
Table 35: Cerebellar peduncle profiles in healthy controls and ALS 176
Table 36: Cerebellar peduncle profiles in healthy controls and ALS-ATXi 177
Table 37: Demographic and clinical profile of thalamus study participants 193
Table 38. Effect sizes for thalamus study for intergroup differences using Cohen's |d|. 194
Table 39: Subcortical grey matter volumes in HC, ALS C9+, ALS C9- and PLS..... 199
Table 40: Clinical and demographic profile of study participants: ALS C9+, ALS C9-, PLS, and HC in amygdala study 222
Table 41. Effect sizes for amygdala study for intergroup differences using Cohen's |d|.. 223
Table 42: Estimated marginal means of amygdala nuclei 225

SUMMARY

Novelty

Because the vast majority of ALS imaging studies focus on evaluating motor pathology, the focus and novelty of this work is the nuanced characterisation of extra-motor involvement in a genetically stratified cohort of ALS patients. Sensory, infratentorial and subcortical structures were assessed comprehensively in multimodal analyses. The thalamus and amygdala were segmented into their individual nuclei to examine their volumetric profile, as the involvement of these nuclei has not been comprehensively characterised to date in ALS. The significance of extra-motor involvement in ALS is that subcortical and frontotemporal disease burden may contribute to neuropsychological deficits with implications for multidisciplinary management, clinical trial participation, caregiver burden, adherence to therapy and compliance with supportive interventions. Cerebellar pathology in ALS has also been prooly characterised to date despite its contribution to speech, swallowing, gait and cognitive difficulties.

Rationale

The core neuroimaging signature of ALS includes motor cortex, brainstem, corticospinal tract, and spinal cord degeneration. It is increasingly recognised as a multi-system disorder and extra-motor involvement is observed to be part of the disease process. Sensory dysfunction is relatively under evaluated. There is a prevailing notion that sensory pathways may be relatively spared in ALS despite evidence of

sensory disturbance that has been observed in ALS patients clinically, in electrophysiology, neuroimaging and neuropathology for several decades. We hypothesised that cerebral structures involved in somatosensory processes are not spared in ALS and sought to evaluate cerebral structures involved in sensory processes.

While ALS is primarily characterized by the degeneration of upper and lower motor neurons, it is now recognized as a multi-system disorder. Cerebellar pathology in ALS has been demonstrated by a multitude of neuroimaging and neuropathology studies, however, anatomical patterns of cerebellar disease-burden are poorly characterised *in vivo*, cerebro-cerebellar connectivity changes are mostly inferred from functional studies, and the cerebellar signatures of specific genotypes are not firmly established. Based on these considerations, our main hypothesis is that focal cerebellar pathology may be detected instead of global cerebellar degeneration with the selective vulnerability of specific cerebellar lobules. Additionally, we hypothesised that focal intra-cerebellar pathology is accompanied by selective cerebro-cerebellar disconnection. Our objective was the systematic evaluation of cerebellar grey and white matter alterations, cerebellar peduncle integrity and cerebro-cerebellar connectivity in ALS.

Subcortical grey matter degeneration has been consistently observed both post mortem and in vivo. Thalamus pathology in ALS has been evaluated by dedicated structural, metabolic, and functional imaging studies. The thalamus however is typically evaluated as a single structure in ALS. Overall thalamic atrophy has been

identified by both neuroimaging and post mortem histopathology studies in ALS, but the involvement of specific nuclei has not been comprehensively characterised to date. Based on the review of the literature, we hypothesised, that the 'global' thalamus pathology reported by previous imaging studies in ALS is driven by focal changes in susceptible nuclei. Building on accruing evidence of overall thalamic involvement in ALS, the main objective was the characterisation of regional thalamic pathology in sporadic, *C9orf72* negative ALS at a nuclear level. An additional objective was to evaluate if PLS and *C9orf72* positive ALS patients have distinctive thalamic signatures.

Dedicated amygdala studies are not only sparse in the ALS imaging literature but their findings are strikingly inconsistent. Some of the inconsistency may be explained by differences in imaging methodology and patient selection, but the most likely cause of the inconsistency is that the amygdala is typically evaluated as a single structure in ALS. The involvement of specific nuclei has not been systematically evaluated to date. Based on the available histopathology literature we hypothesised that selective nuclear degeneration may be captured in the amygdala of ALS patients using high-resolution structural imaging, in-depth genetic and clinical profiling and conservative structural analysis pipelines. Based on the clinical phenotype of GGGGCC hexanucleotide repeat expansion carriers in *C9orf72* we additionally hypothesised that genotype-specific amygdalar signatures may be captured. Accordingly, our objective was the systematic evaluation of amygdala pathology in vivo in a large cohort of

genetically and phenotypically characterised motor neuron disease patients using both measures of the entire amygdala and evaluating alterations in specific nuclei.

Main objectives

The main objectives of this thesis were:

1. To perform a systematic review of existing presymptomatic and symptomatic studies in ALS to identify common themes, stereotyped shortcomings, and key learning points for future studies.
2. To perform a systematic review of existing neuroimaging, electrophysiological, biopsy, post-mortem and animal studies that report sensory deficits in ALS and other motor neuron diseases to identify evidence of sensory involvement.
3. To systematically evaluate cerebral grey and white matter structures involved in the processing, relaying and mediation of sensory information.
4. To review *in vivo* and *post mortem* evidence for cerebellar degeneration in ALS.
5. To perform a comprehensive and multiparametric evaluation of both intra-cerebellar pathology and cerebro-cerebellar connectivity in a genetically stratified cohort of patients with ALS.
6. Individually evaluate nuclei of the thalamus to identify genotype and phenotype-specific focal thalamic involvement in C9+ ALS, C9- ALS and PLS patients in comparison to healthy controls.
7. Individually evaluate nuclei of the amygdala to comprehensively characterise amygdala pathology in C9+ ALS, C9- ALS and PLS patients in comparison to healthy controls.

Clinical relevance

The degeneration of somatosensory, auditory and visual pathways was observed. This may have important clinical ramifications which are easily overlooked in the context of predominant pyramidal and LMN degeneration. Subtle sensory dysfunction, such as proprioceptive deficits, may exacerbate mobility, contribute to fall risk, impair dexterity, and worsen bulbar dysfunction, therefore comprehensive sensory testing should be considered as part of the multidisciplinary assessments. Selective, genotype-associated patterns of cerebellar degeneration were observed. Pathognomonic ALS symptoms which are typically attributed to other anatomical regions, such as dysarthria, dysphagia, pseudobulbar affect, eye movement abnormalities and cognitive deficits may be modulated, exacerbated or partially driven by cerebellar changes in ALS. The thalamus is implicated in both motor and cognitive dysfunction, as degeneration of the motor and sensory nuclei of the thalamus as well as nuclei which mediate memory and executive functions was observed. Pathology in the amygdala which plays a role in a variety of sensory, cognitive and emotional was also demonstrated. Multi-parametric neuroimaging has the potential to facilitate the monitoring of disease progression by tracking changes in selected regions of interest over time and to facilitate the classification of heterogeneous cohorts which will enable meaningful interpretation of individual scans in diagnostic, monitoring and prognostic applications.

GLOSSARY

AAA - anterior amygdaloid area **; ABN** - Accessory basal nucleus ; **ACE-R** - Addenbrooke's Cognitive Examination revised Score ; **AD** - Alzheimer's disease ; **AD** - axial diffusivity ; **ADC** - apparent diffusion coefficient ; **ADI-12** - ALS-Depression Inventory ; **ALFF**- amplitude of low-frequency fluctuations ; **ALLFTD** - ARTFL–LEFFTDS Longitudinal Frontotemporal Lobar Degeneration ; **ALS** - amyotrophic lateral sclerosis ; **ALS C9-** - *C9orf72* negative ALS ; **ALS C9+** - *C9orf72* positive ALS ; **ALS T1** – ALS cohort at the first timepoint **; ALS T2** - ALS cohort at the second timepoint **; ANCOVA -** Analysis of covariance ; **ALS-FTD** - amyotrophic lateral sclerosis and frontotemporal dementia ; **ALS-FTD-Q** – Amyotrophic Lateral Sclerosis-Frontotemporal Dementia-Questionnaire ; **ALS-PK** - Amyotrophic lateral sclerosis with parkinsonian symptoms ; **ALSci** – amyotrophic lateral sclerosis with cognitive impairment ; **ALSFRS-R** - Amyotrophic Lateral Sclerosis Functional Rating Scale ; **ANCOVA** - Analysis of covariance ; **ANG** - angiogenin ; **APEX1** - Apurinic/Apyrimidinic Endodeoxyribonuclease 1 ; **APOE4** - Apolipoprotein E4 ; **APP** - amyloid precursor protein ; **ASCA** - Amnestic Comparative Self Assessment ; **ASO** - antisense oligonucleotide-mediated therapies ; **ATF3** - AMP-dependent transcription factor ; **ATXN1**- ataxin 1 gene ; **ATXN2**- ataxin 2 gene ; **AUC** - area under the receiver operator characteristic curves ; **AV** - antero-ventral nuclei ; **AVLT** - Auditory Verbal Learning Test ; **BADA** - Batteria per l'Analisi del Deficit Afasico ; **BADL** - basic activities of daily living ; **BAEP** – brainstem auditory evoked potential ; **BDI** - Beck Depression Inventory ; **BDI-2** - Beck Depression Inventory-II ; **BG -** Basal ganglia ; **BN** - Basal nucleus ; **BNT** - Boston naming test ; **BSRT** - Babcock Story Recall Test ; **bvFTD** – behavioural variant frontotemporal dementia ; **C-CFT** - C-Labeled 2-β-carbomethoxy-3-β-(4-fluorophenyl)tropane ; **C-PiB** - C-Pittsburgh compound B ; **C9-**

ALS - *C9orf72* negative ALS patients **; C9+ ALS -** *C9orf72* positive ALS patients **; C9orf72** - chromosome 9 open reading frame 72 gene ; **CAPG** - Macrophage-capping protein ; **CAT** - Cortico-amygdaloid transition ; **CBF** - cerebral blood flow ; **CBI-R** - Cambridge Behavioural Inventory revised ; **CCAS** - cerebellar cognitive affective syndrome ; **CDR** - Clinical Dementia Rating Scale ; **CDR-SUM** - Clinical Dementia Rating sum of box score ; **CeM** - central medial nucleus ; **CHEP -** contact heat-evoked potential **; CHI3L1** - chitinase 3-like protein 1 ; **CHI3L2** - chitinase 3-like protein 2 ; **CHIT1** - chitotriosidase-1 ; **CHMP2B** - charged multivesicular body protein 2b ; **CL** - central lateral nucleus ; **CM** - centromedian nucleus ; **CMAP** - Compound muscle action potential ;**CN** - Cortical nucleus ; **CN-V -** Trigeminal nerve **; CNS-LS** - Center of Neurologic Study Lability Scale ; **CPM** - conditioned pain modulation ; **Cr** - Creatine ; **CRP** - C-reactive protein ; **CSAP** - compound sensory action potential ; **CSF** - Cerebrospinal fluid ; **CST** - corticospinal tract ; **CT -** cortical thickness **; CV** – conduction velocity ; **CVLT** - California Verbal Learning test ; **CVLT-II** - California verbal learning test II ; **D-KEFS** - Delis–Kaplan Executive Function System ; **DC** - degree centrality ; **DCTN** - dynactin subunit 1 ; **DKI -** diffusion kurtosis imaging **; DN** – dentate nucleus ; **DRG** - dorsal root ganglion ; **DRS** - dementia rating scale ; **DRTC** - dentato-rubro-thalamo-cortical ; **DTI** - diffusion tensor imaging ; **E/I** - excitation/inhibition ; **ECAS** - Edinburgh Cognitive ALS Screen ; **ECLIA** - electrochemiluminescence immunoassay ; **ELISA** - enzyme-linked immunosorbent assays ; **EMG** - Electromyography ; **EMM -** estimated marginal mean **; ENG** – electronystagmography ; **EPI -** echo-planar imaging **; EPs**- evoked potentials ; **EXAMINER** - Executive Abilities: Measures and Instruments for Neurobehavioral Evaluation and Research ; **F-FDG** – (18)F-fluorodeoxyglucose ; **FA** - fractional anisotropy ; **FAB** - Frontal Assessment Battery ; **fALFF** - Fractional Amplitude of Low Frequency

Fluctuation ; **fALS** - familial ALS ; **FBB** - Florbetaben fluorine-18 ; **FBI** - Frontal behavioral inventory ; **FC** - functional connectivity ; **FD** - fractal dimensionality ; **FDA -** United States Federal Drug Administration **; FDA** – Food and Drug Administration ; **FDG-PET** - fluorodeoxyglucose (FDG)-positron emission tomography ; **FEESST** - fiber-optic endoscopic evaluation of swallowing with sensory testing ; **FEW -** familywise error **; FLAIR -** fluid-attenuated inversion recovery **; fMRI** - functional magnetic resonance imaging ; **FOSMN**- facial onset sensory and motor neuronopathy ; **FOV -** field of view **; FrSBe** - Frontal Systems Behavioral Evaluation ; **FSL** - FMRIB Software Library ;**FTD** – frontotemporal degeneration ; **FTD-CDR** - FTD-specific Clinical Dementia Rating ; **FTD-CDR-SOB** - FTD modified Clinical Dementia Rating Scale Sum of Boxes ; **FTLD** - Frontotemporal lobar degeneration ; **FUS** - fused in sarcoma ; **FVC** - forced vital capacity ; **FWE** - Familywise error ; **GENFI** - Genetic Frontotemporal dementia Initiative ; **GM** - grey matter ; **GMV** – grey matter volume ; **GPNMB** - glycoprotein non-metastatic B ; **GRN** - progranulin ; **HADS** - Hospital Anxiety and Depression Scale **; HARDI -** high angular resolution diffusion imaging **; HC -** healthy control **;** ; **HD** - Huntington's disease ; **HFE** - High FE2+ ; **HIST1H2B** - histone cluster 1H2b ; **HIST1H4A** - histone cluster 1H4 ; **HSP** - hereditary spastic paraplegia ; **HTT** - huntingtin ; **HVLT** - Hopkins Verbal Learning Test ; **i-TRAQ** - Isobaric tags for relative and absolute quantitation ; **IADL** - instrumental activities of daily living ; **IENFD** – Intraepidermal nerve fiber density ; **ihMT** – inhomogeneous magnetization transfer ; **IR-SPGR -** inversion recovery prepared spoiled gradient recalled echo **; IR-TSE -** inversion recovery turbo spin echo sequence **; K-BNT** - Korean version of the Boston Naming Test ; **L-SG** - limitans/suprageniculate nuclei ; **LD** - latero-dorsal nuclei ; **LDST** - Letter Digit Substitution Test ; **LEFFTDS** - Longitudinal Evaluation of Familial Frontotemporal

Dementia Subjects ; **LEP** - laser evoked potentials ; **LGN -** Lateral geniculate nucleus **;** **LLL -** left lower limb **; LMN** - lower motor neuron ; **LN** - Lateral nucleus ; **LOX** – lysyl oxidase ; **LP** - lateral posterior nuclei ; **LRRK2** - Leucine Rich Repeat Kinase 2 ; **Lt -** Left **;** **LUL -** left upper limb **; M -** Mean ;**MAP2** - microtubule-associated protein 2 ; **MAPT** - microtubule-associated protein tau ; **MATR** – matrin ; **MCV** – motor conduction velocity ; **MD** - mean diffusivity ; **MDI** - mediodorsal lateral parvocellular nuclei ; **MDm** - mediodorsal medial magnocellular nuclei ; **MDRS** - Mattis Dementia rating scale ; **MDRS-2** - Mattis Dementia Rating Scale-2 ; **MDS-UPDRS** - Movement Disorders Society Unified Parkinson's Disease Rating Scale ; **MEG** - magnetoencephalography ; **MEP** - motor evoked potential ; **MGN -** Medial geniculate nucleus **; MIQ-rs** - Movement Imagery Questionnaire revised 2nd version ; **MLe -** Medial Lemniscus **; MMSE** - Mini Mental State Examination ; **MN** - Medial nucleus ; **MND -** Motor neuron disease **;** **MNI152 -** Montreal Neurological Institute 152 standard space **; MOCA** - Montreal Cognitive Assessment ; **MR** - magnetic resonance ; **MRC** - Medical Research Council rating scale ; **MRI** – magnetic resonance imaging ; **MRM** - Multiple reaction monitoring ; **MRS** - magnetic resonance spectroscopy ; **mtDNA** - mitochondrial DNA ; **MUNE** - Motor Unit Number Estimation ;**MUNIX** - Motor Unit Number Index ; **MV-re** - reuniens/medial ventral nuclei ; **MVIC** - maximal voluntary isometric contraction ; **Myo** - myo-inositol ; **Na/Cr** - N-acetyl to creatine resonance intensity ratios ; **NAA** - N-Acetylaspartate ; **NCS** – nerve conduction study ; **NCV** - nerve conduction velocity ; **NEFH** - neurofilament heavy ; **NEFL** - neurofilament light ; **NEFM** - neurofilament medium ; **NfL** - neurofilament light ; **NFTs** - neurofibrillary tangles ; **NHPT** - nine hole peg test ; **NMS** – non-motor symptoms ; **NODDI** - Neurite orientation dispersion and density imaging ; **NPI** - Neuropsychiatric Inventory ; **NPI-Q** - Neuropsychiatric Inventory

Questionnaire ; **NPTXR** - neuronal pentraxin receptor ; **OCT -** optical coherence tomography **; OEP** - olfactory-evoked response ; **OPTN** - optineurin ; **PARP** – poly (ADP-ribose) polymerase ; **PBA -** pseudobulbar affect ;**Pc** - paracentral nuclei ; **PCL -** pathological crying and laughing ; **PD** - Parkinson's disease ; **PERK** - PKR-like endoplasmic Reticulum Kinase ; **PET** - positron emission tomography ; **Pf** - parafascicular nuclei ; **PINK1** - PTEN-induced kinase 1 ; **PLS** - Primary lateral sclerosis ; **PMA** - progressive muscular atrophy ; **PMC -** primary motor cortex **; PN** - Paralaminar nucleus ; **pNfH** - neurofilament heavy ; **PON** - paraoxonase ; **Pre-fALS** - Pre-Familial Amyotrophic Lateral Sclerosis ; **PREV-DEMALS** - Predict to Prevent Frontotemporal Lobar Degeneration and Amyotrophic Lateral Sclerosis Study Group ; **PRISMA** - Preferred Reporting Items for Systematic Reviews and Meta-Analyses ; **PRPH** - peripherin ; **PSEN1** - presenilin 1 ; **PSEN2** - presenilin 2 ; **PSVEP** – pattern-shift visual evoked response ; **Pt** - paratenial nuclei ; **pTDP-43 -** phosphorylated 43kDa TAR DNA-binding protein ; **PTR -** Posterior Thalamic Radiation **; PuA** - pulvinar anterior nuclei ; **PuI** - pulvinar inferior nucleus ; **PuL** - pulvinar lateral nucleus ; **PuM** - pulvinar medial nucleus ; **QC -** quality control **; QoL** – quality of life ; **QST** - quantitative sensory testing ; **RAVLT** - Rey Auditory Verbal Learning Test ; **RBMT** - Rivermead Behavioural Memory test ; **rCBF** - regional cerebral blood flow ; **RCFT** - Rey's Complex Figure Test-Immediate Recall ; **rCMA** - rostral cingulate motor area ; **rCMRO2** – oxygen metabolism ; **RD** - radial diffusivity ; **RE** – Repeat expansion ; **ReHo -** Regional Homogeneity ; **RLL -** right lower limb **; RNFL -** retinal nerve fibre layer **; ROCF** - Rey-Osterrieth Complex Figure ; **ROI -** region of interest **; RPCM** - Raven's Progressive Colored Matrices ; **rsFC** - resting-state functional connectivity ; **rsfMRI** -resting state functional magnetic resonance imaging ; **Rt -** right **; RUL -** right upper limb **; RWT** - phonematic

Regensburger Wortflüssigkeits-test ; **SAPA -** sensory action potential amplitude **; SAPA** - sensory action potential amplitudes ; **SAT** - Semantic Association Test ; **SBMA** - Spinal and bulbar muscular atrophy / Kennedy's disease ; **SC** – spino-cerebellar ; **SCA** – spinocerebellar ataxia ; **SCNV** - sensory nerve conduction velocity ; **SCV** - sensory conduction velocity ; **SD -** standard deviation **; SDMT** - symbol digit modalities test ; **SE** – standard error ; **SE-EPI -** spin-echo echo planar imaging **; SEA** - Social Cognition and Emotional Assessment ; **SENSE -** sensitivity Encoding **; SEP -** somatosensory evoked potential **; SET** - story-based empathy task ; **SETX** - senataxin ; **SF36** - 36-item Short Form Health Survey ; **SGCs** - satellite glial cells ; **SICI** - Short interval intracortical inhibition ; **SIGMAR1** - sigma non-opioid intracellular receptor 1 ; **SMA** - Spinal muscular atrophy ; **SMA** - supplementary motor area ; **SMC** - primary sensorimotor cortex ; **SMN** - superior medial sensory-motor network ; **SMN** - survival motor neuron ; **SNAP -** sensory nerve action potential **; SNAPA** - sensory nerve action potential amplitude ; **SNCA** - Synuclein Alpha ; **SNST-CWIS** - Stroop Neuropsychological Screening Test-Color Word Interference Score ; ***SOD1* -** superoxide dismutase 1 **; SPECT** - single-photon emission computerized tomography ; **SPG** - spatacsin ; **SPIR -** spectral presaturation with inversion recovery **; SPM** - statistical parametric mapping ; **SPSS** – statistical product and service solutions ; **SSCV** - spinal cord conduction velocity ; **SSEP** - somatosensory evoked potentials ; **SVC**- slow vital capacity ; **SVLT** - Seoul Verbal Learning Test ; **svPPA** – semantic variant primary progressive aphasia ; **SWI -** susceptibility weighted imaging **; T1** – Timepoint 1 ;**T1W -** T1-weighted imaging ; **T1W** - T1-weighted imaging ; **T2** – Timepoint 2 ; **TARDBP** - TAR DNA-Binding Protein 43 ; **TBM** - tensor based morphometry ; **TBSS -** tract-based spatial Statistics **; TDP-43** - TAR DNA-binding protein 43 ;**TE** - Echo time ; **TFCE -** threshold-free cluster enhancement **; TI** -

Inversion time ; **TIV -** total intracranial volume **; TMS** - transcranial magnetic stimulation ; **TMT** – trail making test ; **ToM** - Theory of Mind ; **TR -** repetition time **; TRPV** – transient receptor potential cation channel subfamily V ; **UBQLN** - Ubiquilin Like ; **UBQLN2** - ubiquilin-2 ; **UCHL1** - ubiquitin carboxyl-terminal hydrolase 1 ; **UDSNB** - neuropsychological battery of the Uniform Data Set ; **UMN** - upper motor neuron ; **UMN score** - upper motor neuron clinical burden score ; **UPDRS** - Unified Parkinson's Disease Rating Scale ; **UPSIT** - University of Pennsylvania Smell Identification Test ; **UtC** - urge to cough ; **VA** - ventral anterior nuclei ; **VAmc** - ventral anterior magnocellular nuclei ; **VAPB** - vesicle associated membrane protein-associated protein B/C ; **VAT** - Visual Association Test ; **VBM** - voxel based morphometry ; **VBR** - voxel-based relaxometry ; **VCP** - valosin containing protein ; **VEP -** visual evoked potentials **; VLp** - ventral lateral posterior nuclei ; **VM -** Ventromedial nucleus **; VOSP** - The Visual Object and Space Perception Battery ; **VP** - ventral posterior nucleus ; **VPL -** Ventral posterolateral nucleus **; WAIS** - Wechsler Adult Intelligence Scale ; **WCST** - Wisconsin Card Sorting Test ; **WM** – white matter ; **WRAT** - Wide Range Achievement Test

CHAPTER 1: Presymptomatic and symptomatic findings in ALS

Introduction

One of the latest developments in amyotrophic lateral sclerosis (ALS) is the emergence of genotype-specific pharmacotherapies heralding a paradigm shift from generic neuroprotective strategies to precision, genotype-specific interventions (1, 2). The fundamental heterogeneity of the disease is now universally recognised and genotype- and phenotype-specific clinical traits, radiological signatures and disease trajectories have been characterised (3-5). The notion that a long presymptomatic phase precedes symptom manifestation and that neurodevelopmental factors may contribute to the pathogenesis of ALS is increasingly accepted (6). The presymptomatic phase of ALS has been relatively arcane until the publication of seminal presymptomatic papers which confirmed considerable pathological changes years before symptom manifestation (7, 8). Existing presymptomatic studies in ALS invariably suffer from sample size limitations and are strikingly diverse with regards to their study design, methodological approach and conclusions. The systematic review of these papers, the frank discussion of their limitations, and the careful integration of their findings is particularly timely with the emergence of genotype-specific therapies (1, 2). One of the key contributions of recent imaging studies in ALS is the confirmation that by the time patients fulfil diagnostic criteria for ALS, considerable disease burden can already be detected, limiting the therapeutic potential of putative disease-modifying drugs. These observations suggest that the optimal therapeutic window is likely to be at an earlier stage in high-risk, genetically susceptible populations. The presymptomatic phase of

ALS has long been of academic interest (9), and inspired small-scale studies (10), dedicated terminology (9), but the advent of antisense oligonucleotide therapies (ASOs) highlights the urgency for large presymptomatic studies and the meticulous integration of molecular, pathological and radiological observations in asymptomatic mutation carriers. ASO-mediated drugs have already been approved by the US Food and Drug Administration for the treatment of spinal muscular atrophy and Duchenne muscular dystrophy (11-13), and currently being trialled for ALS (1). The nuanced characterisation of pathophysiological processes before perceptible disability develops may help to identify the optimal therapeutic window for pharmacological intervention before irreversible functional impairment ensues. Longitudinal studies of mutation carriers spanning from the adolescence to significant disability would provide an opportunity to describe anatomical patterns of disease spread, validate current staging systems, evaluate prognostic indicators and test prevailing propagation theories such as corticofugal spread, network-wise propagation, selective vulnerability, trans-synaptic spread etc. (9, 14, 15) Reports of considerable presymptomatic cerebral pathology without overt functional impairment also suggest a degree of 'motor reserve', network redundancy or possible compensatory processes to maintain function until a critical threshold is reached and symptoms develop. Large presymptomatic studies also permit the systematic assessment of the sensitivity profile of our current biomarkers. For example, detecting white matter changes in a patient with significant disability may be less challenging than capturing early asymptomatic changes in white matter integrity decade before projected symptom manifestation. Despite the dual academic and clinical relevance of characterising the presymptomatic course of ALS (16-18), striking inconsistencies exist in the current

literature due to the sample size limitations and methodological differences (19-21). Our objective is the careful integration of the lessons of existing presymptomatic studies in ALS, to identify key learning points from individual studies, reflect on common methodological shortcomings and distil a robust framework for future studies.

Methods

A formal systematic literature review was conducted using the following search terms on PubMed: “amyotrophic lateral sclerosis”, “motor neuron disease”, “*C9orf72*”, “frontotemporal lobar degeneration”, “frontotemporal dementia” combined with each of the following keywords “presymptomatic”, “premanifest”, “asymptomatic”. An additional search combined the above search terms with the following keywords: “magnetic resonance imaging”, “MRI”, “positron emission tomography”, “PET”, “electromyography”, “neuroimaging”, “electrophysiology”, “neurophysiology”, “transcranial magnetic stimulation”, “motor unit number estimation”, “motor unit number index”, “neurofilament”, “biomarkers”. Only original research papers were systematically reviewed. Conference abstracts published in supplements of neuroscience journals were not considered. Only human studies were systematically reviewed. No exclusion criteria were set based on year of publication, but only articles written in English were reviewed. Animal studies, review papers, opinion pieces, editorials, case reports, and case series were excluded. Based on the above criteria a total of 48 original research papers investigating presymptomatic carriers of gene mutations implicated in ALS were selected and reviewed in accordance with the Preferred Reporting Items for Systematic Reviews and Meta-Analyses (PRISMA) recommendations. The identified papers were systematically reviewed based on the following criteria.

(1) Core study design parameters (target cohort: pre-symptomatic/pre-manifest, control group: healthy controls/non-carrier relatives/disease controls, sample size, cross sectional/longitudinal, prospective/retrospective, multi-centre/single centre,

follow-up interval, number of follow-up time points, number of participants, attrition rates, follow-up into the symptomatic phase)

(2) Clinical and laboratory assessments (Genetic testing, demographic profiles, availability of electrophysiological assessment, neurological or neuropsychological data, functional rating scales)

(3) Neuroimaging methods (cerebral/spinal, whole-brain/region-of-interest, MRI / PET, structural/diffusion/spectroscopy/rs-fMRI, field strength 1,5 Tesla/3 Tesla / 7 Tesla, single/multi-modal analyses, post-mortem validation.

An additional 20 imaging papers of presymptomatic FTD gene mutation carriers were also identified and reviewed. We also reviewed a selection of presymptomatic imaging papers in Huntington's disease (11 papers), Alzheimer's disease (13 papers) and Parkinson's disease (13 papers).

Results

While the terms ‘preclinical’, ‘premanifest’ and ‘presymptomatic’ are widely used, the term ‘asymptomatic mutation carrier’ is preferred by many. It has been proposed (19) that term ‘preclinical’ should be reserved for the period where there are no identifiable pathological changes and the term ‘presymptomatic’ used for the phase when neuroimaging, electrophysiology or detailed cognitive assessment may already detect abnormalities. Despite these recommendations the above terms are often used interchangeably. The number of papers identified stratified by the key study methodology are shown in **Figure 1**.

Figure 1*: Number of studies identified by core search criteria*

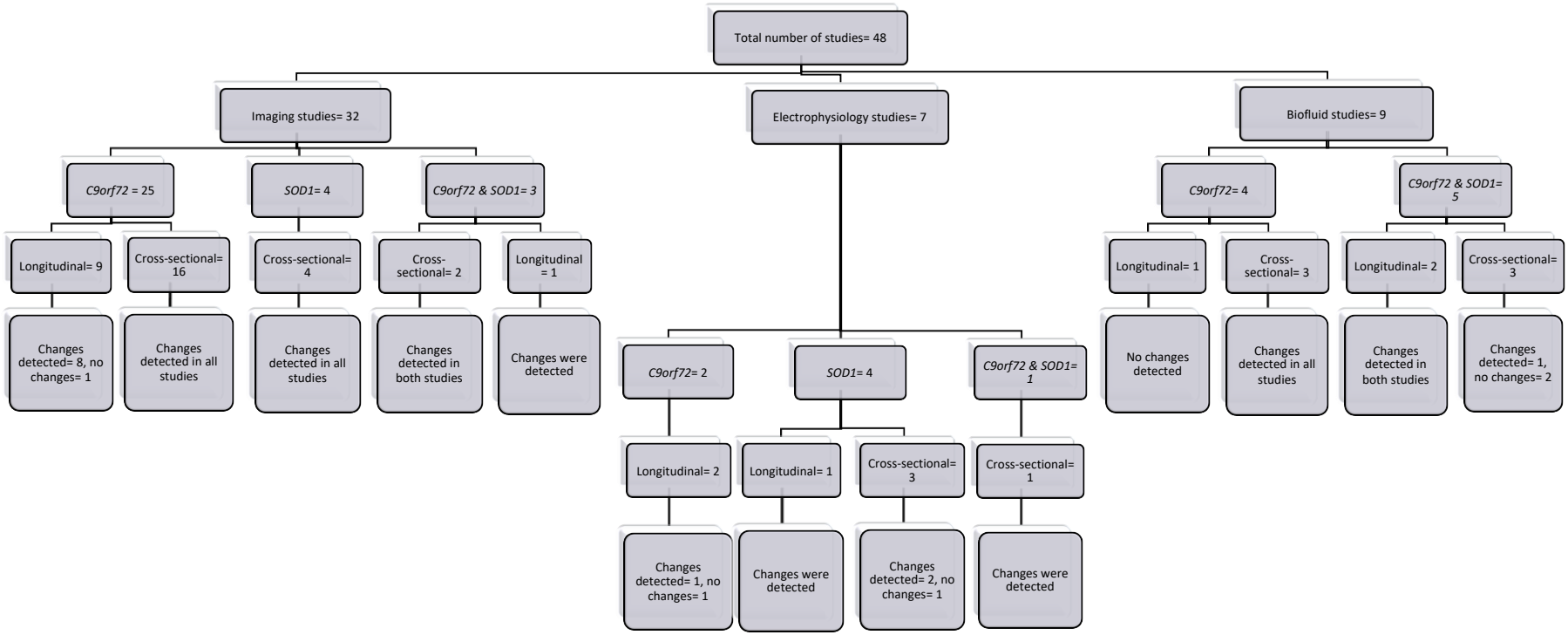

Neuroimaging studies of asymptomatic mutation carriers

Cohort characteristics

Based on our search criteria we have identified twenty-five imaging studies investigating presymptomatic *C9orf72* hexanucleotide carriers (7, 8, 22-28), four studies focusing on presymptomatic *SOD1* carriers (10, 29-33), and three studies evaluating both (29, 30). We also identified a study which included *NEK1*, *TARDBP* and *FUS* gene mutation carriers in addition to participants with the *C9orf72* and the *SOD1* (29). The number of presymptomatic subjects included in single studies showed significant variation ranging from 2 (33) to 249 (34). Eight studies had included over 100 presymptomatic carriers (34-40). The number of presymptomatic *C9orf72* carriers included ranges from 2 (30) to 83 (27) and the number of presymptomatic *SOD1* carriers ranges from 2 (33) to 24 (10) in the current literature. Thirteen studies also included symptomatic patients (27, 38, 41-43), and 19 studies only focussed their investigation on presymptomatic cohorts (8, 26, 28, 35, 36). The strategy to select symptomatic participants was inconsistent; some studies only included symptomatic gene carriers (10, 22, 23, 27, 29, 33, 38, 39, 41-44) while others included sporadic patients (23, 30). The size of the symptomatic cohort also shows great variation ranging from as little as 12 subjects (30) to 270 (29). Symptomatic control cohorts included patients with ALS (10, 23, 27, 29, 33), FTD (23, 27) and ALS-FTD (23, 27). Without exception, all identified studies included a cohort of healthy controls. These cohorts were either unrelated healthy controls (10, 23, 27-31, 33, 38), or more

commonly, gene negative relatives of symptomatic patients (8, 22, 32, 34, 35, 40, 45). A common shortcoming of the available papers is that when unrelated healthy controls were used as a reference group, their gene profile was not reported. Furthermore, none of the reviewed studies used 'disease controls', which would have helped to gauge the specificity of findings to ALS. The mean age of asymptomatic *C9orf72* subjects ranged from 39.8 years (7) to 51 (28) and in the case of *SOD1* Carriers from 32.3 years (32) to 47.2 years (46). In studies where a symptomatic cohort was included, their mean age ranged was 47.8 years (30) to 65.2 years (39). Presymptomatic cohorts were generally relatives of symptomatic ALS (8, 26, 30), ALS-FTD or FTD patients (8, 26, 34). **Table 1.**

Cohort size observations

Existing presymptomatic studies vary considerably with regards to overall sample size and statistical power. The total number of participants ranges from as few as 21 (32) to as many as 472 subjects (34). While several studies included over 300 participants, these are invariably multi-centre studies necessitating some degree of inter-rater reliability testing for clinical assessments, sequence harmonisation for imaging and standard operating procedures for biomarker collection, storage and analysis (27, 29, 34, 38, 39). Irrespective of the overall sample size, almost half all identified presymptomatic studies in ALS-FTD (15 out of 32) resulted from data generated from multi-site consortia such as the Genetic Frontotemporal dementia Initiative (GENFI) (27, 34, 36-44), the ARTFL–LEFFTDS Longitudinal Frontotemporal Lobar Degeneration (ALLFTD)(35, 45) research consortium and the Predict to Prevent Frontotemporal

Lobar Degeneration and Amyotrophic Lateral Sclerosis Study Group (PREV-DEMALS) (7). More than half of the identified studies (17 out of 32) were single centre studies (10, 22-25, 30-33, 47). Very few single-centre studies reached cohort sizes over 100 (46, 48-50), and the largest single-centre recruited included 113 participants (49). The most asymptomatic *C9orf72* participants included in a single centre study were 40 participants (8). **Table 1**

Study methods

The vast majority, 22 out of the 32 presymptomatic imaging studies are cross-sectional (10, 31, 37, 43, 47), and only 10 longitudinal presymptomatic studies can be presently identified (8, 23, 27, 36, 41, 42, 45, 46, 49, 50). Significant variability can also be observed with regards to follow-up intervals, which range from 6 months (23) to 2 years (49, 50). The longest overall follow-up period was 6 years (50). The majority of longitudinal studies are 2 time-point studies, with a select few assessing subjects across three timepoints (23, 45, 50). Only one study evaluated participants up to 4 times longitudinally (27). T1-weighted structural MRI data were appraised in the majority (24) of presymptomatic imaging studies (27, 35, 36, 38-41, 43-45), diffusion MRI data in 14 studies (7, 8, 22, 26, 29, 31, 32, 46) and functional MRI data in 6 studies (24, 30, 34, 42, 48, 50). MR spectroscopy was performed in one study (10) and one study used arterial spin labelling (37). Two presymptomatic PET studies were identified (28, 33), one using flumazenil (33), and the other used fluorodeoxyglucose (F-FDG) (28) as a tracer. While many studies investigated a single parameter, 14 studies implemented a multi-modal approach (7, 22-25, 28, 30-32, 37, 48-50). The majority of

MRI studies were performed on a 3 Tesla MRI platform (7, 8, 10, 27, 31). Seven studies relied on imaging data from a 1.5T scanner (32) and of these, 5 were multi-site studies relying on mixed data from 1.5T and 3T scanners (29, 36, 38, 39, 42). No ultra-high field (7T) human presymptomatic studies were identified at the time of this review.

Table 1

Imaging findings in presymptomatic ALS

In *C9orf72* hexanucleotide repeat expansion carriers, frontal (27), temporal, parietal, occipital (22), thalamic (24, 25), cerebellar (25) and striatal (24) atrophy was consistently detected. Diffusion MRI captured reduced WM integrity in the corticospinal tracts (8, 24), corpus callosum, cingulum, uncinate and inferior longitudinal fasciculi (7, 24, 26) and in the WM axonal structures projecting to the orbitofrontal cortex (46). Neurite orientation dispersion and density imaging (NODDI) is thought to be more sensitive in detecting white matter alterations than traditional DTI metrics (26). A PET study of presymptomatic *C9orf72* participants confirmed hypometabolism in frontotemporal, insular, thalamic and basal ganglia regions (28). It is noteworthy, that some studies did not detect cerebral changes in asymptomatic *C9orf72* carriers (23).

In asymptomatic *SOD1* carriers, white matter degeneration was observed in the posterior limb of the internal capsule (32), reduced flumazenil binding in the left fronto-temporal junction (33), and reduced NAA/Cr and NAA/Myo ratios in the

superior spinal cord (10). A multimodal study of 7 asymptomatic SOD1 carriers found no significant abnormalities on diffusion tensor imaging and threshold tracking transcranial magnetic stimulation (31).

In asymptomatic mixed-genotype cohorts frontal, temporal, parietal (47) and cerebellar (39) atrophy was noted as well as subcortical grey matter degeneration including the caudate (47), hypothalamus (29), and thalamus (39, 47). White matter alterations were observed in the anterior thalamic radiation (49). Marked connectivity changes were detected by some functional MRI studies (30, 34), while others identified functional resilience despite structural degeneration (42). **Table 1**

Table 1*: A selection of presymptomatic neuroimaging studies in ALS/FTD *GENFI assessments include physical examination, FDR, CBI-R, Uniform data set: Weschler memory scale revised, digit symbol, TMT, BNT, category fluency, letter fluency, Wechsler Abbreviated Scale of Intelligence Block Design, MMSE (51)*

Authors, year of publication	Study participants	Clinical assessments	Imaging modality	Key findings in the presymptomatic cohort
Lulé 2020 (46)	21 presymptomatic *C9ORF72* 15 presymptomatic *SOD1* 56 non carrier family members 35 healthy controls	HADS, ACSA, ECAS, RWT, design fluency, visual memory, verbal memory, TMT	Diffusion MRI	-alterations in WM axonal structures projecting to orbitofrontal cortex
de Vocht et al., 2020 (28)	17 presymptomatic *C9orf72* 25 healthy controls	Neurological exam, ECAS, MMSE, BDI	PET	-hypometabolism in frontotemporal regions, insular cortices, basal ganglia, and thalami
Le Blanc et al., 2020 (27)	83 presymptomatic *C9orf72* 54 symptomatic carriers 249 healthy controls	MMSE, CBI	Structural MRI	-reduced cortical thickness/cortical surface area in more restricted areas of medial frontoparietal lobes, in addition to scattered lateral frontal, parietal, and temporal areas
Staffaroni et al., 2020 (35)	127 presymptomatic 101 non carrier family members	Neurological and neuropsychological assessments, cognitive test- UDSNB-3, CDR	Structural MRI	-individualized quantification of baseline brain atrophy is promising predictor of progression in asymptomatic familial FTD
Staffaroni et al., 2020 (45)	34 presymptomatic *C9orf72* 28 presymptomatic *GRN* 31 presymptomatic *MAPT* 78 non carrier family members	UDSNB, MOCA, TMT, CDR, NIH-EXAMINER	structural MRI	-NIH-EXAMINER sensitive to cognitive changes and declines were associated with worsening clinical symptoms and brain volume loss
Cury et al., 2019 (43)	76 presymptomatic carriers 37 symptomatic carriers 98 non carrier family members	*all participants underwent GENFI assessments	Structural MRI	-differences in shape in anterior region of thalamus at least five years before mutation carriers develop clinical symptoms
Feis et al., 2019 (48)	12 presymptomatic *C9orf72* 35 presymptomatic *GRN* 8 presymptomatic *MAPT* 48 non carrier family members	Neurological exam, neuropsychiatry tests, MMSE	structural, diffusion & functional MRI	-using newly created carrier-control classification model, mutation carriers can be separated from controls with a modest AUC even before symptom-onset
Feis et al., 2019 (50)	12 presymptomatic *C9orf72* 35 presymptomatic *GRN* 8 presymptomatic *MAPT* 48 non carrier family members	Neurological exam, neuropsychiatry tests, MMSE	structural, diffusion & functional MRI	-mutation carriers did not have higher classification score increase over time than controls
Gazzina et al., 2019 (36)	31 presymptomatic *C9orf72* 65 presymptomatic *GRN* 20 presymptomatic *MAPT* 113 non carrier family members	*all participants underwent GENFI assessments MMSE scores reported in this study	Structural MRI	-highly educated at-risk subjects had better cognition and higher GM volume at baseline -higher educational attainment was associated with slower loss of GM over time
Mutsaerts et al., 2019 (37)	34 presymptomatic *C9orf72* 55 presymptomatic *GRN* 18 presymptomatic *MAPT* 113 non carrier family members	*all participants underwent GENFI assessments MMSE, CBI-R and FDRS	Structural, arterial spin labelling	-CBF differences first appeared 12.5 years before expected symptom onset -CBF lower in mutation carriers closer to and beyond their expected age of symptom onset

		scores reported		
Panman et al., 2019 (49)	12 presymptomatic *C9orf72* 33 presymptomatic *GRN* 15 presymptomatic *MAPT* 53 non carrier family members	Neurological exam, neuropsychological assessment, MMSE, NPI-Q	Structural & diffusion MRI	-lower GM volume in cerebellum and insula -WM differences in anterior thalamic radiation, at baseline and follow-up
Premi et al., 2019 (34)	82 presymptomatic *C9orf72* 122 presymptomatic *GRN* 45 presymptomatic *MAPT* 223 non carrier family members	*all participants underwent GENFI assessments TMT, MMSE, CBI scores reported in this study	Functional MRI	-diminished dynamic fluidity -visiting less meta-states -shifting less often across them -travelling through a narrowed meta-state distance
Querin et al., 2019 (8)	40 presymptomatic *C9orf72* 32 non carrier family members	UMN and LMN signs, bulbar signs, cognitive and behavioural changes, neuropsychological exam, ALSFRS-R, MMSE, FAB, MDRS	Diffusion MRI	-significant CST FA reduction at baseline
Rittman et al., 2019 (42)	17 presymptomatic *C9orf72* 13 presymptomatic *MAPT* 38 presymptomatic *GRN* 24 symptomatic carriers 80 non carrier family members	*all participants underwent GENFI assessments scores not reported in this study	Functional MRI	-despite loss of both brain volume and functional connections, there is maintenance of efficient topological organization of brain's functional network in years leading up to estimated age of FTD symptom onset
Tavares et al., 2019 (41)	13 presymptomatic *C9orf72* 29 presymptomatic *GRN* 4 presymptomatic *MAPT* 18 symptomatic carriers 56 non carrier family members	*all participants underwent GENFI assessments scores not reported in this study	structural MRI	-ventricular volume differences are detectable
Wen et al., 2019 (26)	38 presymptomatic *C9orf72* 29 non carrier family members	Neurological exam, neuropsychological and behavioural assessments, MMSE, FAB, MDRS	Structural & diffusion (NODDI) MRI	-WM abnormalities in 10 tracts with neurite density index and only 5 tracts with DTI metrics
Bertrand et al., 2018 (7)	41 presymptomatic *C9orf72* 39 non carrier family members	Neurological exam, neuropsychological and behavioural scores, MMSE, MDRS, FBI, FAB, SEA, Praxis score, Benson figure, Free and cued recall test, Fluency tasks	structural, diffusion MRI	-atrophy in 4 cortical regions of interest and in right thalamus -WM alterations in 2 tracts in young *C9orf72* positive individuals
Cash et al., 2018 (39)	40 presymptomatic *C9orf72* 65 presymptomatic *GRN* 23 presymptomatic *MAPT* 47 symptomatic carriers	*all participants underwent GENFI assessments MMSE scores reported	Structural MRI	-GM atrophy in the thalamus and cerebellum

	144 non carrier family members	in this study		
Fumagalli et al., 2018 (38)	42 presymptomatic *C9orf72* 66 presymptomatic *GRN* 24 presymptomatic *MAPT* 63 symptomatic carriers 148 non carrier family members	*all participants underwent GENFI assessments	Structural MRI	-widespread atrophy in *C9orf72*
Popuri et al., 2018 (47)	15 presymptomatic *C9orf72* 9 presymptomatic *GRN* 38 non carrier family members	Neurological exam including motor and reflexes, FAB, FBI, MMSE	Structural MRI	-cortical thinning in temporal, parietal and frontal regions -reduced volumes of bilateral thalamus and left caudate
Gorges et al., 2017 (29)	18 presymptomatic *C9orf72* 11 presymptomatic *SOD1* 1 presymptomatic *NEK1* 1 presymptomatic *TARDBP* 1 presymptomatic *FUS* 270 symptomatic patients 112 healthy controls	Neurological exam, ALSFRS-R	Structural & diffusion MRI	-atrophy of the hypothalamus
Papma et al., 2017 (25)	18 presymptomatic *C9orf72* 15 non carrier family members	neuropsychiatric tests	Structural & diffusion MRI	-WM integrity loss in tracts connecting frontal lobe, thalamic radiation, and tracts associated with motor functioning -GM volume loss in thalamus, cerebellum, and parietal and temporal cortex in C9orf72 positive above 40 years of age
Premi et al., 2017 (40)	33 presymptomatic *C9orf72* 14 presymptomatic *MAPT* 61 presymptomatic *GRN* 123 non carrier family members	*all participants underwent GENFI assessments	Structural MRI	-lower GM volume
Sudre et al., 2017 (44)	28 presymptomatic *C9orf72* 25 presymptomatic *GRN* 8 presymptomatic *MAPT* 43 symptomatic carriers 76 non carrier family members	*all participants underwent GENFI assessments scores not reported in this study	Structural MRI	-Significant differences in symptomatic *GRN* group -no differences in the *MAPT* or *C9orf72* groups
Floeter et al., 2016 (23)	7 asymptomatic *C9orf72* 42 symptomatic carriers/sporadic 28 healthy controls	Neurological exam, ALSFRS-R, D-KEFS, MMSE, MDRS	Structural MRI	- study unable to identify structural changes in asymptomatic carriers
Lee et al., 2016 (24)	15 presymptomatic *C9orf72* 67 non carrier family members	Neurological exam- UMN and LMN signs, cognitive testing, MMSE, CVLT, CDR, neuropsychology	Structural, diffusion & functional MRI	-GM volume deficits in cingulate, insula, thalamus, and striatum -Reduced WM integrity found in corpus callosum, cingulum bundles, corticospinal tracts, uncinate fasciculi and inferior longitudinal fasciculi.
Menke et al., 2016 (30)	2 presymptomatic *C9orf72* 10 presymptomatic *SOD1* 12 symptomatic sporadic patients 12 healthy controls	Neuromuscular exam, neuropsychological test, ALSFRS-R	structural, diffusion & functional MRI	-widespread FA and RD differences - FC between cerebellum and network comprising precuneus, cingulate & middle frontal lobe significantly higher
Walhout et al., 2015 (22)	16 presymptomatic *C9orf72* 14 symptomatic carriers 51 non carrier family members	NA	Structural & diffusion MRI	-cortical thinning in temporal, parietal, and occipital - left caudate and putamen atrophy

Carew et al., 2011 (10)	24 presymptomatic *SOD1* 23 symptomatic carriers 29 healthy controls	Neurological exam- UMN and LMN signs, ALSFRS-R, FVC	MRS	- reduced NAA/Cr and NAA/Myo ratios in the superior spinal cord
Vucic et al., 2010 (31)	7 presymptomatic *SOD1* 62 healthy controls	MRC, ALSFRS-R, Triggs hand function score	Diffusion MRI & TMS	-combined anatomical and functional modalities established normal integrity of corticomotoneurons
Ng et al., 2008 (32)	8 presymptomatic *SOD1* 13 non carrier family members	Neurological exam, neuropsychology	Structural & diffusion MRI	-decreased FA and increased tensor trace (TT) at posterior limb of internal capsule - Increased RD was detected on both sides
Turner et al., 2005 (33)	2 *SOD1* 34 symptomatic carriers 24 healthy controls	Neurological exam, ALSFRS-R, UMN-score	PET	-small focus of reduced [11C]flumazenil binding at left fronto-temporal junction similar to the pattern seen in the clinically affected patients

The clinical profile of mutation carriers

Accompanying clinical assessments

Most presymptomatic imaging studies incorporate a brief neurological assessment to screen for clinical signs (23, 26, 28-30, 32, 33, 35, 48-50), but the details of the exam are seldom reported (8, 10, 24, 47). In symptomatic patients, the revised amyotrophic lateral sclerosis functional rating scale (ALSFRS-r) (8, 10, 23, 29-31, 33), Medical Research Council (MRC) scale (31), Trigg's hand function score (31), and composite upper motor neuron (UMN) scores (33) are typically administered. Nineteen out of 32 studies also commented on neuropsychological performance. The battery of neuropsychological instruments varied greatly across the identified studies. Many studies used generic, non-ALS specific, screening tests such as the Mini Mental State Examination (MMSE) (7, 8, 23, 24, 26-28, 34, 36, 39, 40, 47-50), the Montreal Cognitive Assessment (MOCA) (45), the Frontal Assessment Battery (FAB) (7, 26, 47), the Clinical Dementia Rating Scale (CDR) (45), or the Mattis Dementia rating scale (MDRS). Some centres relied on ALS-specific screening tools such as the (ECAS) (24, 28, 46), while others used an extensive battery of neuropsychological tests assessing memory, visuospatial, language, executive domains, social cognition, anxiety and depression (24). Some studies focused on specific cognitive domains known to be preferentially affected in ALS, such as executive function. This was typically interrogated by digit span (40), Stroop test (25), trail making test (TMT) (34, 40, 45), fluency tasks (7, 25, 40), the Delis–Kaplan Executive Function System (D-KEFS) (23) or symbol digit modalities test (SDMT) (40). Language was either assessed by the Boston naming test (7, 40) or the Wide Range Achievement Test (WRAT) (24). Memory performance was

appraised using the California Verbal Learning test (CVLT) and Benson figure recall (24) and other recall tests (7, 40). Visuospatial function was assessed using the Benson figure and The Visual Object and Space Perception Battery (VOSP) (24). Possible neuropsychiatric manifestations have been assessed by the Neuropsychiatric Inventory Questionnaire (NPI-Q) (24, 49), and depression has been screened for by the geriatric depression scale (24) or the Beck Depression Inventory (BDI) (24, 28). Presymptomatic behavioural manifestations were evaluated by the revised Cambridge Behavioural Inventory (CBI-R), (27, 34, 40) and the Frontal Behavioural Inventory (FBI) (7, 23, 47). Other instruments used in presymptomatic studies included the neuropsychological battery of the Uniform Data Set (UDSNB) and the Executive Abilities: Measures and Instruments for Neurobehavioral Evaluation and Research (EXAMINER) (45).

Clinical findings in presymptomatic cohorts

A study of presymptomatic *C9orf72* carriers identified subtle deficits in executive functioning, verbal fluency and memory (28) while another study detected significant memory impairment (24). Several studies found that MMSE scores are slightly lower in presymptomatic *C9orf72* carriers, but still within normal range (7, 24, 27, 28, 47). Performance on other tests such as the MDRS (7), FAB (7, 47), FBI (7, 47), Benson figure (7, 24), Boston naming test (7, 24), Stroop, verbal fluency, and digit span (24) is thought to be relatively preserved and comparable to healthy controls.

Electrophysiology studies of asymptomatic mutation carriers

Presymptomatic mutation carriers at risk of developing ALS have also been extensively investigated by quantitative electrophysiology tools (**Table 2**), such as motor unit number estimation (MUNE) (20, 21, 52), magnetoencephalography (MEG) (53), and transcranial magnetic stimulation (TMS) (31, 54-56). Some of these studies also interrogated accompanying MRI data (31, 53, 56). Asymptomatic *C9orf72* (53, 54, 56) and *SOD1* (20, 21, 31, 52, 53, 55) mutation carriers are typically either compared to unrelated healthy controls (31, 53-55), gene-negative family members (56) or both (20, 21, 52). Longitudinal studies (20, 54, 56) followed patients for up to 3 years (20, 54) with a follow-up interval as short as 6 months (20). The number of total participants in presymptomatic electrophysiology studies range from 52 (53) to 186 (56) with up to 19 presymptomatic *SOD1* (20, 52) and up to 11 presymptomatic *C9orf72* (54) carriers included in any one study. The majority of these studies also include a group of symptomatic patients (20, 21, 53-55), and often symptomatic mutation carriers (56). Symptomatic patients were mostly ALS (20, 21, 53-55) or FTD patients (56), but one study also included PLS patients (53). None of the reviewed studies included neurodegenerative 'disease-controls'. The age profile of presymptomatic mutation carriers in electrophysiology studies range from 40 (55) to 51.7 (53) but several studies did not report demographic data in detail. In presymptomatic electrophysiology studies, the presymptomatic cohort was on average 10 years younger than the symptomatic cohort. On TMS, alterations in intracortical facilitation transmission are seen up to 3 decades before expected symptom onset (56). One study showed that SICI was absent in only 2 presymptomatic *SOD1* carriers and reduced in one (55). A

study investigating MUNE showed no changes in presymptomatic *SOD1* carriers (21), but a follow-up study reported that 2 of 19 *SOD1* carriers showed reduction in MUNE just months before the symptom onset (20). Cortical hyperexcitability was detected in symptomatic *C9orf72* carriers but not asymptomatic carriers (54). Some electrophysiology studies report the clinical profile, including MRC scores in presymptomatic cohorts (20, 52, 55) or ALSFRS-r in symptomatic patients (53-55). Cognitive screening with ECAS (53) or MMSE (56) was also implemented in some studies.

Table 2*: A selection of presymptomatic electrophysiology studies in ALS*

Authors and year of publication	Study participants	Clinical assessments	Methods	Significant findings in presymptomatic cohort
Benussi et al., 2019 (56)	4 presymptomatic *C9orf72* 48 presymptomatic *GRN* 61 symptomatic carriers 73 non carrier family members	Neuropsychological assessment, CBI-R, MMSE, TMT	TMS, structural MRI	-biological changes and intracortical facilitation transmission abnormalities occur 3 decades before, followed by intracortical inhibition transmission deficits 2 decades before expected symptom onset, followed by an increase of WM lesions, brain atrophy, and cognitive impairment
Proudfoot et al., 2017 (53)	10 presymptomatic *SOD1* 2 presymptomatic *C9orf72* 20 symptomatic carriers/sporadic 20 healthy controls	cognitive tests, ALSFRS-R, ECAS, ACE-R	MEG, structural MRI	-Movement execution coincided with excess beta desynchronization
Geevasinga et al., 2015 (54)	11 presymptomatic *C9orf72* 88 symptomatic carriers/sporadic 74 healthy controls	ALSFRS-R, MRC, UMN score	TMS- MEP, CMAP	-cortical hyperexcitability is an intrinsic feature of symptomatic c9orf72 but not asymptomatic
Aggarwal et al., 2012 (52)	19 presymptomatic *SOD1* 34 non carrier family members 16 healthy controls	Neurological exam, MRC	MUNE	-MUNE is more sensitive for monitoring disease progression than maximal voluntary isometric contraction (MVIC), as MUNE correlates with number of functional motor neurones
Vucic et al., 2008 (55)	17 presymptomatic *SOD1* 57 symptomatic carriers/sporadic 55 healthy controls	Neurological exam, neuropsychological test, ALSFRS-R, MRC, Triggs hand function score	TMS	- SICI was completely absent in 2 pre-symptomatic SOD-1, in 1 subject there was a 32% reduction in SICI -These three individuals subsequently developed clinical features of ALS
Aggarwal et al., 2002 (20)	19 presymptomatic *SOD1* 12 symptomatic sporadic 34 non carrier family members 23 healthy controls	Neurological exam, MRC	MUNE	-in 2 of 19 mutation carriers, there was a sudden reduction in MUNE several months before the onset of weakness
Aggarwal et al., 2001 (21)	18 presymptomatic *SOD1* 12 symptomatic sporadic 34 non carrier family members 23 healthy controls	N/a	MUNE	-no detectable difference in the number of motor units

Biofluid studies of asymptomatic mutation carriers

In the era of 'omics' (proteomics, lipidomics, metabolomics etc.) biofluid markers are also increasingly evaluated in asymptomatic mutation carriers including neurofilament light (NfL) (57-59) or (NEFL) (60), neurofilament heavy (pNfH) (58, 59, 61) or NEFH (60), poly(GP) proteins (62, 63), chitotriosidase-1 (CHIT1) (60, 61, 64), chitinase 3-like protein 1 (CHI3L1) (60, 61), chitinase 3-like protein 2 (CHI3L2) (61), C-reactive protein (CRP) (61), mitochondrial DNA (mtDNA) (65), ubiquitin carboxyl-terminal hydrolase 1 (UCHL1) (60, 64), microtubule-associated protein 2 (MAP2) (60), macrophage-capping protein (CAPG) (60), glycoprotein non-metastatic B (GPNMB) (60), histone cluster 1, H4 (HIST1H4A) (60), histone cluster 1, H2b (HIST1H2B) (60), neurofilament medium (NEFM) (60, 64), neuronal pentraxin receptor (NPTXR) (64) . Some studies focused on protein profiles in a single biofluid either in the CSF (60, 61, 63, 64) or serum (65), while others 22valuated both CSF and serum (57-59, 62). The most commonly used methods to quantify the concentration of these markers are enzyme-linked immunosorbent assays (ELISA) (58, 59, 61), electrochemiluminescence immunoassay (ECLIA) (57, 59), mass spectroscopy (60, 64), meso scale discovery-based immunoassay (62) and poly-GP immunoassay (63). Some longitudinal studies, followed asymptomatic mutation carriers for over 3 years (57, 58), and in some studies controls were also assessed longitudinally (57, 58). Most biofluid studies investigated asymptomatic *SOD1* (57-60, 65) and *C9orf72* (57-65) cohorts, but some included *TARDBP* (59, 60) or *FUS* (59) mutation carriers. The biggest biofluid study included 84 subjects, including 52 *SOD1* and 27 *C9orf72* hexanucleotide carriers among other mutation carriers (57). All identified studies also concurrently assessed a symptomatic

cohort of either ALS (57-64), ALS-FTD(62) or FTD (63) patients. Some studies included a PLS cohort (61, 62), as well as disease controls such as Alzheimer's disease (62, 63), Lewy body dementia (62), Parkinson's disease (63), or Kennedy's disease (61). Mean age of asymptomatic mutation carriers ranged from 39.7 (61) to 48.3 (59) years. Some biofluid studies screened for the presence of UMN and LMN signs (59). In symptomatic patients, ALSFRS-r was invariably recorded, and some studies also reported UMN (58, 61), ECAS (58, 61) or FTD-CDR scores (63). Presymptomatic neurofilament studies are inconsistent; many did not detect elevated levels (59-61). Altered protein profiles were identified by some studies (62-64), especially in the years preceding phenoconversion (57, 58).**Table 3**

Table 3*: A selection of presymptomatic biofluid studies*

Authors	Proteins investigated	Study participants	Clinical tests	Methods	Findings in presymptomatic subjects
Barshcke et al., 2020 (64)	2095 proteins identified, eight candidates validated- UCHL1, NPTXR, etc	**Discovery**- 11 presymptomatic *C9orf72* **MRM validation**- 28 presymptomatic *C9orf72* **SIMOA validation**- 13 presymptomatic *C9orf72* 27 controls- either healthy controls/non carrier family members	ALSFRS-R, FTLD-CDR	iTRAQ, mass spectroscopy-Multiple reaction monitoring (MRM)	-decreased neuronal pentraxin receptor (NPTXR) levels in *C9orf72*-FTD versus carriers
Oeckl et al., 2020 (60)	UCHL1, MAP2, CAPG, GPNMB, HIST1H4A, HIST1H2B, NEFL, NEFH, NEFM, CHIT1, CHI3L1	**Discovery**: 8 presymptomatic *C9orf72* 5 presymptomatic *SOD1* 1 presymptomatic *TARDBP* 26 symptomatic carriers/sporadic 16 non carrier family members **Validation** 85 symptomatic carriers/sporadic 32 healthy controls	ALSFRS-R	iTRAQ, mass spectroscopy-MRM	-No significant alteration observed in asymptomatic mutation carriers
Benatar et al., 2019 (58)	neurofilament heavy (pNfH), neurofilament light (NfL)	25 presymptomatic *C9orf72* 49 presymptomatic *SOD1* 5 other presymptomatic gene carriers 36 symptomatic carriers/sporadic 34 non carrier family members	ALSFRS-R, UMN burden score, ECAS	ELISA	-Serum and CSF pNfH increase prior to phenoconversion -changes observed 6-12 months in *SOD1*, 2 years in *C9orf72*, and 3.5 years in *FUS* prior to disease onset
Thompson et al., 2019 (61)	CHIT1, CHI3L1, CHI3L2, pNFH, CRP	5 Asymptomatic *C9orf72* 92 symptomatic sporadic 12 ALS-mimics 25 healthy controls	ALSFRS-R, UMN burden score, ECAS	ELISA	-Chitinase levels were similar in asymptomatic mutation carriers and healthy controls
Benatar et al., 2018 (57)	neurofilament light (NfL)	52 presymptomatic *SOD1* 27 presymptomatic *C9orf72* 5 other presymptomatic 34 non carrier family members	ALSFRS-R	ECLIA	-among phenoconverters, NfL levels were raised ~12 months preceding the emergence of the earliest clinical symptoms
Stoccoro et al., 2018 (65)	mtDNA	N/A	N/A	N/A	-significant decrease in D-loop methylation levels
Gendron et al., 2017 (62)	poly(GP) proteins	27 presymptomatic *C9orf72* 107 symptomatic *C9orf72* carriers 48 gene-negative healthy controls 57 gene-negative ALS patients	ALSFRS-R	Meso Scale Discovery-based immunoassay	-Poly(GP) proteins detected in CSF and in peripheral blood mononuclear cells

Lehmer et al., 2017 (63)	poly(GP) proteins	10 presymptomatic *C9orf72* 49 symptomatic carriers/sporadic 20 healthy controls 8 non carrier family members 38 disease controls	Neuropsychological testing, ALSFRS-R, FTLD-CDR	poly-GP immunoassay	-Significant poly-GP levels detectable similar to symptomatic carriers
Weydt et al., 2016 (59)	neurofilament heavy (pNfH), neurofilament light (NfL)	7 presymptomatic *C9orf72* 3 presymptomatic *SOD1* 1 presymptomatic *TARDBP* 1 presymptomatic *FUS* 64 symptomatic carriers 19 non carrier family members	Neurological exam- UMN and LMN signs, ALSFRS-R	ELISA, ECLIA	-NF-L and pNF-H are normal before symptom onset

Lessons from other neurodegenerative conditions

Despite the clinical differences, frontotemporal dementia studies offer ample learning opportunities for ALS study designs. In addition *C9orf72*, other FTD-associated mutations have been extensively investigated, including *GRN* (66-78), *MAPT*(69, 79-82) and CHMP2B (83-85) carriers. Mutation carriers were more commonly compared to gene-negative first-degree relatives (66, 69, 70, 72-74, 82-85), but also to healthy controls (67, 68, 71, 75, 80, 81) or both (76, 78). The average age of presymptomatic cohorts in FTD ranges from 31 (82) to 56 (85) years. Many of the reviewed studies also investigated a symptomatic cohort, but a few only focussed on their presymptomatic cohort (68-70, 78, 81, 83-85). Similarly to ALS, no studies included 'disease controls'. Neuropsychological data was more commonly included than in ALS studies, including screening tests such as the CDR (66, 73-75), MOCA (66) and MMSE (67, 68, 72, 76, 81), behavioural tools such as the FBI (72) and FAB (72), neuropsychiatric instruments such as the NPI (72, 76) or BDI (81), as well as executive (67-69, 76, 81), language (67, 68, 81), visuospatial (67, 76) and memory tests (67, 76, 81, 82). While a minority of studies investigated a single imaging parameter (66, 74, 83), most studies presented structural data as well as diffusion (68, 69, 78, 80), functional (67, 69, 71, 73, 75, 76) or PET data (70, 72, 79, 85). Most of the longitudinal studies were two time-point studies (66, 68, 70, 81, 83-85), but one multi-timepoint study followed patients over 11 years (82). Robust multi-centre initiatives such as Longitudinal Evaluation of Familial Frontotemporal Dementia Subjects (LEFFTDS) (66, 82) and The Genetic Frontotemporal dementia Initiative (GENFI) have been particularly successful at gathering large datasets. One of the most widely studied neurodegenerative condition in its

presymptomatic phase is Huntington's disease which has been extensively evaluated by structural (86-92), diffusion (89, 93) and functional (91, 94) MRI studies. These studies tend to be much larger than ALS studies and often include data from hundreds of participants (86, 88). Multi-centre initiatives such as PREDICT-HD (86, 88), IMAGE-HD (87, 92) and TRACK-On HD (89, 91) have facilitated these robust collaborative studies. In presymptomatic Alzheimer's studies, APP (95-99), PSEN1 (95-101), PSEN2 (95-99) and APOE4 (95, 98, 99, 102-104) mutation carriers were investigated with some studies including over 300 participants (96, 97). In presymptomatic Parkinson's disease, LRRK2 (105-112), parkin (108, 112-114), PINK1 (112), ATP13A2 (112) and SNCA (115) mutation carriers were evaluated. These studies are relatively smaller than those conducted in HD and AD, but can include as much as 130 participants (112).

Discussion

Irrespective of their methodology and genetic focus, the majority of existing presymptomatic ALS studies have confirmed considerable biological changes before symptom manifestation. They are also consistent in identifying changes in brain regions which are characteristically affected in symptomatic mutation carriers. The demographic analysis of existing *C9orf72* studies highlights that mutation carriers in their 30s already exhibit considerable structural degeneration, decades before typical symptom manifestation (7, 8). The considerable pathological changes detected in young mutation carriers raises questions about neurodevelopmental factors (6), but this could only be appraised if mutation carriers in their teens and twenties were also included subject to appropriate approvals and genetic counselling. Existing studies

suggest a relatively divergent imaging signature in asymptomatic *C9orf72* and *SOD1* carriers, but in the absence of well-powered studies including large cohorts of both mutations, these genotype-specific traits are not firmly established. Nonetheless, the presymptomatic signature of *C9orf72* seems to be associated with more widespread frontotemporal and subcortical grey matter degeneration than those observed in association with SOD1 (7, 26). While the available studies are conceptually important, stereotypical shortcomings can be readily identified. The sample size of asymptomatic mutation carriers in ALS imaging studies range from 2-83, which coupled with the considerable variation in the age of participants, prevents making conclusive observations regarding presymptomatic biology. The sample size limitations of presymptomatic ALS studies are particularly striking in contrast to the available AD and HD literature. The systematic review of the literature also highlights that in contrast to presymptomatic AD and HD studies, the majority of presymptomatic studies in ALS are single-centre, or national studies. Several ALS studies have included both *SOD1* and *C9orf72* carriers in a single presymptomatic group to demonstrate structural changes before symptom manifestation. However, with the emergence of ASO therapies, it seems paramount to describe genotype-specific changes in a specific presymptomatic mutation cohort rather than characterising admixed cohorts. The importance of defining genetically homogenous groups cannot be underestimated, as carriers of specific mutation may exhibit different rate of progression and anatomical involvement. The strategy to ascertain presymptomatic changes also varies considerably in ALS studies; some research groups contrast their presymptomatic cohort to healthy controls alone, others to symptomatic patients, and others to gene-negative family members. Another common problem is the selection of symptomatic

patients. Including a symptomatic patient cohort in presymptomatic studies is particularly useful if they carry the same mutation as the presymptomatic cohort, but the inclusion of a mixed gene-positive and gene-negative sporadic patients, or symptomatic patients without genetic profiling hinders data interpretability. If the symptomatic cohort carries the same mutation, their "affected" brain regions can be specifically evaluated in the presymptomatic group in targeted region-of-interest analyses. Another potential shortcoming of existing studies is the lack of disease-controls which makes it difficult to appraise how specific the findings are to ALS or to a given genotype. For example, corpus callosum degeneration is regarded as pathognomonic of ALS by the ALS research community, despite being observed in a range of other conditions such as HSP to AD. Similarly, increased neurofilament levels were observed in a number of presymptomatic ALS studies, but they are also raised in many other neurological conditions. If no disease-controls are included, the specificity of a biomarker to ALS is impossible to assess and its ability to distinguish between neurodegenerative processes remain questionable. For example if a proposed biomarker such as CSF neurofilaments, corticospinal tract FA or a TMS parameter is similarly affected in ALS, PLS and CBD, it won't distinguish between these conditions rendering their diagnostic value relatively limited. In real life clinical scenarios the question is seldom whether a patient is healthy or not, the question is typically whether the constellation of symptoms presage ALS or PLS or CBD, as these conditions carry distinctly different prognoses. Not only existing studies don't include disease controls, they don't include other motor neuron disease phenotypes either. This seems like a missed opportunity. The inclusion of relatively pure UMN and LMN phenotypes, such as adult SMA or PLS may help to gauge the sensitivity of a proposed marker to

the UMN versus LMN system. Another contentious aspect of existing studies is the generalisation of observations from small presymptomatic *C9orf72* and *SOD1* cohorts as representative of presymptomatic ALS as a whole. Depending on the population, the vast majority of ALS patients test negative for ALS-associated mutations and are seemingly sporadic. Accordingly, the presymptomatic phase of sporadic patients remains a conundrum and may differ in anatomical involvement and chronological dynamics from the traits observed in *C9orf72* or *SOD1*. This also applies to PLS, which is not closely linked to single mutations and very little is known about cerebral and spinal disease burden prior to symptom onset. PLS exhibits overlapping albeit UMN predominant clinical and radiological characteristics with ALS (116), and in the absence of specific mutations to carry out presymptomatic studies, research groups attempted to characterise 'early' symptomatic cohorts before fulfilling diagnostic criteria (117, 118). These therefore cannot be regarded as presymptomatic studies, rather pre-diagnosis studies of suspected cohorts. The lessons of these studies can be integrated in future ALS studies, namely that gene negative 'suspected ALS' patients should also be included in imaging and biomarker studies in an attempt to characterise early pathology in sporadic cohorts. Additionally, presymptomatic gene-positive cohorts should be followed beyond symptom manifestation and at least until they fulfil current diagnostic criteria for ALS. Characterising disease burden by quantitative imaging, electrophysiology and wet biomarker protocols at the time of fulfilling diagnostic criteria, may help to highlight the limitations of existing diagnostic criteria. The refinement of diagnostic criteria may enable an earlier diagnosis in suspected patients and in turn earlier inclusion in clinical trials. One aspiration would be the introduction of 'radiologically-supported ALS' based on objective radiological variables. Another

important question is the optimal timing ASO therapy. Once brain and cord pathology is detected and electrophysiology changes ascertained in mutation carriers there may be an argument to introduce therapy early before widespread irreversible changes ensue. Existing presymptomatic studies also raise important question re: motor reserve. The observation that both electrophysiology and MRI detects considerable pyramidal tract, motor cortex and spinal cord degeneration long before projected symptom manifestation suggest a degree of network resilience or redundancy. A simplistic interpretation may be that compensatory processes and redundant networks offset degenerative changes until a critical threshold is reached.

While cross-sectional studies have provided pioneering insights, they provide limited information on progressive changes as they average radiological signatures across different age groups. With few exceptions (7), existing presymptomatic studies in ALS rely on convenience samples of asymptomatic mutation carriers with considerable dispersion in their demographic profile. For the meaningful analysis of early alterations, demographically homogenous samples would be desirable. Longitudinal studies have the potential to provide a nuanced picture of progressive changes; map anatomical propagation patterns, progressive functional alterations and evolving CSF/serum signatures overtime. However these studies should also ideally recruit demographically homogenous cohorts. The limitations of two–timepoint longitudinal designs are also clear, as these don't permit the modelling of non-linear changes and the assessment of ceiling- and flooring-effects (119). The lessons of large AD and HD studies also apply here, namely that large multi-timepoint designs are necessary to

characterise progressive structural degeneration in ALS. A limitation of existing longitudinal presymptomatic studies in ALS is that mutation carriers are seldom followed until phenoconversion or beyond. The availability of radiological, electrophysiology or wet biomarker panel in mutation carriers before and after symptom manifestation would also permit the evaluation of prognostic indicators. There are two practical deliverables which were not addressed by existing studies, both of which seem relevant for individualised patient care and future pharmacological trials. One of them is the estimation of projected age of symptom onset based on disease burden in the presymptomatic phase. This would be possible if mutation carriers would be meticulously followed until symptom manifestation. The other practical aspect of presymptomatic studies pertains to *C9orf72* from a phenotype point-of-view; namely can patterns of cerebral or spinal cord involvement be used to predict if an individual GGGGCC repeat expansion carrier is more likely to develop FTD or ALS (ALS-FTD). These observations highlight another shortcoming of existing presymptomatic studies in ALS; with very few exceptions (8, 10) nearly all presymptomatic radiology studies are brain studies. Spinal cord involvement is a key aspect of ALS, which encompasses anterior horn (LMN) and descending pyramidal tract (UMN) degeneration and is now readily detected by novel imaging applications (120, 121). Given the availability of robust quantitative spinal protocols, these should be carefully integrated into future presymptomatic studies to assess if they detect changes earlier than brain protocols and if they can presage age of onset, site of onset, or UMN/LMN predominance. It is conceivable that a hexanucleotide carrier with ample extra-motor cerebral involvement with no spinal cord abnormalities is more likely to develop FTD, than ALS, but unless such studies are conducted and patients followed

until disease manifestations the predictive value of presymptomatic imaging is difficult to gauge. The practical deliverables of robust presymptomatic studies therefore include phenotypic prediction, age of onset estimation and optimising the timing of pharmacological interventions. **Table 4**. Very few presymptomatic studies report negative or unexpected findings (31, 54). The candid reporting of negative results is hugely important as they either reveal genotype-specific traits or reflect on the detection sensitivity of the methods implemented. Similarly, the comparative evaluation of several imaging metrics in the same cohort is helpful to appraise the detection sensitivity of specific methods. Some pioneering spectroscopy studies for example did not perform accompanying structural assessments and vice versa (10). With the current imaging technology at our disposal the detection of white and grey matter alterations in symptomatic ALS cohorts is no longer challenging (122, 123), but the concomitant implementation of several imaging modalities in the presymptomatic phase enables the critical comparison of various techniques. For example NODDI is thought to be superior to characterise white matter degeneration in presymptomatic cohorts than standard DTI (26). Multimodal longitudinal imaging in presymptomatic cohorts may additionally help to establish if certain imaging indices exhibit early ceiling effect (119) which would limit its utility to track the post-symptomatic changes in clinical trials (124). Robust presymptomatic studies can also deliver on important academic objectives. A myriad of environmental factors have been proposed in ALS which could be objectively evaluated in vivo if mutation carriers were tracked from a young age over multiple timepoints and environmental factors would carefully recorded.

Table 4*: Lessons of existing presymptomatic studies in ALS, learning points for future study designs*

Common shortcomings of existing studies	Desirable design features for future studies	Potential deliverables
• Significant cohort size limitations • Predominantly single-centre studies especially in relation to *SOD1* • Mixed presymptomatic cohorts of several mutations e.g. mixed *SOD1*/*C9orf72* • Admixed symptomatic cohorts (sporadic patients and mutation carriers) • Symptomatic cohorts without genetic testing • Scarcity of projects on mutations other than *SOD1*/*C9orf72* • Lack of 'disease controls' in the symptomatic group • Single modality studies (either imaging or wet biomarkers) • Scarcity of spinal MRI studies • Electrophysiology studies dominated by TMS studies, paucity of presymptomatic MUNE/MUNIX studies • Limited clinical assessment • Neuropsychological testing is often more detailed or better documented than neurological testing • Cross-sectional or two-timepoint study designs • Subjects not followed until symptom manifestation • Subjects not followed until fulfilling diagnostic criteria • Study entry in the mid-thirties or forties • ALS-associated presymptomatic changes inferred from specific genotypes overlooking the fact the majority of ALS patients are sporadic	• Several genotypes contrasted • Large samples, multicentre initiatives with standardised assessments, biomarkers SOPS, inter-rater reliability testing, harmonised pulse-sequences for imaging • Multi-timepoint longitudinal study designs • Relatively uniform age at study entry • Inclusion of mutation carriers in their late teens early twenties to assess for developmental factors • Follow-up beyond symptom manifestation • Evaluation of disease burden at the time of fulfilling diagnostic criteria • Combined wet biomarker imaging protocols • Inclusion of spinal imaging protocols • Combined LMN-UMN electrophysiology protocols • Study of gene-negative suspected ALS patients to characterise early changes in sporadic patients	• Phenotypic indicators • Disease onset estimation • Informing timing of ASO therapy • Evaluation of motor reserve • Evaluation of cognitive reserve • Evaluation of adaptive mechanisms • Biomarker supported assessment of environmental factors in presymptomatic mutation carriers • Exploration of epigenetic factors • Refinement of current diagnostic criteria to integrate emerging biomarkers e.g. "Radiologically supported ALS" • Integration of emerging biomarkers into pharmacological trials • Development of a framework for presymptomatic clinical trials before widespread degenerative changes ensue

Conclusions

From an academic perspective, presymptomatic studies offer invaluable learning opportunities to study propagation patterns, characterise early genotype-associated signatures, assess functional resilience, explore concepts like motor reserve or cognitive reserve, and evaluate neurodevelopmental or environmental factors. However, with the advent of ASO therapies, the meticulous study of presymptomatic cohorts in ALS gained practical relevance and unprecedented urgency. Future studies have to be designed to address specific clinical objectives such as informing the timing of pharmacological interventions, monitoring response to therapy, validating phenotypic indicators, and develop novel, biomarker-supported diagnostic criteria to facilitate earlier entry in clinical trials.

Corpus Callosum degeneration in ALS

Corpus callosum degeneration is a recognised feature of amyotrophic lateral sclerosis; it has been consistently highlighted by post mortem studies and repeatedly demonstrated in vivo by computational neuroimaging (125-128). While corpus callosum pathology is widely regarded as pathognomonic of ALS, its clinical correlates, contribution to disease propagation and specificity to ALS are relatively poorly characterised. Tu et al. explore corpus callosum degeneration from a clinical perspective, comparing its integrity in patients with unilateral and bilateral motor disability. They identify more widespread white matter alterations in patients with unilateral limb weakness. The novelty of their study stems from the stratification of

patients based on their disability profile. The majority of imaging studies contrast spinal and bulbar onset patients, and the imaging correlates of unilateral versus bilateral involvement are seldom evaluated (129). Tu et al. evaluate four diffusivity metrics and parcellate the corpus callosum into the rostrum, genu, rostral body, anterior midbody, posterior midbody, isthmus, and splenium providing a painstaking analysis of regional corpus callosum involvement. They identify the preferential vulnerability of the rostral body, posterior mid-body and isthmus. Consistent with the considerable anterior-posterior extension of the corpus callosum and its functionally distinct sub-regions, several previous studies have examined its segmental diffusivity profile in ALS (130-135). Sporadic cases without cognitive impairment typically exhibit pathology in the body of the corpus callosum (136), but significant anterior disease burden has been detected in ALS-FTD (137) and in association with GGGGCC hexanucleotide repeat expansions in *C9orf72* (138). The majority of corpus callosum studies in ALS rely on diffusivity measures, but morphometric changes (139), density alterations (140), cross-sectional area reductions (130), functional connectivity impairment (141), transcranial magnetic stimulation abnormalities (142), and delayed beta rebound on MEG (53) have also been linked to corpus callosum degeneration. There is a scarcity of histopathologically validated imaging studies in ALS (143), but a recent 7 Tesla, ex-vivo study has successfully mapped FA reductions to focal myelin pallor and increased CD68 immunostaining indicative of microglial inflammation (133). Similarly to the presymptomatic corticospinal tract changes observed in asymptomatic mutation carriers (8, 32), presymptomatic corpus callosum degeneration has also been detected in *C9orf72* hexanucleotide repeat expansion carriers (24). Novel white matter techniques such as neurite orientation dispersion and density imaging (NODDI), have

captured both presymptomatic (26) and post-diagnosis (144) corpus callosum alterations and are thought to be more sensitive to pathological change than conventional diffusion tensor metrics. (145, 146) From a practical point of view, the evaluation of white matter regions which exhibit presymptomatic changes may be useful for diagnostic purposes (122, 123, 147), but if they exhibit a ceiling effect early in the course of the disease, they may be ill-suited to track longitudinal changes (124) or utilised in prognostic models (148, 149). Longitudinal studies have been somewhat inconsistent in relation to progressive corpus callosum changes in ALS. While some studies captured progressive white matter degeneration (150), others detected relatively limited progression over time (151). Multimodal imaging studies have the advantage of relying on complementary techniques which compensate for the limitations of single methods and aid the integrative interpretation of seemingly contradictory findings. With the myriad of novel connectivity measures at our disposal, the concomitant analysis of commissural diffusivity patterns seems indispensable. (152-154) In ALS, corpus callosum degeneration has been linked to increased connectivity on EEG (155), altered post-movement beta rebound on MEG (53), and functional connectivity changes on resting-state fMRI (156). From a clinical viewpoint, corpus callosum degeneration has been associated with clinical staging (132), executive dysfunction (134), mirror movements (157), and motor disability (135). One of the common limitations of imaging studies in ALS is the lack of disease controls which would permit the appraisal of the specificity of radiological findings to ALS. In the ALS research community, corpus callosum degeneration is widely regarded as a disease-defining feature of the condition (15). However, it may be far from unique to ALS as it has been consistently demonstrated in other neurodegenerative conditions

such as MCI (158), AD (159), PD (160), and FTD (161). Furthermore, corpus callosum degeneration can be readily detected in other motor neuron diseases, such as PLS (116) and HSP (162) underscoring the notion that corpus callosum pathology is not specific to ALS. Another important aspect of characterising corpus callosum changes in ALS is its considerable sexual dimorphism. Physiological gender differences in corpus callosum morphology are well established in healthy populations (163), but not always accounted for in ALS studies (164). The paper of Tu et al. illustrates that despite the wealth of existing corpus callosum studies in ALS, innovative patient stratification, meticulous anatomical segmentation, and the multiparametric characterisation of commissural white matter tracts add novel insights to an established facet of ALS pathology.

CHAPTER 2: Review of sensory findings in ALS

Introduction

Amyotrophic lateral sclerosis (ALS) is a neurodegenerative disease characterized by the degeneration of upper and lower motor neurons (165, 166). The core neuroimaging signature of ALS includes motor cortex, brainstem, corticospinal tract, and spinal cord degeneration, with subcortical grey matter degeneration also being observed (154). It is increasingly recognised as a multi-system disorder, with extra-motor involvement being observed to be part of the disease process (166, 167). Pathology of sensory neurons in the dorsal root ganglia and sensory neuropathy is not widely acknowledged as part of the ALS syndrome (168), and there is a prevailing notion that ALS spares sensory networks (15), despite evidence of sensory disturbance that has been observed in ALS patients clinically (169-172), in electrophysiology (169, 173-176), neuroimaging (174, 177, 178) and neuropathology (169, 179-182) for several decades (166). Numbness (166), pain (183) and paraesthesia (170, 184-186) are among some the sensory changes described by patients. While frank visual and auditory deficits are rarely observed, changes in smell (187-189) and taste (190, 191) are more frequently reported. Proprioceptive deficits are also observed (192) and may have implications with regards to gait and dexterity. Additionally, sensory dysfunction may contribute to impaired cough (193) and swallow (194, 195). However, the findings of sensory pathology in ALS are conflicting with negative findings being reported in several studies (196-202). Of note, sensory disturbance is also observed in other motor neuron

disease phenotypes such as primary lateral sclerosis (PLS) (203-205). The comprehensive characterisation of sensory pathology in ALS is crucial for our understanding of disease heterogeneity, and findings of sensory pathology may have implications with regards to the debate of corticofugal versus corticopetal spread. In addition to this, sensory dysfunction may have significant impact on patient quality of life. The objective of this review is to investigate findings of sensory pathology in ALS and other motor neuron disease phenotypes.

Methods

A formal literature search was performed on PubMed using the core search terms "amyotrophic lateral sclerosis", "motor neuron disease" combined with each of the following keywords: "electrophysiology", "magnetic resonance imaging", "spinal imaging", "biopsy" and "sensory", "sensory cortex", "postcentral gyrus", "dorsal column", "clinical", "proprioception", "thermoception", "nociception", "bulbar sensation", "taste", "enjoyment of food", "facial sensation", "tingling" and "paraesthesia". We also performed an additional search of sensory alterations in "primary lateral sclerosis", "progressive muscular atrophy", "spinal and bulbar muscular atrophy", "Kennedy's disease", and "post-polio syndrome". Only original research papers were systematically reviewed. Review papers, conference abstracts, opinion pieces and editorials were excluded. No exclusion criteria were set based on year of publication. Based on the above criteria a total of 211 original research papers

were selected and reviewed in accordance with the Preferred Reporting Items for Systematic Reviews and Meta-Analyses (PRISMA) recommendations.

Results

Clinical

Sensory symptoms and signs are reported in ALS. According to one study, the most common symptom reported was numbness, followed by neuropathic pain, tingling and reduced temperature sensation (166). Sensory disturbance is more common in familial ALS than in sporadic ALS (165, 206). One study showed 20% of familial ALS (fALS) cases manifest atypical features such as pain, paraesthesia or urgency micturition (184). Pain is commonly reported in patients with ALS, with a study reporting a prevalence of 66% (183). Pain was most commonly located in the neck and shoulders (183). Neuropathic pain was reported in 9% of patients (183). Pain was not correlated with measures of disease duration or severity (183). Paraesthesia is observed in patients (170, 185, 186), but it is a common adverse event of riluzole treatment (207-209). A small proportion of patients were found to have changes on the quantitative sensory testing (QST) battery (180). There are conflicting reports on the impairments of thermal sensory pathways. One study reports thermal threshold abnormalities (210), while another which investigated contact heat-evoked potentials (CHEPs) in ALS patients proposed that the nociceptive pathway is not affected, suggesting small fibres are spared in ALS (198).

High correlations are shown between abnormal postural reactions and motor and balance deficits, and it is suggested that abnormal axial control leads to postural abnormalities (211) and impaired gait (212, 213). Extrapyramidal involvement is also suspected to contribute to stiffness and balance impairment in ALS (214, 215). Vestibular deficits have also been observed (216). 25% of patients assessed in one study had proprioceptive impairments (192).

Patients complain of other sensory abnormalities such as perceived reduction in taste (191, 217), which can have a negative impact on quality of life. Impaired taste, smell and swallow are observed in motor neuron disease (MND) (190) according to some studies, while other studies find no changes in olfaction and gustation (218). One study reports 35% of patients were anorexic, 43.8% reported taste disorders, and 70% had dysphagia, which was significantly associated with salivary stasis (219). Changes in taste perception may have profound negative consequences on quality of life (191). Sensory changes in the larynx are also observed on fiber-optic endoscopic evaluation of swallowing with sensory testing (FEEST) (194, 195). 33% of ALS patients had sensory deficit of the larynx in one study (194) while another shows deficits in as many as 54.5% of patients (195). Sensory deficits are more commonly observed in bulbar-onset ALS patients (194). Olfactory impairment has also been observed (187-189). One study showed changes in respiratory function correlate with deficits in olfaction (189).

Autonomic dysfunction is observed in ALS patients at various disease stages in sporadic and familial ALS (220-227). One study showed impaired cardiac autonomic

control and parasympathetic dysfunction in ALS patients (221). Cutaneous sensory and autonomic denervation in ALS and primary lateral sclerosis (PLS) is reported, but the pathophysiological mechanisms behind these changes are still unknown (181). Understanding the pathophysiology behind the various autonomic symptoms observed in ALS could facilitate improvements in the quality of life of patients with ALS (228). Normal findings in the sensory system are also observed (197, 218, 229). **Table 5**

Table 5: *A selection of clinical studies ALS*

Author and year of publication	Study participants	Method of assessment	Significant findings
Tabor-Gray et al., 2021 (193)	32 ALS, 34 healthy controls	sensory patients-rated urge to cough (UtC), cough spirometry metrics	-ALS show increased sensitivity to an upper airway irritant -ALS have slower and weaker expiratory cough motor output
Krieg et al., 2019 (211)	12 ALS, 12 healthy controls	spontaneous sway measures, measures of postural reactions	-spontaneous sway amplitudes and velocities significantly larger in patients -sway frequencies higher in patients -high correlations between abnormal postural reactions and motor or balance deficits
Simmatis et al., 2019 (192)	17 ALS	robot based sensorimotor, cognitive and proprioceptive performance	-20-69% displayed sensorimotor impairments -25% have proprioceptive impairments
Tarlarini et al., 2019 (191)	32 ALS	taste observations	-perceived reduction in taste in ALS -loss of taste negatively related to QoL
Gunther et al., 2018 (189)	94 ALS, 81 healthy controls	olfactory performance- Sniffin Sticks	-impairment of olfaction detected in patients
Lopes et al., 2018 (230)	80 MND, 32 healthy controls	QST, CPM, clinical	-pain frequently reported
Isak et al., 2017 (180)	32 ALS, 32 healthy controls	QST and IENFD skin biopsy	-mean values of QST and IENFD in normal range
Marjanovic et al., 2017 (225)	241 ALS	clinical	-sensory and sphincter disturbances dominant in patients with *SOD1 L114F* -significant sensory involvement in *SOD1 D90A*
Gunther et al., 2016 (190)	90 MND, 96 healthy controls	NMS questionnaire	-impaired taste and smell observed in MND
Moisset et al., 2016 (183)	96 ALS	pain assessment	-66% of patients report pain, 9% of patients report neuropathic pain
Ruoppolo et al., 2016 (194)	114 ALS	evaluation of swallowing, including a fiber-optic endoscopic evaluation of swallowing with sensory testing and biopsy	-38 patients (33%) had sensory deficit of the larynx -sensory deficit of larynx was more common in bulbar-onset ALS
Truini et al., 2015 (231)	24 ALS	SNAP, NCV, QST	-normal thermal-pain perceptive thresholds
Ferrari et al., 2014 (232)	8 ALS, 7 healthy controls	corneal confocal microscopy	-reduced corneal small fibre sensory nerve number and branching in patients
Radovanovic et al., 2014 (212)	27 ALS, 29 healthy controls	simple walking test, dual-motor task, dual-mental task, combined motor and mental tasks	-impaired gait in dual tasks in spinal and bulbar onset ALS
Sanjak et al., 2014 (215)	19 ALS, 15 healthy controls	clinical	-nearly 37% of ambulatory ALS with normal clinical balance testing have reduced ability to use vestibular input

Hineno et al., 2012 (224)	24 ALS	clinical, neurophysiology, neuropathology	-half of patients had neurogenic bladder and sensory impairment
Jesus et al., 2012 (219)	40 ALS	clinical	-43.8% of patients report taste disorders
Lang et al., 2011 (218)	26 ALS, 26 healthy controls	olfactory performance- Sniffin Sticks	-no difference in ability
Pradat et al., 2009 (214)	39 ALS	clinical	-extrapyramidal involvement plays role in stiffness and balance impairment in some ALS patients
Liao et al., 2008 (213)	13 ALS, 51 healthy controls	gait assymetry	-gait symmetry significantly disturbed
Hammad et al., 2007 (169)	103 ALS	SNAP, biopsy	-sensory symptoms/signs seen in 32% of patients
Amin et al., 2006 (195)	22 ALS	laryngeal sensation	-abnormal sensation in 54.5% of patients -sensory deficits in the larynx present in ALS
Deepika et al., 2006 (197)	20 ALS, 20 healthy controls	QST	-normal thermal thresholds on QST
Khoris et al., 2000 (186)	NA	genetics	-parestesia commonly reported
Camu et al., 1999 (184)	109 ALS	clinical observations	-pain, paresthesia and urgency micturition experienced
Hawkes et al., 1998 (188)	58 MND, 135 healthy controls	UPSIT, OEP	-smell identification slightly worse overall in MND -bulbar patients scored significantly less on UPSIT
Mogyoros et al., 1998 (229)	21 ALS, 14 healthy controls	parasthesia due to ischemic compression	-patients experience less or no paresthesias during and after release of ischemic compression
Rothstein et al., 1992 (233)	13 ALS, 15 Alzheimer's disease, 12 Huntington's, 17 healthy controls	glutamate transport	-reduced maximum velocity of transport of high-affinity glutamate uptake in synaptosomes from somatosensory cortex
Wirguin et al., 1992 (234)	31 ALS	clinical	-normal sensory conduction
Elian et al, 1991 (187)	15 MND, 10 healthy controls	UPSIT	-significant olfactory impairment in MND
Li et al., 1988 (206)	NA	Clinical	-more frequent occurrence of sensory symptoms at presentation in familial cases (15%) than sporadic cases (5%)
Gubbay et al., 1985 (170)	318 ALS	clinical observations	-sphincter disturbance and deep sensation loss observed
Jamal et al., 1985	40 MND, 40 healthy	heat threshold and cold threshold	-abnormal thermal thresholds in 80% of MND patients

(210)	controls		
Hamida et al., 1984 (235)	102 ALS	clinical	-juvenile form associated with sensory symptoms
Jokelainen et al., 1977 (236)	255 ALS	Clinical	-sensory disturbances absent, sphincter abnormalities reported in 3 patients
Alter et al., 1976 (237)	14 ALS	Clinical	-peripheral sensory impairment observed in one family

Electrophysiology

While the autonomic and sensory nervous system were previously thought to be spared (238-240) in the disease, they have increasingly been shown to be impaired at various levels (240, 241). The rate of nerve conduction abnormalities varies with one study showing that the sensory system was damaged in 14.7% (242) of patients and others showing they occur more commonly than this (243, 244), with as high as 66.7% (243) of patients being affected. A study showed that 22.7% patients with ALS had sensory abnormalities in at least one nerve (175). However, another study of 154 patients reports that while motor nerve conduction abnormalities are common, abnormal sensory nerve conduction is only found in a minority of ALS patients (245). It has been shown that ALS patients have a slower sensory conduction velocity (246, 247). It is suggested that sensory involvement is more frequent in *C9orf72* positive ALS with electrophysiological sensory neuropathy observed in 38% of *C9orf72* positive ALS patients as opposed to 21% of *C9orf72* negative ALS patients (248). Sensory deficits are commonly seen in *SOD1* patients as well (225), and sensory disturbance is commonly observed in familial ALS patients (224, 235).

A review of results of electrodiagnostic tests performed in ALS revealed the presence of sensory signs and symptoms in 32%, and in 27% of patients and sural SNAPs were abnormal (169). Reduced conduction velocity (176) and abnormal sensory nerve action potentials (SNAP) are observed (176, 245, 249), and one study showed that SNAP amplitude deteriorated with disease progression although it remained within the

normal range (172). SNAP maybe useful as a prognostic indicator, as one study showed that prognosis was better in the group with lower median nerve SNAP amplitude, but only in patients younger than the 25th percentile (57 years) (250). It is suggested that compound muscle action potential (CMAP) and SNAP amplitudes of the median nerve are independent prognostic factors of sporadic ALS (250).

Abnormal somatosensory evoked potentials (SEPs) were previously used to exclude a diagnosis of ALS (251), however, abnormal SEPs are also observed in ALS patients (173, 252-257) and PLS patients (256). It has been reported that nerve conduction studies and SEPs at baseline show abnormal slowing in the peripheral and central sensory pathways (247). Pathology was detected in median nerve SEP, and sensory cortex hyperexcitability was shown to predict shorter survival (253). Another study reports abnormalities in median and tibial nerve SEPs (255). A study assessed sensory nerve function in 19 patients with amyotrophic lateral sclerosis (ALS) using a battery of clinical and neurophysiological tests at baseline and was repeated after 6-18 months (172). While only 2 patients had mild sensory symptoms and none of the patients had sensory signs, abnormal SEPs and SNAPs were observed, showing sensory deficits maybe subclinical (172, 258). A study shows sensory action potential amplitudes (SAPas) were reduced in 22%, affecting the median, ulnar and sural nerve (259).

A-beta or A-delta sensory fibres and in some cases, both, are shown to be impaired (254). One study suggests that distal sensory nerve conduction measures are more

likely to be pathological than conventional sensory measures (243). Another study showed that 60% of patients had abnormal findings on sensory tests, but suggests that the changes are non-progressive (247). In some studies, sensory conduction is normal (199, 202, 260). Normal findings in the sensory system are detected in a handful of studies (261, 262). **Table 6**

Table 6*: A selection of electrophysiology studies in ALS*

Author and year of publication	Study participants	Methodology	Significant findings
Harada et al., 2021 (263)	23 ALS, 14 healthy controls	SEP	-Pain-related SEP amplitudes significantly lower in ALS -no significant differences in pain-related SEP parameters between patients with or without sensory symptoms
Norioka et al., 2021 (264)	145 ALS, 57 healthy controls	SEP	-ALS demonstrated larger N20o-p, N20p-P25p, and early and late HFO amplitudes
Imai et al., 2020 (250)	190 ALS	SNAP	-SNAP identified as a prognostic factor of sporadic ALS
Nardone et al., 2020 (265)	10 ALS, 10 healthy controls	SEP	-large amplitude reduction of post-synaptic HF-SEP burst in patients with disease duration >2yrs
Hoffken et al., 2019 (266)	15 ALS, 15 healthy controls	SEP	-disinhibition of somatosensory cortex
Liu et al., 2019 (242)	150 ALS	EMG	-sensory system damaged in 22 patients on nerve conduction
Pegat et al., 2019 (248)	53 ALS	clinical and electrodiagnostic data	-38% C9+ ALS and 21% C9- ALS have electrophysiological sensory neuropathy
Matamala et al., 2018 (267)	28 ALS, 20 healthy controls	MUNE, SNAP	-normal axonal membrane properties in myelinated sensory axons
Sangari et al., 2018 (252)	21 ALS, 21 healthy controls	SEPs	-late cortical components more depressed than early ones
Shimizu et al., 2018 (253)	145 ALS, 73 healthy controls	SEP (N13, N20, P25)	-larger amplitude of N20p-P25p in the median nerve SEP -sensory cortex hyperexcitability predicts short survival
Kulkantrakorn et al., 2017 (244)	25 ALS, 11 PMA, 1 PLS, 1 Kennedy disease	NCS	-sensory studies abnormal in 16.3%
Dalla Bella et al., 2016 (179)	57 ALS	sural nerve conduction study	-sural nerve conduction study abnormal in 2 patients
Isak et al., 2016 (254)	18 ALS, 31 healthy controls	LEPs, SSEPs	-longer N2 and P2 latencies, smaller N2P2 LEPs; abnormal LEPs in 72.2% of patients -longer latencies for median and tibial SSEPs; abnormal SSEPs in 56.6%
Ren et al., 2016 (245)	154 ALS	SCV, SNAP	-reduced sensory conduction velocity in 1.22%-2.73% -reduced SNAP amplitude in 0-1.82% and sural nerve SNAP absent in 0-1.22% of patients
Iglesias et al., 2015 (174)	21 ALS, 21 healthy controls	SEPs	-altered SEPs correlated with disease duration -spinal imaging and electrophysiology together identify ~85% of patients with subclinical sensory defect
Jin et al., 2014 (268)	97 ALS, 100 Hiriyama disease, 32 cervical spondylotic amyotrophy	SNAP, conduction velocity	-Conduction velocity of sensory nerve and amplitude of SNAP in unaffected limb normal
Hineno et al., 2012 (224)	24 ALS	neurophysiology,	-half the patients have neurogenic bladder and sensory impairment

		clinical	
Simone et al., 2010 (269)	24 ALS, 23 healthy controls	LEPs	-LEP abnormalities present but no correlation with pain intensity or other clinical features
Xu et al., 2009 (198)	60 ALS, 60 healthy controls	CHEPs	-no significant differences in CHEP suggesting nociceptive pathway is intact
Pugdahl et al., 2008 (176)	35 ALS, 35 healthy controls	SNAP	-reduced SNAP amplitude or reduced conduction velocity or both found in 6 ALS patients
Hamada et al., 2007 (270)	26 ALS, 15 healthy controls	SEPs, CMAP	-altered median nerve SEP amplitude associated with motor disturbances -central sensory conduction time and N20 duration prolonged
Hammad et al., 2007 (169)	103 ALS	SNAP, biopsy	-Sural SNAP amplitudes abnormal in 27%, pathologic abnormalities in 91%
Pugdahl et al., 2007 (175)	88 ALS	SCNV, SNAP	-20 patients had sensory NCS abnormalities in at least one nerve -of these, 11 have electrophysiological polyneuropathy
Argyriou et al., 2006 (199)	23 ALS, 23 healthy controls	sensory conduction study	-sensory conduction study normal
Koszewicz et al., 2005 (260)	19 ALS, 20 healthy controls	sensory conduction study	-sensory conduction parameters do not differ significantly between groups
Ogata et al., 2001 (271)	12 ALS	SEP	-abnormal posterior tibial nerve and median nerve SEPs detected in some patients
de Carvalho et al., 2000 (261)	70 ALS, 35 healthy controls	CMAP, CV, sensory potentials	-no conduction block, and sensory potentials were normal
Matsumoto et al., 1999 (272)	14 ALS	SSCV, SSEP	-degree of reduction in SCCVs correlated with degree of reduction in vibration sense and duration of illness
Rabin et al., 1999 (202)	49 ALS	electrodiagnostic	-sensory conduction studies and quantitative sensory testing were normal
Schulte-Mattler et al., 1999 (273)	23 ALS, 23 healthy controls	SNCV, SNAPA	-median sensory NCV abnormally reduced in 3 patients
Theys et al., 1999 (247)	50 ALS, 20 healthy controls	motor and sensory assessment	-NCS and SEP showed abnormal delay in peripheral and central sensory pathways -at least one sensory test abnormal in 60% of patients -significant decrease in amplitude SNAPs of sural nerves over 6 month follow-up
Zakrzewska-Pniewska et al., 1999 (247)	74 MND	SEP, SNCV	-SEPs altered in 39 (53%) patients -median nerve SNCV abnormal in 14 (19%) patients
Emeryk-Szajewska et al.,1998 (274)	94 ALS, 2 PLS, 3 primary bulbar palsy, 6 primary motor spinal atrophy	nerve conduction	-slowing of conduction velocity in 25% of sensory fibres in median nerve, 11% of sural nerve
Mogyoros et al 1998 (275)	23 ALS, 32 healthy controls	CMAP, CSAP	-strength-duration time constant of sensory fibres declines with age, no difference between patients and controls
Georgesco et al., 1997 (276)	24 ALS, 17 healthy controls	SEP	-alterations in SEPs cortical components of all lower limb nerves
Zanette et al., 1996 (277)	29 ALS, 10 PMA	SEP	-SEPs altered in 22 ALS patients, but unaffected in 10 PMA patients
Georgesco et al., 1994	21 ALS, 7 PLS	SEPs	-SEPs abnormal in ALS and PLS

(256)			
Constantinovici et al.,1993 (257)	10 ALS	SEPs	-9 patients with abnormal parietal SEPs to tibial nerve stimulation
Gregory et al., 1993 (172)	19 ALS, 12 healthy controls	SNAP, SNCV	-significant fall in amplitude of SNAPs in medial, radial and sural nerve -SNCV not altered
Lukomski et al., 1993 (216)	18 ALS	ENG exam	-8 patients have lesion of central part of vestibular system, 2 have peripheral vestibular disturbance
Mondelli et al., 1993 (259)	64 ALS, 60 healthy controls	MCV, SCV, SAPa	-SAPas more affected than SCVs -parallel decrease in SCVs and MCVs over time in 14 patients
Palma et al., 1993 (278)	NA	BAEP, VEP, SEP	-no difference in BAEP and VEP -reduction in N13 amplitude and P22 latency in SEP recordings
Behnia et al., 1991 (249)	133 ALS	SNAP	-SNAP amplitudes maybe abnormal in a small proportion of ALS patients
Gao et al., 1991 (279)	343 MND	Sensory nerve conduction velocities	-sensory nerve conduction velocities were almost always normal
Shefner et al., 1991 (246)	18 ALS	compound sensory action potentials	-18 patients had abnormally reduced minimum conduction velocity
Subramaniam et al., 1990 (255)	27 MND	SEP, PSVEP, BAEP	-median nerve SEPs abnormal in 8 out of 27 patients and tibial nerve SEPs abnormal in 3 out of 21 patients
Zanette et al., 1990 (280)	26 MND, 20 healthy controls	SEPs	-central conduction time was abnormal in 3 patients
Facco et al., 1989 (281)	19 ALS	SEP	-N9-N13 significantly delayed, N13-N20 normal
Berardelli et al., 1987 (262)	11 MND, 20 healthy controls	SEP, MCV	-somatosensory responses from wrist stimulation were normal
Radtke et al., 1986 (173)	17 ALS	sensory evoked potential	-SEPs abnormal in 7 out of 16 patients after lower-extremity stimulation and 2 out of 16 patients after upper-extremity stimulation
Cosi et al., 1984 (282)	45 ALS	SEPs	-decreased amplitude of SEPs from tibial nerve

Post-mortem, biopsy and animal models

According to the 4 stage TDP-43 neuropathological staging, pTDP-43 inclusions are observed in the sensory cortex at stage 3 (283). pTDP-43 immunoreactive oligodendrocytes are observed in white matter in the sensory cortex (284). Studies also show pathology of dorsal root axons and dorsal root ganglion (DRG) cell bodies (285). Loss of neurons in the dorsal root ganglia as well as degeneration of posterior columns is detected (202). One study investigating 78 post-mortem brains (12 ALS, 38 frontotemporal lobar degeneration (FTLD), 28 controls) using 7T MRI and neuropathology reports iron deposition in the thalamus (286). Severe deterioration of somatosensory, auditory and gustatory pathways has also been observed (287).

Biopsy findings are inconsistent. Intraepidermal nerve fiber density has been found to be normal in one skin biopsy study (231) and reduced in another (179, 182). In the larynx, morphological changes have been detected in fibres in some patients. Inflammatory cell infiltrates (288), reduced myelin thickness (289) and axonal loss (290) are observed in the sural nerve. Both large calibre and small calibre fibres are affected (169). There is a reduction of myelinated fibres in the peroneal nerve (185, 291). The sural nerve has been shown to be affected in ALS (290, 292, 293). For patients who underwent sural nerve biopsy, pathology was detected in 91%, and this study also showed that large-calibre myelinated fibres were preferentially affected (169).

TDP43 animal models also show sensory pathology (294, 295). *SOD1* animal models show damage to sensory regions (296-298), neurons in the DRG (165, 167), DRG axons (299) and sensory neuropathy (300, 301). Wallerian degeneration of sensory nerves is observed in *SOD1* mouse models (302). A diffusion tensor imaging (DTI) study on a *SOD1* animal model showed sensory regions were affected during the symptomatic disease phase (296). Other animal studies, however, revealed that sensory white matter fibres were preserved (201, 303). Sensory deficits are not observed in other studies (201, 303, 304). **Table 7**

Table 7*: A selection of postmortem, biopsy and animal studies*

Postmortem			
Author and year of publication	**Study participants**		**Significant findings**
Mehta et al., 2021 (305)	3 *C9orf72* positive ALS/FTD, 2 healthy controls		-selective dysregulation of the mitochondrially encoded transcripts in ventral horn spinal MNs, but not in corresponding dorsal horn sensory neurons
De Reuck et al., 2017 (286)	12 ALS, 38 FTLD, 28 healthy controls		-iron deposition in thalamus
Fatima et al., 2015 (284)	35 ALS, 4 healthy controls		-pTDP43 immunoreactive oligodendrocytes observed in white matter in sensory cortex
Oyanagi et al., 2015 (287)	7 ALS		-severe deterioration in somatosensory, auditory and gustatory pathways in brainstem and spinal cord
Rabin et al., 1999 (202)	49 ALS		-loss of neurons in dorsal root ganglia and degeneration of posterior columns
Shankar et al., 1995 (306)	3 ALS		-involvement of sensory systems
Biopsy			
Author and year of publication	**Study participants**	**Region biopsied**	**Significant findings**
Dalla Bella et al., 2016 (179)	57 ALS	skin	-IENF density reduced in 75.4% of pure ALS and 50% FOSMN patients -IENF density similarly reduced in different subtypes of ALS
Ruoppolo et al., 2016 (194)	114 ALS	Larynx	-morphological changes present in fibres in 2 patients
Truini et al., 2015 (231)	24 ALS	skin	-normal intraepidermal nerve fibre
Luigetti et al., 2012 (290)	17 ALS	Sural nerve	-more than 2/3 biopsies revealed variable degree of axonal loss
Sawa et al., 2012 (289)	3 ALS	Sural nerve	-moderate, marginal reduction in myelin thickness
Devigili et al., 2011 (288)	18 ALS	sural nerve	-11 of 18 ALS+ patients had inflammatory cell infiltrates
Weis et al., 2011 (182)	28 ALS	skin	-significant reduction in epidermal nerve fibre density in distal calf -small-fibre neuropathy significantly higher in patients
Hammad et al., 2007 (169)	103 ALS	Sural nerve	-pathologic abnormalities present in 91% -large-calibre myelinated fibres reduced in 73%, small-calibre myelinated fibres affected in 23%

			-axonal degeneration and regeneration and excessive myelin irregularity
Isaacs et al., 2007 (171)	5 ALS	Sensory nerve	-axonal loss
Rabin et al., 1999 (202)	49 ALS	skin	-intracutaneous sensory fibres in skin biopsies normal
Hawkes et al., 1998 (188)	58 MND, 135 healthy controls	Olfactory bulbs	-olfactory bulbs showed excess lipofuscin deposition
Heads et al., 1991 (293)	NA	sural nerve	-early axonal atrophy, increased remyelination -sensory nerve pathology in ALS correlated with disease duration
Hamida et al., 1987 (291)	16 ALS, 8 healthy controls	Superficial peroneal nerve	-significant reduction of all myelinated fibres
Dyck et al., 1975 (185)	10 ALS	Peroneal nerve	-one nerve had low myelinated fiber density, 7 of 10 have abnormally high frequencies of teased fiber abnormalities
Animal models			
Author and year of publication	**Disease model**		**Significant findings**
Baczyk et al., 2020 (307)	presymptomatic mutSOD1 mice		-excitatory responses evoked by sensory and brainstem inputs reduced in motoneurons of presymptomatic mutSOD1 mice
Park et al., 2020	Drosophilia		-dynamic and reversible changes in TDP-43 localization seen in sensory neurons during development
Peng et al., 2020 (308)	mice with astroglial TDP-43 deletion		-mice with astroglial TDP-43 deletion develop motor but not sensory deficits
Ruiz-Soto et al., 2020 (309)	*SOD1(G93A)* mouse model		-Presymptomatic alterations of satellite glial cells (SGCs) at the dorsal root ganglion might not only be responsible of sensory disturbances in ALS, but could also contribute to anterior horn motor disturbances
Weerasekera et al., 2020 (310)	TDP-43(A315T) mouse model		-[18F]FDG PET demonstrated significantly lowered glucose metabolism in motor and somatosensory cortices of TDP-43A315T mice
Seki et al., 2019 (311)	*SOD1G93A* mouse		-novel reflex circuit-specific proprioceptive sensory abnormality in ALS
Vaughan et al., 2018 (294)	*TDP43A315T* on sensory neurons in culture and in vivo, *SOD1G93A* sensory neurons		-*TDP43* sensory neurons have shorter and less complex neurites and more sensitive to vincristine compared to controls and *SOD1* sensory neurons -levels of ATF3 and PERK are significantly different between *TDP43* and *SOD1* sensory neurons
Marcuzzo et al., 2017 (296)	G93A-*SOD1* mouse model		-main sensory regions affected by neurodegeneration
Bernard-Marissal et al., 2015 (304)	*SIGMAR1* mice		-defects are not observed in cultured sensory neurons
Vaughan et al., 2015 (295)	*SOD1(G93A)* and *TDP43(A315T)*		-degeneration of sensory nerve endings in *TDP43* mice
Sabado et al., 2014	*SOD1(G93A)* mouse model		-large dorsal root ganglion proprioceptive neurons accumulate misfolded *SOD1* and undergo degeneration

(165)		-degenerating sensory axons were detected in association with activated microglial cells in spinal cord dorsal horn
Cowin et al., 2011 (303)	*SOD1* mouse model	-sensory white matter fibres unchanged
Filali et al., 2011 (297)	*SOD1(G37R)* transgenic mouse model	-raised somatosensory thresholds
Underwood et al., 2011 (201)	*SOD1* mice	-sensory white matter fibres preserved
Choi et al., 2010 (298)	*SOD1 G93A* rats	-decreased response in sensorimotor cortex
Guo et al., 2009 (300)	*hSOD1-G93A* mice	-spinal cords of mice exhibit significant damage in the sensory system
Fischer et al., 2005 (299)	*SOD*/Wld(S) mice	-significant degeneration of sensory axons

Imaging

Sensory pathology is reported in the brain in the sensory cortical areas (169, 312-316) especially the postcentral gyrus (177, 178, 315, 317-320) as well as in the thalamus (286, 321-337) on structural (315, 320, 338), diffusion tensor imaging (DTI) (174, 339-341), functional MRI (fMRI) (316) and magnetic resonance spectroscopy (MRS) (342, 343). Atrophy of the postcentral gyrus has been observed in several studies (315, 320). One study investigating specific regions and nuclei of the thalamus shows degeneration of sensory nuclei of thalamus (344). Dorsal column degeneration has been shown in several spinal MR studies (174, 339, 340). One study reported a significant correlation between abnormal DTI measures of sensory fibres and N9 amplitude (174). Functional imaging reveals changes in the somatosensory cortex (345). Reduced right regional coherence in the postcentral gyrus was seen to correlate with high disease severity, while increased regional coherence in the left postcentral gyrus was associated with longer disease duration (317). Reduced fractional amplitude of low-frequency fluctuations (fALFF) was also observed in the right postcentral gyrus (319). Reduced Na/Cr resonance intensity ratio is demonstrated on spectroscopy in the postcentral gyrus (343).

Combining spinal imaging and neurophysiology has shown sub-clinical deficits of the sensory system in up to 85% of ALS patients (174). Dorsal column changes are observed soon after symptom onset, therefore it is possible that sensory involvement has been highly underestimated and is an early feature of ALS (174, 339). One study

specifically investigated involvement of the sensory pathway in 29 ALS patients with spinal onset ALS who were compared to 21 healthy controls. Diffusion tensor imaging (DTI), magnetization transfer and atrophy index were measured in the spinal cord and found damage to the dorsal columns within a year of symptom onset (339). Several studies note negative findings in the sensory areas (346, 347). **Table 8**

Table 8*: A selection of imaging studies in ALS*

Author and year of publication	Study participants	Methodology	Significant findings
Structural			
Ahmed et al., 2021 (337)	52 ALS, 41 ALS-FTD, 58 bvFTD, 58 healthy controls	Structural (volumetry)	-marked subcortical atrophy of thalamus in ALS-FTD and bvFTD
Barry et al., 2021 (338)	12 ALS, 9 healthy controls	structural, MRS, rsfMRI	-disruption in long-range functional connectivity between superior sensorimotor cortex and bilateral cerebellar lobule VI -decreased functional connectivity that predominantly mapped to bilateral postcentral and precentral gyri
Chen et al., 2020 (348)	22 ALS, 20 healthy controls	structural	-decreased fractal dimensionality (FD) values in right postcentral gyrus
Chipika et al., 2020 (344)	100 ALS, 33 PLS, 117 healthy controls	Structural (volumetry, shape analysis, ROI morphometry)	-degeneration of sensory nuclei of thalamus in *C9orf72* negative ALS and PLS
Bede et al., 2018 (154)	36 ALS, 26 ALS-FTD, 10 bvFTD, 11nfvPPA, 5 svPPA, 50 healthy controls	Structural (volumetry, cortical thickness), diffusion	-*C9orf72* ALS-FTD have reduced density in thalamic sub-region connected to sensory cortex
Bueno et al 2018 (349)	20 ALS, 15 healthy controls	structural, diffusion, rsfMRI	-thalamus is preserved
Chen et al., 2018 (350)	65 ALS, 65 healthy controls	structural	-GM volume reduced in left postcentral gyrus in spinal onset ALS
Buhour et al., 2017 (324)	37 ALS, 37 healthy controls	structural	-GM atrophy in right thalamus
Kim et al., 2017 (351)	62 ALS, 57 healthy controls	structural	-atrophy of postcentral region in limb-onset ALS
de Albuquerque et al., 2016 (352)	32 ALS, 32 healthy controls	Structural	-higher values for parameter correlation in both thalami
Masuda et al., 2016 (326)	44 ALS, 7 ALS-FTD, 24 healthy controls	Structural (VBM), diffusion	-atrophic changes in thalamus in ALS-FTD
Devine et al., 2015 (178)	30 ALS, 17 healthy controls	structural	-assymetric atrophy of the left somatosensory cortex in ALS patients with right-sided onset of limb weakness
Machts et al., 2015 (327)	42 ALS-nci, 7 ALS-FTD, 18 ALS-plus, 39 healthy controls	Structural (Volumetry, shape, density)	-pathologic changes bilateral thalami
Irwin et al., 2013 (353)	143 ALS	Structural	-greater atrophy in thalamus
Mioshi et al., 2013 (354)	22 ALS, 17 ALS-FTD, 18 healthy controls	Structural (VBM)	-atrophy in somatosensory region in ALS-plus

Thorns et al., 2013 (355)	14 ALS, 14 healthy controls	Structural (cortical thickness)	-significant cortical thinning in postcentral gyrus bilaterally
Cosottini et al., 2012 (320)	20 ALS, 16 healthy controls	Structural (VBM), fMRI	-decreased cortical GM in postcentral gyri -significant hypoactivation of primary sensory motor cortex
Mohammadi et al., 2009 (356)	20 ALS, 20 healthy controls	structural, fMRI	-ALS patients without bulbar involvement show activations in postcentral areas and thalamus
Grosskreutz et al., 2006 (315)	17 ALS, 17 healthy controls	structural	-decreased GM volume in postcentral gyrus bilaterally
Chang et al., 2005 (336)	10 ALS, 10 ALS-FTD, 22 healthy controls	Structural-VBM	-GM atrophy in left posterior thalamus
Kato et al., 1993 (357)	22 ALS	structural	-gradually progressive atrophy in postcentral gyrus -high intensity T2 signals rarely in the thalamus
Diffusion			
Rajagopalan et al., 2021 (341)	75 ALS, 14 disease controls	diffusion	-ALS-FTD showed significantly lower primary motor and sensory cortex GM fractal dimension values compared to other ALS groups.
Rajagopalan et al., 2017 (347)	45 ALS, 14 healthy controls	diffusion	-fibres projecting to postcentral gyrus spared
Zhang et al., 2017 (325)	38 ALS, 35 healthy controls	diffusion	-thalamocortical connections remained relatively in tact
Sheelakumari et al., 2016 (346)	17 ALS, 15 healthy controls	diffusion, SWI	-no significant differences in sensory cortex
Trojsi et al., 2015 (358)	54 ALS, 18 healthy controls	diffusion	-reduced FA and increased RD and MD in WM underneath postcentral gyri
Barbagallo et al., 2014 (329)	24 ALS, 22 healthy controls	diffusion, structural	-MD values of ALS significantly higher in thalamus
Kim et al., 2014 (359)	14 ALS, 16 healthy controls	diffusion	-no significant changes in primary sensory cortex
Sharma et al., 2013 (335)	14 ALS, 12 healthy controls	diffusion, Structural	-MD significantly higher in thalamus
Rose et al., 2012 (318)	15 ALS, 20 healthy controls	Diffusion, structural	-abnormal intrahemispheric pathways include CST involving right postcentral gyrus
Agosta et al., 2011 (360)	26 ALS, 15 healthy controls	diffusion	-significantly increased functional connectivity between left sensorimotor cortex and other cortical areas and cerebellum -different changes in functional connectivity in patients with CST damage versus those without
Thivard et al., 2007 (332)	15 ALS, 25 healthy controls	Diffusion, structural	-decreased FA in thalamus
Sach et al., 2004 (334)	15 ALS, 12 healthy controls	diffusion, structural,	-decreased FA in thalamus
Functional			

Wei et al., 2021 (361)	20 ALS, 22 healthy controls	fMRI	-ALS group had significantly increased functional stability in post-central gyrus
Qiu et al., 2019 (362)	60 ALS, 60 healthy controls	rsfMRI, structural, diffusion	-reduced functional connectivity in bilateral postcentral gyrus
Menke et al., 2017 (322)	13 ALS, 3 PLS	rsfMRI, Structural (volumetry, shape analysis), diffusion	-reduced functional connectivity between sensorimotor resting state network and frontal pole
Xu et al., 2017 (323)	20 ALS, 21 healthy controls	rsfMRI	-decreased nodal efficiency in right thalamus
Zhang et al., 2017 (141)	38 ALS, 35 healthy controls	rsfMRI, diffusion	-reduced voxel mirrored homotopic connectivity in postcentral gyrus
Fang et al., 2016 (345)	20 ALS, 21 healthy controls	rsfMRI	-significant regional activity alterations in left primary somatosensory cortex
Zhou et al., 2016 (177)	43 ALS, 44 healthy controls	rsfMRI	-significant decrease of DC in bilateral sensory motor region
Zhou et al., 2014 (317)	12 ALS, 12 healthy controls	rsfMRI	-decreased coherence in superior medial sensory-motor network (SMN) -increased coherence in peripheral SMN areas -decreased regional coherence in right postcentral gyrus correlated with high disease severity -enhanced regional coherence in left postcentral gyrus related to longer disease duration -increased coherence in left postcentral gyrus corresponds to fast disease progression rate
Poujois et al., 2013 (313)	19 ALS, 21 healthy controls	fMRI, diffusion	-overactivations in ipsilateral and contralateral somatosensory cortex -correlation of ipsilateral somatosensory activations with severity of right arm deficit
Luo et al., 2012 (319)	20 ALS, 20 healthy controls	fMRI, structural (VBM)	-significant reduction in ALFF in right postcentral gyrus
Mohammadi et al., 2011 (314)	22 ALS, 22 healthy controls	fMRI	-size of activated area in contralateral sensorimotor cortex increased to similar degree in all 3 ALS groups compared to controls regardless of weakness on clinical examination
Lule et al., 2010 (316)	14 ALS, 18 healthy controls	fMRI	-reduced response in sensory intergration areas of parietal lobe
Li et al., 2009 (331)	10 ALS, 10 healthy controls	fMRI, diffusion, structural	-reduced activation of sensorimotor cortex in patients with dysphagia -MD increased in thalamus
Other			
De Reuck et al., 2017 (286)	12 ALS, 38 FTLD, 28 healthy controls	iron deposition	-significant increase of iron deposition in thalamus
Pioro et al., 1994 (343)	12 MND, 6 healthy controls	1H-MRSI	-significant decrease in Na/Cr resonance intensity ratios in primary sensory region
Spinal imaging			
Pisharady et al., 2020 (363)	20 ALS, 20 healthy controls	diffusion	- tracts and spinal levels affected in ALS, involvement of sensory pathways
Olney et al., 2018 (364)	3 ALS, 2 ALS-FTD, 1 PLS, 2 PMA, 2 FOSMN, 10 healthy controls	structural- Axial 2D PSIR images and diffusion	-spinal cord GM and WM atrophy
Rasoanandrianina et al., 2017 (340)	10 ALS, 20 healthy controls	diffusion, ihMT	-changes in posterior spinocerebellar tract

Wang et al., 2017 (365)	14 ALS, 14 healthy controls	MRS	-significantly decreased Naa/Cr ratios in postcentral gyrus
Iglesias et al., 2015 (174)	21 ALS, 21 healthy controls	diffusion	-damage to ascending sensory fibres in ~60% of patients
Wang et al., 2014 (366)	24 ALS, 16 healthy controls	structural, diffusion	-no abnormal findings in cervical spine detected with conventional MR imaging
Cohen-Adad et al., 2013 (339)	29 ALS, 21 healthy controls	structural, diffusion, magnetization transfer	-impairment of spinal sensory pathways detected in early stage disease

PLS, PMA, SBMA, PPS

Reports of sensory changes in PLS vary. One study showing increased functional connectivity in the sensorimotor network including the postcentral gyrus and increased pathology was seen in patients with a faster progression and greater disability (203). Thalamic changes are shown in some studies (367, 368) while another study shows a trend towards a smaller thalamus in PLS patients (369). However, cortical thickness of primary sensory cortex did not differ from controls (370). Some imaging and electrophysiology studies also report that PLS spares the postcentral gyrus (116, 371).

In primary muscular atrophy (PMA), while SEPs were abnormal in the majority of ALS patients assessed, they were unaltered in 10 PMA patients. In spinal and bulbar muscular atrophy (SBMA), significantly reduced (204, 205, 372-378) or absent (379) SNAP is observed in many studies. SNAP does not appear to be related to CAG repeat size (380). Axonal degeneration and loss of myelinated nerve fibres is observed in the sural nerve (381). Altered visual and auditory EPs (382), decreased somatosensory EPs (382) and prolonged somatosensory evoked field (383) are also observed. Abnormal SEPs and other sensory derangements have been observed in aging polio survivors (384), however, an imaging study of patients with post-polio syndrome reported no significant changes in grey or white matter in the postcentral gyrus or thalamus (385).

Discussion

Sensory disturbance is rarely evaluated clinically or otherwise in motor neuron disease due to the enormous clinical burden caused by motor as well as cognitive and behavioural pathology (4, 386). While patients may have little to no symptoms and signs of sensory dysfunction, they could have subclinical sensory deficits which can be observed on electrophysiology (172). Observations of electrophysiological neuropathy as evidenced by alterations in SNAP, SEP, and SAPA show that while the absence of sensory changes supports a diagnosis of ALS, the presence of sensory abnormalities does not completely exclude ALS (387). In post-mortem and biopsy findings, the dorsal root ganglia, dorsal columns, thalamus and sensory cortex are affected, and degeneration of sensory nerves is also observed (202, 284, 286, 290). On neuroimaging, dorsal column degeneration (174, 339, 340), damage to the nuclei of the thalamus involved in sensation (344) is observed. The ventral posterolateral and ventromedial nuclei located in the thalamus have a primary sensory function, relaying somatosensory information from the head and body. Pathology in the postcentral gyrus, which is the location of the primary somatosensory cortex processing somatosensory inputs from the entire body and integrating sensory and motor signals (315, 320) is also reported. Objective markers of damage to the dorsal column-medial lemniscus pathway support clinical reports of sensory symptoms and signs observed in a subset of patients.

The majority of sensory findings are observed in single timepoint studies, therefore it is challenging to determine whether sensory pathology is an early or late feature.

There are some reports of sensory pathology preceding motor pathology (171, 388), but confidently ascertaining chronology of pathology requires multi-timepoint studies. Longitudinal observation of the progression of sensory deficits would be more informative in showing when and in which subset of patients sensory pathology develops and how it progresses over time. Many of the imaging studies reporting deficits in the sensory pathway are not dedicated to the assessment of sensory pathology. Findings of damage to components of the sensory pathway are reported but seldom discussed comprehensively. Few studies assess sensory pathology using multiple different methods. Practically, it often proves challenging to collect clinical, electrophysiology, imaging and biopsy data, and while it would be desirable, ascertaining correlations between findings on one modality versus another is often unsuccessful. However, it may be of use if future studies were designed in a manner that captures multiple points of potential pathology in the sensory pathway, for example, the collection of brain and spinal imaging data. In the studies reviewed, patients were commonly stratified by phenotype, but not commonly stratified by genotype. The stratification of patients by genotype as well as the inclusion of presymptomatic ALS mutation carriers is essential to determine genotype and phenotype specific patterns of sensory involvement. Findings of sensory involvement are common in SBMA, but variable and inconsistent in PLS, polio and PMA. These conditions may mimic ALS, and there is a need for the comprehensive characterisation of sensory pathology in these varying phenotypes to elucidate genotype and phenotype-specific patterns of disease pathology in varying neurodegenerative conditions. This will ultimately improve prognostication in individual patients, which would allow patients to make better informed decisions about their future.

It is possible that in ALS, varying aspects of sensorimotor control may contribute to deficits in dexterity. ALS patients show a impaired dexterity on tests such as the nine hole peg test (NHPT) which has a moderate negative correlation with the ALSFRS-R handwriting scores (389). In other conditions such as autism spectrum disorders, sensorimotor integration deficits are observed in both gross and fine manual dexterity tasks (390). This is also reported in other conditions including stroke (391) and schizophrenia (392). Such deficits, if observed in ALS could contribute to difficulty with tasks such as writing, typing, getting dressed among other essential daily tasks. There is evidence of disturbances in gait which in some cases are attributed to abnormal postural reactions (211) and reduced ability to integrate vestibular input (215). Proprioceptive deficits are more commonly reported, but their contribution to gait impairment is often neglected. Proprioceptive deficits would put ALS patients at increased risk of falls due to poor balance or improper coordination of movements, particularly when navigating uneven surfaces or stairs, and consequently would lead to a reduced quality of life. The precise degree to which sensory dysfunction contributes to gait impairment in ALS patients is difficult to assess clinically due to extensive lower motor neuron involvement and pyramidal weakness. Current rehabilitation strategies in ALS focus primarily on motor dysfunction and spasticity. Recognition of proprioceptive deficits may guide falls prevention strategies.

Sensory changes with respect to swallow and cough are detected. In the larynx, sensory deficits are noted to be more common in bulbar-onset ALS as revealed with

fibre-optic endoscopic evaluation of swallowing with sensory testing (194, 195). ALS patients report increased sensitivity to an upper airway irritant (193). Somatosensory deficits can contribute to speech impairment as seen in Parkinson's disease where decreased laryngeal sensitivity to airburst stimulation is reported (393). Progressive dysphagia, aspiration and dysarthria is often attributed to muscle weakness with little consideration given to the contribution of sensory impairment to swallowing and speech problems in ALS. Symptoms of paraesthesia, mild pain and numbness are often overshadowed by extensive and progressive limb weakness and bulbar dysfunction. In addition to this, riluzole, the first FDA approved for the treatment of ALS is reported to be associated with sensory deficits such as circumoral paraesthesia (207, 208). While moderate to severe pain and paraesthesia are likely to be addressed by clinicians if present, patients may underreport mild pain and paraesthesia, therefore if these symptoms and signs are not regularly assessed, they may never be addressed satisfactorily.

There are glaring research gaps. Several sensory domains are under-evaluated or not evaluated at all. For example, while visual, auditory, olfactory and gustatory deficits are rarely assessed and commonly overlooked, abnormal visual evoked potentials (394, 395), retinal changes on optical coherence tomography (OCT) (396) and changes in auditory evoked potentials (173, 395) have been demonstrated in ALS, as well as alterations in olfaction (187-189) and taste (190, 191). Impaired visuospatial ability has been shown in a proportion of patients (225, 397). Pathology in the lateral posterior nucleus of the thalamus, which has a role in visual saliency and visually guided

behaviours with afferents from the superior colliculus, primary visual, auditory and somatosensory cortices and efferents to the parietal association cortex has also been observed (344). Visual pathology may negatively impact basic activities of daily living such as driving and reading, and auditory deficits may further complicate communication for patients particularly for those battling with dysarthria. Impaired taste and smell may have considerable impact on quality of life as it impacts on patients' appetite and ability to enjoy food and consequently their ability to acquire adequate nutrition (191).

Genetic, functional and pathological studies suggest ALS originates in the motor cortex and that propagation occurs away from the cerebral cortex along the corticofugal projections (398, 399). It is theorised that corticofugal spread occurs either via prion-like propagation of misfolded proteins (400, 401) or via cortical hyperexcitability resulting in aberrant corticofugal neurons excitability and activity and subsequent excitotoxicity downstream (402, 403). Brettschneider defines four neuropathological stages of ALS, suggesting the first lesions begin in the motor cortex, brainstem and spinal cord. Stage 2 involves the reticular formation and precerebellar nuclei, stage 3 the prefrontal neocortex and basal ganglia and stage 4 involves the temporal lobe and hippocampal formation (404). However, several studies have shown concomitant subcortical grey matter and other extra-motor pathology very early in the disease process (344, 405, 406). Short association fibres interconnect the motor cortex with the primary somatosensory cortex. Whether there is a link between pathology developing in the motor and somatosensory cortices is yet to be elucidated. The

theory of corticopetal spread proposes ALS originates in peripheral tissues with a retrograde signalling cascade leading to motor neuron death (407, 408). The simultaneous evaluation multiple locations within the skeletal muscle, peripheral nerves, spinal cord and brain over multiple timepoints from the presymptomatic to the symptomatic phase is necessary to elucidate which mechanism of propagation drives neurodegeneration in ALS. Because the somatosensory system is multi-synaptic, it may be useful to evaluate propagation patterns and confront prevailing views on unidirectional spread.

Table 9*: Shortcomings of current study design and desirable design*

Shortcomings in study design	**Desirable study design**
Cross-sectional study design	Longitudinal study design with multiple timepoints
Commonly single modal studies	Multi-modal studies assessing neurological features of sensory deficits clinically, as well as using electrophysiology, imaging and biopsy
Assessment of single point in dorsal column-medial lemniscus pathway	Assessment of multiple points in dorsal column-medial lemniscus pathway
Studies commonly assessing pathology of various pathways	Studies dedicated to the assessment of sensory pathology in motor neuron disease
Imaging studies either assess the brain or spine	Combination of brain and spinal imaging
Patients commonly stratified by phenotype only	Inclusion of mutation carriers and stratification of patient cohorts by genotype as well as phenotype
Primarily assessment of symptomatic patients	Assessment of presymptomatic ALS mutation carriers
Few studies evaluate more than one motor neuron disease phenotype	Assessment of other motor neuron disease phenotypes as disease controls
No post-mortem validation in the majority of studies	Post-mortem validation of in-vivo findings

Conclusions

ALS should no longer be considered a condition exclusively involving motor and frontotemporal regions. In addition to motor and cognitive changes, sensory alterations are also a feature of ALS and other motor neuron disease phenotypes as evidenced by clinical, electrophysiology, imaging, biopsy, post-mortem and animal studies. Sensory deficits are under-evaluated, despite the fact that they may contribute to impairments in swallowing, dexterity and gait and reduced enjoyment of food. Consequently, the recognition and assessment of changes in the sensory pathway may be an important factor in improving the quality of life of ALS patients.

CHAPTER 3: Alterations in somatosensory, visual and auditory pathways in amyotrophic lateral sclerosis

1. Introduction

1.1 Background

Amyotrophic lateral sclerosis (ALS) is a neurodegenerative disease which is primarily characterized by the degeneration of upper and lower motor neurons [1, 2]. While frontotemporal involvement is often observed [3], sensory neuropathy, dorsal root ganglion pathology and the degeneration of brain structures involved in sensory processing are not recognised as core features of the disease. However, sensory disturbances have been observed clinically [4-7], and demonstrated by electrophysiology [4, 8-11], neuroimaging [9, 12, 13] and neuropathology studies [4, 14-17]. Sensory dysfunction is thought to be more common in familial ALS than in sporadic ALS [1, 18], and sensory disturbances have also been observed in other motor neuron disease phenotypes [19-22]. The literature of sensory involvement in ALS is conflicting. Most studies report negative findings [23-25], but very few studies have evaluated sensory regions specifically [9]. Clinically, subtle paraesthesia [5, 26-28], numbness [2], pain [29], vestibular symptoms [30], proprioceptive deficits [31] and changes in olfaction [32-34] and taste [35, 36] may be overshadowed by progressive limb weakness and bulbar dysfunction [37]. It is noteworthy, that Riluzole, the first FDA approved for the treatment of ALS has been associated with mild circumoral paresthesia [38] but this is rarely a cause for discontinuation. Sensory changes have

also been observed in the larynx on fibre-optic endoscopic evaluation of swallowing with sensory testing (FEEST) [39, 40].

The substrate of sensory symptoms is most commonly studied by electrophysiology or post mortem and it is seldom specifically evaluated on neuroimaging [41]. Alterations in sensory nerve action potentials (SNAP) [11, 42], somatosensory evoked potentials (SEP) [8, 43-46], visual evoked potentials (VEP) [47, 48], auditory evoked potentials [8, 48] and sensory action potential amplitudes (SAPA) [49] have been sporadically described. There are inconsistent reports on the impairments of thermal sensory pathways, but study protocols differ considerably [24, 50]. Overt visual deficits are rarely reported by the patients, but impaired visuospatial function has been consistently demonstrated in ALS [51, 52]. Microscopically, dorsal root ganglion, dorsal column, thalamus, sensory cortex and sensory nerve degeneration has also been observed [25, 53, 54]. Occipital lobe pathology has been described in both familial and sporadic ALS patients [55] and occipital pTDP-43 pathology has also been described [56]. On neuroimaging, dorsal column degeneration [9, 57, 58], focal thalamic pathology [59, 60] and postcentral gyrus [61, 62] atrophy have been reported. Structural [63], diffusion [64], functional [65], susceptibility [66], and MR spectroscopy [67] have all captured some degree of parietal and occipital lobe involvement. Despite these reports, there is a prevailing notion that ALS spares sensory networks [68], and no dedicated cerebral studies have systematically investigated the cortical, subcortical and white matter components of sensory pathways.

1.2 Objectives, aims and hypotheses

The primary objective of this study is the systematic evaluation of cortical, subcortical and white matter structures involved in the processing, relaying and mediation of sensory information. Accordingly, a comprehensive panel of cerebral structures was defined associated with specific somatosensory, visual and auditory processes **(Table 10)**. Some of the selected regions such as the postcentral gyrus, the ventral posterolateral (VPL), ventromedial (VM), lateral geniculate (LGN) and medial geniculate (MGN) nuclei of the thalamus and the medial lemniscus are either exclusively or primarily involved in sensory functions. Other regions included in the panel, such as the insular cortex, supramarginal gyrus, superior temporal gyrus, and the posterior thalamic radiation mediate a combination of sensory and non-sensory functions. We hypothesised that cerebral structures involved in somatosensory processes are not spared in ALS. Direct clinico-radiological correlations were not sought, as peripheral and spinal components of sensory pathways were not evaluated in this study [9, 69].

Table 10*: Panel of anatomical regions evaluated; key functions and connections.*

Region	Main functions	Key connections
Cortical regions		
Postcentral gyrus	-primary somatosensory cortex -processing afferent somatosensory inputs (touch, pressure, pain and temperature) -integration of sensory and motor signals necessary for skilled movement	-third-order neurons from thalamic VPL and VM ascend to the primary somatosensory cortex -visual and auditory cortices -subcortical structures encoding different sensory modalities -motor cortices
Insula	-multimodal sensory processing, interoception, perceptual self-awareness, autonomic control and emotional guidance of social behaviour -posterior insula receives inputs from pain, temperature, visceral, and vestibular pathways, which are processed in mid-insular cortex and transferred to anterior insula for further processing and interaction with areas involved in cognitive and emotional control	Posterior insula: -projects to lateral and central amygdaloid nuclei -connects reciprocally with the secondary somatosensory cortex -receives input from ventral posterior inferior and VM nuclei of thalamus Anterior insula: -projects to anterior amygdaloid area (AAA) and lateral, medial, cortical, accessory basal magnocellular and medial basal amygdaloid nuclei
Supramarginal gyrus	-part of the somatosensory association cortex -interprets tactile sensory data and involved in perception of space and limb location -involved in identifying postures and gestures of other people, a part of the mirror neuron system	-located just anterior to the angular gyrus -these two structures make up the inferior parietal lobule forming a multimodal complex that receives somatosensory, visual, and auditory inputs from the brain
Lateral occipital cortex	-object recognition and visual object processing - facial recognition and motion perception	-middle longitudinal fasciculus, inferior longitudinal fasciculus, vertical occipital fasciculus, inferior fronto-occipital fasciculus, optic radiations, and U-shaped fibres connect lateral occipital lobe to itself as well as parts of the temporal, parietal, and medial occipital cortices

Superior temporal gyrus	-location of part of primary auditory cortex -part of the high-order associative auditory cortex -encodes sound features that are more complex and heterogeneous -contains Wernicke's area	-auditory radiation from medial geniculate body to primary auditory cortex
Transverse temporal gyrus	-Also known as Heschl's gyrus -Location of primary auditory cortex	-auditory radiation from medial geniculate body to primary auditory cortex
Thalamic nuclei		
Ventral posterolateral	somatic sensation for contralateral trunk and limbs	-somatic afferents from trunk and limbs -efferents to somatic sensory cortex
Ventromedial	somatic sensation for contralateral head/face	-somatic afferents from head -efferents to somatic sensory cortex
Lateral posterior	-determining visual saliency, visually guided behaviours and multisensory processing of information related to aversive stimuli	-afferents from superior colliculus, primary visual, auditory and somatosensory cortex -efferents to parietal association cortex
Lateral geniculate	-primary visual relay centre that receives retinofugal fibers and transmits visual information to the visual cortex	-afferent from optic tract -efferent to primary visual cortex
Medial geniculate	-central role in auditory processing	-afferent from brachium of inferior colliculus -efferent to primary auditory cortex
Amygdala nuclei		

Lateral nucleus	-involved in tactile, auditory, visual, olfactory, nociceptive processes as well as cognition and attention	-subcortical afferents- VP nucleus of thalamus, MGN, hypothalamus, midbrain reticular formation, cerulean nucleus -cortical afferents- parietal, superior temporal gyrus, occipital, piriform lobe, hippocampus/entorhinal cortex, insula, orbital cortex, Basal nucleus of Meynert -receives extrinsic sensory inputs and sends projections to other amygdala nuclei
Medial nucleus	-generates innate emotional responses to chemosignals -key role in innate emotional behaviours, relaying olfactory information to hypothalamic nuclei involved in reproduction and defence	-termination of olfactory fibres from olfactory bulb -projections to ventromedial nucleus of hypothalamus
Cortical nucleus	-processing of pheromonal information and olfaction -presumably participates in ingestive, defensive and reproductive behaviours as a part of the vomeronasal amygdala	-termination of olfactory fibres from olfactory bulb -projections to ventromedial nucleus of hypothalamus
White matter		
Medial lemniscus	-part of the dorsal column-medial lemniscus pathway -transmits proprioception, touch and vibration	-internal arcuate fibres cross over at great sensory decussation then ascend as the medial lemniscus, synapsing at VPL nucleus of thalamus
Posterior thalamic radiation	-connect the caudal parts of the thalamus with the parietal and occipital lobes through posterior thalamic peduncle and posterior limb of the internal capsule	-connect thalamus, parietal and occipital lobes

AAA, anterior amygdaloid area; MGN, Medial geniculate nucleus; VM, Ventromedial nucleus; VP, ventral posterior nucleus; VPL, Ventral posterolateral nucleus.

2. Methods

2.1 Participants

A total of 287 participants, 160 patients with ALS ('ALS') 127 healthy controls ('HC') were included in a prospective, single-centre imaging study. All participants provided informed consent as required by the Ethics Approval of this research project (Beaumont Hospital, Dublin, Ireland). Exclusion criteria included a history of traumatic brain injury, cerebrovascular events, neoplastic, paraneoplastic and neuroinflammatory diagnoses. Additionally, a total of 7 patients were excluded after enrolment because of incidental radiological findings. Patients with ALS were diagnosed according to the revised El Escorial criteria. Key demographic and clinical variables (ALSFRS) were recorded for all participants at the time of their scan and a dedicated sensory assessment was performed in a subset of *C9orf72* negative patients (n = 45). The cohort of patients who underwent sensory assessment had no cervical or lumbar spondylosis, carpal tunnel syndrome, type I diabetes or pharmacotherapy associated with sensory symptoms. Methods for genetic screening for hexanucleotide repeat expansions in *C9orf72* have been described previously [70]. Repeat-primed PCR was used and expansions longer than 30 repeats were considered pathological.

2.2 Sensory assessment

Forty-five patients with ALS were systematically assessed for clinical signs of sensory dysfunction. Nociception was assessed using a 'neurotip' on the face, upper limbs and

lower limbs bilaterally. Vibrioception and proprioception were assessed in the upper and lower limbs bilaterally. For nociception, vibrioception and proprioception, a score of '2' indicated normal sensation in the relevant body region, '1' indicated reduced sensation, and '0' indicated sensory loss in the investigated sensory domain. Graphaestesia, the ability to recognise symbols traced on the skin, and stereognosis, the ability to perceive the form of solid objects by touch, were assessed in the upper limbs bilaterally. For graphaestesia and stereognosis, the patient was given a score of '1' for each correct answer, and '0' for each incorrect answer. A composite score of 84 indicated no sensory deficits and lower scores corresponded with more severe sensory deficits.

2.3 Screening for sensory symptoms

Additionally, a brief 7-item questionnaire was administered to screen for subjective symptoms pertaining to (1) upper limb paraesthesia, (2) lower limb paraesthesia, (3) cold sensitivity, (4) perioral paraesthesia, (5) tongue numbness, (6) changes in taste and (7) deterioration in sense of smell. Each item was scored 0–2, '0' meaning no symptoms in the relevant sensory domain.

2.4 Magnetic resonance imaging

Images were acquired on a 3 Tesla Philips Achieva Magnetic resonance (MR) platform as part of a standardised neuroimaging protocol. T1-weighted (T1w) images were acquired with a 3D Inversion Recovery prepared Spoiled Gradient Recalled echo (IR-SPGR) sequence with the following key parameters: field-of-view (FOV) of 256 × 256 ×

160 mm, flip angle = 8°, spatial resolution of 1 mm^3, SENSE factor = 1.5, TR/TE = 8.5/3.9 ms, TI = 1060 ms. Diffusion tensor images (DTI) data were acquired with a spin-echo echo planar imaging (SE-EPI) pulse sequence with a 32-direction Stejskal-Tanner diffusion encoding scheme; FOV = 245 × 245 × 150 mm, 60 slices with no interslice gap, spatial resolution = 2.5 mm^3, TR/TE = 7639/59 ms, SENSE factor = 2.5, b-values = 0, 1100 s/mm^2, dynamic stabilisation and spectral presaturation with inversion recovery (SPIR) fat suppression. Fluid-attenuated inversion recovery (FLAIR) images were acquired with an Inversion Recovery Turbo Spin Echo (IR-TSE) sequence to screen for comorbid inflammatory or vascular pathologies. FLAIR data were acquired in axial orientation: FOV = 230 × 183 × 150 mm, spatial resolution = 0.65 × 0.87 × 4 mm, 30 slices with 1 mm gap, TR/TE = 11,000/125 ms, TI = 2800 ms, 120° refocusing pulse, with flow compensation and motion smoothing and a saturation slab covering the neck region. Clinical sequences (T1w and FLAIR) were radiologically reviewed for incidental findings and datasets from all participants underwent quality control review for movement artifacts before computational analyses.

2.5 Grey matter metrics

The standard anatomical reconstruction pipeline of the FreeSurfer image analysis suite [71], was implemented, including non-parametric non-uniform intensity normalization, affine registration to the MNI305 atlas, intensity normalization, skull striping, automatic subcortical segmentation, linear volumetric registration, neck removal, tessellation of the grey matter-white matter boundary, surface smoothing, inflation to minimize metric distortion, and automated topology correction [72]. The relevant

cortical labels of the Desikan-Killiany atlas were utilized to retrieve average cortical thickness and cortical volumes values from the postcentral gyrus, insula, superior temporal, transverse temporal, supramarginal, and lateral occipital cortices in the left and right cerebral hemispheres separately. The thalamus was parcellated into 25 sub-regions by Bayesian inference using a probabilistic atlas developed based on histological data [73]. The volumes of the following thalamic nuclei were evaluated in the two hemispheres separately: ventral posterolateral (VPL), ventromedial (VM), lateral posterior (LP), lateral geniculate (LGN), medial geniculate (MGN). The amygdala was segmented into 9 sub-regions using a probabilistic atlas developed based on histological [73, 74]. The volumes of the lateral (LN), medial (MN), and cortical nuclei (CN) were estimated in each hemispheres separately.

2.6 White matter metrics

Raw diffusion tensor data were eddy current corrected, skull stripped, and a tensor model was fitted in FMRIB's software library to create maps of axial diffusivity (AD), fractional anisotropy (FA), mean diffusivity (MD), and radial diffusivity (RD). FSL's tract-based statistics (TBSS) module was implemented for non-linear registration, skeletonisation and the creation of a mean FA mask. Diffusivity values were retrieved from the four (AD, FA, MD, RD) concatenated diffusivity files using the medial lemniscus and posterior thalamic radiation labels of the ICBM-DTI-81 white-matter atlas [75].

2.7 Statistics

Assumptions of normality were examined using the Kolmogorov-Smirnov test. Skewness and kurtosis were assessed separately for each study group. Since all variables followed a normal distribution, parametric statistics were applied. The age and ALSFRS-r profile of the study groups were compared multivariate analysis of variance (MANOVA). Sex, symptom onset and handedness proportions in the study groups were contrasted using Pearson's chi-squared test. White matter variables and cortical thickness measures were contrasted using multivariate analysis of covariance (MANCOVA) with age and sex and covariates. Volumetric profiles (cortical, thalamic nuclei, amygdalar nuclei) of the study groups were also appraised in MANCOVAs with the following covariates, age, sex and total intracranial volume (TIV). Bonferroni corrections were used to account for multiple comparisons and reduce Type I error. Output statistics were summarised in comprehensive tables to report estimated marginal means (EMM), standard error (SE), *p*-values and post hoc pairwise comparisons. To further illustrate focal pathology, radar plots were generated for the two patients groups where EMMs were expressed as the percentage of reference (HC) EMM in the given anatomical region.

3. Results

3.1 Demographic profiles

The study groups were matched for age, sex and handedness. Patient groups were matched for site of onset and functional disability **(Table 11)**. Forty-five patients were

specifically evaluated for the presence of sensory signs and symptoms, and all of these patients tested negative for the *C9orf72* gene.

Table 11*: The demographic and clinical profile of study participants.*

Study groups	C9+ ALS	C9- ALS	HC	*p* value
	n = 22	n = 138	n = 127	
Age (years)	59.05 (6.176)	61.46 (10.161)	59.30 (10.960)	0.195
Sex (male)	13 (59.09%)	81 (58.70%)	74 (58.27%)	0.996
Onset (bulbar)	2 (9.09%)	22 (15.94%)	N/a	0.403
Onset (spinal)	20 (90.91%)	116 (84.06%)	N/a	0.403
Handedness (right)	19 (86.36%)	122 (88.41%)	112 (88.19%)	0.963
ALSFRS-R	37.91 (6.852)	37.17 (6.121)	N/a	0.604

ALSFRS-r, revised ALS functional rating scale.

3.2 Clinical signs and symptoms

On clinical examination, vibrioception was the most commonly affected sensory domain detected in 80.0% of the patients, subtle nociceptive deficits were identified in 57.8%, and proprioceptive deficits were ascertained in 28.9% of patients. Graphaesthesia was abnormal in 48.9% and stereognosis was abnormal in 28.9% of the 45 patients who had a dedicated sensory assessment at the time of their scan. Subtle facial sensory deficits were identified in 11.1% of patients. On the sensory symptom questionnaire, 68.9% reported at least one sensory symptom, and only 31.1% patients reported having no sensory symptoms at all. 33.3% had paraesthesia in the hands/fingers, 20.0% had paraesthesia in the feet/toes and 24.4% of patients reported cold sensitivity in hands/fingers. Tingling around the lips was reported in 8.9% and

tongue numbness in 11.1%. 24.4% reported changes in taste and 17.8% of patients reported some change in smell **(Table 12)**.

Table 12*: Clinical sensory assessment scores in C9orf72 negative patients (n = 45) Lower scores indicate more severe sensory deficits.*

	Scores	% of patients with some deficit	Min. Score	Max. Score	Mean	Std. Deviation
Sensory deficits	Nociception (0–36)	57.8	21	36	33.47	3.641
	Vibrioception (0–24)	80.0	6	24	19.16	4.537
	Proprioception (0–12)	28.9	6	12	11.49	1.141
	Graphaesthesia (0–6)	48.9	2	6	4.98	1.234
	Stereognosis (0–6)	28.9	2	6	5.51	0.944
	Total deficit score (0–84)	95.6	48	84	74.60	7.381
Symptoms	Paraesthesia hands/fingers (0–2)	33.3	0	2	0.42	0.656
	Paraesthesia feel/toes (0–2)	20.0	0	2	0.29	0.626
	Cold sensitivity hands/fingers (0–2)	24.4	0	2	0.38	0.716
	Tingling around lips (0–2)	8.9	0	2	0.11	0.383
	Tongue numbness (0–2)	11.1	0	2	0.16	0.475
	Changes in taste (0–2)	24.4	0	2	0.33	0.640
	Changes in smell (0–2)	17.8	0	2	0.22	0.517
	Total Symptoms Score (0–14)	68.9	0	6	1.89	1.921

Number of patients systematically assessed n = 45, CN-V, Trigeminal nerve; LLL, left lower limb; LUL, left upper limb; RLL, right lower limb; RUL, right upper limb.

3.3 Cortical alterations

C9- ALS patients exhibited cortical volume reductions in the insula bilaterally, and the left supramarginal and right superior temporal gyrus compared to healthy controls **(Table 13)**. Each cortical region associated with sensory processing showed atrophic change in C9+ ALS bilaterally in comparison to both healthy controls and to C9- ALS. C9- ALS patients showed cortical thickness reductions in all evaluated regions except the lateral occipital region bilaterally and the right postcentral cortex. Cortical thickness changes were observed in all regions bilaterally in C9+ ALS in contrast to healthy controls, and in all regions except the transverse temporal bilaterally and the right insula when compared to C9- ALS **(Figure 2)**.

3.4 Subcortical nuclear degeneration

In C9- ALS, volumes of all thalamic nuclei involved in sensory processing were reduced except the lateral geniculate nucleus (LGN) bilaterally and the left lateral posterior nucleus **(Table 14)**. Sensory nuclei volumes were also reduced in C9+ ALS in comparison to healthy controls bilaterally except in the left medial geniculate nucleus. In the amygdalae of C9- ALS patients, volumetric reduction was observed in the right lateral and right cortical nuclei in comparison to healthy controls. Volumes reductions were also observed in the amygdalae of C9+ ALS patients in comparison to healthy controls in the lateral and cortical nuclei bilaterally and the left medial nucleus. When C9+ ALS patients are contrasted with C9- ALS patients, the volume of the left lateral nucleus was observed to be significantly reduced **(Figure 3)**.

3.5 White matter alterations

Significant inter-group AD and MD differences were observed in the right medial lemniscus and post hoc comparisons revealed AD differences between C9+ ALS and C9- ALS patients (p = 0.038). A trend of FA reduction was observed in C9- ALS compared to healthy controls in the left medial lemniscus (p = 0.054) **(Table 15)**. FA reductions and increased RD were observed in the bilateral posterior thalamic radiation in both C9+ and C9- ALS in comparison to healthy controls. Increased posterior thalamic radiation MD was also detected in C9- ALS in contrast to healthy controls in the right hemisphere (Fig. 2).

Table 13*: Cortical grey matter volumes (mm³) and cortical thickness (mm) in C9orf72 positive ALS patients (C9+ ALS), C9orf72 negative ALS patients (C9- ALS) and healthy controls (HC). For cortical volume values, estimated marginal means and standard error are adjusted for age (60.32), sex (1.41) and total intracranial volume (TIV) (1542959.99). For cortical thickness values, estimated marginal means and standard error are adjusted for age (60.32) and sex (1.41).*

Structure	Study group	EMM	Standard error	*p* value	Post-hoc comparisons		
					C9+ vs HC	C9- vs HC	C9+ vs C9-
CORTICAL VOLUMES							
left postcentral	C9+ ALS	7916.754	239.708	**<0.001**	**<0.001**	0.862	**<0.001**
	C9- ALS	8983.901	96.087				
	HC	9132.497	99.762				
right postcentral	C9+ ALS	7610.712	227.482	**<0.001**	**<0.001**	1.000	**<0.001**
	C9- ALS	8711.645	91.186				
	HC	8757.073	94.673				
left insula	C9+ ALS	6309.209	162.726	**<0.001**	**<0.001**	**0.037**	**0.005**
	C9- ALS	6873.812	65.229				
	HC	7111.916	67.723				
right insula	C9+ ALS	6234.165	169.753	**<0.001**	**<0.001**	**0.032**	**0.003**
	C9- ALS	6853.342	68.045				
	HC	7107.363	70.648				
left supramarginal	C9+ ALS	9121.066	301.457	**<0.001**	**<0.001**	**0.024**	**<0.001**
	C9- ALS	10569.938	120.839				
	HC	11039.497	125.460				
right supramarginal	C9+ ALS	8268.990	278.070	**<0.001**	**<0.001**	0.258	**<0.001**
	C9- ALS	9426.911	111.464				
	HC	9705.642	115.727				
left lateral occipital	C9+ ALS	10573.185	317.292	**0.002**	**0.014**	0.490	**0.001**
	C9- ALS	11804.076	127.186				

	HC	11546.145	132.051				
right lateral occipital	C9+ ALS	10313.655	315.875	**<0.001**	**<0.001**	1.000	**<0.001**
	C9- ALS	11854.095	126.618				
	HC	11726.933	131.461				
left superior temporal	C9+ ALS	10641.573	318.005	**<0.001**	**<0.001**	0.073	**0.003**
	C9- ALS	11774.368	127.472				
	HC	12193.572	132.347				
right superior temporal	C9+ ALS	9812.695	269.843	**<0.001**	**<0.001**	**<0.001**	**0.001**
	C9- ALS	10910.344	108.167				
	HC	11530.403	112.303				
left transverse temporal	C9+ ALS	1006.992	44.887	**0.003**	**0.002**	0.361	**0.033**
	C9- ALS	1131.138	17.993				
	HC	1171.835	18.681				
right transverse temporal	C9+ ALS	776.246	33.451	**0.001**	**0.001**	0.653	**0.010**
	C9- ALS	883.787	13.409				
	HC	907.819	13.922				
CORTICAL THICKNESS							
left postcentral	C9+ ALS	1.857	0.025	**<0.001**	**<0.001**	**0.012**	**<0.001**
	C9- ALS	1.998	0.010				
	HC	2.041	0.011				
right postcentral	C9+ ALS	1.859	0.025	**<0.001**	**<0.001**	0.080	**<0.001**
	C9- ALS	1.986	0.010				
	HC	2.018	0.010				
left insula	C9+ ALS	2.691	0.039	**<0.001**	**<0.001**	**0.001**	**<0.001**
	C9- ALS	2.855	0.015				
	HC	2.940	0.016				
right insula	C9+ ALS	2.765	0.039	**<0.001**	**<0.001**	**<0.001**	0.053[t]
	C9- ALS	2.864	0.015				
	HC	2.961	0.016				

left supramarginal	C9+ ALS	2.270	0.029	**<0.001**	**<0.001**	**<0.001**	**<0.001**
	C9- ALS	2.439	0.012				
	HC	2.508	0.012				
right supramarginal	C9+ ALS	2.249	0.028	**<0.001**	**<0.001**	**<0.001**	**<0.001**
	C9- ALS	2.396	0.011				
	HC	2.473	0.012				
left lateral occipital	C9+ ALS	2.012	0.027	**<0.001**	**<0.001**	1.000	**<0.001**
	C9- ALS	2.130	0.011				
	HC	2.130	0.011				
right lateral occipital	C9+ ALS	2.036	0.024	**<0.001**	**<0.001**	1.000	**<0.001**
	C9- ALS	2.143	0.010				
	HC	2.144	0.010				
left superior temporal	C9+ ALS	2.551	0.036	**<0.001**	**<0.001**	**<0.001**	**0.027**
	C9- ALS	2.652	0.014				
	HC	2.766	0.015				
right superior temporal	C9+ ALS	2.591	0.036	**<0.001**	**<0.001**	**<0.001**	**0.026**
	C9- ALS	2.694	0.015				
	HC	2.832	0.015				
left transverse temporal	C9+ ALS	2.206	0.046	**<0.001**	**0.002**	**0.010**	0.178
	C9- ALS	2.300	0.018				
	HC	2.378	0.019				
right transverse temporal	C9+ ALS	2.213	0.051	**0.001**	**0.001**	**0.025**	0.102
	C9- ALS	2.330	0.020				
	HC	2.409	0.021				

Significant intergroup differences at $p < 0.05$ after Bonferroni correction for multiple comparisons are highlighted in bold print, ^{t} indicates a statistical trend of $0.05 < p_{cor} < 0.07$.

Figure 2*: Cortical thickness profile in C9orf72 positive ALS patients (C9+ ALS), C9orf72 negative ALS patients (C9- ALS), healthy controls (HC), based on estimated marginal means adjusted for age and sex. Error bars represent 95% confidence intervals. Left denoted by (L) and right denoted by (R). Significant inter-group differences corrected for multiple comparisons are highlighted with asterisks: * p value between 0.01 and 0.05, ** p value between 0.001 and 0.01, *** p value < 0.001.*

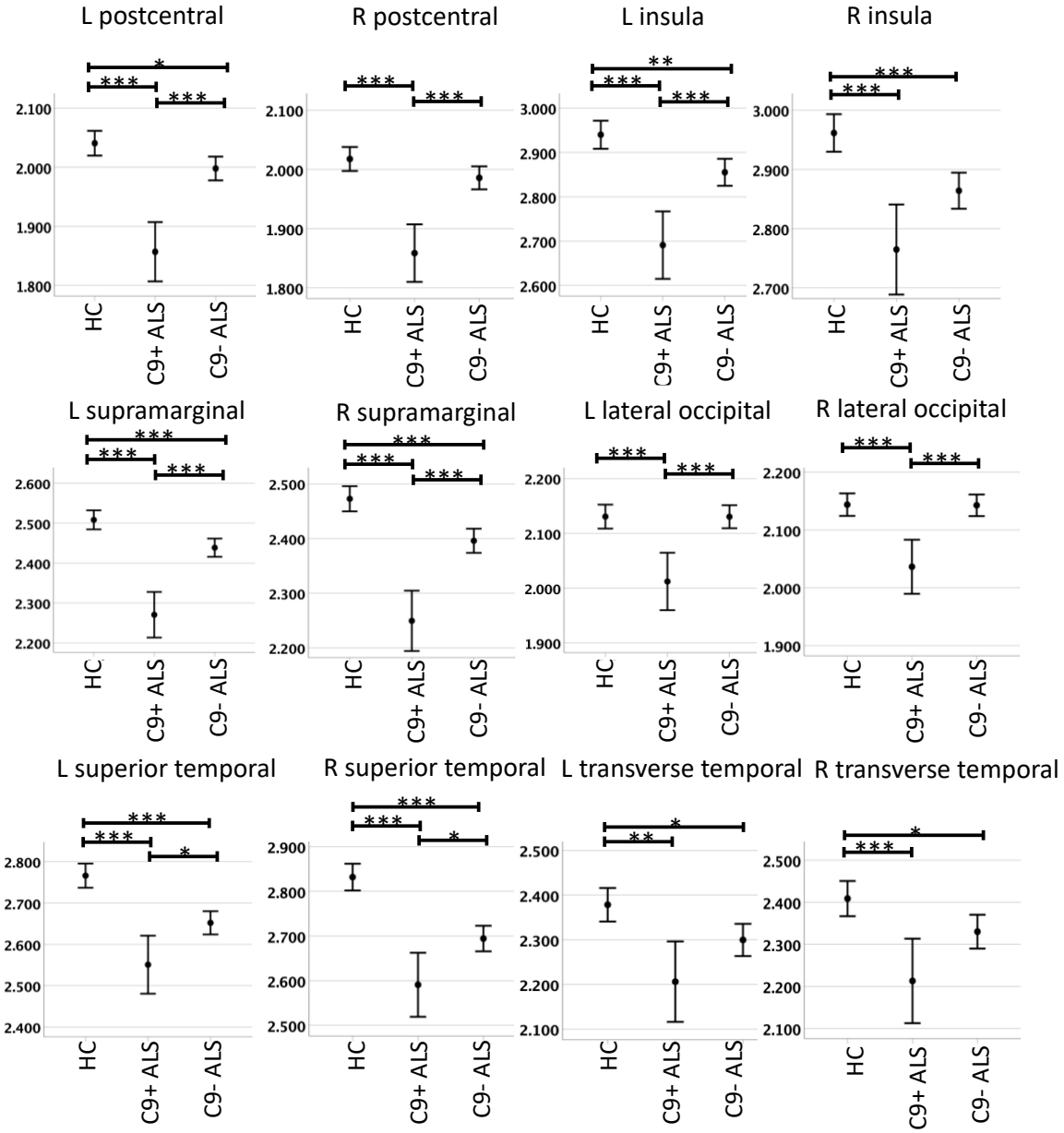

Table 14*: Thalamic and amygdalar nuclear volumes (mm^3) in C9orf72 positive ALS patients (C9+ ALS), C9orf72 negative ALS patients (C9- ALS) and healthy controls (HC). Estimated marginal means and standard error are adjusted for age (60.32), sex (1.41) and total intracranial volume (TIV) (1542959.99).*

Structure	Study group	EMM	standard error	*p* value	Post-hoc comparisons		
					C9+ vs HC	C9- vs HC	C9+ vs C9-
left thalamus proper	C9+ ALS	6279.851	154.835	**<0.001**	**<0.001**	**0.002**	**<0.001**
	C9- ALS	6968.154	62.066				
	HC	7282.553	64.439				
right thalamus proper	C9+ ALS	5922.869	137.042	**<0.001**	**<0.001**	**0.002**	**<0.001**
	C9- ALS	6593.957	54.933				
	HC	6873.343	57.034				
left ventral posterolateral (thalamus)	C9+ ALS	808.611	23.181	**<0.001**	**0.004**	**<0.001**	1.000
	C9- ALS	821.560	9.292				
	HC	890.153	9.647				
right ventral posterolateral (thalamus)	C9+ ALS	740.267	20.922	**<0.001**	**0.003**	**<0.001**	0.617
	C9- ALS	768.988	8.386				
	HC	815.432	8.707				
left ventromedial (thalamus)	C9+ ALS	18.802	0.590	**<0.001**	**0.001**	**<0.001**	1.000
	C9- ALS	19.396	0.236				
	HC	21.230	0.245				
right ventromedial (thalamus)	C9+ ALS	17.468	0.638	**<0.001**	**<0.001**	**<0.001**	0.404
	C9- ALS	18.504	0.256				
	HC	20.158	0.266				
left lateral posterior (thalamus)	C9+ ALS	94.283	4.323	**<0.001**	**<0.001**	0.062[t]	**0.002**
	C9- ALS	110.495	1.733				
	HC	116.344	1.799				
right lateral posterior (thalamus)	C9+ ALS	88.676	3.816	**<0.001**	**<0.001**	**0.017**	**0.004**
	C9- ALS	102.224	1.530				

	HC	108.403	1.588				
left lateral geniculate nucleus	C9+ ALS	146.082	5.403	**<0.001**	**<0.001**	0.510	**0.004**
	C9- ALS	165.165	2.166				
	HC	169.490	2.249				
right lateral geniculate nucleus	C9+ ALS	139.186	5.126	**0.001**	**<0.001**	1.000	**0.002**
	C9- ALS	158.301	2.055				
	HC	160.663	2.133				
left medial geniculate nucleus	C9+ ALS	103.127	3.749	**0.030**	0.425	**0.036**	1.000
	C9- ALS	103.568	1.503				
	HC	109.090	1.560				
right medial geniculate nucleus	C9+ ALS	96.508	3.267	**0.002**	**0.009**	**0.021**	0.395
	C9- ALS	101.851	1.309				
	HC	107.026	1.360				
left lateral nucleus (amygdala)	C9+ ALS	587.603	18.059	**<0.001**	**0.001**	0.094	**0.029**
	C9- ALS	638.607	7.239				
	HC	661.328	7.516				
right lateral nucleus (amygdala)	C9+ ALS	621.303	17.962	**<0.001**	**0.002**	**0.015**	0.170
	C9- ALS	658.510	7.200				
	HC	688.082	7.476				
left medial nucleus (amygdala)	C9+ ALS	16.070	1.118	**0.018**	**0.017**	0.592	0.114
	C9- ALS	18.595	0.448				
	HC	19.436	0.465				
right medial nucleus (amygdala)	C9+ ALS	20.066	1.316	0.437	0.628	1.000	0.673
	C9- ALS	21.801	0.528				
	HC	21.855	0.548				
left cortical nucleus (amygdala)	C9+ ALS	20.734	1.055	**0.001**	**0.001**	0.050[t]	0.071
	C9- ALS	23.331	0.423				
	HC	24.809	0.439				
right cortical nucleus (amygdala)	C9+ ALS	23.693	0.978	**<0.001**	**0.001**	**0.020**	0.123

	C9- ALS	25.864	0.392				
	HC	27.416	0.407				

Significant intergroup differences at $p < 0.05$ after Bonferroni correction for multiple comparisons are highlighted in bold print, ^{t} indicates a statistical trend of $0.05 < p_{cor} < 0.07$.

Table 15: *Axial diffusivity (AD), fractional Anisotropy (FA), mean diffusivity (MD) and radial diffusivity (RD) in C9orf72 positive ALS patients (C9+ ALS), C9orf72 negative ALS patients (C9- ALS) and healthy controls (HC). Estimated marginal means and standard error are adjusted for age (60.32) and sex (1.41).*

Structure	Study group	EMM	standard error	*p* value	Post-hoc comparisons		
					C9+ vs HC	C9- vs HC	C9+ vs C9-
AD medial lemniscus left	C9+ ALS	0.001148	0.000015	0.149	0.154	1.000	0.295
	C9- ALS	0.001174	5.853586E-6				
	HC	0.001179	6.096982E-6				
AD medial lemniscus right	C9+ ALS	0.001154	1.410245E-5	**0.044**	0.096	1.000	**0.038**
	C9- ALS	0.001192	5.644191E-6				
	HC	0.001187	5.878880E-6				
FA medial lemniscus left	C9+ ALS	0.568855	0.009018	0.212	1.000	0.322	0.805
	C9- ALS	0.558068	0.003609				
	HC	0.566511	0.003759				
FA medial lemniscus right	C9+ ALS	0.561060	0.008291	0.060[t]	1.000	0.054[t]	1.000
	C9- ALS	0.556778	0.003318				
	HC	0.568222	0.003456				
MD medial lemniscus left	C9+ ALS	0.000671	9.836082E-6	0.165	0.342	1.000	0.174
	C9- ALS	0.000691	3.936673E-6				
	HC	0.000688	4.100363E-6				
MD medial lemniscus right	C9+ ALS	0.000678	9.294528E-6	**0.035**	0.542	0.228	0.066[t]
	C9- ALS	0.000702	3.719929E-6				
	HC	0.000692	3.874606E-6				
RD medial lemniscus left	C9+ ALS	0.000433	9.959697E-6	0.188	1.000	0.605	0.331
	C9- ALS	0.000450	3.986148E-6				
	HC	0.000443	4.151894E-6				
RD medial lemniscus right	C9+ ALS	0.000441	9.336970E-6	0.058[t]	1.000	0.092	0.370
	C9- ALS	0.000456	3.736915E-6				

	HC	0.000444	3.892298E-6				
AD posterior thalamic radiation left	C9+ ALS	0.001265	1.389886E-5	0.312	0.387	1.000	0.667
	C9- ALS	0.001283	5.562710E-6				
	HC	0.001288	5.794011E-6				
AD posterior thalamic radiation right	C9+ ALS	0.001236	1.392658E-5	0.362	0.500	1.000	0.521
	C9- ALS	0.001256	5.573804E-6				
	HC	0.001257	5.805567E-6				
FA posterior thalamic radiation left	C9+ ALS	0.510931	0.008419	**<0.001**	**<0.001**	**0.001**	0.077
	C9- ALS	0.531271	0.003369				
	HC	0.549686	0.003509				
FA posterior thalamic radiation right	C9+ ALS	0.502567	0.008459	**<0.001**	**<0.001**	**<0.001**	0.078
	C9- ALS	0.522972	0.003385				
	HC	0.542817	0.003526				
MD posterior thalamic radiation left	C9+ ALS	0.000783	1.113229E-5	0.159	0.558	0.268	1.000
	C9- ALS	0.000778	4.455453E-6				
	HC	0.000767	4.640713E-6				
MD posterior thalamic radiation right	C9+ ALS	0.000770	1.040189E-5	**0.035**	0.363	**0.046**	1.000
	C9- ALS	0.000767	4.163127E-6				
	HC	0.000752	4.336233E-6				
RD posterior thalamic radiation left	C9+ ALS	0.000543	1.160346E-5	**0.002**	**0.015**	**0.017**	0.553
	C9- ALS	0.000526	4.644025E-6				
	HC	0.000507	4.837127E-6				
RD posterior thalamic radiation right	C9+ ALS	0.000537	1.088973E-5	**<0.001**	**0.006**	**0.001**	0.659
	C9- ALS	0.000522	4.358372E-6				
	HC	0.000500	4.539596E-6				

Significant intergroup differences at $p < 0.05$ after Bonferroni correction for multiple comparisons are flagged in bold print. [t] indicates a statistical trend of $0.05 < p_{cor} < 0.07$.

Figure 3*: Radar plots of integrity measures expressed as % of estimated marginal means of controls (green) in regions of interest associated with sensory processing. * indicates significant intergroup differences (p value < 0.05).*

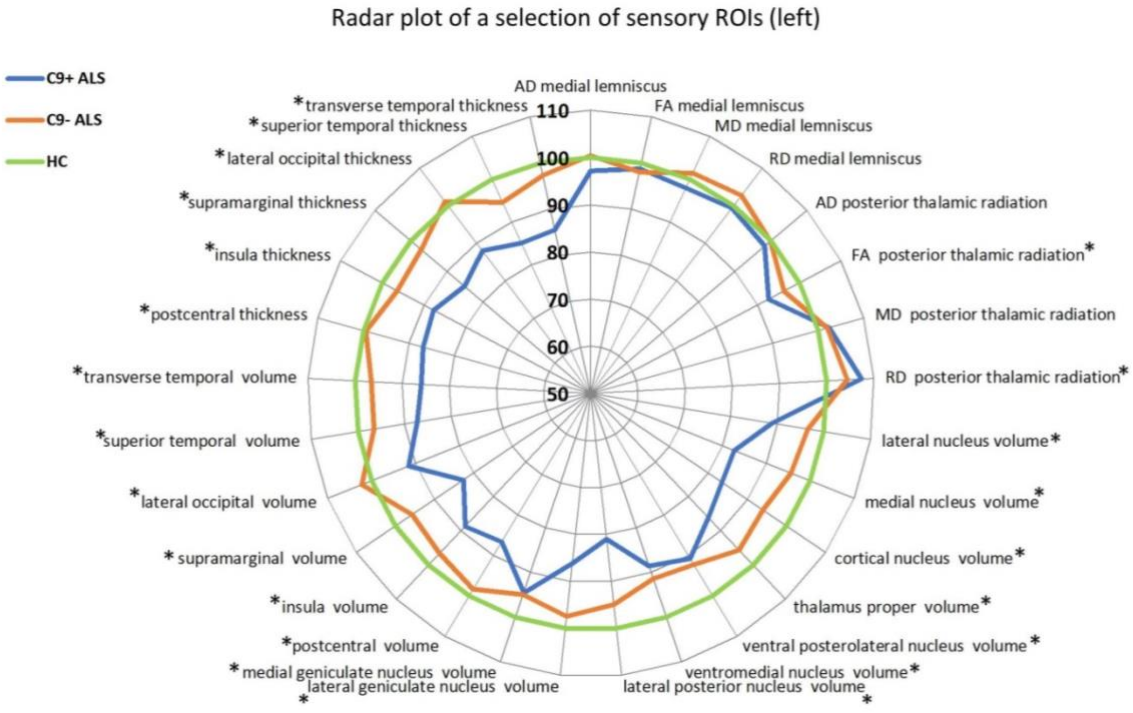

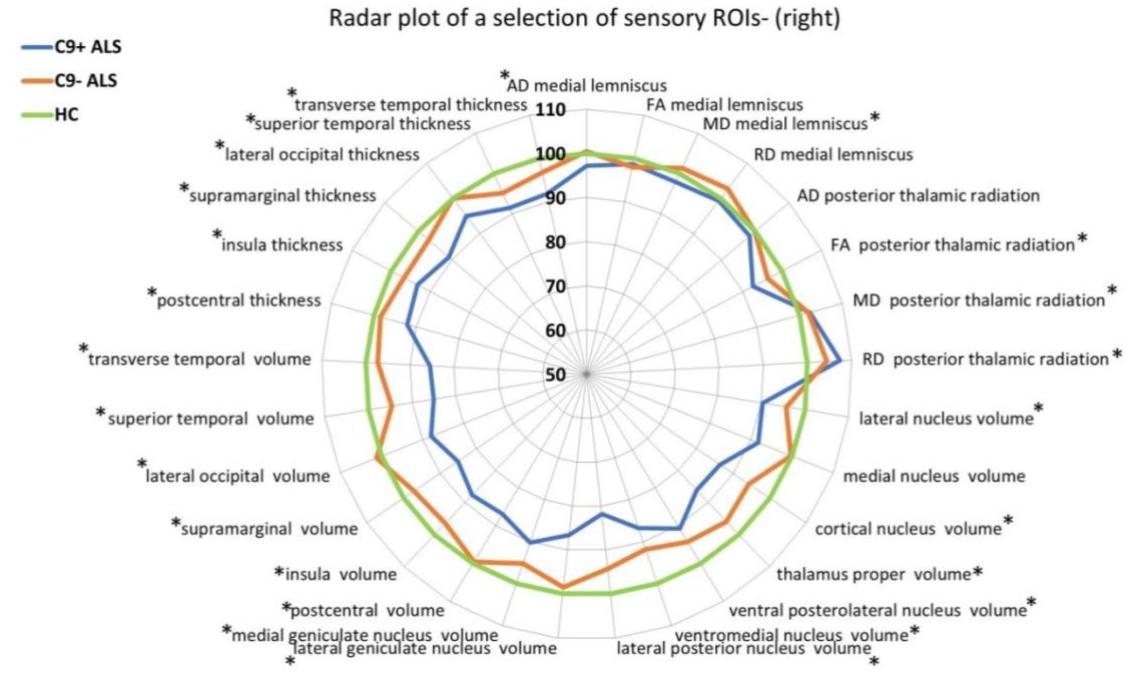

4. Discussion

While ALS is primarily associated with motor and frontotemporal dysfunction [76-80], we have demonstrated the degeneration of anatomical structures involved in somatosensory, visual and auditory processing. Both cortical volumes and cortical thickness were significantly reduced in the postcentral, insular, supramarginal, lateral occipital, superior temporal and transverse temporal cortices bilaterally in C9+ ALS patients in comparison to healthy controls. Bilateral insular, supramarginal, superior temporal and transverse temporal as well as left postcentral cortical thickness reductions were also observed in C9- ALS patients.

The postcentral gyrus is the location of the primary somatosensory cortex which processes somatosensory inputs from the entire body and integrates sensory and motor signals. It is abundantly interconnected with subcortical structures encoding sensory modalities [81] and our data indicate that it is affected in both C9+ ALS and C9- ALS. Our data also confirm insular cortex degeneration irrespective of hexanucleotide repeat status. The insular cortex has ample connections to the secondary somatosensory cortex, sensory nuclei in the thalamus and the amygdala and is involved in multimodal sensory processing, interoception, autonomic control and integration of sensory signals with cognition and emotion. The supramarginal gyrus is part of the somatosensory association cortex and is involved in the perception of space and limb location and the interpretation of tactile sensory data. There is a benefit associated with evaluating multiple cortical measures as imaging indices have different

sensitivity profiles to capture pathological changes. For example, left postcentral cortex involvement in C9-ALS was only detected on cortical thickness analyses. C9+ ALS patients predominantly exhibited symmetrical cortical changes, whereas C9- ALS patients showed more selective cortical pathology which was unilateral in certain regions.

We have confirmed previous reports of overall thalamus volume reduction in C9+ ALS [60], and additionally, demonstrated focal changes in nuclei relaying sensory information; the ventral posterolateral, ventromedial, lateral posterior and lateral geniculate nuclei bilaterally and right medial geniculate nucleus. In C9- ALS, we observed bilateral ventral posterolateral, ventromedial and medial geniculate nucleus degeneration as well as right lateral posterior nucleus pathology. Physiologically, the ventral posterolateral and ventromedial nuclei have a primary sensory function; they relay somatosensory information from the head and body. Our cross-sectional study captures the degeneration of structures involved in sensory processing both at a subcortical and cortical level. Longitudinal data are required to clarify the chronology of cortical and subcortical involvement which may contribute to the corticofugal versus corticopetal spread debate [82-84].

The amygdala mediates a multitude of functions including reward processing, memory consolidation, fear conditioning *etc*., but also integrates somatosensory, visual, auditory, olfactory, gustatory and visceral sensory modalities. Amygdalar degeneration had been previously implicated in both ALS and in primary lateral sclerosis [85-88][70]. In our C9+ ALS cohort, volumes of the lateral and cortical nuclei bilaterally and the left medial nucleus were reduced. In C9- ALS patients, the volumes of the right lateral and

cortical nuclei were reduced compared to healthy controls. The lateral nucleus is involved in relaying nociceptive, tactile, auditory, visual and olfactory processes. The medial nucleus is recipients of olfactory information and is also involved in pheromone-processing. The integration of our cortical and subcortical grey matter findings suggests that GGGGCC repeats in *C9orf72* are associated with more severe and more widespread degeneration of sensory regions compared to C9- ALS and these changes are more likely to be bilateral.

Overt visual symptoms are seldom experienced in ALS, but alterations in visual evoked potentials [47, 48] and retinal changes on optical coherence tomography (OCT) [89] have been reported. Our radiological findings indicate that multiple components of the visual pathway are affected. Both the volume and thickness of the lateral occipital cortex which is involved in object and facial recognition, as well as the volume of the right lateral geniculate nucleus, which is the primary visual relay centre to the visual cortex is reduced in C9+ ALS. Volume of the lateral posterior nucleus is reduced bilaterally in C9+ ALS, but only the right nucleus is reduced in C9- ALS. The lateral posterior nucleus has a role in visual saliency and visually guided behaviours with afferents from the superior colliculus, primary visual, auditory and somatosensory cortices and efferents to the parietal association cortex.

Hearing problems are not commonly associated with ALS, but abnormal auditory evoked potentials have also been reported [8, 48]. Our imaging findings suggest the involvement of auditory pathways. In C9+ ALS, we detected cortical volume and thickness reductions in the superior temporal and transverse temporal cortices bilaterally and right medial geniculate nucleus atrophy. In C9- ALS, cortical thickness

changes were noted in the superior temporal and transverse temporal cortices bilaterally and volume reductions in the right superior temporal cortex and medial geniculate nucleus bilaterally. The transverse temporal gyrus encompasses the primary auditory cortex and the superior temporal region includes the high-order associative auditory cortex and also possesses a number of non-sensory functions. The medial geniculate nucleus is a key hub of the auditory pathway and forms the thalamic relay between the inferior colliculus and the auditory cortex.

A key finding of this study is the demonstration of medial lemniscus involvement in ALS. Axial diffusivity differences have been captured between C9+ and C9- patients in the right medial lemniscus (p = 0.038) and there is a trend of reduced FA in the left medial lemniscus (p = 0.054) in C9- ALS compared to healthy controls. Despite the plethora of tractography studies in ALS [90, 91], sensory white matter tracts are seldom evaluated specifically and brainstem studies typically focus on motor tract degeneration [92, 93]. The medial lemniscus is part of the dorsal column-medial lemniscus pathway which transmits proprioception, touch and vibration. Internal arcuate fibres cross over at the great sensory decussation then ascend as the medial lemniscus, synapsing at the ventral posterolateral nucleus of the thalamus. The posterior thalamic radiation includes functionally diverse thalamocortical white matter projections encompassing sensory and non-sensory fibres which connect the caudal thalamus with the occipital and parietal lobes. FA reductions and increased RD were observed in the posterior thalamic radiation bilaterally in both C9+ and C9- ALS in comparison to healthy controls.

Complementary to established motor [79, 94] and frontotemporal pathology [80, 95], our results provide structural evidence of somatosensory pathway degeneration in both C9+ ALS and C9- ALS. We have detected evidence of multi-level pathological change spanning from the medial lemniscus, through the thalamic nuclei and thalamocortical radiation to the primary sensory cortex. Our data also provide evidence of the concomitant degeneration of cortical and subcortical components of the auditory and visual pathways. On clinical assessment, the majority of patients only exhibit limited sensory signs and report mild or no symptoms. Accordingly, the pathological changes observed on neuroimaging may be considered sub-clinical. While somatosensory, visual and auditory deficits are not routinely investigated, they may have significant implications for activities of daily living. Proprioceptive deficits may contribute to gait impairment, fall risk and impaired dexterity. The wider recognition of proprioceptive deficits may guide falls prevention strategies. Pharyngeal and laryngeal sensory deficits [39, 40] may exacerbate dysphagia, and altered smell and impaired taste [35, 36, 96] may contribute to diminished appetite [37]. Changes in taste are likely to be multifactorial in ALS and may be exacerbated by other factors such as medications and oral candidiasis [35, 36].

This study is not without limitations. We performed a cross-sectional imaging study of symptomatic ALS patients. The longitudinal interrogation of integrity metrics in these anatomical foci would provide important additional insights [82, 97]. We purposefully did not explore direct clinico-radiological correlations between clinical scores and imaging findings, acknowledging the contribution of spinal [98] and peripheral components of the sensory system to clinical manifestations [69, 98, 99]. Our clinical data pertain to *C9orf72* negative patients only and we did not collect visual, auditory

or olfactory clinical data to complement our neuroimaging findings. Some of the anatomical regions we assessed mediate exclusively sensory functions (postcentral gyrus, medial lemniscus *etc*.), but some of the regions we evaluated (posterior thalamic radiation, insula *etc*.) have both sensory and non-sensory roles and their degeneration is therefore less specific to sensory functions. While we have confirmed the involvement of cerebral hubs of sensory circuits, future studies of sensory dysfunction in ALS should acquire quantitative electrophysiology data to evaluate the spinal and peripheral components of sensory networks. Notwithstanding these limitations, we have demonstrated the degeneration of cortical, subcortical and white matter components of somatosensory pathways in a condition which is primarily associated with motor and frontotemporal dysfunction.

5. Conclusions

Key subcortical hubs, white matter tracts and cortical components of the somatosensory system are affected in ALS. ALS should no longer be regarded as a condition exclusively involving motor and frontotemporal regions. Subclinical or subtle sensory deficits may exacerbate mobility, impact on dexterity, increase fall risk and may have ramifications for bulbar dysfunction. Somatosensory deficits in ALS are important to recognise, should be routinely screened for, and should be taken into account when planning multidisciplinary interventions.

CHAPTER 4: Review of cerebellar pathology in ALS

Introduction

Amyotrophic lateral sclerosis (ALS) is a relentlessly progressive neurodegenerative condition. While it is primarily characterized by the degeneration of upper and lower motor neurons, ALS is now recognized as a multi-system disorder. Cerebellar pathology in ALS has been demonstrated by a multitude of neuropathology and neuroimaging studies (409), but its role in the disease process is poorly characterized. Clinical reports of overt cerebellar signs are sparse, frank dysmetria, dysdiadochokinesia and ataxia are rarely reported in ALS (410-413). The clinical assessment of the cerebellum in ALS is notoriously challenging due to concomitant upper and lower motor neuron degeneration. Eye-movement abnormalities, such as nystagmus (414), pursuit (415-417) and saccadic impairment (416-418) have been consistently described in ALS. Bulbar dysfunction is a pathognomonic feature of ALS (419) which is often exclusively linked to corticobulbar tract and brainstem nuclei degeneration despite the likely contribution of cerebellar pathology to bulbar symptoms (420). Primary lateral sclerosis (PLS) is a progressive, low-incidence upper motor neuron disorder which carries a better prognosis than ALS. A common symptom of both ALS and PLS, is pseudobulbar affect, which is traditionally linked to corticobulbar disconnection, but cerebellar pathology is increasingly recognised as an important aetiological factor (421-423).

Functional anatomy

The cerebellum comprises two hemispheres with deep fissures and folia connected by the vermis. It is located in the posterior cranial fossa, inferior to the occipital and temporal lobes and posterior to the pons. Each hemisphere has three lobes, the flocculonodular lobe, anterior lobe and posterior lobe divided by two fissures – the posterolateral fissure and the primary fissure. **(Figure 4.)** The white matter surrounds four cerebellar nuclei, the fastigial, emboliform, globose and dentate nuclei. Functionally, the cerebellum is classically divided into three zones: (1) the vestibulocerebellum which is the flocculonodular lobe. It is primarily involved in balance and ocular reflexes. Inputs arise from vestibular nuclei and semicircular canals as well as visual inputs from superior colliculi and visual cortex and outputs synaps onto the vestibular nuclei; (2) the spinocerebellum which is made up of the vermis and the paravermis or intermediate zone on either side of the vermis. It is involved in the adjustment of body movements, error correction and proprioception. It receives proprioceptive inputs from the dorsal columns of spinal cord and trigeminal nerve and also visual and auditory inputs and has projections onto the deep cerebellar nuclei and brainstem; (3) the cerebrocerebellum which comprises of the lateral hemispheres, lateral to the intermediate zone. It is involved in planning movements, motor learning as well as cognitive functions. It receives inputs from cerebral cortex and pons and sends outputs to the thalamus and red nuclei (424). Phylogenetically, the cerebellum is divided as follows: (1) the archicerebellum which is the vestibulocerebellum, and is evolutionarily the oldest structure; (2) the paleocerebellum which is the spinocerebellum; (3) the neocerebellum which is the cerebrocerebellum, and is

evolutionarily the newest structure (424). There are three major fibre bundles connecting the cerebellum to the rest of the brain known as the cerebellar peduncles. The superior cerebellar peduncle or brachium conjunctivum is the primary output pathway of cerebellum. It is mostly made up of efferent fibres originating from the dentate nucleus projecting onto the midbrain, thalamus and medulla. The dentato-rubro-thalamo-cortical and cerebello-thalamo-cortical pathways pass through this peduncle. This peduncle is primarily involved in motor planning. The middle cerebellar peduncle or brachium pontis is primarily made up of afferent fibres originating from the pontine nuclei as part of the cortico-ponto-cerebellar tract. The inferior cerebellar peduncle (restiform and juxtarestiform bodies) is made up of both afferent and efferent fibres involved in proprioception and vestibular functions. The dorsal spinocerebellar tract passes through the inferior peduncle. This peduncle is involved in maintenance of posture and balance (424). **(Figure 4.)** Neurulation is the process by which the central portion of the ectoderm forms the neural plate which is the origin of the entire nervous system. At week 3 of gestation, the neural plate folds to form the neural tube, which in week 4 undergoes flexion at the region of the mesencephalon, which is the future midbrain. Above the mesencephalon is the prosencephalon, which is the future forebrain and beneath it is the rhombencephalon, which is the future hindbrain. The caudal rhombencephalon develops into the medulla oblangata and the rostral part becomes the pons and cerebellum (424).

Cerebellar function has been traditionally associated with motor control and motor learning, however, it's physiological role in mediating cognitive and behavioural

functions such as executive functions, language, spatial cognition and mood regulation is also increasingly recognized (425). The 'Dysmetria of thought' theory was coined to denote cognitive and emotional disorders arising from cerebellar pathology (426). Cerebellar lobules are not only activated during motor and sensorimotor task, but during executive, working memory, language and emotional processing paradigms (427). Cerebellar pathology has been consistently implicated in impaired social cognition (428), pathological crying and laughing (429, 430) and language deficits (431). Neuropsychological domains that show focal cerebellar activity on cerebellar imaging studies include attention (432), working memory (433) and envisioning future events (434). Attention and visuospatial skills are noted to be particularly impaired in subjects with cerebellar insults (435). Emotional dysregulation including irritability, disinhibition and impulsivity has been linked to lesions of the vermis (436). While lesions in the anterior lobe have been primarily linked to motor deficits, pathology of the posterior lobe is associated with cerebellar cognitive affective syndrome (CCAS), encompassing problems with language, speech, executive and visuospatial functions and emotional affect (437, 438). Evidence is slowly mounting that specific lobules have specific roles in mediating cognitive processes (427, 438). Based on the expanding spectrum of physiological roles of the cerebellum and the high number of recently published imaging studies in ALS, the main aim of this review is to summarise cerebellar neuroimaging and post-mortem findings in ALS and other motor neuron disease phenotypes. An additional objective of this manuscript is to examine the evidence for cerebellar neuroplasticity in ALS and link radiological observations to post mortem findings.

Figure 4*: Gross anatomy of the cerebellum: (a) dorsal view of the cerebellum, (b) ventral view of the cerebellum, (c) lobes of the cerebellum and (d) sagittal view of the cerebellum.*

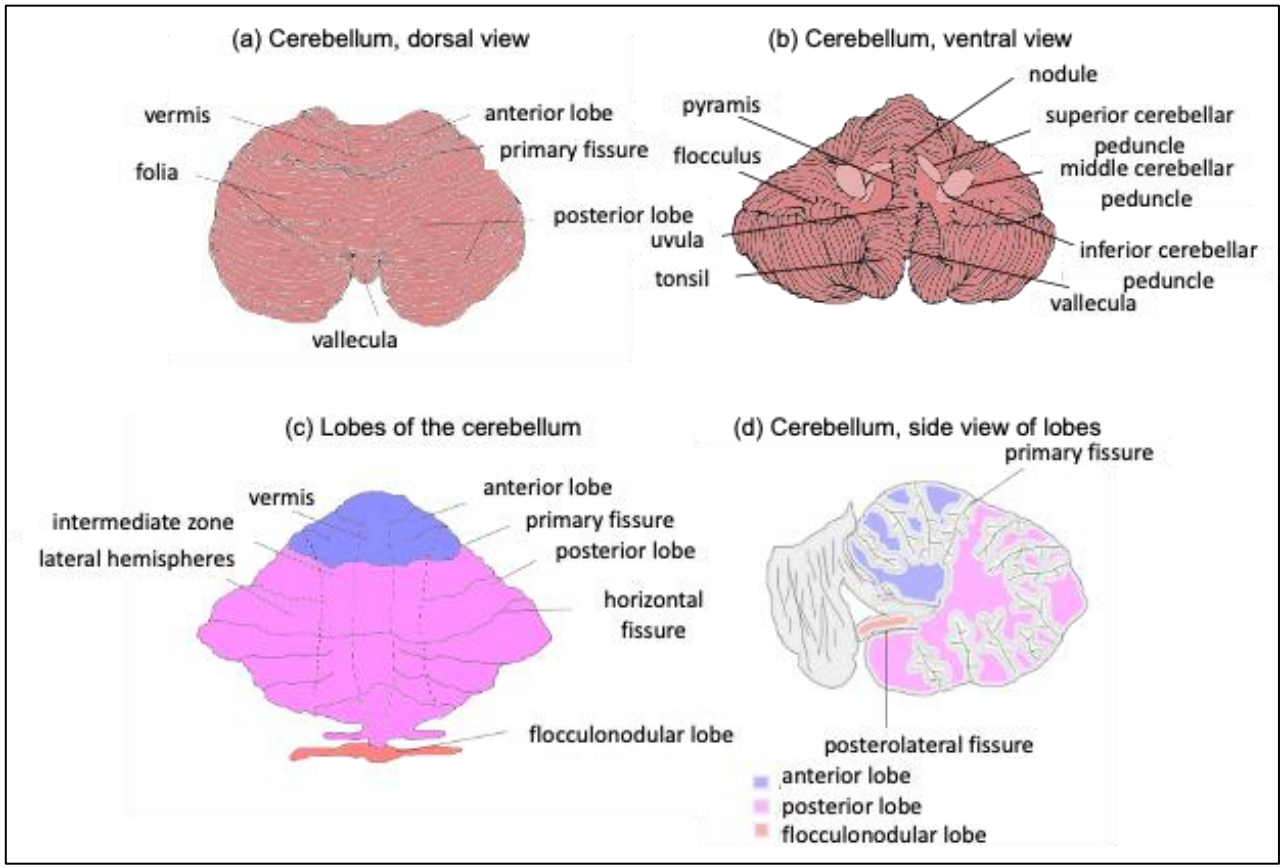

Search strategy and selection criteria

A systematic literature search was performed on PubMed using the core search terms "amyotrophic lateral sclerosis", "primary lateral sclerosis" and "motor neuron disease" combined individually with each of the following keywords as search word pairs: "cerebellum", "cerebellar", "magnetic resonance imaging", "positron emission tomography" and "post mortem". Only original research papers were systematically reviewed. Conference abstracts, review papers, opinion pieces and editorials were excluded. No exclusion criteria were set based on year of publication. Based on the above criteria, a total of 69 original research papers were identified, selected and reviewed.

Results

I. Imaging

Only two cerebellar studies included pre-symptomatic patients (25, 30). About half of the identified studies collected genetic information, but only 11 studies stratified their ALS cohort by genotype (128, 138, 439-447). The vast majority of identified studies were cross-sectional with only 4 longitudinal imaging studies describing cerebellar changes (151, 322, 447, 448). Sample size limitations are evident, with only a minority of studies including over 100 participants. Four studies investigated over 200 participants and most of these were PET studies (449-452). The majority of studies were case-control studies, with only a few exceptions. While most studies reported

complementary clinical or neuropsychological assessments, only a handful of studies performed clinic-radiological correlations (440, 453-456). A minority of studies acquired data on 1.5 Tesla (T) scanners, 3T scanners were most commonly used and only one study collected data on a 7T platform (338). Over half the studies assessed multiple imaging parameters.

1. Grey matter alterations

While the cerebellar imaging data are characteristically challenging to quantitatively interpret, novel pipelines have been developed to evaluate infratentorial structures. Cerebellar changes are often observed on whole-brain analyses (409). Structural imaging readily captures cerebellar grey matter atrophy in ALS and ALS-Plus patients (446, 457, 458) and progressive cerebellar degeneration has been detected longitudinally (151). Cerebellar degeneration has been described in *C9orf72* positive ALS patients (445), as well as in pre-symptomatic GGGGCC hexanucleotide carriers above 40 years of age (25). A study specifically investigating genotype-associated cerebellar profiles in ALS patients revealed symmetrical patterns of cerebellar atrophy in *C9orf72* ALS preferentially affecting lobules I–IV, V, VIIIA/B, IX and the vermis (406). In C9orf72 *negative* sporadic ALS patients, more focal changes were observed in lobules I–IV and V on morphometric analyses (406). Structural cerebellar changes in the anterior lobule have been correlated to disease severity, and changes in the posterior lobule have been linked to cognitive impairment (453). Interestingly, one study reported increased grey matter volume in the cerebellum in ALS (362), and another detected no cerebellar atrophy (442, 459). **(Table 16.)**

2. White matter changes

Cerebellar white matter alterations have also been specifically studied (128, 138, 448, 460, 461) and genotype-associated patterns have recently been proposed (128, 406). Decreased fractional anisotropy (FA) and increased axial diffusivity (AD) and radial diffusivity (RD) in lobules I–IV, V have been observed in *C9orf72* ALS, while in sporadic ALS, decreased FA in lobules I–IV, V, IX and crura I and II and increased RD in lobules I–IV, V and VI was detected (406). Cerebro-cerebellar tractography in ALS reveals preferential white matter degeneration in the cerebellar peduncles and ponto-cerebellar tracts (406, 423, 462-467). Significant alterations were also observed in the dentato-rubro-thalamo-cortical tract proximal to the motor cortex in both ALS and PLS (468). Progressive diffusion tensor imaging (DTI) changes were noted in the cerebellum in a longitudinal study conducted over two years (322). **(Table 16.)**

3. Functional and metabolic studies

Functional MRI findings are relatively inconsistent(469). Both decreased (338, 467, 470) and increased cerebro-cerebellar connectivity have been reported (30, 360, 439, 471), the latter postulated to represent a compensatory process (439, 452). Increase in functional connectivity has been observed between the cerebellum and a network comprising the precuneus, cingulate and middle frontal lobe in both presymptomatic and symptomatic ALS (30). Increased functional connectivity (FC) between bilateral superior parietal lobule and right anterior inferior cerebellum is thought to correlate with disease severity (471), but direct clinico-radiological correlations are widely seen as contentious (456). In the paradigm-based studies increased cerebellar activation is

often observed during various motor tasks (472, 473), and particularly in patients with upper motor neuron (UMN) predominant symptoms (439, 440). In ALS with cognitive impairment, alterations of regional homogeneity (ReHo) in the right inferior cerebellar area have been noted (441). Increased cerebellar 'degree centrality' (DC) was observed in the posterior lobes and bilateral cerebellum crura (177). The involvement of the cerebellar nuclei has also been demonstrated. While no volume reductions were noted in the dentate nucleus, the resting state FC of the dentate nucleus is thought to correlate with WM changes at superior cerebellar peduncle (463). **(Table 17.)** Significantly reduced mean regional cerebral blood flow (rCBF) has been also observed in the cerebellar hemispheres (444). The cerebellum is rarely evaluated by spectroscopy, but one study found that the cerebellar N-acetylaspartate (NAA) concentrations are unaltered in MND patients (474). **(Table 17.)** While some PET studies detect no changes in the cerebellum (475), some describe hypometabolism (447), the majority of PET studies identify cerebellar hypermetabolism in ALS (443, 476-478), both in spinal-onset disease (449, 455), bulbar-onset (455), as well as in ALS-FTD (451). The reports are conflicting, with another study reporting **(Table 18.)**

Table 16*: A selection of grey and white matter studies investigating cerebellar pathology in MND*

Author and year of publication	Study participants (patients/ healthy controls)	Methodology	Clinical assessments	Main findings
Bede et al., 2021 (406)	161/110	Structural (volumetry, cortical thickness), diffusion (DTI)	ALSFRS-r, cerebellar assessment	-cerebellar pathology confined to lobules I-V of anterior lobe in patients with sporadic ALS -considerable posterior lobe and vermis disease burden identified in *C9orf72* mutation carriers -patients with intermediate *ATXN2* expansions did not exhibit significant cerebellar pathology
Baek et al., 2020 (462)	96/47	diffusion (DTI)	ALSFRS-r	-significant differences between ALS and healthy controls in cerebellar peduncle
De Marchi et al., 2020 (464)	41/0	diffusion (DTI)	ALSFRS-r, FVC, MMSE, RCPM, Cognitive Estimates Test, FAB, Clock Drawing Test, Digit Span test, Short Story Test, Trail Making A-B Test, Attentive Matrices, verbal fluency and comprehension, NPI	-revealed significant FA reduction and ADC increase in all selected regions including cerebellar peduncle
Consonni et al., 2019 (453)	66/28	Structural (cortical thickness, cortical volume)	ALSFRS-R, phonemic fluency index, object naming, SET, stroop, RAVLT, FBI	-disease severity correlated with cerebellar cortical volume reduction in anterior lobules -decreased cerebellar cortical volume in posterior lobules related to cognitive impairment
Qiu et al., 2019 (362)	60/60	structural (VBM), diffusion (DTI)	ALSFRS-r, MOCA	-ALS patients have increased GMV in bilateral cerebellum -decreased FC in cerebellum anterior lobe
Tu et al., 2019 (468)	19/17	diffusion (DTI)	ALSFRS-r	-Significant alterations across diffusion metrics in the DRTC proximal to the motor cortex were found in both ALS and PLS patient groups -PLS patients have independent diffusion abnormality in cerebellar region of DRTC and SC tracts
Bede et al., 2018 (151)	32/69	structural (VBM, cortical thickness), diffusion (DTI)	ALSFRS-r	-gradually progressive cerebellar grey matter degeneration throughout three time-points

Christidi et al., 2018 (423)	56/25	structural (VBM), diffusion (DTI)	ALSFRS-r, CNS-LS, ADI-12, neuropsychological assessment	-WM abnormalities detected in WM associative and ponto-cerebellar tracts
Christidi et al., 2018 (446)	50/25	structural (VBM), diffusion (DTI)	ALSFRS-r, MMSE, TMT, SNST-CWIS, WCST, RAVLT, BSRT, RCFT, WAIS, Age-Scale Score	-reduced GMV in cerebellar areas in ALS -reduced GMV in cerebellum in ALS-Plus
Christidi et al., 2018 (457)	17/22	structural (VBM), TMS	ALSFRS-r	-decreased GM density in cerebellar regions in ALS
Feron et al., 2018 (459)	31/14	Structural (VBM, volumetry)	ALSFRS-R, MRC, Ashworth scale, Berg Balance scale, CVLT, Stroop, verbal fluency test, WCST, forward and backward digit span, computational gait analysis	-no cortical changes in the cerebellum
Menke et al., 2018 (322)	16/0	Structural (VBM), diffusion (DTI), functional (rsfMRI)	ALSFRS-r, UMN score, ACE-R	-progressive DTI changes -increased RD, AD, MD in cerebellum
Schoenecker et al., 2018 (442)	58/19	Structural (volumetry)	MMSE, FTD-CDR-SOB	-no significant atrophy of cerebellar regions
Agosta et al., 2017 (445)	86/22	structural (cortical thickness, volume), diffusion (DTI), functional (rsfMRI)	ALSFRS-r, UMN score, MMSE, RPCM, Phonemic fluency, Semantic fluency, Digit span backward, Cognitive estimation task, WCST, Weigl test, Digit span forward, Rey's list immediate recall, Rey's list delay recall, Oral noun confrontation naming subtest of BADA, FBI, ALS-FTD questionnaire	-C9orf72 patients showed cerebellar and thalamic atrophy
Kim et al., 2017 (458)	47/28	structural (VBM)	ALSFRS-R, contrasting program go, no-go test, category verbal fluency test (animal item), phonemic fluency test, Stroop test color reading and backward digit span test, forward digit span test, K-BNT, auditory comprehension test, calculation, RCFT, SVLT, Korean HVLT, K-MMSE, CDR, Caregiver-Administered Neuropsychiatric	-ALSci group show decreased volume in the left cerebellum compared to healthy controls -ALSci show decreased brain volume in the bilateral cerebellum compared to pure ALS

			Inventory	
Papma et al., 2017 (25)	18/15	structural (VBM), diffusion (DTI)	neuropsychological tests	-*C9orf72RE* carriers above 40 years of age, have grey matter volume loss in cerebellum
Bae et al., 2016 (479)	42/37	Structural (VBM), diffusion (DTI), TMS	ALSFRS-r, ACE-R, CBI-R	-more grey-matter changes in the cerebellum in ALS compared to controls -in bvFTD, severe degenerative changes observed in the cerebellum
Trojsi et al., 2015 (461)	54/18	structural (VBM), diffusion (DTI)	ALSFRS-R, ACE-R, FrSBe, UMN score, FVC	-ALS patients had decreased FA and increased MD and RD in left cerebellar hemisphere and brainstem precerebellar nuclei
Bede et al., 2014 (164)	27/42	structural (cortical thickness), diffusion (DTI)	ALSFRS-r	-higher FA in association with male gender in cerebellum
Bede et al., 2014 (128)	36/42	diffusion (DTI)	0	-FA and RD also captured diffusivity differences in the cerebellum -bilateral symmetrical cerebellar white matter pathology detected in *C9orf72* negative cohort -*C9orf72* positive patients have reduced AD, MD and RD in comparison to *C9orf72* negative patients
Floeter et al., 2014 (422)	47/0	diffusion (DTI)	ALSFRS-r, MDRS-2, MMSE, BDI-2, FrsBe, University of California Los Angeles (UCLA) Neuropsychiatric Index	-patients with PBA had increased MD of WM tracts underlying middle cerebellar peduncle -disruption of corticopontocerebellar pathways supports hypothesis that PBA can be viewed as a "dysmetria" of emotional expression resulting from cerebellar dysmodulation
Hartung et al., 2014 (460)	30/37	diffusion (VBI)	ALSFRS-r	-widespread WM intensity increases in cerebellum
McCluskey et al., 2014 (480)	30/0	structural (VBM), diffusion (DTI)	clinical assessment, ALSFRS-r	-greater cerebellar disease in ALS-plus patients
Bede et al., 2013 (138)	39/44	structural (cortical thickness, VBM), diffusion (DTI)	executive function, letter fluency, category fluency, attention, memory, language, visuospatial skills, and behavioral domains	-WM changes in *C9orf72* negative group confined to corticospinal and cerebellar pathways
Keil et al., 2012 (448)	24/24	diffusion (DTI)	ALSFRS-r, MMSE, FAB, SF36	-reduced FA in cerebellum in ALS

Prudlo et al., 2012	22/21	Diffusion (DTI)	ALSFRS-r	-widespread white matter changes in all fibre groups of the brain including cerebellum
Minnerop et al., 2009 (465)	12/12	structural (VBM), relaxometry (VBR)	0	-reduced WM in right middle cerebellar peduncle
Kassubek et al., 2005 (481)	22/22	statistical parametric mapping (SPM) and VBM	NA	-white matter alterations in cerebellum

ACE-R - Addenbrooke's Cognitive Examination Score; **AD** – axial diffusivity; **ADC** - apparent diffusion coefficient; **ADI-12** - ALS-Depression Inventory; **ALS** - amyotrophic lateral sclerosis; **ALS-FTD** - amyotrophic lateral sclerosis and frontotemporal dementia; **ALSci** – amyotrophic lateral sclerosis with cognitive impairment; **ALSFRS-r** – revised Amyotrophic Lateral Sclerosis Functional Rating Scale; **ATXN2**- ataxin 2 gene; **BADA** - Batteria per l'Analisi del Deficit Afasico;; **BDI-2** - Beck Depression Inventory-II; **BSRT** - Babcock Story Recall Test; **bvFTD –** behavioural variant frontotemporal dementia; **C9orf72** - chromosome 9 open reading frame 72 gene; **CBI-R** - Cambridge Behavioural Inventory Revised; **CDR** - Clinical Dementia Rating; **CNS-LS** - Center of Neurologic Study Lability Scale ; **CVLT-II** - California verbal learning test II**; DRTC** - dentato-rubro-thalamo-cortical ; **DTI** - diffusion tensor imaging; **FA** – fractional anisotropy; **FA** – fractional anisotropy; **FAB** - Frontal Assessment Battery; **FBI** - Frontal behavioral inventory; **FC** - functional connectivity; **FrSBe** - Frontal Systems Behavioral Evaluation; **FTD-CDR-SOB** - FTD modified Clinical Dementia Rating Scale Sum of Boxes; **FVC** – forced vital capacity **; GM** – grey matter; **GMV** – grey matter volume; **HVLT** - Hopkins Verbal Learning Test; **K-BNT** - Korean version of the Boston Naming Test; **MD** – mean diffusivity; **MDRS-2** - Mattis Dementia Rating Scale-2; **MMSE** – mini mental state exam; **MOCA** – montreal cognitive assessment; **MRC** – the Medical Research Council score; **NPI** - Neuropsychiatric Inventory; **PBA** – pseudobulbar affect; **PLS** - primary lateral sclerosis; **RAVLT** - Rey Auditory Verbal Learning Test; **RCFT** - Rey's Complex Figure Test-Immediate Recall; **RD** – radial diffusivity; **RPCM** - Raven's Progressive Colored Matrices; **rsfMRI** -resting state functional magnetic resonance imaging; **SC** – spino-cerebellar; **SET** - story-based empathy task; **SF36** - 36-item Short Form Health Survey; **SNST-CWIS** - Stroop Neuropsychological Screening Test-Color Word Interference Score; **SPM** - statistical parametric mapping; **SVLT** - Seoul Verbal Learning Test; **TMS** - Transcranial Magnetic Stimulation; **TMT** – trail making test; **UMN** – upper motor neuron; **VBM** – voxel based morphometry; **VBR** - voxel-based relaxometry; **WAIS** - Wechsler Adult Intelligence Scale ; **WCST** - Wisconsin Card Sorting Test; **WM** – white matter

Table 17*: A selection of functional MR studies evaluating cerebellar pathology in ALS: fMRI & spectroscopy*

Author and year of publication	Study participants (patients/ healthy controls)	Methodology	Clinical assessments	Main findings
Abidi et al., 2021 (439)	31/14	structural, functional (fMRI)	ALSFRS-r, CVLT II, Stroop, Verbal fluency test, WCST, digit span, MIQ-rs	-UMN predominant ALS patients show increased cerebellar signal during imagined locomotion -increased effective connectivity of striato-cerebellar and parieto-cerebellar circuits may represent compensatory process
Barry et al., 2021 (338)	12/9	functional (fMRI)	ALSFRS-R, SVC, quantitative muscle strength test using hand-held dynamometry	-disruption in long range functional connectivity between superior sensorimotor cortex and bilateral cerebellar lobule VI
Abidi et al., 2020 (440)	31/14	structural, functional (fMRI)	ALSFRS-r, CVLT II, Stroop, Verbal fluency test, WCST, digit span	-increased cerebellar activation in UMN predominant ALS patients in comparison to healthy controls and LMN predominant ALS -increased effective connectivity between cerebellum and caudate -decreased connectivity between SMA and cerebellum when performing self-initiated movement -UMNp patients, a positive correlation detected between clinical variables and striato-cerebellar connectivity
Bharti et al., 2020 (463)	71/56	structural, functional (rsfMRI), diffusion tensor imaging (DTI)	ALSFRS-r, ECAS, finger tapping, foot tapping, UMN burden	-no dentate nucleus (DN) volumetric changes -DN rsFC correlated with WM abnormalities at superior cerebellar peduncle -altered cerebellar rsFC connectivity with motor and extra-motor regions in ALS & impaired rsFC likely due to observed cerebellar peduncular WM damage
Hu et al., 2020 (441)	42/21	structural (VBM), functional (rsfMRI)	ALSFRS-r, ACER-R	-alterations of ReHo in the right inferior cerebellar area in ALS with cognitive impairment

Trojsi et al., 2020 (467)	32/21	structural (VBM), functional (rs-fMRI), diffusion (DTI)	ALSFRS-r, MMSE, ECAS, digit span, Stroop, fluency, RAVLT-immediate and delayed recall, RCPM, HADS, ALS-FTD-Q	-reduced functional connectivity between bilateral hippocampus, bilateral parahippocampal gyri and cerebellum in ALS patients
Menke et al., 2016 (30)	24/12	structural (VBM), diffusion (DTI), functional (rs-fMRI)	ALSFRS-R	-FC between cerebellum and a network comprising precuneus, cingulate & middle frontal lobe significantly higher in presymptomatic ALS and symptomatic ALS in comparison to controls
Zhou et al., 2016 (177)	43/44	functional (rsfMRI)	ALSFRS-r	-ALS patients showed significant increase of DC in the left cerebellum posterior lobes & bilateral cerebellum crus in comparison to controls
Fekete et al., 2013 (470)	40/30	functional (rsfMRI)	ALSFRS-r	-widespread alterations in motor functional connectivity including in cerebellum
Zhou et al., 2013 (471)	12/12	functional (rsfMRI)	ALSFRS-r	-Increased FC between bilateral superior parietal lobule and right anterior inferior cerebellum found to be correlated with disease severity
Agosta et al., 2011 (360)	26/15	functional (rsfMRI)	ALSFRS-r, MRC score	-significantly increased functional connectivity between left SMC and right cingulate cortex, parahippocampal gyrus, and cerebellum-crus II
Han et al., 2006 (472)	15/15	functional (fMRI)	NA	-activation areas in ipsilateral cerebellum significantly larger in ALS in comparison to healthy controls
Konrad et al., 2006 (473)	10/10	functional (fMRI)	0	-activation increase observed in cerebellum
Schoenfeld et al., 2005 (482)	6/6	structural, functional (fMRI)	ALSFRS-R, motor task	-difficulty–related activity in the left cerebellum observed in patients
Gredal et al., 1997 (474)	10/8	spectroscopy (MRS)	NA	-concentration of NAA in the cerebellum unaltered in MND patients
Tanaka et al., 1993 (444)	13/13	regional cerebral blood flow (rCBF) and oxygen metabolism (rCMRO2)	NA	-significant reduction in the mean rCBF was also found in the cerebellar hemispheres in progressive dementia with ALS

ACE-R - Addenbrooke's Cognitive Examination Score; **ALS** - amyotrophic lateral sclerosis; **ALS-FTD-Q** – Amyotrophic Lateral Sclerosis-Frontotemporal Dementia-Questionnaire; **ALSFRS-r** – revised Amyotrophic Lateral Sclerosis Functional Rating Scale; **CVLT-II** - California verbal learning test II; **DC** - degree centrality; **DN** – dentate nucleus; **DTI** - diffusion tensor imaging; **ECAS** - Edinburgh Cognitive and Behavioural ALS Screen; **FC** - functional connectivity; **fMRI** – functional magnetic resonance imaging; **HADS** - Hamilton depression rating scale; **LMN**- lower motor neuron; **MIQ-rs** - Movement Imagery Questionnaire revised 2nd version; **MMSE** – mini mental state exam; **MRC** – the Medical Research Council score; **NAA** - N-acetylaspartate ; **RAVLT** - Rey Auditory Verbal Learning Test; **rCBF** - regional cerebral blood flow; **ReHo** - regional homogeneity; **RPCM** - Raven's Progressive Colored Matrices; **rsFC** - resting-state functional connectivity; **rsfMRI** -resting state functional magnetic resonance imaging; **SMA** - supplementary motor area; **SVC**- slow vital capacity; **UMN** – upper motor neuron; **VBM** – voxel based morphometry; **WCST** - Wisconsin Card Sorting Test; **WCST** - Wisconsin Card Sorting Test; **WM** – white matter

Table 18*: A selection of PET studies commenting on cerebellar pathology in ALS*

Author and year of publication	Study participants (patients/ healthy controls)	Methodology	Clinical assessments	Significant findings
Canosa et al., 2021 (454)	165/0	F-FDG PET	FrsBe	-FrsBe apathy before-after gap positively correlated with cerebellar and pontine clusters
Canosa et al., 2021 (483)	111/40	18F-FDG-PET	ALSFRS-r, ECAS	-negative correlation between medial frontal cluster and cerebellum found in ALS patients may reflect cerebellar compensation
Canosa et al., 2020 (451)	274/0	18F-FDG-PET	ALSFRS-r, MMSE, The Letter and Category Fluency Test, FAB, Digit Span Forward and Backward, The Trail-Making Test (TMT) A and B, RAVLT, BSRT, ROCF, RPCM (CPM47)	-ALS-FTD patients showed cerebellar relative hypermetabolism
Calvo et al., 2019 (447)	101/0	structural, diffusion (DTI), 123I-ioflupane (123I-FP-CIT) SPECT, 18F-FDG-PET18F-FDG-PET	ALSFRS-R, MRC score, Ashworth scale, neuropsychology battery, MDS-UPDRS	-ALS-PK patients showed a relative hypometabolism in left cerebellum
Sala et al., 2019 (455)	95/0	18F-FDG-PET	ALSFRS-r, cognitive tests	-hypermetabolism in cerebellum in both spinal onset and bulbar onset ALS patients -severity of motor symptoms correlates with cerebellar hypermetabolism in bulbar-onset ALS
Buhour et al., 2017 (476)	37/37	structural (VBM), FDG-PET	ALSFRS-r, MRC, Muscle Strength Scale, TMT, letter verbal fluency, episodic memory, theory of mind, Mattis	-hypermetabolism in cerebellum

Canosa et al., 2016 (443)	170/NA	18F-FDG-PET	NA	-Hypometabolism in frontal regions was associated to hypermetabolism in cerebellum
Matias-Guiu et al., 2016 (477)	18/24	F-FDG PET, amyloid-PET with (18)F-florbetaben	ALSFRS-r, ACE-III, MMSE, memory span, visuospatial span (Corsi block-tapping test), TMT, ROCF, Free and Cued Selective Reminding Test, VOSP, Stroop Color-Word Interference Test, letter verbal fluency, category fluency test, Tower of London, action fluency tests, picture-sentence matching tasks, semantic association tests, the Hayling Test, ECAS, CBI-R) Anosognosia Questionnaire for Dementia	-ALS exhibit hypometabolism in frontal area and hypermetabolism in cerebellum compared to healthy controls -changes in metabolism in cerebellum in ALS with or without cognitive impairment
Pagani et al., 2016 (450)	259/40	FDG-PET	ALSFRS-r	-cerebellar/midbrain component accounted for highest accuracy in separating ALS patients from controls
Pagani et al., 2014 (449)	195/40	(18)F-FDG-PET	0	-spinal patients have relative hypermetabolism in right cerebellum
Cistaro et al., 2012 (478)	32/22	F-FDG PET	phonological verbal fluency test (FAS), TMT, Stroop, WCST	-Highly significant relative increases in glucose metabolism distribution in cerebellum in ALS compared to healthy controls
Ludolph et al., 1992 (475)	18/NA	PET	neuropsychological assessment	-no changes seen in cerebellum
Dalakas et al., 1987 (484)	12/11	[18F]FDG-PET	0	-hypometabolism did not extend to cerebellum

ACE-III - Addenbrooke's cognitive examination III; **ALS** - amyotrophic lateral sclerosis; **ALS-FTD** - amyotrophic lateral sclerosis and frontotemporal dementia; **ALS-PK** - Amyotrophic lateral sclerosis with parkinsonian symptoms; **ALSFRS-r** – revised Amyotrophic Lateral Sclerosis Functional Rating Scale; **BSRT** - Babcock Story Recall Test; **CBI-R** - Cambridge Behavioural Inventory Revised; **DTI** - diffusion tensor imaging **; ECAS** - Edinburgh Cognitive and Behavioural ALS Screen; **F-FDG** – (18)F-fluorodeoxyglucose; **FAB** - Frontal Assessment Battery; **FrSBe** - Frontal Systems Behavioral Evaluation; **MDS-UPDRS** - Movement Disorders Society Unified Parkinson's Disease Rating Scale; **MMSE** – mini mental state exam; **MRC** – the Medical Research Council score; **PET** - positron emission tomography; **RAVLT** - Rey

Auditory Verbal Learning Test ; **ROCF** - Rey-Osterrieth Complex Figure; **RPCM** - Raven's Progressive Colored Matrices; **SPECT** - single-photon emission computerized tomography; **TMT** – trail making test; **VOSP** - Visual Object and Space Perception Battery; **WCST** - Wisconsin Card Sorting Test

II. Post-mortem findings

While cerebellar changes are seldom evaluated specifically, cerebellar pathology is readily observed post-mortem (485, 486). UBQLN-positive cytoplasmic inclusions in cerebellar granular layer (487), neurofibrillary tangles (NFTs) (488) and neuronal and glial TDP-43 pathology have been consistently described (489). Cerebellar degeneration has been linked to bulbar ALS (490), but other studies do not identify significant cerebellar alterations (491, 492). **(Table 19.)** p62 positive, p-TDP-43 negative neuronal intranuclear inclusions (493) have been observed in *C9orf72* and the severity of cerebellar changes are thought to depend on repeat length expansion (494). In PLS, cerebellar involvement is clearly established. Some studies observed ballooning of dendrites in molecular and Purkinje cell layers of the cerebellum (495), and dentate nucleus degeneration (496), while other found no significant changes (497).

III. Animal models

With few exceptions (498), animal models of ALS also exhibit cerebellar pathology. In *SOD1(G93A)* transgenic mice, PARP-immunoreactive astrocytes (499) and pERK-immunoreactive astrocytes (500) were observed in cerebellar nuclei. Reduced tau-mRNA expression was observed at the symptomatic stage of ALS (501). Increased cerebellar TRPV4 expression (502) and enhanced LOX gene expression (503) have also been shown. Cerebellar Purkinje cell degeneration and neuroinflammation was noted in *MATR3 S85C* knock-in mice (504), *C9orf72* mice (505) as well as in *SOD1* mice (503).

Table 19*: A selection of post mortem studies describing cerebellar pathology in ALS*

Author and year of publication	Summary of findings
Jones et al., 2021 (506)	HML6_3p21.31c consistently upregulated in ALS in cerebellum tissue
Yang et al., 2019 (507)	similar levels of nonphosphorylated TDP-43 were found in all 3 regions (motor cortex, spinal cord, cerebellar vermis) between ALS groups (ALS with repeat expansions in the *ATXN2* or *C9orf72* genes and sporadic disease)
Blitterswijk et al., 2013 (494)	Repeat lengths in the cerebellum were smaller than those in the frontal cortex and those in blood in *C9orf72* symptomatic patients Substantial variation in repeat sizes between samples from cerebellum, frontal cortex, and blood Longer repeat sizes in the cerebellum associated with survival disadvantage
Brettschneider et al., 2012 (487)	UBQLN pathology showed a highly distinct pattern in ALS and FTLD-TDP cases with the *C9orf72* expansion, with UBQLN-positive cytoplasmic inclusions in cerebellar granular layer
Kobayashi et al., 2011 (486)	degeneration in posterior cerebellar tract
Al-Sarraj et al., 2011 (493)	Abundant p62 positive, p-TDP-43 negative neuronal intranuclear inclusions (NIIs) observed in 6 out of 14 cases in the cerebellar granular layer in *C9orf72* symptomatic patients
Geser et al., 2008 (489)	neuronal and glial TDP-43 pathology present in multiple areas of the central nervous systems of ALS patients, including cerebellum
Ishihara et al., 2006 (485)	severe and widespread degeneration in CNS including in cerebellum
Petri et al., 2006 (491)	no disease-specific differences of the mRNA expression of the investigated subunits in cerebellar cortex
Yokota et al., 2006 (488)	neurofibrillary tangles (NFTs) found in cerebellum
Przedborski et al., 1996 (492)	glutathione peroxidase activity not significantly altered in the cerebellar cortex in ALS compared to controls
Plaitakis et al., 1988 (508)	glutamate levels significantly decreased in all areas investigated (frontal and cerebellar cortex and two areas of spinal cord)

ALS - amyotrophic lateral sclerosis; **ATXN2**- ataxin 2 gene; **C9orf72** - chromosome 9 open reading frame 72 gene; **NFTs** - neurofibrillary tangles; **TDP-43** - TAR DNA-binding protein 43; **UBQLN** - Ubiquilin Like

Discussion

Neuroimaging and post-mortem infratentorial pathology in ALS

It is increasingly recognised that symptom manifestation in ALS is preceded by a long pre-symptomatic phase (19, 119), and to clarify the role of the cerebellum in the pathogenesis and verify proposed compensatory processes, more pre-symptomatic imaging studies are needed specifically evaluating infratentorial changes (25, 30). Cerebellar findings in ALS are strikingly inconsistent; many studies report widespread cerebellar degeneration (406, 468), others detect no changes (442, 474, 491, 492). Both increased (362) and decreased grey matter volumes (446) have been reported, both increased (30, 360, 439, 471) and reduced functional cerebro-cerebellar connectivity (467), cerebellar hypermetabolism (443, 476, 477) and hypometabolism (447) have been observed. Very few imaging studies assessed disease burden in specific cerebellar lobules (338, 406, 453), cerebellar nuclei (463) or the cerebellar peduncles (422, 462-465). Because of the considerable clinical heterogeneity of ALS, stratification by genotype and phenotype -specific changes is essential. Delineating disease heterogeneity and objective stratification in ALS are particularly critical for drug development (124). Only a minority of cerebellar imaging studies investigated different subtypes of ALS contrasting LMN versus UMN predominant (439, 440), ALS with and without cognitive impairment (441-444), ALS-motor and ALS-plus (446), and *C9orf72* positive and *C9orf72* negative ALS (128, 138, 442, 445). Only a handful of studies included PLS (322, 422, 468), PMA (474), FTD and ALS-FTD (442, 479) cohorts. The strikingly different stratification strategies illustrate just one of the many

methodological differences across cerebellar imaging studies that may explain the inconsistencies in the literature. It is also noteworthy that the vast majority of ALS imaging studies are cross-sectional encompassing patients at various stages of their disease trajectories adding to sample heterogeneity (124). Sample heterogeneity (genetic, phenotypic, symptom duration) coupled with sample size limitations are likely to be key contributors the contradictory findings. It is also widely recognised the imaging studies in ALS have an inherent inclusion bias to patients with less severe disability, limited bulbar impairment, less severe sialorrhoea, and relatively good respiratory function. Patients with frank orthopnoea, patients reliant on continuous non-invasive ventilation, patients with very poor mobility are much less likely to participate in imaging studies, therefore our insights gained from lengthy imaging protocols may not be fully representative of disease burden across the entire clinical spectrum of ALS (146).

There is often an expectation in imaging studies to explore clinico-radiological correlations even though cerebellar signs, gait abnormalities, eye-movement abnormalities and cognitive deficits are confounded by coexisting UMN, LMN and frontotemporal degeneration in ALS (456, 509, 510). Nevertheless, cerebellar changes have been linked to disease severity (453), motor symptoms (455), cognitive impairment (453) and apathy (454). One study using computational gait analysis reveals the contribution of extrapyramidal deficits rather than cerebellar pathology to gait impairment highlighting the need for objective measures of clinical findings (459). The majority of cerebellar imaging studies evaluate multiple parameters which is helpful to determine which biomarkers are most sensitive to detect and track progressive cerebellar changes. Despite the overwhelming focus on spinal and

supratentorial changes, cerebellar pathology has also been evaluated post-mortem (485). UBQLN-positive cytoplasmic inclusions (487), neurofibrillary tangles (NFTs)(488) and TDP-43 pathology (489) have been described in the cerebellum. The predilection to specific cerebellar lobules, vermis or deep cerebellar nuclei however has not been systematically characterised post mortem in specific ALS phenotypes and genotypes. There is a notion that neuronal networks underpinning phylogenetically "recent" skills, such as fine motor skills, vocalisation, ambulation etc. are particularly vulnerable to ALS (511, 512), which may explain the preferential atrophy of certain cerebellar regions, but these associations remain to be elucidated. It is also unfortunate that large imaging studies of well-characterise patients don't typically offer complementary post-mortem analyses to interpret their ante-mortem imaging findings.

A multitude of fMRI studies showed increased cerebellar activation when performing motor tasks (406, 409, 469, 473), and resting-state fMRI studies often reveal increased cerebro-cerebellar connectivity (30, 360, 439, 471). These two observations are often interpreted as a compensatory, adaptive change to motor cortex degeneration despite the lack of supporting structural findings and compelling post mortem evidence. Neuroplasticity is an intrinsic property of the nervous system, allowing some degree of reorganisation at a molecular, cellular, or anatomical level (513) which enables the nervous system to adopt to insult and compensate for injury (514). Effective neuroplasticity has been demonstrated in a multitude of neurological conditions such as traumatic brain injury (514), stroke (515), multiple sclerosis (516), Alzheimer's disease (517) and spinal cord injury (518), and similar adaptive mechanisms have also

been proposed in ALS (314). Based largely on abnormal activation patterns during motor tasks, it has been proposed that additional brain regions compensate for primary motor cortex degeneration such as the ipsilateral motor cortex, supplementary motor and premotor areas (519), as well as in the basal ganglia (154, 520) and cerebellum (409, 469, 472, 482). The cerebellum in particular is thought to exhibit remarkable neuroplasticity, withstand considerable cerebellar insults (521) and adapt to extra-cerebellar pathologies (522). The activation shift from primary motor areas to the cerebellum during movement execution (452) is often interpreted as evidence of an adaptive or compensatory process, but very few structural studies (362) and no post mortem studies have actually captured frank hypertrophy. An alternative explanation for increased functional connectivity centres on the loss of cortical inhibition (409, 469).

Cerebellar findings in related neurodegenerative conditions

The link between ALS and FTD is increasingly accepted based on shared clinical, genetic and imaging features (3, 510, 523). Frontotemporal dysfunction is a key dimension of clinical heterogeneity in ALS and the concept of an ALS-FTD spectrum or continuum is now widely accepted. Cerebellar changes have been consistently described in GGGGCC hexanucleotide repeat carriers in *C9orf72* (406, 524-526). While comorbid FTD was once primarily associated with hexanucleotide repeats, recent data have shown that frontotemporal degeneration is not exclusively caused by *C9orf72* repeat expansions in ALS (527). Cerebellar changes have also been reported in FTD cohorts without ALS and without GGGGCC repeat expansions. (528) For example, preferential vermis atrophy

was described in *MAPT* carriers (528). Other cerebellar studies of FTD stratified their patients by the clinical phenotype (525, 529-531) and associations were identified between cerebellar pathology and performance in specific cognitive domains such as attention, working memory, visuospatial skills and language (529, 530). Lobule VI, VIIb, VIIIb atrophy was noted in bvFTD and crus I and lobule VI volume loss seen in semantic variant primary progressive aphasia (svPPA) (532). Cerebellar grey matter atrophy was captured pre-symptomatic *C9orf72* carriers (533) and ALS-FTD (534). PLS is a low incidence disorder of the upper motor neurons with a relatively limited imaging literature (535, 536) and overlapping clinical, radiological and genetic features with ALS (5, 537, 538). Very few imaging studies have specifically commented on cerebellar changes in PLS. Intra-cerebellar white matter alterations (368), dentato-rubro-thalamo-cortical (DRTC) and spino-cerebellar (SC) tract diffusivity changes (468) and increased functional connectivity was reported between the cerebellum and cortical motor, frontal and temporal areas (539). PLS patients with cognitive deficits are thought to exhibit FA reductions and increased RD in cerebellar white matter (540). In spinal muscular atrophy (SMA) preferential lobule VIIIB, IX and X atrophy has been observed without notable correlations with clinical metrics (541). Hereditary spastic paraplegia (HSP), which can be mistaken for UMN-predominant ALS or PLS, is also associated with considerable cerebellar grey and white matter degeneration (542-547). Cerebellar changes are also commonly observed in spinal and bulbar muscular atrophy (SBMA) or Kennedy's disease which is an X-linked recessive, slowly progressive, LMN-predominant MND (548, 549). Interestingly, cerebellar integrity metrics are typically superior in poliomyelitis survivors compared to demographically-

matched healthy controls (550), which is often regarded as evidence of neuroplasticity and compensation for longstanding spinal anterior horn insult (551, 552).

Clinical relevance

Though woefully understudied in ALS, cerebellar pathology is thought to contribute to pseudobulbar affect (422, 429), cognitive deficits (406, 453), behavioural dysfunction (454, 479), bulbar symptoms (419, 455), respiratory problems (553), gait impairment (410, 411) and eye movement abnormalities (554). The role of the cerebellum in mediating cognitive, and behavioural processes is increasingly well established (428, 555-557). Multi-time point longitudinal studies have shown that the corticospinal tracts (CST) and the corpus callosum (CC) are involved very early in the disease process (7, 8, 26, 131), whereas cerebellar changes exhibit progressive change in the symptomatic phase of the disease (151, 322). Regions that are affected early in the disease process may help diagnostic or phenotypic classification (121, 122, 149), but region which exhibit progressive change in the later disease phases are better suited as tracking biomarkers (119, 124). It is noteworthy that commonly used image analysis suites which evaluate cortical thickness profiles, such as FreeSurfer, only provide supratentorial segmentation, therefore many longitudinal ALS studies using these software don't evaluate cerebellar changes at all (558). The prevailing clinical understanding of ALS-associated disability is overwhelmingly centred in UMN/LMN degeneration and the wider recognition of cerebellar pathology would also inform and refine multidisciplinary rehabilitation strategies, fall prevention, occupational therapy, speech and language therapy, management of pseudobulbar affect and

synchronisation with non-invasive ventilation (NIV). ALS is now universally regarded as part of the ALS-FTD spectrum, but mounting clinical and genetic evidence suggests that an ataxia-ALS continuum also exists. Ataxia-ALS overlap syndromes have been described in association with spinocerebellar ataxia type 1 (SCA1) and type 2 (SCA2) (559, 560). While 33 or more CAG repeats in the *ATXN1* and *ATXN2* genes are linked to spinocerebellar ataxia, an intermediate number of repeats in these genes is a risk factor for ALS (560, 561). ALS patients with intermediate *ATXN1* and *ATXN2* mutations often have a positive family history of spinocerebellar ataxia (560, 562) and SCA1 and SCA2 patients can present with or eventually develop an ALS-like phenotype (562, 563). Despite the emerging recognition of an ataxia-ALS continuum, ALS patients are not routinely screened for trinucleotide repeat expansions in *ATXN1* and *ATXN2* and a targeted cerebellar examination is seldom performed in ALS clinics (406). Subtle cerebellar manifestations in ALS are notoriously difficult to ascertain due to confounding UMN and LMN signs which dominate the clinical picture. Spinocerebellar ataxias also share some clinical features with ALS such as dysphagia, and even muscle wasting and dementia, particularly in advanced stages (564, 565). A key lesson of the emerging *ATXN1* and *ATXN2* literature is that patients presenting to ataxia clinics should be carefully evaluated for UMN and LMN signs, and patients attending ALS clinics should be assessed for cerebellar signs.

Future directions

The contribution of cerebellar pathology to the clinical manifestations of ALS are poorly characterised and robust dedicated cerebellar studies are needed to dissect the

role of infratentorial and supratentorial changes to motor disability, cognitive deficits, behavioural disturbances, pseudobulbar affect, dysphagia and respiratory regulation. While putative compensatory processes were inferred from functional imaging studies, these have not been demonstrated by compelling structural and post mortem data to date. Emerging genetic data reveal an ataxia-ALS spectrum, the anatomical correlates of which have not been duly explored by dedicated imaging and post mortem studies. Cerebello-spinal connectivity is particularly poorly explored in ALS, despite emerging quantitative spinal imaging techniques (120, 566). From an academic perspective, the role of the cerebellum in the pathogenesis of ALS and disease propagation is not established, despite its ample projections to key ALS-associated foci; the spinal cord and motor cortex. At present, cerebellar disease-burden remains an overlooked facet of ALS despite its wide-ranging clinical and academic relevance.

The field of MND imaging has seen unprecedented technological innovations in recent years, including the emergence of ultra-high-field platforms, a gradual transition to cloud-based applications, the increasing implementation of machine-learning frameworks, emphasis on longitudinal modelling, and a shift to non-Gaussian diffusion imaging (145, 567-569). Methods for evaluating the cerebellum have also improved considerably; robust cerebellar analysis pipelines have been published, high-resolution cerebellar atlases have been made available and novel cerebellar normalisation templates have been developed (570-573). Thanks to momentous methodological advances in neuroimaging, animal model technologies and immunohistochemistry, the armamentarium of clinical, radiological and biological tools are finally at our disposal to conduct authoritative integrative cerebellar studies.

Conclusions

While the cerebellum is recognised to be involved in the disease process in ALS, the specific contribution of cerebellar pathology to cardinal clinical manifestations are poorly characterised. There is a disproportionate emphasis on supratentorial changes in imaging and post mortem studies. Recent advances in genetics, imaging technology and data analysis pipelines offer unprecedented opportunities to clarify the role of the cerebellum in mediating disease propagation in ALS and its contribution to clinical symptoms.

CHAPTER 5: Genotype associated cerebellar profiles in ALS

Introduction

While cerebellar involvement is a recognised feature of amyotrophic lateral sclerosis (ALS), anatomical patterns of cerebellar disease-burden are poorly characterised *in vivo*, cerebro-cerebellar connectivity changes are mostly inferred from functional studies, and the cerebellar signatures of specific genotypes are not firmly established. The majority of imaging studies in ALS conjecture that the cerebellum assumes a compensatory role as progressive supratentorial degeneration ensues, yet post-mortem studies have not confirmed such changes. Cognitive, behavioural and extra-pyramidal manifestations are now all accepted facets of ALS and supported by compelling post mortem and radiological observations. While the link between FTD and ALS has been cemented, the notion of an ALS-ataxia continuum remains contentious despite the association of intermediate-length CAG repeat expansions in *ATXN2* with ALS,(574) and shared clinical features with spinocerebellar ataxias. Even though cerebellar changes in ALS have been confirmed by seminal post mortem and TDP-43 studies,(534, 575, 576) their clinical manifestations are less clear than those linked to frontotemporal pathology. Common clinical manifestations of ALS, such as pseudobulbar affect, dysarthria, dysphagia, eye movement abnormalities, behavioural dysfunction, and deficits in social cognition are often exclusively linked to corticobulbar tract degeneration, brainstem and cranial nerve pathology, orbitofrontal atrophy etc. which overlooks the likely contribution of cerebellar pathology to these symptoms.(419, 420, 577) The pitfalls of linking imaging findings directly to clinical observations are well recognised,(456) but the real value of computational imaging in ALS lies in its ability to characterise disease-burden patterns *in vivo* in an impartial, descriptive, observer-independent fashion. Varying patterns of cerebellar changes have been noted on whole-brain analyses,(409) but relatively few dedicated cerebellar studies have been

undertaken.(468, 479) Cerebellar imaging studies in ALS have led to strikingly inconsistent findings,(409) which may stem from methodological differences, sample size limitations, differences in inclusion criteria and divergent patient stratification strategies. Few imaging studies reported focal changes in specific lobules,(446) implemented longitudinal designs across multiple timepoints,(151) evaluated the integrity of cerebellar peduncles,(466) investigated cerebellar nuclei,(463) or commented on presymptomatic changes.(30) Popular MRI analysis pipelines are often confined to the evaluation of supratentorial changes, and EEG and MEG studies do not typically acquire cerebellar data at all.(578) PET studies often detect hypermetabolism in various cerebellar regions(443) including the vermis, lobules IV and V, but propose strikingly different biological explanations such as microglial activation, loss of inhibition or compensatory process. Reports of cerebellar degeneration in *C9orf72*-positive ALS are also inconsistent; while post mortem studies consistently confirmed *C9orf72*-associeted cerebellar changes,(576, 579) some imaging studies did not detect cerebellar atrophy *in vivo*.(442) *ATXN2*-associated cerebellar changes in ALS have not been systematically evaluated to date.

Based on these considerations, our main objective is the comprehensive and multiparametric evaluation of both intra-cerebellar pathology and cerebro-cerebellar connectivity in a genetically stratified cohort of patients with ALS. We are not seeking to explore direct clinical correlates,(456) but endeavour to characterise anatomical patterns of cerebellar disease burden distribution. Our main hypothesis is that focal cerebellar pathology may be detected instead of global cerebellar degeneration with the selective vulnerability of specific cerebellar lobules. We hypothesise that cerebellar changes may also be readily detected in patients who test negative for established ALS-associated genetic variants. Additionally, we hypothesise that intra-cerebellar pathology is accompanied by cerebro-cerebellar disconnection.

Methods

Participants

A total of 271 participants, 161 patients with ALS and 110 healthy controls were included in a prospective, single-centre imaging study of cerebellar degeneration in amyotrophic lateral sclerosis. All participants provided informed consent in accordance with the Medical Ethics Approval of the research project (Beaumont Hospital, Dublin, Ireland). Exclusion criteria included prior traumatic brain injury, cerebrovascular events, comorbid neoplastic, paraneoplastic or neuroinflammatory diagnoses. Participating ALS patients with 'probable' or 'definite' ALS according to the revised El Escorial research criteria were drawn from a larger cohort (n=808) genotyped for repeat expansions in *C9orf72* and *ATXN2* (see 'Genotyping') and were stratified into three groups: (1) those testing positive for GGGGCC repeat expansions in *C9orf72* ('ALS-C9', n=22), (2) those carrying an intermediate repeat expansion in *ATXN2* with a max allele length of 27-33 ('ALS-ATXi', n=5) and patients who tested negative for both *ATXN2* and *C9orf72* ('ALS-NEG', n=133). Additionally the cerebellar profile of a single ALS patient was evaluated who had a max *ATXN2* allele length of 62. Hundred and twenty-five ALS patients had a uniform cerebellar assessment by the same neurologist (PB) at the time of scan. This included screening for dysdiadochokinesis, dysmetria, and rebound assessing rapid alternating movements, finger-to-nose / heel-to-shin coordination, and gait where disability from UMN/LMN degeneration permitted.

Magnetic resonance imaging

A uniform imaging protocol was implemented on a 3 Tesla Philips Achieva Magnetic resonance (MR) platform. T1-weighted (T1w) images were acquired with a 3D Inversion Recovery

prepared Spoiled Gradient Recalled echo (IR-SPGR) sequence with the following parameters; field-of-view (FOV) of 256 x 256 x 160 mm, flip angle = 8°, spatial resolution of 1 mm^3, SENSE factor = 1.5, TR/TE = 8.5/3.9 ms, TI =1060 ms. Diffusion tensor images (DTI) were acquired with a spin-echo echo planar imaging (SE-EPI) pulse sequence using a 32-direction Stejskal-Tanner diffusion encoding scheme, FOV = 245 x 245 x 150 mm, 60 slices with no interslice gap, spatial resolution = 2.5 mm^3, TR/TE = 7639 / 59 ms, SENSE factor = 2.5, b-values = 0, 1100 s/mm^2, dynamic stabilisation and spectral presaturation with inversion recovery (SPIR) fat suppression. To assess for comorbid vascular and inflammatory pathologies, FLAIR images were also acquired from each participant. Axial orientation was used for FLAIR imaging with an Inversion Recovery Turbo Spin Echo (IR-TSE) sequence: FOV = 230 x 183 x 150 mm, spatial resolution = 0.65 x 0.87 x 4 mm, 30 slices with 1 mm gap, TR/TE = 11000 / 125 ms, TI = 2800 ms, 120° refocusing pulse, with flow compensation and motion smoothing and a saturation slab covering the neck region.

Cortical thickness and volume analyses

To evaluate cerebellar cortical thickness and lobular volume alterations, the cerebellum was parcellated using a validated segmentation algorithm.(570) Pre-processing included the 'denoising' of raw structural data in native space, inhomogeneity corrections, affine registration to the Montreal Neurological Institute (MNI) space, inhomogeneity corrections in MNI space, cerebellar cropping, low dimensional non-linear registration estimation, and intensity normalization. A patch-based segmentation algorithm was subsequently applied to generate cerebellar volume metrics for each lobule,(580) separately for the right and left cerebellar hemispheres. The accuracy of anatomical segmentation and tissue-type parcellation was individually verified for each subject. White matter volumes in each lobule were calculated by subtracting grey matter volume values from total lobule volume estimates. The following

anatomical labels were considered to retrieve regional cortical thickness and volume values: Lobules I-II, III, IV, V, VI, VIIB, VIIIA, VIIIB, IX, X, Crus I and Crus II. The outputs considered for statistical interpretation included cortical thickness, grey matter volumes, and white matter volumes in each lobule and crus.

Morphometry

Imaging analyses were carried out in a Linux environment on a multi-CPU server running CentOS.

First, total intracranial volumes (TIV) were estimated for each subject to be used as a covariate in subsequent region-of interest (ROI) morphometric analyses. TIV was estimated by linearly aligning each participant's brain image to the MNI152 standard, and the inverse of the determinant of the affine registration matrix was calculated and multiplied by the size of the template. FMRIB's FSL-FLIRT was used for spatial registration and FSL-FAST for tissue type segmentation. Resulting partial grey matter, white matter and CSF volumes were added for TIV estimation. Cerebellar grey matter pathology was appraised by ROI morphometry using FMRIB's FSL suite. Pre-processing included skull-removal (BET), motion-corrections and tissue-type segmentation, followed by the individual visual inspection of the outputs for quality control. Affine registration was then utilised to align individual grey-matter partial volume images to the MNI152 standard space. A study-specific grey matter template was generated representing each study group to which the grey matter images of each participant were then non-linearly co-registered. For the voxelwise analyses, permutation based non-parametric inference was utilised to contrast the three patient groups to healthy control implementing the threshold-free cluster enhancement (TFCE) method. Design matrices included group membership, age, sex and TIV. Voxelwise statistics were constrained to a cerebellar ROI mask defined by 'label 1' of the MNI structural atlas. Resulting statistical maps were thresholded at p

< 0.05 FWE TFCE and visualised in FSLeyes. The labels of the Diedrichsen probabilistic atlas was used as underlay to aid the localisation of statistically significant clusters.

White matter analyses

Raw DTI data first underwent eddy current corrections and skull removal; a tensor model was then fitted to generate maps of fractional anisotropy (FA), axial diffusivity (AD), and radial diffusivity (RD). FMRIB's software library's tract-based statistics (TBSS) module was utilised for non-linear registration and skeletonisation of individual DTI images. A mean FA mask was created and each subject's individual FA, AD and RD images were merged into 4-dimentional (4D) AD, FA and RD image files. The study specific white matter skeleton was masked by atlas-defined labels for the entire cerebellum to restrict analyses to the cerebellum. Permutation-based non-parametric inference was used for the two-way, voxelwise comparison of diffusivity parameters between each patient group and controls using design matrix-defined contrasts which included age and sex as covariates. The threshold-free cluster enhancement (TFCE) method was applied and results considered significant at a $p < 0.01$ TFCE family-wise error (FWE).

Segmentation for superior cerebellar peduncle volumetry

A Bayesian segmentation pipeline was implemented for the parcellation of the superior cerebellar peduncle which is based on a probabilistic atlas generated based on 49 scans.(581) The FreeSurfer image analysis suite was used for the pre-processing; the removal of non-brain tissue, segmentation of the subcortical white matter and deep grey matter structures, intensity normalization, tessellation of the grey matter-white matter boundary, and

automated topology correction. Following pre-processing, segmentation, and quality checks, raw superior cerebellar peduncle volume values were retrieved for each study participant for subsequent statistical interpretation with the appropriate covariates.

Cerebro-cerebellar connectivity

Cerebro-cerebellar connectivity was evaluated with deterministic tractography, and in a supplementary analysis, diffusivity metrics in the cerebellar peduncles were evaluated separately. Tractography was performed using BrainanceMD (Advantis Medical Imaging, Eindhoven, The Netherlands). Before formal analyses, all DTI datasets were first corrected for motion and Eddy-currents using a scanner registration tool and a co-registration protocol. Region-of-interest (ROI) fibre tractography (thresholds: FA = 0.15, angle = 70^{o}, step size = 1) was implemented for the main cortico-ponto-cerebellar tracts: (1) fronto-ponto-cerebellar (FPC), (2) parieto-ponto-cerebellar (PPC), (3) occipito-ponto-cerebellar (OPC), (4) temporo-ponto-cerebellar (TPC), and (5) dentate-rubro-thalamo-cortical (DRTC). ROI definitions and gating has been presented previously(582) and is illustrated in **Figure 5**. The following indices were extracted from each tract: fractional anisotropy (FA), axial diffusivity (AD), and radial diffusivity (RD). All DTI datasets were analysed twice by a single experienced rater (F.C.) within an interval of 3 weeks to verify intra-observer consistency. To evaluate inter-observer consistency, the same dataset was also analysed by a second experienced rater (E.K.), who was blinded to the results of the first rater. Intra- and inter-rater consistencies were verified with intra-class correlation coefficient (ICC) and ICC values greater than 0.80 were found in all cases [(ICC) > 0.8].

In a supplementary analysis, the integrity of the cerebellar peduncles was also specifically evaluated. Labels 1,11,12,13,14 of the 1mm JHU-ICBM atlas was utilised to generate masks for

the left and right inferior, the middle and the left and right superior cerebellar peduncles. Average FA, AD and RD values were retrieved from the merged skeletonised diffusion data using these masks from each subject for statistical analysis.

Figure 5: *Tractography methods and anatomical targets for the fronto-ponto-cerebellar (FPC), parieto-ponto-cerebellar (PPC), occipito-ponto-cerebellar (OPC), temporo-ponto-cerebellar (TPC) and dentate-rubro-thalamo-cortical (DRTC) tracts.*

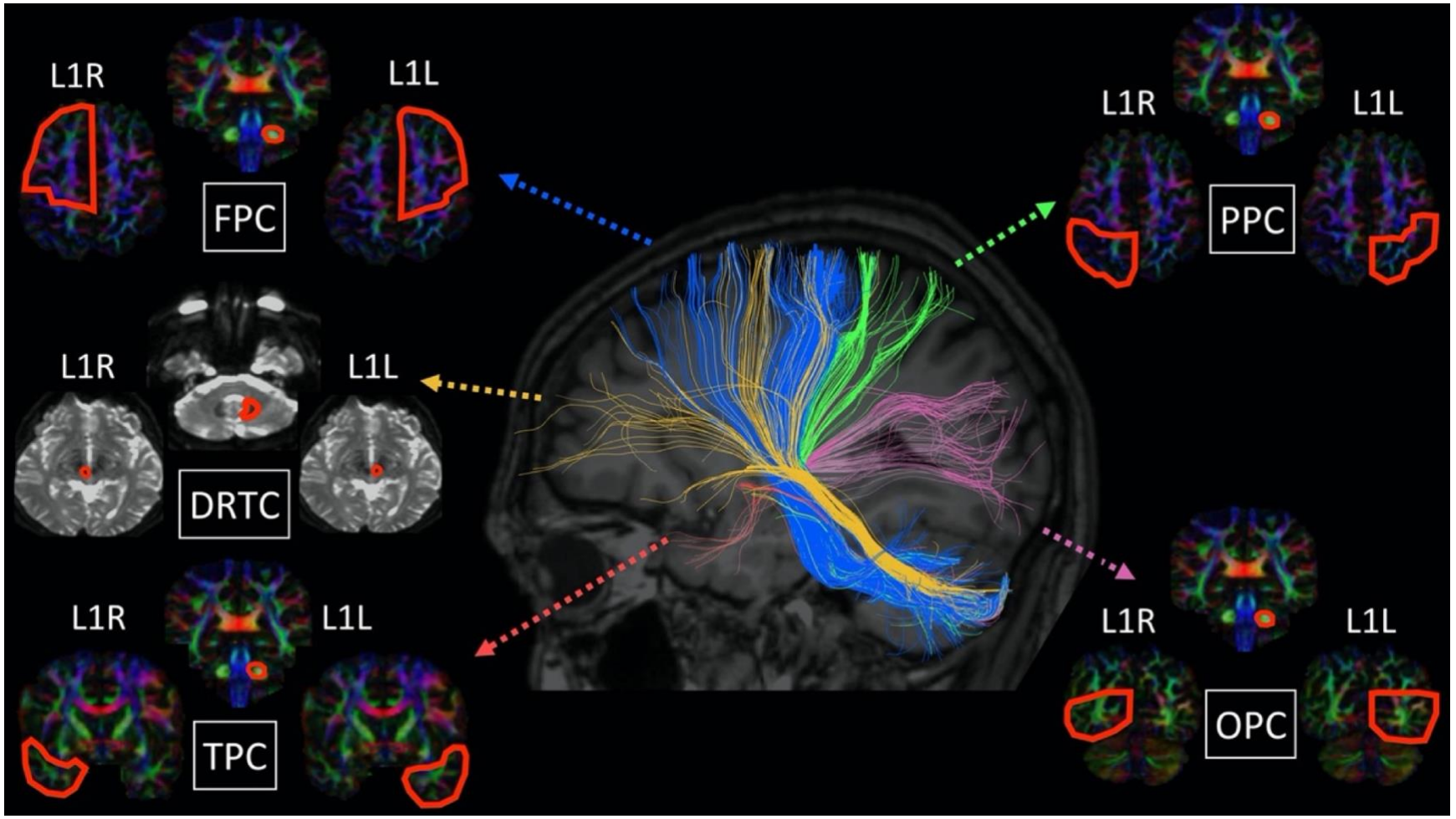

Statistical analyses

Voxelwise statistics, covariates and design matrices are described above for morphometric and tract-based statistics. Multivariate analyses of covariance (MANCOVAs) were used to evaluate the effect of group membership on lobular cortical thickness, designating lobular cortical thickness values as dependent variables, the grouping variable as independent factor and age and sex as covariates. To test the effect of group membership on cerebellar GM volumes, a MANCOVA was also conducted, including lobular GM volumes as dependent variables, the grouping variable as independent factor and age, sex and TIV as covariates. To test the effect of group membership on diffusivity metrics (FA, AD, RD), diffusivity values were included as dependent variables, the grouping variable as independent factor and age and gender as covariates. To test the effect of group membership on SCP volume, an ANCOVA was conducted using SCP volume as dependent variable, the grouping variable as independent factor and age, sex and TIV as covariates. Due to cohort size considerations, only the imaging profile of the HC, ALS-NEG and ALS-C9 groups are presented in the main manuscript. Differences between HC and ALS-ATXi patients are reported in the supplementary material. In case of a significant multivariate omnibus test (or univariate for the SCP volume), post-hoc comparisons were considered significant at $p<0.05$, following Bonferroni corrections for multiple comparisons to reduce Type I error. For the interpretation of the imaging metrics of the single ALS-SCA patient, an age and sex-matched subgroup of 55 controls were used, implementing supplementary Bayesian statistics and using the SINGLEBAYES pipeline.(583) The ALS-SCA patient's lobular CT, GM, WM and peduncular diffusivity values were compared to the age-match HC values at $p < 0.05$, using Bonferroni correction for multiple comparisons.

Genotyping

Nine hundred and seventy-seven ALS patients from the Irish ALS DNA bank were included in genotyping analyses. DNA was extracted commercially from whole blood drawn from ALS patients along with 562 age- and population-matched healthy control subjects. All patients provided written informed consent and genotyping was approved by the Beaumont Hospital Research Ethics Committee. The *ATXN2* $(CAG)_n$ repeat locus was amplified by polymerase chain reaction (PCR) using primers (5'-3') ATXN2-F 6-FAM-CCCCGCCCGGCGTGCGAGCCGGTGTATG and ATXN2-R CGGGCTTGCGGACATTGG.(584) Between 40 and 70 ng of genomic DNA was amplified using Q5 Hot Start High-fidelity Polymerase (New England BioLabs inc) along with the provided high-GC enhancer. Resulting PCR products were purified using Agencourt Ampure XP beads (Beckman Coulter) and analysed for amplified fragment length polymorphism commercially by Eurofins Medigenomix GmbH on an Applied Biosystems 3730xl capillary electrophoresis instrument. All patients were also genotyped for the intronic GGGGCC repeat expansion in *C9orf72* by repeat-primed PCR. Resulting capillary electrophoresis traces were visualised using GeneMapper version 4.0; patients unambiguously exhibiting 30 or more repeats were labelled *C9orf72*-positive. Additionally, all participating patients were screened for a panel of protein-altering, exonic or splice-site variants present in 32 genes linked to ALS in the ALS online database (ALSod).(585)

Results

The frequency of pathogenic *C9orf72* repeat expansions across the genotyped cohort was 7.6%. *ATXN2* alleles contained between 8 and 91 trinucleotide repeats, with the most common alleles containing 22, 23 and 27 repeats at frequencies (cases and controls combined) of 87.4%, 8.2% and 1.7% respectively. Consistent with previous reports, we observed an excess of ALS cases in which the larger *ATXN2* allele was in the intermediate range of 27 to 33 repeats,

as well as 6 ALS patients and 1 healthy control with >33 repeats (**Figure 6A**). Trinucleotide repeat counts ≥28, ≥29, ≥30 and ≥31 for the larger allele were significantly associated with ALS (Fisher's exact test, $p < 2.4 \times 10^{-3}$, corresponding to $\alpha = 0.05$ corrected for 21 tests; (**Figure 6B**) and the odds ratio for ALS in the established ALS risk range (27-33 repeats) (574) was 1.72 (95% CI 1.04-2.84).

MRI data from a total of 161 patients with ALS and 110 healthy controls ('HC', mean age: 59.2±10.5) were available for analyses. Patients with ALS were categorised into three groups; (1) patients with sporadic disease testing negative for established mutations ('ALS-NEG', n=133, mean age: 61.6±10.2, mean ALSFRS-r:36.8±6.6, mean symptom duration: 19.6±9.2), (2) patients carrying the GGGGCC repeat expansion in *C9orf72* ('ALS-C9', n=22, mean age: 56.4±8.9, mean ALSFRS-r: 37.9±6.8, mean symptom duration: 20.8±6.2), and (3) patients with intermediate *ATXN2* repeat expansions ('ALS-ATXi', n=5, mean age: 59.6±15.1, mean ALSFRS-r: 35.8±3.7, mean symptom duration: 18.8±5.9). The groups were matched for age, sex, handedness, symptom duration and ALSFRS-r. The comparative demographic and clinical profile of the patients groups are presented in **Table 20**. All patients tested negative for a panel of protein-altering, exonic or splice-site variants in 32 genes linked to ALS.

Figure 6: *Profile of ATXN2 repeat expansions in 977 Irish patients with ALS and 562 population-matched healthy controls. (A) Allele frequencies for ALS cases and controls for the larger ATXN2 allele observed per individual. (B) OR ±95% CI for ATXN2 repeat expansions in ALS, thresholded by each observed allele as a lower limit. Asterisks indicate repeat expansion size categories significantly associated with ALS (Fisher's exact test $p<2.4\times10^{-3}$). ALS, amyotrophic lateral sclerosis.*

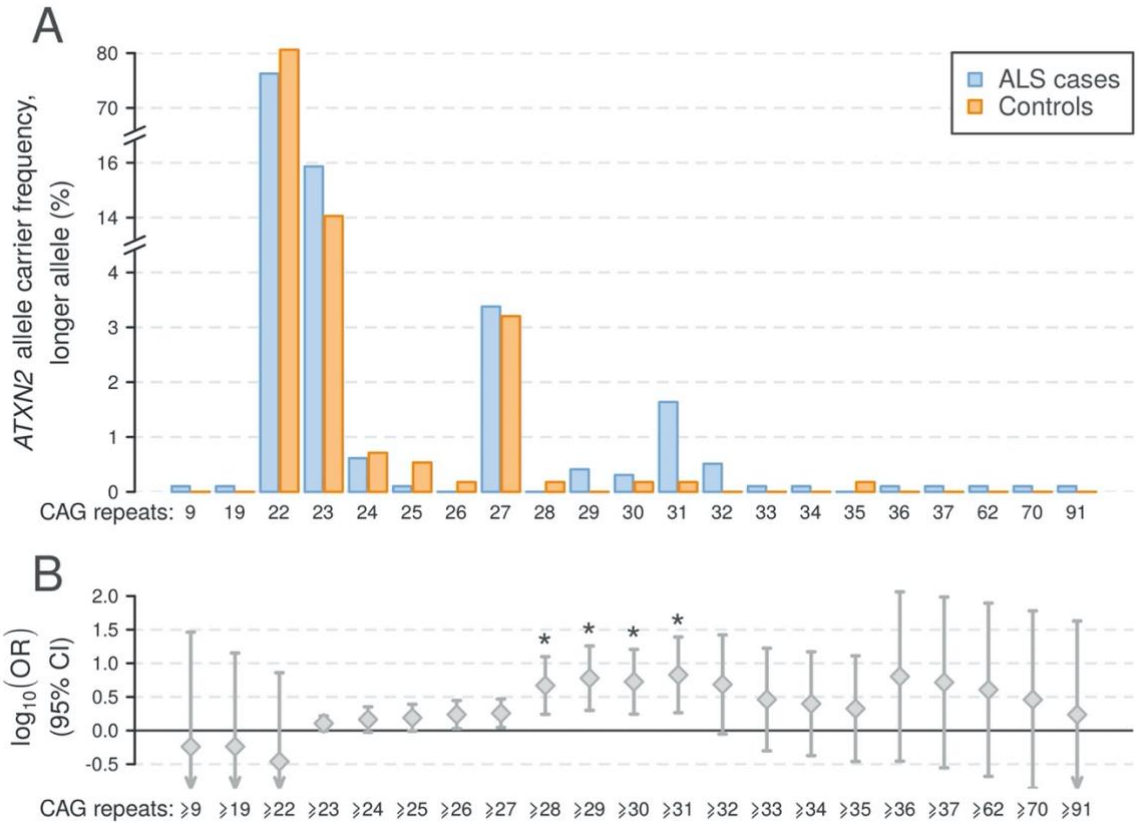

Table 20*: The comparative demographic and clinical profile of patient cohorts*

	HC n=110	**ALS-NEG n=133**	**ALS-C9 n=22**	**ALS-ATXi n=5**	**p - value**
Age	59.2(10.5)	61.6(10.2)	56.4(8.9)	59.6(15.1)	.09
Gender -male	65(59%)	74(55%)	12(54.5%)	5(100%)	.25
Handedness – right n(%)	102 (92%)	124 (93%)	19 (86%)	4 (80%)	.50
Symptom onset – spinal n(%)	n/a	113 (85%)	16 (72%)	4 (80%)	.35
Symptom Duration (months)	n/a	19.6(9.2)	20.8(6.2)	18.8(5.9)	.82
ALSFRS-r (max.48)	n/a	36.8(6.6)	37.9(6.8)	35.8(3.7)	.73
Availability of cerebellar exam n(%)	n/a	101(75%)	19(86%)	4(80%)	.55
Comorbid FTD n(%)	n/a	15(11%)	13(59%)	1(20%)	**.00***
Availability of ECAS n(%)	n/a	93(69%)	14(63%)	4(80%)	.73
Abnormal ECAS in those available n(%)	n/a	23(24%)	9(64%)	1(25%)	**.01***

Patients carrying hexanucleotide repeat expansion in *C9orf72* exhibited cortical thickness reductions in lobules IV, V, VI and crura I and II in the left cerebellar hemisphere, and lobules V, VI, VIIb and crura I and II in the right cerebellar hemisphere. (**Table 21**.) This cohort also demonstrated volume reductions in left lobule IV. (**Table 22**.) ALS-NEG patients showed cortical thinning in crus I on the left (**Table 21**) and volume reduction in the right and left lobules IV. (**Table 22**). ALS-ATXi patients exhibited no cerebellar cortical thinning or volume loss. (**Tables 23 and 24**). No cerebellar white matter volume reductions were observed in any of the patient groups. (**Tables 25 and 26**.)

Table 21*: Cerebellar cortical thickness in healthy controls and ALS-NEG and ALS-C9*

Cerebellar CT		Estimated marginal means ± S.E. for groups			Statistics		
		Controls n=110	ALS-NEG n=133	ALS-C9 n=22	Univariate effect size	HC vs ALS-NEG	HC vs ALS-C9
Left Lobules[a]	**I-II**	1.423 ± 0.036	1.506 ± 0.033	1.541 ± 0.080	$\eta^2p = 0.014$	0.273	0.525
	III	3.221 ± 0.036	3.225 ± 0.033	3.248 ± 0.081	$\eta^2p = 0.000$	1.000	1.000
	IV	4.916 ± 0.014	4.894 ± 0.013	4.812 ± 0.032	$\eta^2p = 0.034$	0.764	**0.009**
	V	4.899 ± 0.017	4.893 ± 0.015	4.780 ± 0.037	$\eta^2p = 0.033$	1.000	**0.012**
	VI	4.979 ± 0.011	4.963 ± 0.010	4.881 ± 0.025	$\eta^2p = 0.048$	0.849	**0.001**
	VIIB	4.605 ± 0.021	4.595 ± 0.019	4.522 ± 0.046	$\eta^2p = 0.010$	1.000	0.307
	VIIIA	4.651 ± 0.017	4.682 ± 0.016	4.674 ± 0.039	$\eta^2p = 0.007$	0.552	1.000
	VIIIB	4.522 ± 0.033	4.533 ± 0.030	4.509 ± 0.073	$\eta^2p = 0.000$	1.000	1.000
	IX	3.570 ± 0.044	3.588 ± 0.040	3.449 ± 0.099	$\eta^2p = 0.006$	1.000	0.784
	X	2.499 ± 0.044	2.511 ± 0.040	2.561 ± 0.099	$\eta^2p = 0.001$	1.000	1.000
	Crus I	4.571 ± 0.021	4.499 ± 0.019	4.386 ± 0.046	$\eta^2p = 0.058$	**0.032**	**0.001**
	Crus II	4.358 ± 0.024	4.314 ± 0.022	4.169 ± 0.054	$\eta^2p = 0.038$	0.549	**0.005**
Right Lobules[b]	**I-II**	1.362 ± 0.034	1.453 ± 0.031	1.538 ± 0.076	$\eta^2p = 0.024$	0.150	0.104
	III	3.097 ± 0.033	3.156 ± 0.030	3.183 ± 0.074	$\eta^2p = 0.008$	0.584	0.869
	IV	4.777 ± 0.017	4.759 ± 0.016	4.739 ± 0.039	$\eta^2p = 0.004$	1.000	1.000
	V	4.756 ± 0.018	4.731 ± 0.016	4.650 ± 0.040	$\eta^2p = 0.022$	0.930	**0.049**
	VI	4.930 ± 0.011	4.914 ± 0.010	4.847 ± 0.025	$\eta^2p = 0.035$	0.901	**0.007**
	VIIB	4.789 ± 0.016	4.751 ± 0.014	4.620 ± 0.035	$\eta^2p = 0.070$	0.240	**<0.001**
	VIIIA	4.645 ± 0.017	4.646 ± 0.015	4.599 ± 0.037	$\eta^2p = 0.006$	1.000	0.763
	VIIIB	4.580 ± 0.026	4.600 ± 0.024	4.492 ± 0.059	$\eta^2p = 0.011$	1.000	0.530
	IX	3.765 ± 0.039	3.807 ± 0.035	3.658 ± 0.087	$\eta^2p = 0.010$	1.000	0.778
	X	2.254 ± 0.038	2.154 ± 0.034	2.159 ± 0.084	$\eta^2p = 0.015$	0.162	0.921
	Crus I	4.634 ± 0.020	4.576 ± 0.018	4.494 ± 0.045	$\eta^2p = 0.036$	0.109	**0.015**
	Crus II	4.574 ± 0.021	4.527 ± 0.019	4.413 ± 0.046	$\eta^2p = 0.040$	0.287	**0.005**

Estimated marginal mean ± standard error for cortical thickness adjusted for age and gender. [a]Wilks' Lambda = 0.828; F = 2.055; p = 0.001; η^2p = 0.090. [b]Wilks' Lambda = 0.821; F = 2.146; p = 0.001; η^2p = 0.94. Bold p-values are significant at $p < 0.05$, after Bonferroni correction for multiple comparisons. Partial η^2 effect size is interpreted as small ($\eta^2p = 0.01$), medium ($\eta^2p = 0.06$) or large ($\eta^2p = 0.14$).

Table 22*: Cerebellar grey matter volumes in healthy controls and ALS-NEG and ALS-C9*

Cerebellar GM		Estimated marginal means ± S.E. for groups			Statistics		
		Controls n=110	ALS-NEG n=133	ALS-C9 n=22	Univariate effect size	HC vs ALS-NEG	HC vs ALS-C9
Left Lobules[a]	**I-II**	0.030 ± 0.001	0.029 ± 0.001	0.030 ± 0.002	$\eta^2p = 0.000$	1.000	1.000
	III	0.505 ± 0.011	0.483 ± 0.010	0.518 ± 0.026	$\eta^2p = 0.011$	0.484	1.000
	IV	2.080 ± 0.029	1.984 ± 0.026	1.844 ± 0.065	$\eta^2p = 0.049$	**0.045**	**0.003**
	V	3.590 ± 0.047	3.612 ± 0.042	3.394 ± 0.106	$\eta^2p = 0.014$	1.000	0.276
	VI	7.880 ± 0.101	7.946 ± 0.092	7.822 ± 0.231	$\eta^2p = 0.001$	1.000	1.000
	VIIB	4.031 ± 0.059	3.944 ± 0.054	3.782 ± 0.135	$\eta^2p = 0.012$	0.851	0.286
	VIIIA	4.921 ± 0.062	5.017 ± 0.057	5.015 ± 0.142	$\eta^2p = 0.005$	0.767	1.000
	VIIIB	3.334 ± 0.053	3.476 ± 0.048	3.294 ± 0.121	$\eta^2p = 0.018$	0.155	1.000
	IX	2.672 ± 0.045	2.719 ± 0.041	2.638 ± 0.102	$\eta^2p = 0.003$	1.000	1.000
	X	0.584 ± 0.007	0.573 ± 0.007	0.592 ± 0.017	$\eta^2p = 0.007$	0.816	1.000
	Crus I	11.106 ± 0.153	10.760 ± 0.140	10.371 ± 0.350	$\eta^2p = 0.019$	0.300	0.169
	Crus II	6.893 ± 0.099	6.782 ± 0.090	6.551 ± 0.225	$\eta^2p = 0.008$	1.000	0.500
Right Lobules[b]	**I-II**	0.035 ± 0.001	0.037 ± 0.001	0.039 ± 0.002	$\eta^2p = 0.012$	0.711	0.305
	III	0.495 ± 0.010	0.480 ± 0.009	0.506 ± 0.024	$\eta^2p = 0.006$	0.896	1.000
	IV	1.950 ± 0.029	1.846 ± 0.027	1.891 ± 0.067	$\eta^2p = 0.025$	**0.030**	1.000
	V	3.317 ± 0.045	3.349 ± 0.041	3.214 ± 0.103	$\eta^2p = 0.006$	1.000	1.000
	VI	7.873 ± 0.102	7.892 ± 0.093	7.519 ± 0.233	$\eta^2p = 0.009$	1.000	0.495
	VIIB	4.210 ± 0.061	4.089 ± 0.056	3.852 ± 0.140	$\eta^2p = 0.023$	0.450	0.061
	VIIIA	4.821 ± 0.064	4.906 ± 0.058	4.691 ± 0.146	$\eta^2p = 0.009$	0.980	1.000
	VIIIB	3.411 ± 0.058	3.505 ± 0.053	3.370 ± 0.133	$\eta^2p = 0.007$	0.708	1.000
	IX	2.836 ± 0.045	2.893 ± 0.041	2.809 ± 0.102	$\eta^2p = 0.004$	1.000	1.000
	X	0.582 ± 0.007	0.566 ± 0.007	0.588 ± 0.017	$\eta^2p = 0.013$	0.292	1.000
	Crus I	11.108 ± 0.149	10.797 ± 0.136	10.566 ± 0.340	$\eta^2p = 0.013$	0.380	0.436
	Crus II	7.088 ± 0.103	6.954 ± 0.094	6.985 ± 0.235	$\eta^2p = 0.004$	1.000	1.000

Estimated marginal mean ± standard error for GM volumes adjusted for age, gender and total intracranial volume. [a]Wilks' Lambda = 0.854; F = 1.695; p = 0.022; $\eta^2p = 0.076$. [b]Wilks' Lambda = 0.857; F = 1.662; p = 0.026; $\eta^2p = 0.074$. Bold p-values are significant at $p < 0.05$, after Bonferroni correction for multiple comparisons. Partial η^2 effect size is interpreted as small ($\eta^2p = 0.01$), medium ($\eta^2p = 0.06$) or large ($\eta^2p = 0.14$).

Table 23*: Cerebellar cortical thickness in healthy controls and ALS-ATXi*

Cerebellar CT	Estimated marginal means ± S.E. for groups		Statistics	
	HC N=110	ALS-ATXi n=5	Univariate effect size	HC vs ALS-ATXi
Left Lobules[a]				
I-II	1.416 ± 0.033	1.715 ± 0.158	η2p = 0.030	0.067
III	3.213 ± 0.035	3.438 ± 0.169	η2p = 0.015	0.197
IV	4.911 ± 0.014	4.909 ± 0.066	η2p = 0.000	0.973
V	4.898 ± 0.014	4.882 ± 0.068	η2p = 0.000	0.818
VI	4.978 ± 0.010	4.939 ± 0.050	η2p = 0.005	0.451
VIIB	4.608 ± 0.019	4.657 ± 0.093	η2p = 0.002	0.604
VIIIA	4.648 ± 0.017	4.723 ± 0.081	η2p = 0.007	0.371
VIIIB	4.513 ± 0.033	4.647 ± 0.157	η2p = 0.006	0.407
IX	3.569 ± 0.042	3.833 ± 0.202	η2p = 0.015	0.204
X	2.491 ± 0.043	2.829 ± 0.205	η2p = 0.023	0.110
Crus I	4.577 ± 0.020	4.520 ± 0.093	η2p = 0.003	0.557
Crus II	4.366 ± 0.026	4.271 ± 0.123	η2p = 0.005	0.452
Right Lobules[b]				
I-II	1.354 ± 0.030	1.764 ± 0.143	η2p = 0.066	0.006
III	3.092 ± 0.034	3.242 ± 0.161	η2p = 0.007	0.363
IV	4.771 ± 0.017	4.702 ± 0.083	η2p = 0.006	0.417
V	4.751 ± 0.018	4.653 ± 0.086	η2p = 0.011	0.270
VI	4.927 ± 0.012	4.844 ± 0.055	η2p = 0.019	0.143
VIIB	4.787 ± 0.016	4.782 ± 0.078	η2p = 0.000	0.943
VIIIA	4.641 ± 0.016	4.713 ± 0.077	η2p = 0.008	0.361
VIIIB	4.572 ± 0.025	4.762 ± 0.121	η2p = 0.021	0.127

IX	3.761 ± 0.037	3.991 ± 0.179	η2p = 0.014	0.211
X	2.250 ± 0.037	2.260 ± 0.175	η2p = 0.000	0.956
Crus I	4.636 ± 0.021	4.604 ± 0.102	η2p = 0.001	0.760
Crus II	4.576 ± 0.020	4.576 ± 0.098	η2p = 0.000	0.996

Estimated marginal means ± standard error for cortical thickness adjusted for age and gender. Post-hoc univariate comparisons across groups were only considered significant if the multivariate omnibus test reached significance (neither hemisphere)**: aWilks' Lambda = 0.919; F = 0.739; p = 0.710; η2p = 0.081. bWilks' Lambda = 0.859; F = 1.367; p = 0.194; η2p = 0.141.** Partial η2 effect size is interpreted as small (η2p = 0.01), medium (η2p = 0.06) or large (η2p = 0.14).

Table 24*: Cerebellar grey matter volumes in healthy controls and ALS-ATXi*

Cerebellar GM	Estimated marginal means ± S.E. for groups		Statistics	
	HC n=110	ALS-ATXi n=5	Univariate effect size	HC vs ALS-ATXi
Left Lobules[a]				
I-II	0.030 ± 0.001	0.036 ± 0.005	η2p = 0.015	0.202
III	0.508 ± 0.011	0.568 ± 0.053	η2p = 0.011	0.270
IV	2.093 ± 0.032	2.031 ± 0.153	η2p = 0.001	0.690
V	3.608 ± 0.043	3.507 ± 0.208	η2p = 0.002	0.637
VI	7.946 ± 0.096	7.985 ± 0.463	η2p = 0.000	0.934
VIIB	4.050 ± 0.059	4.148 ± 0.284	η2p = 0.001	0.736
VIIIA	4.951 ± 0.060	5.730 ± 0.290	η2p = 0.059	0.010
VIIIB	3.359 ± 0.052	3.447 ± 0.248	η2p = 0.001	0.729
IX	2.690 ± 0.044	2.846 ± 0.210	η2p = 0.005	0.468
X	0.587 ± 0.007	0.533 ± 0.036	η2p = 0.019	0.149
Crus I	11.179 ± 0.155	11.412 ± 0.744	η2p = 0.001	0.760
Crus II	6.936 ± 0.098	7.081 ± 0.472	η2p = 0.001	0.764
Right Lobules[b]				
I-II	0.035 ± 0.001	0.041 ± 0.004	η2p = 0.019	0.145
III	0.498 ± 0.010	0.543 ± 0.046	η2p = 0.008	0.334
IV	1.962 ± 0.028	1.708 ± 0.133	η2p = 0.031	0.065
V	3.330 ± 0.043	3.233 ± 0.208	η2p = 0.002	0.650
VI	7.937 ± 0.099	7.830 ± 0.476	η2p = 0.000	0.827
VIIB	4.230 ± 0.055	4.279 ± 0.264	η2p = 0.000	0.854
VIIIA	4.851 ± 0.060	5.286 ± 0.287	η2p = 0.020	0.141
VIIIB	3.436 ± 0.057	3.545 ± 0.277	η2p = 0.001	0.701
IX	2.854 ± 0.044	3.032 ± 0.210	η2p = 0.006	0.411

X	0.585 ± 0.007	0.528 ± 0.035	η2p = 0.022	0.120
Crus I	11.180 ± 0.149	11.685 ± 0.716	η2p = 0.004	0.493
Crus II	7.120 ± 0.108	7.419 ± 0.519	η2p = 0.003	0.574

Estimated marginal means ± standard error for GM volumes adjusted for age, gender and total intracranial volumes. Post-hoc univariate comparisons across groups were only considered significant if the multivariate omnibus test reached significance (neither hemisphere): aWilks' Lambda = 0.880; F = 1.120; p = 0.353; η2p = 0.120. bWilks' Lambda = 0.875; F = 1.181; p = 0.307; η2p = 0.125. Partial η2 effect size is interpreted as small (η2p = 0.01), medium (η2p = 0.06) or large (η2p = 0.14).

Table 25*: Cerebellar white matter volume profiles in healthy controls and ALS-NEG and ALS-C9*

Cerebellar WM	Estimated marginal means ± S.E. for groups			Statistics		
	HC n=110	ALS-NEG n=133	ALS-C9 n=22	Univariate effect size	HC vs ALS-NEG	HC vs ALS-C9
Left Lobules[a]						
I-II	0.031 ± 0.001	0.029 ± 0.001	0.025 ± 0.003	η2p = 0.024	0.494	0.051
III	0.216 ± 0.006	0.204 ± 0.006	0.210 ± 0.014	η2p = 0.008	0.437	1.000
IV	0.328 ± 0.007	0.320 ± 0.006	0.293 ± 0.016	η2p = 0.015	1.000	0.154
V	0.592 ± 0.013	0.572 ± 0.012	0.549 ± 0.030	η2p = 0.009	0.771	0.564
VI	0.886 ± 0.017	0.889 ± 0.015	0.923 ± 0.038	η2p = 0.003	1.000	1.000
VIIB	0.760 ± 0.016	0.742 ± 0.014	0.782 ± 0.036	η2p = 0.006	1.000	1.000
VIIIA	0.959 ± 0.018	0.923 ± 0.017	0.948 ± 0.042	η2p = 0.008	0.457	1.000
VIIIB	0.792 ± 0.020	0.796 ± 0.018	0.747 ± 0.046	η2p = 0.004	1.000	1.000
IX	0.888 ± 0.025	0.867 ± 0.023	0.813 ± 0.057	η2p = 0.006	1.000	0.695
X	0.057 ± 0.003	0.052 ± 0.002	0.043 ± 0.006	η2p = 0.022	0.351	0.086
Crus I	1.940 ± 0.038	1.946 ± 0.035	1.983 ± 0.088	η2p = 0.001	1.000	1.000
Crus II	1.201 ± 0.203	1.215 ± 0.021	1.264 ± 0.053	η2p = 0.005	1.000	0.815
Right Lobules[b]						
I-II	0.030 ± 0.001	0.029 ± 0.001	0.026 ± 0.003	η2p = 0.005	0.682	0.255
III	0.227 ± 0.006	0.213 ± 0.005	0.217 ± 0.014	η2p = 0.012	0.074	0.501
IV	0.350 ± 0.008	0.324 ± 0.007	0.292 ± 0.017	η2p = 0.045	0.015	0.002
V	0.669 ± 0.014	0.681 ± 0.013	0.656 ± 0.031	η2p = 0.003	0.500	0.707
VI	1.002 ± 0.016	1.009 ± 0.015	0.982 ± 0.037	η2p = 0.002	0.768	0.624
VIIB	0.629 ± 0.016	0.639 ± 0.015	0.659 ± 0.037	η2p = 0.002	0.644	0.466
VIIIA	0.866 ± 0.019	0.879 ± 0.017	0.898 ± 0.042	η2p = 0.002	0.600	0.487
VIIIB	0.633 ± 0.017	0.648 ± 0.016	0.661 ± 0.039	η2p = 0.003	0.520	0.510
IX	0.835 ± 0.023	0.816 ± 0.021	0.800 ± 0.053	η2p = 0.002	0.548	0.539

X	0.071 ± 0.003	0.070 ± 0.003	0.069 ± 0.007	η2p = 0.000	0.851	0.823
Crus I	1.975 ± 0.034	2.030 ± 0.031	2.047 ± 0.078	η2p = 0.006	0.240	0.401
Crus II	1.176 ± 0.022	1.201 ± 0.020	1.315 ± 0.051	η2p = 0.023	0.409	0.014

Estimated marginal means ± standard error for WM volumes adjusted for age, gender and total intracranial volumes. Post-hoc univariate comparisons across groups were only considered significant if the multivariate omnibus test reached significance (neither hemisphere): aWilks' Lambda = 0.905; F = 1.062; p = 0.384; η2p = 0.049. bWilks' Lambda = 0.904; F = 1.073; p = 0.370; η2p = 0.049. Partial η2 effect size is interpreted as small (η2p = 0.01), medium (η2p = 0.06) or large (η2p = 0.14).

Table 26*: Cerebellar white matter volume profiles in healthy controls and ALS-ATXi*

Cerebellar WM	Estimated marginal means ± S.E. for groups		Statistics	
	HC n=110	ALS-ATXi n=5	Univariate effect size	HC vs ALS-ATXi
Left Lobules[a]				
I-II	0.031 ± 0.001	0.031 ± 0.005	η2p = 0.000	0.824
III	0.218 ± 0.005	0.211 ± 0.025	η2p = 0.001	0.790
IV	0.331 ± 0.007	0.277 ± 0.036	η2p = 0.019	0.143
V	0.594 ± 0.013	0.553 ± 0.062	η2p = 0.004	0.512
VI	0.893 ± 0.015	0.925 ± 0.073	η2p = 0.002	0.669
VIIB	0.764 ± 0.017	0.748 ± 0.081	η2p = 0.000	0.847
VIIIA	0.967 ± 0.020	1.024 ± 0.096	η2p = 0.003	0.563
VIIIB	0.804 ± 0.019	0.727 ± 0.092	η2p = 0.006	0.414
IX	0.901 ± 0.024	0.747 ± 0.115	η2p = 0.015	0.193
X	0.058 ± 0.003	0.033 ± 0.012	η2p = 0.033	0.056
Crus I	1.945 ± 0.037	2.105 ± 0.179	η2p = 0.007	0.386
Crus II	1.203 ± 0.023	1.254 ± 0.111	η2p = 0.002	0.657
Right Lobules[b]				
I-II	0.030 ± 0.001	0.021 ± 0.005	η2p = 0.021	0.130
III	0.230 ± 0.005	0.242 ± 0.025	η2p = 0.002	0.644
IV	0.352 ± 0.008	0.321 ± 0.037	η2p = 0.006	0.416
V	0.673 ± 0.013	0.661 ± 0.063	η2p = 0.000	0.852
VI	1.010 ± 0.016	1.059 ± 0.076	η2p = 0.004	0.532
VIIB	0.631 ± 0.015	0.680 ± 0.073	η2p = 0.004	0.516
VIIIA	0.874 ± 0.020	0.884 ± 0.096	η2p = 0.000	0.924
VIIIB	0.644 ± 0.015	0.558 ± 0.074	η2p = 0.012	0.258
IX	0.847 ± 0.021	0.714 ± 0.101	η2p = 0.015	0.201

X	0.072 ± 0.003	0.070 ± 0.014	η2p = 0.000	0.879
Crus I	1.980 ± 0.029	2.236 ± 0.140	η2p = 0.028	0.076
Crus II	1.174 ± 0.022	1.257 ± 0.104	η2p =0.005	0.440

Estimated marginal means ± standard error for WM volumes adjusted for age, gender and total intracranial volumes. Post-hoc univariate comparisons across groups were only considered significant if the multivariate omnibus test reached significance (neither hemisphere): aWilks' Lambda = 0.921; F = 0.709; p = 0.739; η2p = 0.079. bWilks' Lambda = 0.904; F = 0.878; p = 0.572; η2p = 0.096. Partial η2 effect size is interpreted as small (η2p = 0.01), medium (η2p = 0.06) or large (η2p = 0.14).

Morphometric analyses captured predominantly symmetrical patterns of cerebellar atrophy in hexanucleotide repeat expansion carriers selectively affecting lobules I-IV, V, $VIII_{a/b}$, IX, and the vermis (**Figure 7**.) ALS-NEG patients showed more focal and less widespread changes in lobules I-IV and V. No voxelwise partial volume reductions were captured in the ALS-ATXi cohort.

Tract-based spatial statistics detected decreased FA and increased AD and RD in lobules I-IV, V, in GGGGCC repeat carriers. Additionally, decreased FA was also detected in Crura I and II in ALS-C9. (**Figure 8**.) Symmetric patterns of FA reductions were also readily detected in the ALS-NEG group, which involved lobule IX in both hemispheres, in addition to lobules I-IV, V, crura I and II. Increased RD in ALS-NEG was less widespread, predominantly involving lobules I-IV, V and VI. Changes in AD did not reach significance in the ALS-NEG group. The ALS-ATXi cohort did not exhibit voxelwise diffusivity alterations.

Figure 7*: Cerebellar grey matter alterations as indicated by focal partial volume reductions at p<0.05 FWE TFCE corrected for age, gender and total intracranial volumes. (A) Focal changes in ALS-C9 are indicated in blue and (B) changes in ALS-NEG patients in red-yellow. The Diedrichsen probabilistic cerebellar atlas is presented as underlay to aid localisation. MNI coordinates are provided on the right side of the figure for sagittal (x), coronal (y) and axial (z) views. ALS, amyotrophic lateral sclerosis; ALS-C9, patients who tested positive for GGGGCC repeat expansions in C9orf72; ALS-NEG, patients who tested negative for both ATXN2 and C9orf72; FWE, family-wise error; MNI, Montreal Neurological Institute; TFCE, threshold-free cluster enhancement.*

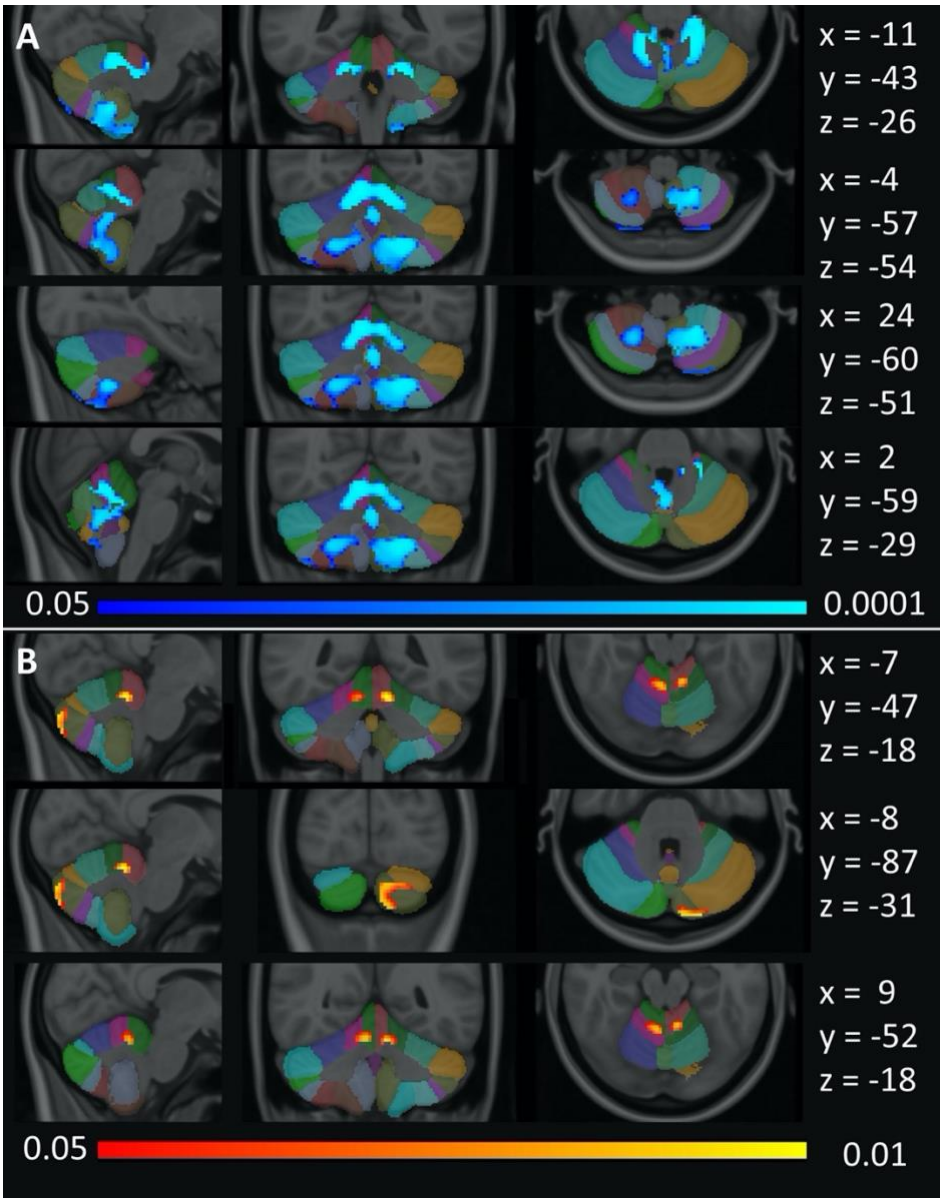

Figure 8: *Tract-based white matter changes in ALS as identified by FA, AD and RD alterations at p<0.01 TFCE adjusted for age and gender. Changes in ALS-C9 are indicated in blue (top), and changes in ALS-NEG are shown in red-yellow (bottom). The Diedrichsen probabilistic cerebellar atlas is presented as underlay to aid localisation. MNI coordinates are provided on the right side of the figure for sagittal (x), coronal (y) and axial (z) views. AD, axial diffusivity; ALS, amyotrophic lateral sclerosis; ALS-C9, patients who tested positive for GGGGCC repeat expansions in C9orf72; ALS-NEG, patients who tested negative for both ATXN2 and C9orf72; FA, fractional anisotropy; MNI, Montreal Neurological Institute; RD, radial diffusivity; TFCE, threshold-free cluster enhancement.*

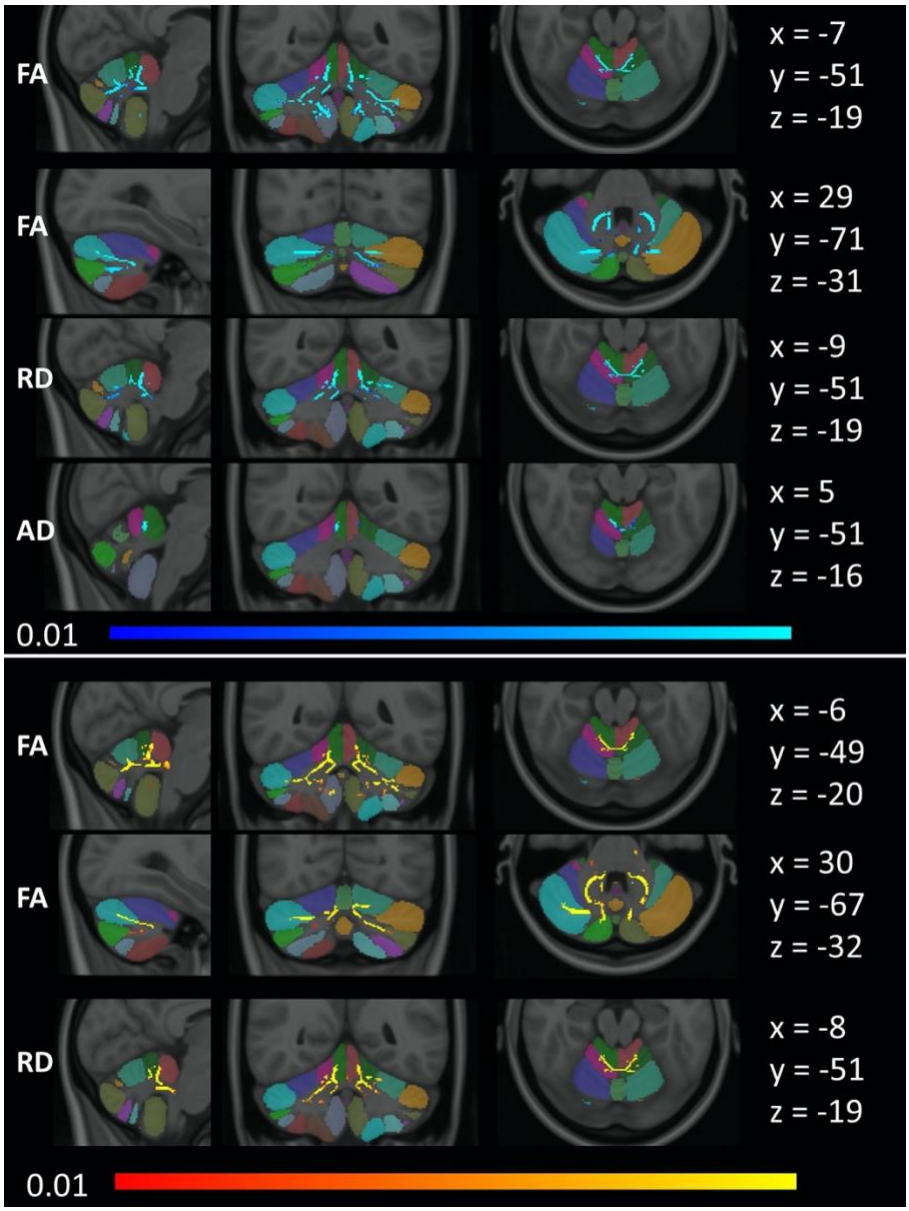

The comparison of superior peduncle volumes between the study groups did not reach significance, after corrections for age, gender and TIV. (**Tables 27 and 28**)

Table 27*: Superior cerebellar peduncle (SCP) volumes in healthy controls, ALS-NEG and ALS-C9*

	Estimated marginal means ± S.E. for groups			**Statistics**	
	HC n=110	**ALS-NEG n=133**	**ALS-C9 n=22**	**HC vs ALS-NEG**	**HC vs ALS-C9**
SCP volume	260.202 ± 5.246	250.211 ± 4.778	238.923 ± 12.069	0.491	0.325

Estimated marginal means ± standard error for SCP volume adjusted for age, gender and total intracranial volume. Post-hoc univariate comparisons across groups were only considered significant if the multivariate omnibus test reached significance (not applicable): F = 1.774; p = 0.172; η2p = 0.014. Partial η2 effect size is interpreted as small (η2p = 0.01), medium (η2p = 0.06) or large (η2p = 0.14).

Table 28*: Superior cerebellar peduncle (SCP) volumes in healthy controls and ALS-ATXi*

	Estimated marginal means ± S.E. for groups	
	HC n=100	**ALS-ATXi n=5**
SCP volume	260.254 ± 4.763	224.205 ± 22.908

Estimated marginal means ± standard error for SCP volume adjusted for age, gender and total intracranial volume. The comparison between HC and ALS-ATXi was not significant: F = 2.363; p = 0.127; η2p = 0.021.

Cerebro-cerebellar tractography in ALS-NEG identified FA reductions in the FPC (left cerebellar hemisphere to contralateral cerebrum) and in the DRTC (left cerebellar hemisphere to contralateral

cerebrum) (**Table 29**.) as well as increased RD in the left to contralateral FPC and in the left to contralateral DRTC. (**Table 30**) ALS-C9 patients exhibited FA reductions in left to contralateral FPC and left to contralateral PPC (**Table 29**.) as well as increased RD in the left to contralateral FPC and left to contralateral PPC (**Table 30**). No cerebro-cerebellar AD changes have been detected in the ALS-NEG or ALS-C9 group. (**Supplementary Table 31**.) Cerebro-cerebellar tractography did not capture FA, RD or AD alterations in the ALS-ATXi group. (**Supplementary Tables 32-34**.) The diffusivity profiles of the cerebellar peduncles were evaluated in dedicated region-of-interest analyses. Both ALS-NEG and ALS-C9 patients exhibited FA reductions in left and right inferior peduncles, whereas ALS-NEG showed additional FA reductions in right superior and middle cerebellar peduncles. ALS-NEG and ALS-C9 also showed increased RD in right superior, left and right inferior cerebellar peduncles. Furthermore, ALS-C9 exhibited increased AD in right superior cerebellar peduncle. (**Table 35**). No FA, AD or RD changes were detected in the ALS-ATXi group. (**Supplementary Table 13**). No significant CT, GM, or WM volume reductions and peduncular diffusivity alterations were identified in the single ALS-ATX patient with respect to matched controls.

Table 29. *FA values for the cerebro-cerebellar tracts in healthy controls and ALS-NEG and ALS-C9*

Cerebro-cerebellar FA values			Estimated marginal means ± S.E. for groups			Statistics		
			HC n=110	ALS-NEG n=133	ALS-C9 n=22	Univariate effect size	HC vs ALS-NEG	HC vs ALS-C9
Left[a]	**FPC**	**L1L**	0.453 ± 0.005	0.446 ± 0.005	0.439 ± 0.005	η^2p = 0.064	0.953	0.125
		L1R	0.465 ± 0.006	0.445 ± 0.006	0.432 ± 0.006	η^2p = 0.220	**0.035**	**<0.001**
	PPC	**L1L**	0.445 ± 0.005	0.439± 0.005	0.430 ± 0.005	η^2p = 0.073	1.000	0.093
		L1R	0.452 ± 0.006	0.442 ± 0.006	0.423 ± 0.006	η^2p = 0.143	0.763	**0.006**
	TPC	**L1L**	0.353 ± 0.008	0.342 ± 0.008	0.343 ± 0.008	η^2p = 0.019	0.991	1.000
		L1R	0.338 ± 0.008	0.347 ± 0.008	0.335 ± 0.008	η^2p = 0.020	1.000	1.000
	OPC	**L1L**	0.416 ± 0.008	0.410 ± 0.008	0.392 ± 0.008	η^2p = 0.071	1.000	0.117
		L1R	0.389 ± 0.010	0.362 ± 0.011	0.363 ± 0.011	η^2p = 0.063	0.226	0.256
	DRTC	**L1L**	0.395 ± 0.005	0.399 ± 0.005	0.394 ± 0.005	η^2p = 0.006	1.000	1.000
		L1R	0.381 ± 0.007	0.345 ± 0.007	0.362 ± 0.007	η^2p = 0.173	**0.002**	0.179
Right[b]	**FPC**	**R1R**	0.451 ± 0.005	0.444 ± 0.005	0.434 ± 0.005	η^2p = 0.072	1.000	1.000
		R1L	0.447 ± 0.005	0.436 ± 0.005	0.437 ± 0.005	η^2p = 0.043	1.000	1.000
	PPC	**R1R**	0.439 ± 0.005	0.442 ± 0.006	0.425 ± 0.006	η^2p = 0.075	1.000	1.000
		R1L	0.426 ± 0.006	0.417 ± 0.006	0.425 ± 0.006	η^2p = 0.021	1.000	1.000
	TPC	**R1R**	0.343 ± 0.007	0.348 ± 0.007	0.333 ± 0.007	η^2p = 0.042	1.000	1.000
		R1L	0.352 ± 0.008	0.347 ± 0.008	0.338 ± 0.008	η^2p = 0.026	1.000	1.000
	OPC	**R1R**	0.409 ± 0.008	0.401 ± 0.009	0.401 ± 0.009	η^2p = 0.010	1.000	1.000
		R1L	0.392 ± 0.009	0.371 ± 0.009	0.377 ± 0.009	η^2p = 0.049	1.000	1.000
	DRTC	**R1R**	0.390 ± 0.005	0.391 ± 0.005	0.387 ± 0.005	η^2p = 0.005	1.000	1.000
		R1L	0.356 ± 0.007	0.367 ± 0.007	0.365 ± 0.007	η^2p = 0.020	1.000	1.000

Estimated marginal means ± standard error for fractional anisotropy adjusted for age and gender. Post-hoc univariate comparisons across groups were only considered significant if the multivariate omnibus tests reached significance (left hemisphere): [a]Wilks' Lambda = 0.565; F = 1.782; p = 0.031; η^2p = 0.248, [b]Wilks' Lambda = 0.667; F = 1.212; p = 0.259; η^2p = 0.183. Bold p-values are significant at $p < 0.05$, after Bonferroni correction for multiple comparisons. Partial η^2 effect size is interpreted as small (η^2p = 0.01), medium (η^2p = 0.06) or large (η^2p = 0.14).

Table 30*: Radial diffusivity (RD) in cerebro-cerebellar tractography in healthy controls and ALS-NEG and ALS-C9*

Cerebro-cerebellar RD×10-3 values		Estimated marginal means ± S.E. for groups			Statistics		
		HC n=110	ALS-NEG n=133	ALS-C9 n=22	Univariate effect size	HC vs ALS-NEG	HC vs ALS-C9
Left[a]							
FPC	**L1L**	0.520 ± 0.006	0.529 ± 0.006	0.534 ± 0.006	η2p = 0.038	0.984	0.373
	L1R	0.508 ± 0.009	0.544 ± 0.010	0.552 ± 0.010	η2p = 0.169	**0.023**	**0.004**
PPC	**L1L**	0.537 ± 0.006	0.546 ± 0.006	0.557 ± 0.006	η2p = 0.081	0.944	0.065
	L1R	0.540 ± 0.013	0.563 ± 0.013	0.589 ± 0.013	η2p = 0.102	0.657	**0.029**
TPC	**L1L**	0.648 ± 0.020	0.697 ± 0.021	0.711 ± 0.021	η2p = 0.078	0.288	0.096
	L1R	0.709 ± 0.029	0.689 ± 0.031	0.746 ± 0.031	η2p = 0.028	1.000	1.000
OPC	**L1L**	0.575 ± 0.013	0.584 ± 0.013	0.615 ± 0.013	η2p = 0.078	1.000	0.095
	L1R	0.635 ± 0.025	0.688 ± 0.026	0.658 ± 0.026	η2p = 0.033	0.437	1.000
DRTC	**L1L**	0.592 ± 0.009	0.580 ± 0.009	0.603 ± 0.009	η2p = 0.048	1.000	1.000
	L1R	0.643 ± 0.020	0.721 ± 0.021	0.677 ± 0.021	η2p = 0.100	**0.032**	0.433
Right[b]							
FPC	**R1R**	0.504 ± 0.006	0.517 ± 0.006	0.535 ± 0.006	η2p = 0.167	0.382	0.002
	R1L	0.543 ± 0.009	0.548 ± 0.009	0.547 ± 0.009	η2p = 0.004	1.000	1.000
PPC	**R1R**	0.530 ± 0.008	0.536 ± 0.008	0.557 ± 0.008	η2p = 0.092	1.000	0.056
	R1L	0.593 ± 0.013	0.598 ± 0.014	0.590 ± 0.014	η2p = 0.003	1.000	1.000
TPC	**R1R**	0.632 ± 0.024	0.676 ± 0.024	0.690 ± 0.024	η2p = 0.049	0.593	0.272
	R1L	0.683 ± 0.019	0.671 ± 0.020	0.700 ± 0.020	η2p = 0.018	1.000	1.000
OPC	**R1R**	0.565 ± 0.014	0.587 ± 0.014	0.594 ± 0.014	η2p = 0.034	0.868	0.484
	R1L	0.617 ± 0.022	0.690 ± 0.023	0.665 ± 0.023	η2p = 0.080	0.074	0.420
DRTC	**R1R**	0.578 ± 0.010	0.599 ± 0.010	0.607 ± 0.010	η2p = 0.064	0.464	0.151
	R1L	0.650 ± 0.017	0.651 ± 0.018	0.674 ± 0.018	η2p = 0.019	1.000	0.986

Estimated marginal means ± standard error for radial diffusivity adjusted for age and gender. Post-hoc univariate comparisons across groups were only considered significant if the multivariate omnibus test reached significance (left hemisphere): aWilks' Lambda = 0.552; F = 1.869; p = 0.022; η2p = 0.257, bWilks' Lambda = 0.643; F = 1.336; p = 0.172; η2p = 0.198. Bold p-values are significant at $p < 0.05$, after Bonferroni correction for multiple comparisons. Partial η2 effect size is interpreted as small (η2p = 0.01), medium (η2p = 0.06) or large (η2p = 0.14).

Table 31: *Axial Diffusivity (AD) in cerebro-cerebellar tractography in healthy controls and ALS-NEG and ALS-C9*

Cerebro-cerebellar AD×10-3 values		Estimated marginal means ± S.E. for groups			Statistics		
		HC n=110	ALS-NEG n=133	ALS-C9 n=22	Univariate effect size	HC vs ALS-NEG	HC vs ALS-C9
Left[a]							
FPC	**L1L**	1.092 ± 0.007	1.097 ± 0.007	1.083 ± 0.007	η2p = 0.027	1.000	1.000
	L1R	1.090 ± 0.011	1.110 ± 0.012	1.092 ± 0.012	η2p = 0.025	0.716	1.000
PPC	**L1L**	1.114 ± 0.006	1.120 ± 0.007	1.113 ± 0.007	η2p = 0.009	1.000	1.000
	L1R	1.122 ± 0.016	1.143 ± 0.016	1.137 ± 0.016	η2p = 0.015	1.000	1.000
TPC	**L1L**	1.108 ± 0.023	1.159 ± 0.024	1.173 ± 0.024	η2p = 0.061	0.412	0.181
	L1R	1.167 ± 0.035	1.147 ± 0.036	1.207 ± 0.036	η2p = 0.022	1.000	1.000
OPC	**L1L**	1.117 ± 0.012	1.118 ± 0.012	1.127 ± 0.012	η2p = 0.006	1.000	1.000
	L1R	1.153 ± 0.035	1.182 ± 0.036	1.141 ± 0.036	η2p = 0.010	1.000	1.000
DRTC	**L1L**	1.116 ± 0.010	1.105 ± 0.010	1.138 ± 0.010	η2p = 0.076	1.000	0.432
	L1R	1.158 ± 0.020	1.197 ± 0.021	1.166 ± 0.021	η2p = 0.030	0.565	1.000
Right[b]							
FPC	**R1R**	1.060 ± 0.009	1.073 ± 0.009	1.079 ± 0.009	η2p = 0.036	0.911	0.420
	R1L	1.119 ± 0.010	1.105 ± 0.011	1.105 ± 0.011	η2p = 0.019	1.000	1.000
PPC	**R1R**	1.090 ± 0.008	1.110 ± 0.008	1.106 ± 0.008	η2p = 0.050	0.283	0.506
	R1L	1.163 ± 0.017	1.151 ± 0.017	1.154 ± 0.017	η2p = 0.004	1.000	1.000
TPC	**R1R**	1.064 ± 0.031	1.144 ± 0.033	1.142 ± 0.033	η2p = 0.061	0.245	0.275
	R1L	1.153 ± 0.024	1.128 ± 0.025	1.153 ± 0.025	η2p = 0.011	1.000	1.000
OPC	**R1R**	1.092 ± 0.015	1.110 ± 0.016	1.115 ± 0.016	η2p = 0.018	1.000	0.914
	R1L	1.138 ± 0.026	1.211 ± 0.027	1.174 ± 0.027	η2p = 0.054	0.185	1.000
DRTC	**R1R**	1.087 ± 0.012	1.123 ± 0.013	1.127 ± 0.013	η2p = 0.091	0.128	0.082
	R1L	1.122 ± 0.018	1.151 ± 0.019	1.174 ± 0.019	η2p = 0.059	0.839	0.156

Estimated marginal means ± standard error for axial diffusivity adjusted for age and gender. Post-hoc univariate comparisons across groups were only considered significant if the multivariate omnibus test reached significance (neither hemisphere): aWilks' Lambda = 0.666; F = 1.216; p = 0.256; η2p = 0.184, bWilks' Lambda = 0.723; F = 0.953; p = 0.524; η2p = 0.150. Partial η2 effect size is interpreted as small (η2p = 0.01), medium (η2p = 0.06) or large (η2p = 0.14).

Table 32: *Fractional anisotropy (FA) values for the cerebro-cerebellar tracts in healthy controls and ALS-ATXi*

Cerebro-cerebellar FA values		Estimated marginal means ± S.E. for groups		Statistics	
		HC n=110	ALS-ATXi n=5	Univariate effect size	HC vs ALS-ATXi
Left[a]					
FPC	**L1L**	0.453 ± 0.005	0.462 ± 0.009	η2p = 0.030	0.388
	L1R	0.466 ± 0.005	0.450 ± 0.012	η2p = 0.052	0.252
PPC	**L1L**	0.446 ± 0.003	0.436 ± 0.008	η2p = 0.043	0.299
	L1R	0.453 ± 0.005	0.455 ± 0.012	η2p = 0.002	0.841
TPC	**L1L**	0.353 ± 0.006	0.378 ± 0.013	η2p = 0.104	0.101
	L1R	0.340 ± 0.009	0.313 ± 0.021	η2p = 0.050	0.262
OPC	**L1L**	0.415 ± 0.005	0.424 ± 0.011	η2p = 0.018	0.504
	L1R	0.389 ± 0.010	0.390 ± 0.022	η2p = 0.000	0.985
DRTC	**L1L**	0.396 ± 0.005	0.392 ± 0.012	η2p = 0.003	0.798
	L1R	0.381 ± 0.008	0.364 ± 0.018	η2p = 0.027	0.414
Right[b]					
FPC	**R1R**	0.451 ± 0.004	0.450 ± 0.010	η2p = 0.000	0.938
	R1L	0.447 ± 0.005	0.451 ± 0.011	η2p = 0.004	0.751
PPC	**R1R**	0.440 ± 0.005	0.446 ± 0.012	η2p = 0.011	0.607
	R1L	0.426 ± 0.005	0.418 ± 0.012	η2p = 0.017	0.517
TPC	**R1R**	0.342 ± 0.006	0.339 ± 0.015	η2p = 0.001	0.867
	R1L	0.352 ± 0.007	0.354 ± 0.017	η2p = 0.00	0.905
OPC	**R1R**	0.410 ± 0.008	0.417 ± 0.020	η2p = 0.004	0.755
	R1L	0.394 ± 0.009	0.355 ± 0.021	η2p = 0.096	0.115
DRTC	**R1R**	0.391 ± 0.005	0.389 ± 0.012	η2p = 0.001	0.911
	R1L	0.356 ± 0.008	0.347 ± 0.018	η2p = 0.010	0.619

Estimated marginal means ± standard error for fractional anisotropy adjusted for age and gender. Post-hoc univariate comparisons across groups were only considered significant if the multivariate omnibus test reached significance (neither hemisphere): aWilks' Lambda = 0.522; F = 1.468; p = 0.238; η2p = 0.478, bWilks' Lambda = 0.801; F = 0.397; p = 0.929; η2p = 0.199. Partial η2 effect size is interpreted as small (η2p = 0.01), medium (η2p = 0.06) or large (η2p = 0.14).

Table 33*: Axial Diffusivity (AD) in cerebro-cerebellar tractography in healthy controls and ALS-ATXi*

Cerebro-cerebellar AD×10-3 values		Estimated marginal means ± S.E. for groups		Statistics	
		HC n=110	ALS-ATXi n=5	Univariate effect size	HC vs ALS-ATXi
Left[a]					
FPC	**L1L**	1.092 ± 0.0075	1.073 ± 0.011	η2p = 0.087	0.136
	L1R	1.089 ± 0.007	1.077 ± 0.016	η2p = 0.016	0.528
PPC	**L1L**	1.114 ± 0.004	1.103 ± 0.010	η2p = 0.037	0.336
	L1R	1.122 ± 0.018	1.167 ± 0.042	η2p = 0.036	0.342
TPC	**L1L**	1.108 ± 0.015	1.096 ± 0.034	η2p = 0.004	0.755
	L1R	1.156 ± 0.029	1.274 ± 0.068	η2p = 0.090	0.129
OPC	**L1L**	1.116 ± 0.009	1.102 ± 0.020	η2p = 0.014	0.561
	L1R	1.146 ± 0.022	1.181 ± 0.051	η2p = 0.016	0.532
DRTC	**L1L**	1.118 ± 0.009	1.101 ± 0.022	η2p = 0.021	0.475
	L1R	1.164 ± 0.014	1.065 ± 0.033	η2p = 0.221	0.013
Right[b]					
FPC	**R1R**	1.060 ± 0.006	1.045 ± 0.014	η2p = 0.040	0.316
	R1L	1.117 ± 0.009	1.115 ± 0.021	η2p = 0.000	0.928
PPC	**R1R**	1.091 ± 0.005	1.097 ± 0.013	η2p = 0.008	0.667
	R1L	1.158 ± 0.016	1.197 ± 0.038	η2p = 0.033	0.365
TPC	**R1R**	1.061 ± 0.019	1.095 ± 0.045	η2p = 0.018	0.503
	R1L	1.154 ± 0.023	1.174 ± 0.052	η2p = 0.005	0.734
OPC	**R1R**	1.093 ± 0.013	1.094 ± 0.031	η2p = 0.000	0.988
	R1L	1.137 ± 0.020	1.113 ± 0.048	η2p = 0.008	0.655
DRTC	**R1R**	1.087 ± 0.012	1.108 ± 0.027	η2p = 0.018	0.509
	R1L	1.121 ± 0.021	1.224 ± 0.049	η2p = 0.125	0.071

Estimated marginal means ± standard error for axial diffusivity adjusted for age and gender. Post-hoc univariate comparisons across groups were only considered significant if the multivariate omnibus test reached significance (neither hemisphere): aWilks' Lambda = 0.462; F = 1.864; p = 0.129; η2p = 0.538, bWilks' Lambda = 0.682; F = 0.745; p = 0.676; η2p = 0.318. Partial η2 effect size is interpreted as small (η2p = 0.01), medium (η2p = 0.06) or large (η2p = 0.14).

Table 34*: Radial diffusivity (RD) in cerebro-cerebellar tractography in healthy controls and ALS-ATXi*

Cerebro-cerebellar RD×10-3 values		Estimated marginal means ± S.E. for groups		Statistics	
		HC n=110	ALS-ATXi n=5	Univariate effect size	HC vs ALS-ATXi
Left[a]					
FPC	**L1L**	0.520 ± 0.006	0.499 ± 0.011	η2p = 0.112	0.088
	L1R	0.506 ± 0.007	0.523 ± 0.017	η2p = 0.032	0.375
PPC	**L1L**	0.536 ± 0.004	0.539 ± 0.010	η2p = 0.003	0.791
	L1R	0.539 ± 0.013	0.565 ± 0.031	η2p = 0.022	0.464
TPC	**L1L**	0.648 ± 0.012	0.612 ± 0.028	η2p = 0.051	0.257
	L1R	0.700 ± 0.027	0.814 ± 0.063	η2p = 0.094	0.119
OPC	**L1L**	0.575 ± 0.009	0.560 ± 0.020	η2p = 0.017	0.512
	L1R	0.630 ± 0.021	0.646 ± 0.048	η2p = 0.004	0.768
DRTC	**L1L**	0.593 ± 0.021	0.585 ± 0.022	η2p = 0.004	0.768
	L1R	0.648 ± 0.018	0.618 ± 0.042	η2p = 0.017	0.519
Right[b]					
FPC	**R1R**	0.503 ± 0.005	0.497 ± 0.011	η2p = 0.009	0.634
	R1L	0.541 ± 0.008	0.537 ± 0.017	η2p = 0.002	0.845
PPC	**R1R**	0.528 ± 0.006	0.526 ± 0.014	η2p = 0.001	0.865
	R1L	0.590 ± 0.014	0.622 ± 0.032	η2p = 0.030	0.391
TPC	**R1R**	0.633 ± 0.017	0.654 ± 0.039	η2p = 0.010	0.624
	R1L	0.684 ± 0.019	0.676 ± 0.045	η2p = 0.001	0.880
OPC	**R1R**	0.566 ± 0.012	0.561 ± 0.027	η2p = 0.001	0.872
	R1L	0.615 ± 0.016	0.644 ± 0.036	η2p = 0.020	0.481
DRTC	**R1R**	0.578 ± 0.010	0.594 ± 0.024	η2p = 0.016	0.528
	R1L	0.646 ± 0.022	0.738 ± 0.052	η2p = 0.086	0.138

Estimated marginal means ± standard error for radial diffusivity values adjusted for age and gender. Post-hoc univariate comparisons across groups were only considered significant if the multivariate omnibus test reached significance (neither hemisphere): aWilks' Lambda = 0.582; F = 1.148; p = 0.389; η2p = 0.418, bWilks' Lambda = 0.688; F = 0.725; p = 0.692; η2p = 0.312. Bold p-values are significant at $p < 0.05$, after Bonferroni correction for multiple comparisons. Partial η2 effect size is interpreted as small (η2p = 0.01), medium (η2p = 0.06) or large (η2p = 0.14).

Table 35*: Cerebellar peduncle profiles in healthy controls and ALS*

Anatomical region	Diffusivity index	Estimated marginal means ± S.E. for groups			Statistics		
		HC n=110	ALS-NEG n=133	ALS-C9 n=22	Univariate effect size	HC vs ALS-NEG	HC vs ALS-C9
Left Superior Cerebellar Peduncle	**FA**	0.600 ± 0.004	0.587 ± 0.003	0.584 ± 0.009	$\eta^2p = 0.024$	0.064	0.311
	AD×10^{-3}	1.367 ± 0.007	1.370 ± 0.007	1.384 ± 0.017	$\eta^2p = 0.003$	1.000	1.000
	RD×10^{-3}	0.473 ± 0.005	0.490 ± 0.005	0.502 ± 0.012	$\eta^2p = 0.030$	0.057	0.086
Right Superior Cerebellar Peduncle	**FA**	0.592 ± 0.004	0.576 ± 0.003	0.574 ± 0.009	$\eta^2p = 0.041$	**0.005**	0.148
	AD×10^{-3}	1.374 ± 0.008	1.386 ± 0.007	1.422 ± 0.017	$\eta^2p = 0.025$	0.739	**0.033**
	RD×10^{-3}	0.488 ± 0.005	0.513 ± 0.005	0.532 ± 0.012	$\eta^2p = 0.068$	**0.001**	**0.002**
Left Inferior Cerebellar Peduncle	**FA**	0.482 ± 0.004	0.464 ± 0.003	0.450 ± 0.008	$\eta^2p = 0.072$	**0.001**	**0.001**
	AD×10^{-3}	1.079 ± 0.006	1.092 ± 0.005	1.084 ± 0.013	$\eta^2p = 0.009$	0.404	1.000
	RD×10^{-3}	0.495 ± 0.005	0.519 ± 0.004	0.540 ± 0.011	$\eta^2p = 0.077$	**0.001**	**<0.001**
Right Inferior Cerebellar Peduncle	**FA**	0.479 ± 0.004	0.458 ± 0.003	0.436 ± 0.008	$\eta^2p = 0.112$	**<0.001**	**<0.001**
	AD×10^{-3}	1.079 ± 0.006	1.084 ± 0.005	1.050 ± 0.012	$\eta^2p = 0.024$	1.000	0.104
	RD×10^{-3}	0.492 ± 0.004	0.518 ± 0.004	0.529 ± 0.010	$\eta^2p = 0.081$	**<0.001**	**0.003**
Middle Cerebellar Peduncle	**FA**	0.502 ± 0.003	0.490 ± 0.003	0.485 ± 0.006	$\eta^2p = 0.043$	**0.008**	0.052
	AD×10^{-3}	1.052 ± 0.005	1.053 ± 0.004	1.039 ± 0.010	$\eta^2p = 0.006$	1.000	0.731
	RD×10^{-3}	0.455 ± 0.003	0.466 ± 0.003	0.468 ± 0.007	$\eta^2p = 0.028$	**0.034**	0.274

Estimated marginal means ± standard error for diffusivity values (FA, AD, RD) adjusted for age and gender. Wilks' Lambda = 0.703; F = 3.164; $p < 0.001$; $\eta^2p = 0.162$. Bold p-values are significant at $p < 0.05$, after Bonferroni correction for multiple comparisons. Partial η^2 effect size is interpreted as small ($\eta^2p = 0.01$), medium ($\eta^2p = 0.06$) or large ($\eta^2p = 0.14$). HC- Healthy Control, FA – Fractional Anisotropy, AD – Axial diffusivity, RD – Radial diffusivity

Table 36*: Cerebellar peduncle profiles in healthy controls and ALS-ATXi*

Anatomical region	Diffusivity index	Estimated marginal means ± S.E. for groups		Statistics	
		HC n=110	ALS-ATXi n=5	Univariate effect size	HC vs ALS-ATXi
Left Superior Cerebellar Peduncle	**FA**	0.599 ± 0.004	0.577 ± 0.020	η2p = 0.011	0.273
	AD×10-3	1.365 ± 0.007	1.344 ± 0.035	η2p = 0.003	0.573
	RD×10-3	0.473 ± 0.006	0.499 ± 0.028	η2p = 0.008	0.358
Right Superior Cerebellar Peduncle	**FA**	0.591 ± 0.004	0.564 ± 0.020	η2p = 0.016	0.180
	AD×10-3	1.372 ± 0.007	1.363 ± 0.033	η2p = 0.001	0.789
	RD×10-3	0.488 ± 0.006	0.524 ± 0.028	η2p = 0.015	0.203
Left Inferior Cerebellar Peduncle	**FA**	0.483 ± 0.004	0.481 ± 0.018	η2p = 0.000	0.917
	AD×10-3	1.079 ± 0.005	1.072 ± 0.025	η2p = 0.001	0.778
	RD×10-3	0.494 ± 0.004	0.506 ± 0.021	η2p = 0.003	0.568
Right Inferior Cerebellar Peduncle	**FA**	0.480 ± 0.004	0.464 ± 0.018	η2p = 0.006	0.399
	AD×10-3	1.080 ± 0.005	1.074 ± 0.026	η2p = 0.001	0.800
	RD×10-3	0.491 ± 0.005	0.512 ± 0.022	η2p = 0.008	0.340
Middle Cerebellar Peduncle	**FA**	0.502 ± 0.004	0.511 ± 0.017	η2p = 0.002	0.601
	AD×10-3	1.052 ± 0.005	1.043 ± 0.023	η2p = 0.001	0.695
	RD×10-3	0.454 ± 0.004	0.440 ± 0.019	η2p = 0.005	0.469

Estimated marginal means ± standard error for diffusivity values (FA, AD, RD) adjusted for age and gender. Post-hoc univariate comparisons across groups were only considered significant if the multivariate omnibus test reached significance (not applicable): Wilks' Lambda = 0.849; F = 1.154; p = 0.321; η2p = 0.151. Partial η2 effect size is interpreted as small (η2p = 0.01), medium (η2p = 0.06) or large (η2p = 0.14). HC- Healthy Control, FA – Fractional Anisotropy, AD – Axial diffusivity, RD – Radial diffusivity

Discussion

In this study, we have identified relatively symmetric and focal cerebellar degeneration in ALS. These observations are not driven by intermediate-length alleles of *ATXN2*, indicating that cerebellar pathology is a broader feature of ALS than a simple overlap of clinical features with spinocerebellar ataxia type 2 due to pleiotropy of *ATXN2* repeat expansions. The genetic causes of ALS in the ALS-NEG cohort remain undiscovered, but recent observations of intermediate-length *ATXN1* risk alleles in ALS,(560) coupled with polygenic enrichment in cerebellar genes,(586) indicate that the aetiological agents underlying ALS have functional roles in the biology of the cerebellum, potentially explaining the structural changes that we have observed.

While ALS-NEG patients displayed predominantly anterior lobe pathology, patients carrying the pathogenic hexanucleotide repeat expansion in *C9orf72* exhibited more widespread cerebellar atrophy involving the posterior lobe and the vermis. The posterior lobe of cerebellum, or 'neocerebellum' is regarded the newest part of the cerebellum phylogenetically and is associated with a variety of cognitive functions.(435, 587) The role of posterior lobe lobules in mediating cognitive processes has been consistently demonstrated by activation and lesion studies.(427, 438) While clinically the *C9orf72* genotype in ALS is widely associated with cognitive and behavioural deficits, these symptoms are typically solely linked to frontotemporal degeneration.(510) Cortical thickness analyses in ALC-C9 captured the involvement of lobules VI, VIIb, and crura I & II, while morphometric analyses confirmed considerable posterior lobe pathology showcasing extensive lobule VIIIa, VIIIb, IX and posterior-inferior vermis involvement. The lobular distribution of diffusivity alterations

mirrored the patterns of grey mater degeneration. Cerebro-cerebellar tractography highlighted the pathology of FPC and PPC projections.

The intra-cerebellar patterns identified by the various imaging methods are largely concordant; segmentation-based volumetric analyses mirror the most vulnerable regions identified by morphometry. The most significant white matter alterations were detected subjacent to grey matter regions affected by cortical thickness and partial volume reductions. The relative concordance between the various imaging streams suggests that voxelwise analysis pipelines such as TBSS and morphometry may readily detect focal cerebellar changes potentially obviating the need for computationally demanding segmentation approaches and post-hoc statistics in future studies. Both cerebro-cerebellar tractography and intra-cerebellar tract-based analyses identified widespread FA reductions and increased RD, with relatively limited AD alterations. In contrast to the considerable diffusivity alterations, no white matter volume reductions were detected, which highlights the limitations of T1w data in detecting white matter degeneration.

In the existing literature, increased cerebellar activation during motor task, increased PET signal, and increased functional cerebro-cerebellar connectivity are often interpreted as compensatory(362, 454, 469) change in response to supratentorial degeneration, despite the fact that very few structural studies (362) and no post mortem studies have actually demonstrated adaptive cerebellar hypertrophy. In this study, we have not identified increased cerebellar integrity metrics or increased cerebro-cerebellar connectivity indices. The apparent disparity between high-resolution structural findings and insights inferred from functional studies highlights the risks of interpreting functional observations in isolation without the interrogation of accompanying structural or post mortem data. The evaluation of putative

compensatory processes would require dedicated multiparametric studies combining functional, metabolic and structural protocols.

This study is not without limitations; only a single ALS-SCA patient was included, a small ALS-ATXi sample was evaluated, and a cross-sectional study design was implemented. The interrogation of longitudinal cerebellar data, with the inclusion of presymptomatic mutation carriers, is likely to offer important additional insights regarding the chronology of supra- and infra-tentorial changes. Broader genotyping of SCA-associated genes (e.g. *ATXN1*) and other repeat expansions known to contribute to neurodegeneration(588) may provide a more comprehensive and better-powered categorisation strategy for understanding the pleiotropic expression of this type of genetic variant. Our tractography protocol did not evaluate the segmental profile of cerebro-cerebella projections and the CST, FPC, PPC and DRTC may overlap in certain voxels along their course. High angular resolution protocols, constrained spherical deconvolution and non-Gaussian diffusion models such as NODDI or DKI may be better suited for the nuanced characterisation of these tracts especially with regards to crossing fibres.

Notwithstanding these limitations, we have demonstrated focal anterior lobe degeneration in a large cohort of ALS patients testing negative for *ATX2* and *C9orf72* and have shown posterior dominant and vermis atrophy in *C9orf72* mutation carriers. From a clinical perspective our findings highlight the pitfalls of attributing specific clinical symptoms to single anatomical foci, as cerebellar pathology is likely to modulate a number of cardinal symptoms in ALS, such as dysphagia, dysarthria, pseudobulbar affect, and respiratory rhythmicity.(419, 420, 429, 553) With our descriptive analyses we sought to add the cerebellum to the list of vulnerable

anatomical regions preferentially affected in ALS, and showcase the presence of considerable infratentorial disease burden.

Conclusions

Patients with ALS exhibit cerebellar degeneration and cerebro-cerebellar connectivity alterations which can be readily detected *in vivo*. The contribution of cerebellar pathology to the clinical heterogeneity of ALS, including cognitive, behavioural, pseudobulbar, bulbar, eye movement and gait manifestations need to be carefully considered instead of solely attributing these symptoms to supratentorial and brainstem pathology.

CHAPTER 6: Selective pathology of thalamic nuclei in ALS and PLS

Introduction

While amyotrophic lateral sclerosis (ALS) is a clinically and genetically heterogeneous neurodegenerative condition, patients with ALS have a relatively stereotyped disease trajectory dominated by relentlessly progressive motor disability and ultimately respiratory compromise. The core neuroimaging signature of ALS includes motor cortex, brainstem, corticospinal tract, and spinal cord degeneration. Subcortical grey matter degeneration has also been observed both post mortem and in vivo (589). Thalamus pathology in ALS has been evaluated by dedicated structural, metabolic, and functional imaging studies (316, 321, 327, 590, 591). The thalamus however is typically evaluated as a single structure in ALS. Overall thalamic atrophy has been identified by both neuroimaging (150, 327, 336) and post mortem histopathology studies in ALS (592), but the involvement of specific nuclei has not been comprehensively characterised to date. The thalamus comprises over 60 cytoarchitectonically distinct nuclei with unique cortical connectivity patterns (593), physiological functions, (594) embryonic origin, (595) and vascular supply (596). The risk of evaluating the entire thalamus as a whole is averaging pathological change across affected and unaffected regions. Several radiological approaches exist to segment the thalamus; it may be parcellated based on cortical connectivity patterns (325, 593, 597) or anatomically, based on the histological data (598). The few existing thalamus studies in ALS

segmented the thalamus based on cortical projection patterns (154, 321) and not anatomically, which would allow the systematic assessment of specific nuclei.

Given the strikingly focal cortical grey matter signatures observed in both ALS (316) and PLS (118) we hypothesised that similarly selective thalamic involvement may be detected if thalamic nuclei are appraised individually. Irrespective of the underlying genotype, co-existence of cognitive deficits, familial or sporadic presentation, limb weakness and bulbar impairment are pathognomonic clinical features of ALS (599) which can be linked to motor cortex and spinal cord degeneration on imaging (121). Based on clinical and radiological observations, it is increasingly clear that extra-pyramidal degeneration also contributes to motor disability in ALS (459, 600). Connectivity-based thalamic segmentation in ALS reveals focal degeneration in thalamic regions projecting to motor areas (154) and frontotemporal regions (321). Accordingly, we hypothesised that thalamic pathology in ALS preferentially involves nuclei mediating motor function such as the ventral anterior and ventral lateral nuclei.

While GGGGCC hexanucleotide expansions in *C9orf72* in ALS have been previously linked to orbitofrontal (23), opercular (138), cingulate (590) and temporal lobe alterations (132), widespread extra-motor (527) and subcortical grey matter changes (601) are also readily observed in *C9orf72* negative sporadic ALS patients. The *C9orf72* genotype has also been linked to thalamus pathology in ALS (590, 601), but its thalamic signature has not been characterised at a nuclear level. A recent large FTD study (602) identified that *C9orf72* hexanucleotide repeat carriers exhibit preferential

pulvinar atrophy, which is thought to be unique to the genotype. Based on the available FTD literature (602, 603), one of the objectives of this study is to examine if *C9orf72* mutation carriers in ALS exhibit distinctive patterns of thalamic involvement different from sporadic ALS patients. As GGGGCC hexanucleotide repeat expansions in ALS are associated with neuropsychological deficits (604), we hypothesised that *C9orf72* positive ALS patients may exhibit preferential degeneration in thalamic nuclei mediating cognitive functions.

In contrast to ALS, there is a striking paucity of both imaging and post mortem studies in PLS (118). PLS is associated with longer survival than ALS (605) and the clinical picture is dominated by upper motor neuron dysfunction.(606) Extra-motor (607) and extra-pyramidal (608) manifestations have been sporadically reported in PLS, but thalamic involvement has not been systematically characterised to date in vivo. As clinical heterogeneity is less marked in PLS than ALS, we hypothesised that focal changes will be captured in the ventral anterior and ventral lateral nuclei.

While the clinical symptoms of ALS and PLS are dominated by limb weakness, bulbar impairment and respiratory weakness, sensory deficits have also been reported, captured by electrophysiology studies and sensory tract involvement detected on spinal imaging (174, 252). Patients with ALS often report paraesthesiae, but frank nociceptive, thermoceptive or proprioceptive deficits are seldom detected on clinical assessment. (166) The anatomical segmentation of the thalamus into specific nuclei permits the targeted assessment of ventral posterolateral nuclei which mediate

somatosensory information from the contralateral face and the ventral medial nuclei conveying somatosensory information from the contralateral trunk and limbs.

Building on accruing evidence of overall thalamic involvement in ALS, the main objective of this study was the characterisation of regional thalamic pathology in sporadic, *C9orf72* negative ALS at a nuclear level. An additional objective was to evaluate if PLS and *C9orf72* positive ALS patients have distinctive thalamic signatures. Based on the review of the literature, we hypothesised, that the 'global' thalamus pathology reported by previous imaging studies in ALS is driven by focal changes in susceptible nuclei.

Methods

Ethics statement

All aspects of this study, including recruitment, data management, consent forms and information leaflets were approved by the institutional ethics committee (Beaumont Hospital, Dublin, Ireland), in accordance with the 1964 Helsinki declaration and its later amendments. Study participants provided informed consent prior to inclusion.

Participants

Patients were recruited between September 2017 and September 2020. Hundred patients with ALS, 33 patients with PLS and 117 healthy controls were included in this study. PLS patients were diagnosed based on the Gordon criteria (605) Participating ALS patients had 'probable' or 'definite' ALS according to the El Escorial criteria (609). Exclusion criteria included a known history of traumatic brain injury, cerebrovascular events, neuroinflammatory conditions, neoplastic conditions, and inability to undergo MRI scanning due to metallic devices such as baclofen pumps or pacemakers. Known claustrophobia or orthopnoea were other exclusion criteria. The demographic and clinical profile of each patient was carefully recorded; motor disability was assessed by the revised ALS functional rating scale (ALSFRS-r) (610), the Edinburgh Cognitive ALS Screen (ECAS) (397) was administered for cognitive assessment using population-based normative values (611) and the diagnosis of co-morbid FTD was established based on the revised Strong criteria (612). The healthy controls of the study were unrelated to the participating patients and had no known neurological or psychiatric conditions, previous head injuries or a family history of neurodegenerative conditions.

Neuroimaging methods

T_1-weighted images were acquired with a 3D Inversion Recovery prepared Spoiled Gradient Recalled echo (IR-SPGR) pulse sequence on a 3 Tesla Philips Achieva system using an 8-channel receive-only head coil. The following pulse sequence parameters were used; field-of-view (FOV): 256 x 256 x 160 mm, spatial resolution: 1 mm^3, TR/TE =

8.5/3.9 ms, TI =1060 ms, flip angle = 8°, SENSE factor = 1.5, acquisition time: 7 min 30 s.

TIV volumes

Total intracranial volume (TIV) was estimated for each study participant to be used as a covariate in comparative statistical models. TIV was calculated by adding grey matter, white matter and CSF volume estimates. Registration and tissue type segmentation was carried out in FMRIB's FSL environment. Following skull-stripping (613) and individual quality verification, each subject image was linearly aligned to MNI152 standard space using FMRIB's Linear Image Registration Tool (FLIRT)(614). Tissue-type segmentation was performed using FMRIB's Automated Segmentation Tool (FAST) (615) which accounts for spatial intensity variations. The inverse of the determinant of the affine registration matrix was calculated and multiplied by the size of the template for tissue-type volume estimation.

Thalamic segmentation

A Bayesian inference was used to segment the thalamus into 25 sub-regions as described by Iglesias at al. using a probabilistic atlas developed based on histological data in the FreeSurfer analysis suite. (598) (**Figure 9**.) The thalamus was parcellated into the following nuclei in each hemisphere: antero-ventral (AV), latero-dorsal (LD), lateral posterior (LP), ventral anterior (VA), ventral anterior magnocellular (VA mc), ventral lateral anterior (VLa), ventral lateral posterior (VLp), ventral posterolateral (VPL), ventromedial (VM), central medial (CeM), central lateral (CL), paracentral (Pc),

centromedian (CM), parafascicular (Pf), paratenial (Pt), reuniens/medial ventral (MV-re), mediodorsal medial magnocellular (MDm), mediodorsal lateral parvocellular (MDl), lateral geniculate (LGN), medial geniculate (MGN), limitans/suprageniculate (L-SG), pulvinar anterior (PuA), pulvinar medial (PuM), pulvinar lateral (PuL), and pulvinar inferior (PuI). The raw volume estimates of the above nuclei were averaged between left and right and merged into the following 10 core group of nuclei defined based on their distinctive physiological function: “Anteroventral”, “Lateral geniculate”, “Medial geniculate”, “Pulvinar-limitans” (PuA, PuM, PuL, PuI, L-SG), “Laterodorsal”, “Lateroposterior”, “Mediodorsal-paratenial-reuniens” (MDm, MDl, MV-re, Pt), “Motor hub” (VA, VAmc, VLa, VLp), “Sensory hub” (VPL, VM), “Intralaminar” (CeM, CL, Pc, CM, Pf). “Total thalamic volume” was defined as the mean of the left and right thalamus volume estimates.

Figure 9*: Atlas-based segmentation of the thalamus; anteroventral (AV), central medial (CeM), central lateral (CL), centromedian (CM), laterodorsal (LD), lateral geniculate (LGN), lateral posterior (LP), limitans/suprageniculate (L-SG), mediodorsal lateral parvocellular (MDl), mediodorsal medial magnocellular (MDm), medial geniculate (MGN), reuniens/medial ventral (MV-re), paracentral (Pc), parafascicular (Pf), pulvinar anterior (PuA), pulvinar inferior (PuI), pulvinar lateral (PuL), pulvinar medial (PuM), ventral anterior (VA), ventral anterior magnocellular (VA mc), ventral lateral anterior (VLa), ventral lateral posterior (VLp), ventromedial (VM), ventral posterolateral (VPL)*

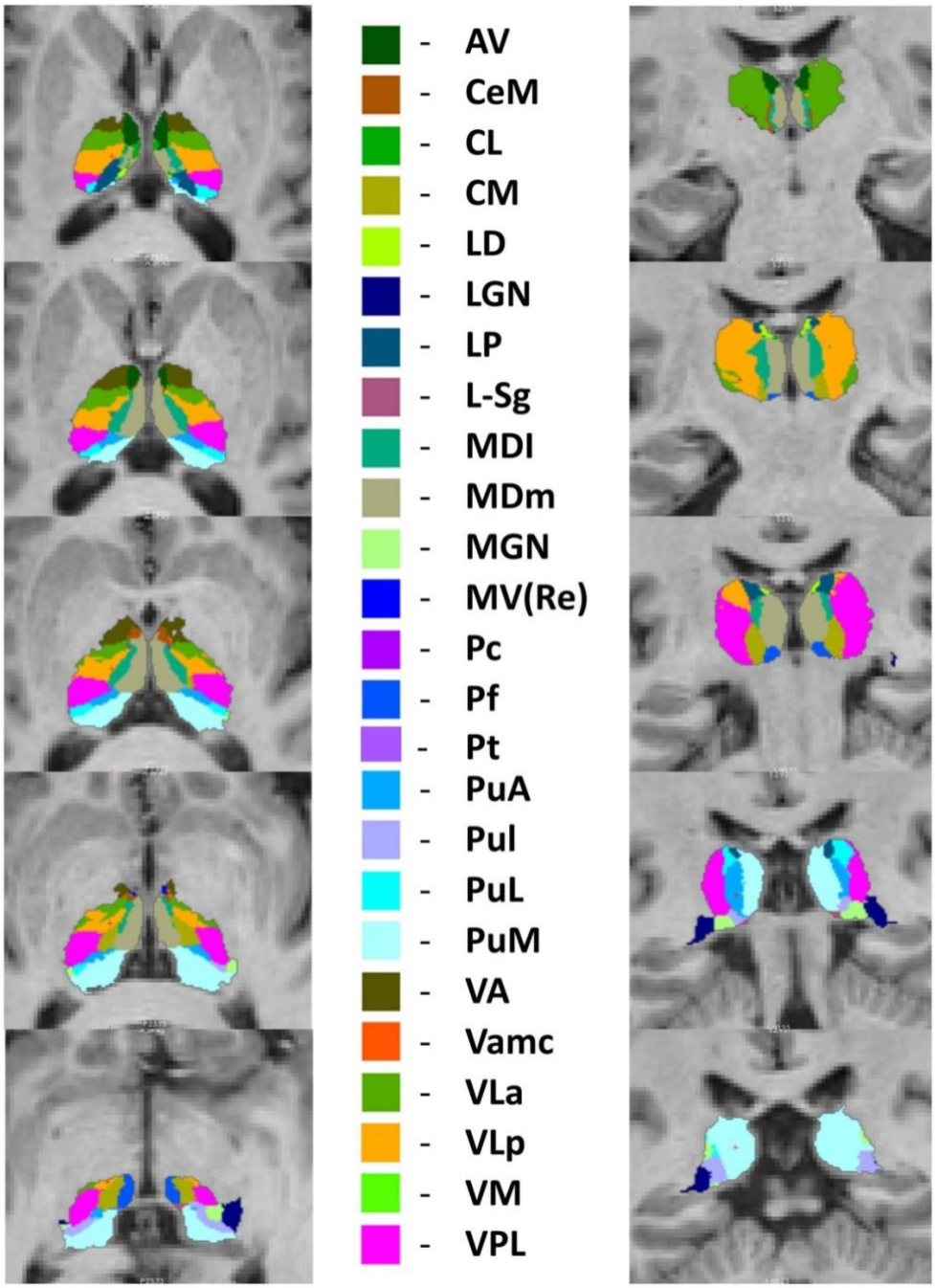

Vertex analyses

Surface projected patterns of atrophy were evaluated using vertex analyses. As described previously (327), FMRIB's subcortical segmentation and registration tool FIRST (616) was utilised to characterise focal thalamic shape deformations. Vertex locations of each participant were projected on the surface of an average thalamic shape template as scalar values, positive value being outside the surface and negative values inside. The average thalamic shape was generated from all participants. Permutation based non-parametric inference was implemented for group comparisons using FMRIB's 'RANDOMISE' module (617). The design matrices included demeaned age, gender, education, total intracranial volumes and education as covariates (617).

Region of interest morphometry

In order to characterise focal pathology beyond shape deformations and volume reductions in the thalamus, region-of-interest morphometry was performed to explore focal density alterations. FMRIB's software library (FSL) was used for skull removal and tissue-type segmentation. Affine registration was used to align grey-matter partial volume images to the MNI152 standard space. A study-specific grey matter template was then created to which the grey matter images of each subject were non-linearly coregistered. The study specific template was generated by the same number of randomly selected subjects from each study group i.e. 12 C9+ ALS patients, 12 C9- ALS patients, 12 healthy controls and 12 PLS patients to ensure that the template is representative of each study group. A voxelwise generalized linear model and permutation-based non-parametric inference were utilised to evaluate density

alterations in a bilateral thalamus mask accounting for age, gender, TIV and education. (617, 618) The labels of the Harvard-Oxford probabilistic structural atlas (619) was used to generate the bilateral thalamus mask.

Genetics

All ALS and PLS patients were tested for *C9orf72* repeat expansions and tested for a panel of mutations implicated in ALS and PLS. DNA samples were tested for pathogenic GGGGCC hexanucleotide repeat expansions by repeat-primed PCR using the Applied Biosystems (Foster City, CA, USA) 3130xl Genetic Analyser and visualised using GeneMapper version 4.0. More than 30 hexanucleotide repeats were considered pathological. All patients were also tested for an extensive panel of ALS and PLS associated mutations including *SOD1, ALS2, SETX, SPG11, FUS, VAPB, ANG, TARDBP, FIG4, OPTN, ATXN2, VCP, UBQLN2, SIGMAR1, CHMP2B, PFN1, ERBB4, HNRNPA1, MATR3, CHCHD10, UNC13A, DAO, DCTN1, NEFH, PRPH, SQSTM1, TAF15, SPAST, ELP3, LMNB1, SARM1, C21orf2, NEK1, FUS, CHMP2B, GRN, MAPT, PSEN1, PSEN2, TBK1*. Sixty-seven ALS patients and all 33 PLS patients underwent whole genome sequencing (620) and the remaining 33 ALS patients underwent target next –generation targeted sequencing. (621) In addition to *C9orf72* testing and genetic screening for established ALS-causing mutations, PLS patients were also screened for a panel of 70 genes linked to HSP. (116, 622)

Statistical analysis

The statistical interpretation of demographic and clinical data was conducted using IBM Statistical Product and Service Solutions (SPSS) verion 25. Group differences in age, education and ALSFRS-r were examined using multivariate analysis of variance (MANOVA). Differences in gender, handedness, disease onset, and the proportion of patients with cognitive impairment were assessed with Chi-square tests. Intergroup differences in thalamic volumes were also evaluated in SPSS. Assumptions of normality were examined using the Kolmogorov-Smirnov test separately for each group. Since all variables followed a normal distribution, parametric statistics were used. Intergroup differences in thalamic volumes were examined using multivariate analysis of covariance with total intracranial volume (TIV), age, gender and education as covariates. If a significant main effect of group membership was identified ($p < 0.05$) for specific thalamic nuclei, post-hoc group comparisons were performed. False discovery rate (FDR-Benjamini Hochberg) corrections were used to account for multiple comparisons. The association between symptom duration and thalamic volumes was further examined in ALS and PLS patients with partial correlation, using age, gender, education and TIV as covariates. Correlations between motor disability (ALSFRS-r) and the volume of motor nuclei were also explored in PLS and ALS patients.

Results

ALS patients were stratified based on their *C9orf72* status. All ALS patients and PLS patients tested negative for other established mutations associated with ALS. The four study groups were matched for age, gender, education and handedness. Patients groups were match for functional disability and site of onset. (**Tables 37 and 38**.)

Table 37*: The demographic and clinical profile of study participants, ECAS: Edinburgh Cognitive ALS Screen, ALSFRS-r: revised ALS functional rating scale, MND-FTD defined by the revised Strong criteria (612)*

Study Groups	***ALS C9+ n=12***	***ALS C9- n=88***	***PLS n=33***	***HC n=117***	***p value***
Age (years)	57.25 (16.454)	60.18 (10.311)	60.48 (10.488)	57.38 (11.914)	.263
Gender (male)	6 (50%)	56 (63.6%)	19 (57.6%)	56 (47.9%)	.598
Education (years)	12.50 (3.205)	13.58 (3.169)	12.88 (3.380)	14.31 (3.294)	.053
Handedness (right)	9 (75%)	81 (92%)	29 (87.9%)	109 (93.2%)	.185
Cognitive impairment on ECAS	7 (58.3%)	19 (21.5%)	8 (24.2%)	n/a	.023
Comorbid FTD as per the Strong criteria	8 (66.66%)	7 (7.95%)	1 (3.03%)	n/a	< .01
Onset (Bulbar)	2 (16.66%)	16 (18.18%)	1 (3.03%)	n/a	.102
Onset (Limb)	10 (83.33%)	72 (81.81%)	32 (96.96%)	n/a	.102
ALSFRS-R	36.08 (7.585)	36.69 (7.495)	34.36 (5.337)	n/a	.272

Table 38. *Effect sizes for intergroup differences using Cohen's |d|. |d| over 0.80 is considered a large effect size and is highlighted in pink; 0.50-0.79 signifies a medium effect size and is highlighted in green, 0.20-0.49 is regarded as a small effect size and is highlighted in yellow, |d| < 0.19 is a negligible effect size and shown in grey.*

Thalamic nuclei	C9+ALS versus HC	C9-ALS versus HC	PLS versus HC	C9+ALS versus C9-ALS	C9+ALS versus PLS	C9-ALS versus PLS
Anteroventral	0.7	0.44	0.27	0.26	0.44	0.18
Lateral geniculate	0.48	0.17	0.79	0.31	0.32	0.62
Medial geniculate	0.66	0.37	0.19	0.3	0.48	0.18
Pulvinar-limitans	0.01	0.07	0.61	0.06	0.61	0.54
Laterodorsal	0.5	0.32	0.28	0.17	0.79	0.6
Lateroposterior	0.58	0.37	0.1	0.21	0.49	0.27
Mediodorsal-paratenial-reuniens	1.27	0.59	0.94	0.68	0.34	0.34
Motor hub	0.56	0.48	0.59	0.08	0.03	0.11
Sensory hub	0.27	0.56	0.88	0.29	0.63	0.32
Intralaminar	0.2	0.49	0.58	0.29	0.39	0.09
Whole Thalamus	0.64	0.53	0.86	0.11	0.23	0.34

Thalamic segmentation revealed study-group specific volumetric profiles. (**Figures 10-12**.) Significant atrophy was identified in the mediodorsal-paratenial-reuniens group of nuclei in all three patient cohorts. Both *C9orf72* negative ALS patients and PLS patients exhibited significant volume reductions in motor nuclei, sensory nuclei and intralaminar nuclei. *C9orf72* negative ALS patients showed additional anteroventral, medial geniculate, and lateroposterior changes compared to healthy controls. PLS patients had a distinctive thalamic signature with preferential pulvinar and lateral geniculate compared to healthy controls but also in contrast to *C9orf72* negative ALS patients. (**Figures 10-12**) While intergroup differences between hexanucleotide carriers and sporadic ALS patients did not reach significance following FDR corrections, reduced mediodorsal-paratenial-reuniens volumes were observed in hexanucleotide carriers compared to C9orf72 negative ALS patients. ($p = 0.085$) (**Table 39**.)

Figure 10*: The volumetric profile of thalamic nuclei in healthy controls (HC), primary lateral sclerosis (PLS), C9orf72 positive ALS patients (C9+ALS), and C9orf72 negative ALS patients (C9-ALS) based on estimated marginal means adjusted for age, gender, total intracranial volumes (TIV) and education. Error bars represent 95% confidence intervals. Inter-group differences corrected for multiple comparisons are highlighted with asterisks * p < 0.05 ** p< 0.01*

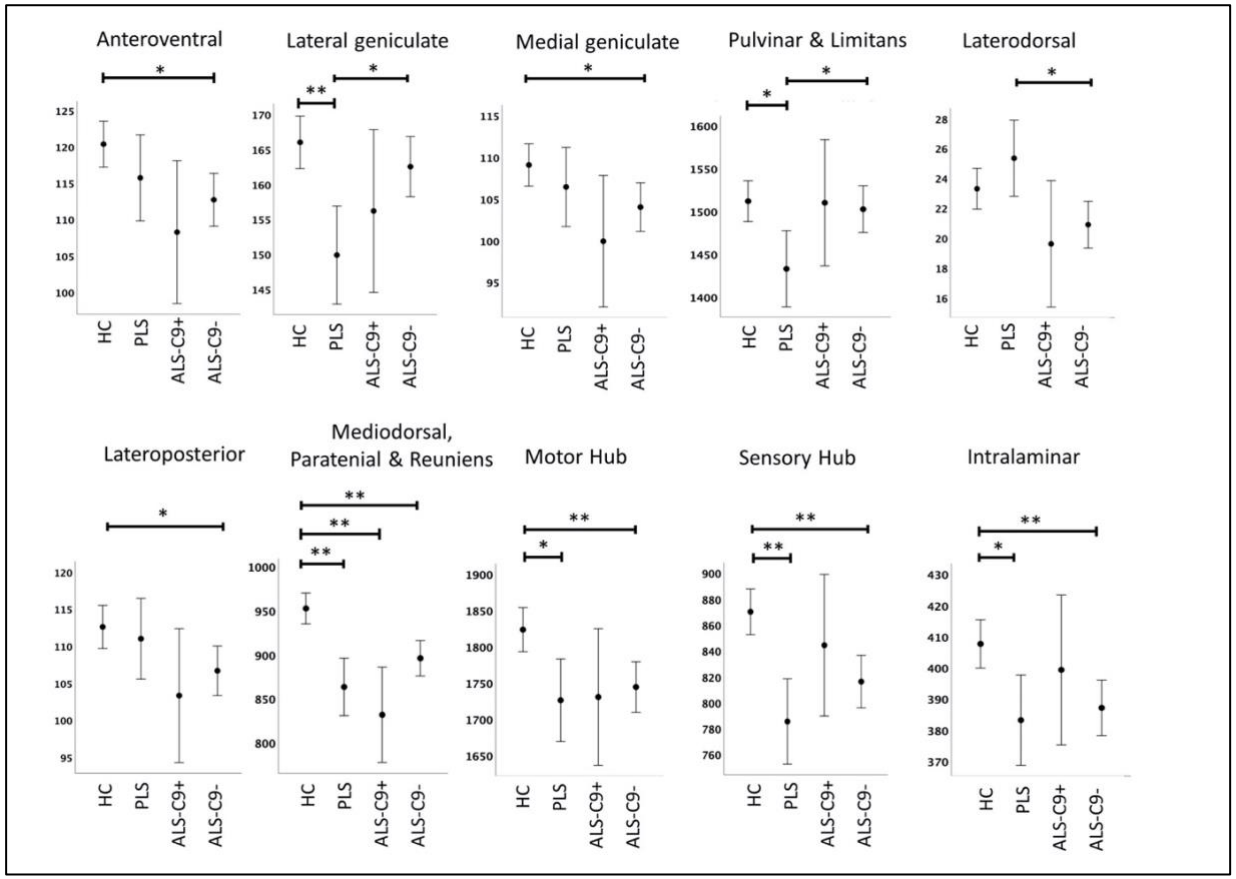

Figure 11*: The volumetric profile of thalamic nuclei in C9orf72 hexanucleotide carrying ALS patients (ALS C9+), C9orf72 negative amyotrophic lateral sclerosis patients (ALS C9-), primary lateral sclerosis patients (PLS) and healthy controls (HC). Statistically significant intergroup differences following correction for age, gender, intracranial volumes and multiple comparisons are indicated with asterisks. * p < 0.05 ** p < 0.01*

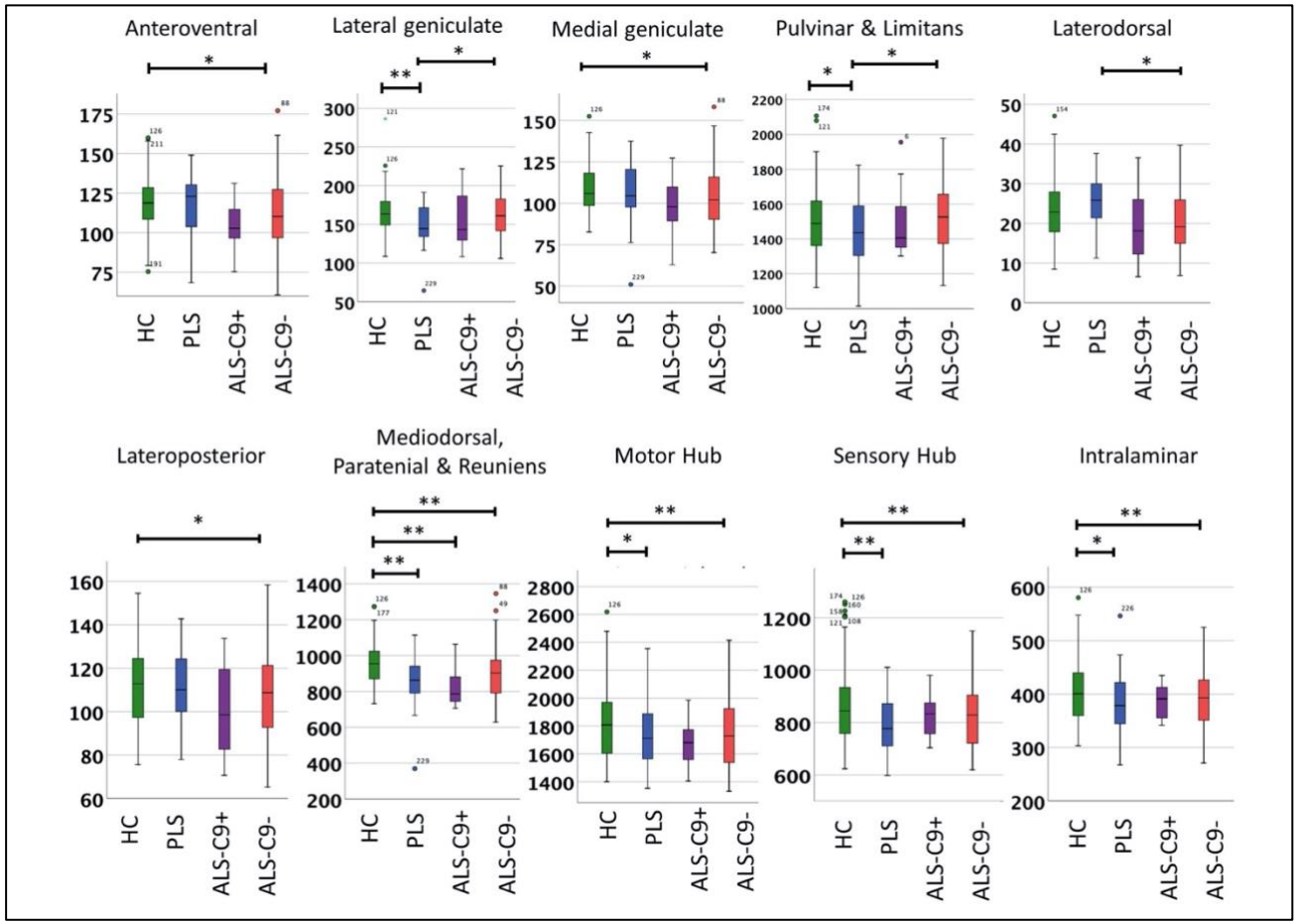

Figure 12. *The segmental thalamus profile of C9+ ALS, C9- ALS, and PLS with reference to healthy controls. 100% represents the estimated marginal mean of healthy controls for each structure. Estimated marginal means of volumes were calculated with the following values age = 59.07, gender = 1.43, Education = 13.68, total intracranial volume = 1432347.15.*

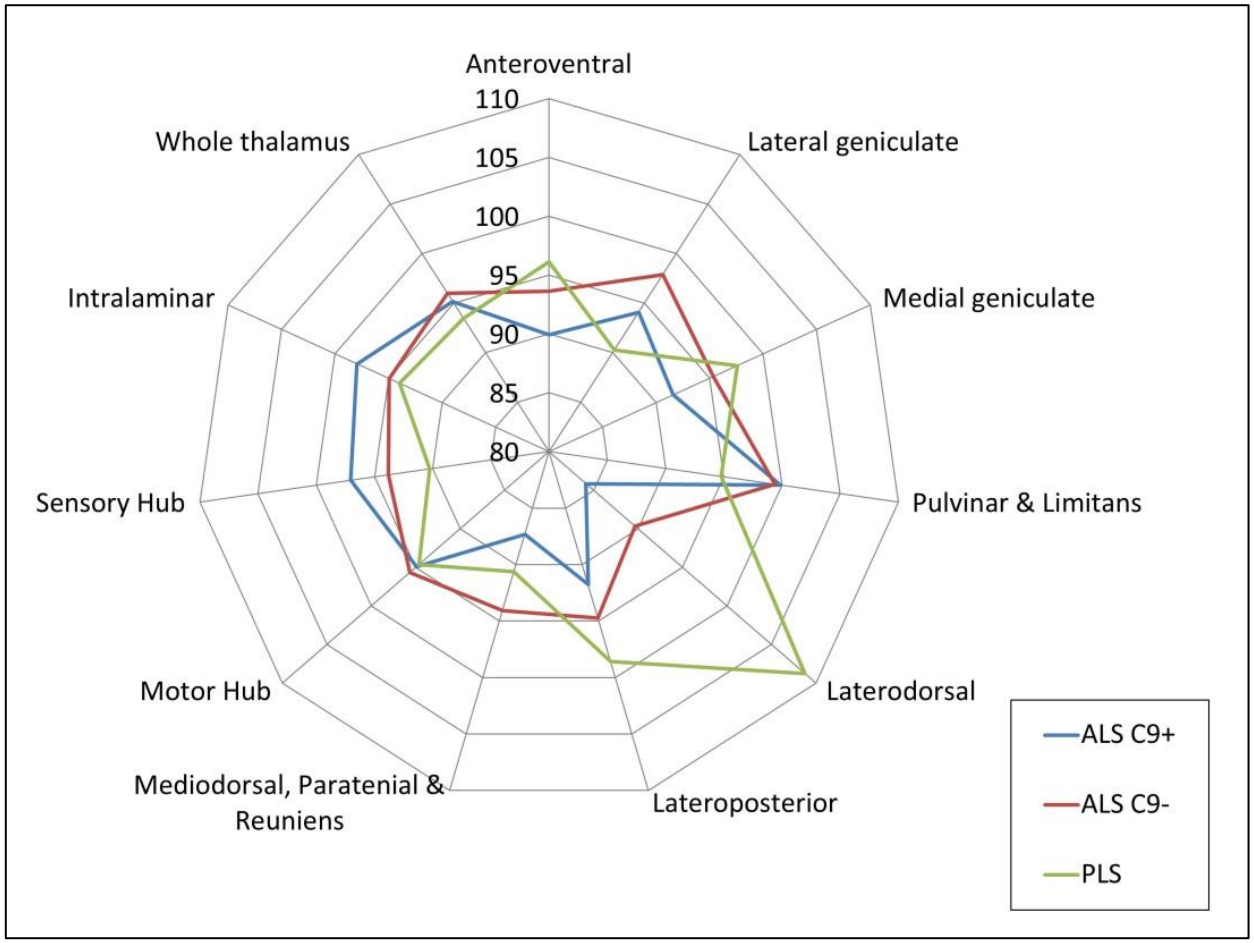

Table 39: *Subcortical grey matter volumes (mm3) in healthy controls (HC), C9orf72 positive ALS patients (ALS C9+), C9orf72 negative ALS patients (ALS C9-) and PLS patients (PLS). Estimated marginal means and standard error are adjusted for age, gender, education and total intracranial volume (TIV). Significant intergroup differences at p < 0.05 after FDR-correction for multiple comparisons are flagged in bold print.*

Nuclei	*Study group*	*Estimated marginal mean*	*Standard error*	*ANCOVA p value*	*C9+ ALS vs HC*	*C9- ALS vs HC*	*PLS vs HC*	*C9+ vs C9-*	*C9+ ALS vs PLS*	*C9- ALS vs PLS*
Anteroventral	HC	120.348	1.606	.006	**.022**	**.002**	.178	.403	.200	.391
	ALS-C9+	108.247	4.985							
	ALS-C9-	112.701	1.843							
	PLS	115.716	3.004							
Lateral geniculate	HC	166.002	1.903	.001	.115	.235	**<.001**	.315	.361	**.003**
	ALS-C9+	156.178	5.908							
	ALS-C9-	162.525	2.184							
	PLS	149.874	3.560							
Medial geniculate	HC	109.069	1.289	.027	**.031**	**.011**	.338	.338	.164	.392
	ALS-C9+	99.915	4.000							
	ALS-C9-	104.013	1.479							
	PLS	106.428	2.411							
Pulvinar-limitans	HC	1511.829	12.094	.022	.963	.618	**.002**	.852	.078	**.009**
	ALS-C9+	1510.012	37.536							
	ALS-C9-	1502.542	13.880							
	PLS	1432.716	22.622							
Laterodorsal	HC	23.301	.692	.008	.103	**.024**	.168	.575	**.023**	**.004**
	ALS-C9+	19.607	2.148							
	ALS-C9-	20.893	.794							
	PLS	25.344	1.295							
Lateroposterior	HC	112.576	1.480	.031	.056	**.010**	.614	.495	.153	.182
	ALS-C9+	103.304	4.594							
	ALS-C9-	106.652	1.699							

	PLS	110.981	2.769							
Mediodorsal-paratenial-reuniens	HC	952.485	8.870	<.001	**<.001**	**<.001**	**<.001**	**.030**	.325	.094
	ALS-C9+	831.611	27.532							
	ALS-C9-	895.909	10.180							
	PLS	863.272	16.593							
Motor Hub	HC	1823.542	15.441	.001	.066	**.001**	**.003**	.788	.936	.589
	ALS-C9+	1730.548	47.926							
	ALS-C9-	1744.318	17.721							
	PLS	1726.039	28.884							
Sensory Hub	HC	870.109	8.949	<.001	.377	**<.001**	**<.001**	.344	.070	.117
	ALS-C9+	844.262	27.777							
	ALS-C9-	816.158	10.271							
	PLS	785.381	16.740							
Intralaminar	HC	407.634	3.941	.002	.517	**.001**	**.004**	.352	.259	.646
	ALS-C9+	399.285	12.231							
	ALS-C9-	387.102	4.523							
	PLS	383.145	7.371							
Whole thalamus	HC	6096.895	43.005	<.001	**.037**	**<.001**	**<.001**	.727	.504	.103
	ALS-C9+	5802.968	133.480							
	ALS-C9-	5852.813	49.356							
	PLS	5698.896	80.445							

Vertex analyses

Vertex analyses also confirmed considerable thalamic atrophy in both ALS cohorts. In C9+ ALS patients strikingly symmetric patterns of atrophy were observed with superior-inferior predominance as well as posterior involvement. Similar patterns were noted in the C9- ALS group compared to healthy controls. The direct comparison of hexanucleotide carrying ALS patients with C9 negative patients revealed asymmetric superior-inferior-posterior atrophy in the right thalamus. Anterior and posterior deformations were observed in PLS compared to C9 negative ALS. Widespread superior, inferior and posterior shape alterations were noted in PLS compared to healthy controls. (**Figure 13**)

Figure 13: *Shape deformations in C9 positive ALS in comparison to healthy controls (1), C9 negative ALS compared to healthy controls (2), C9 positive ALS compared to C9 negative ALS (3), PLS compared to C9 negative ALS (4), and PLS patients in contrast to healthy controls (5). Average thalamic mesh is shown in blue and surface projected patterns of atrophy are shown in orange colour at p<0.05 corrected for age, gender, education, and TIV. Anterior, superior lateral from the right, superior lateral from the left and posterior inferior views are presented. Rt – right, Lt. – left.*

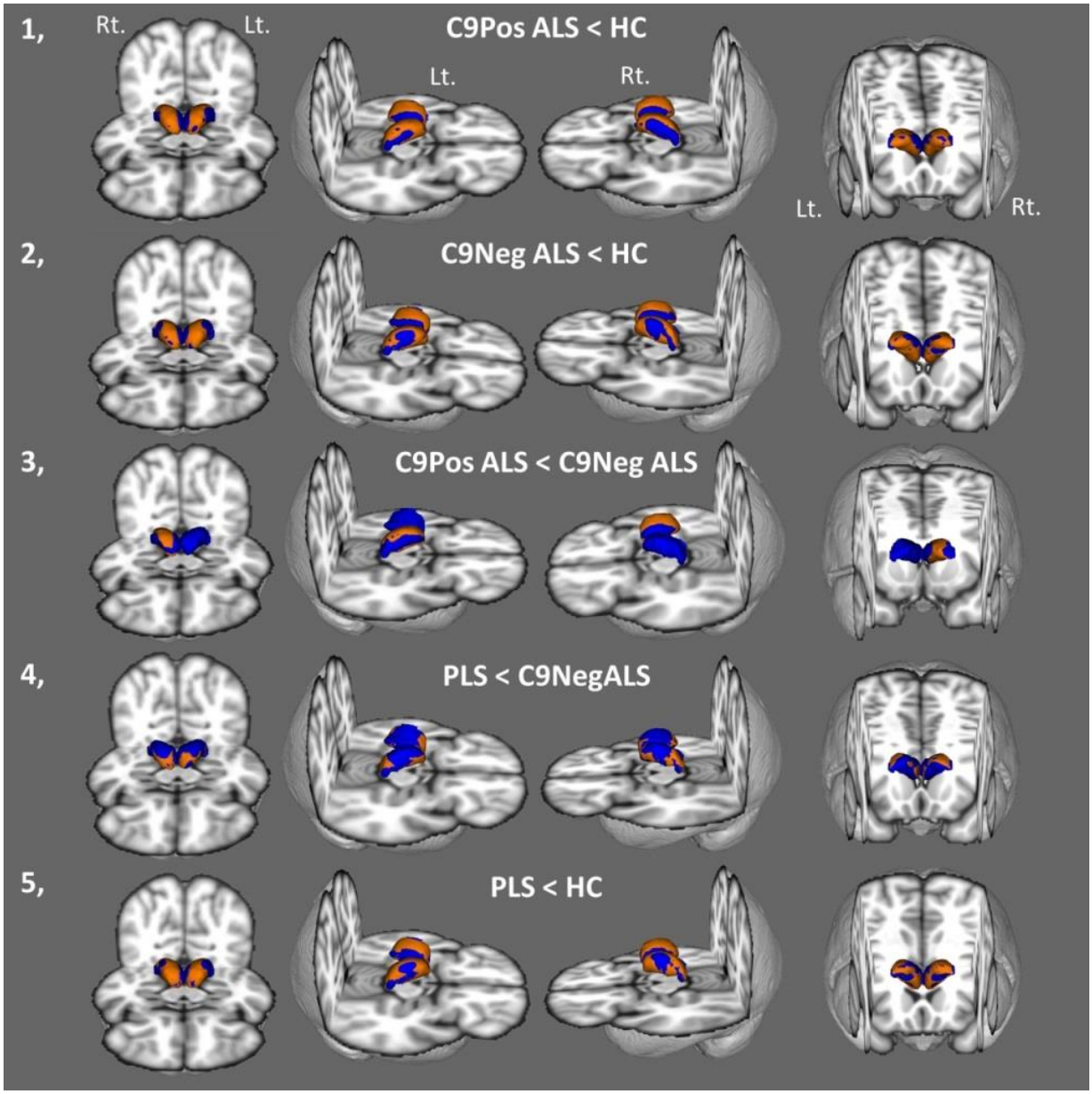

Morphometric alterations

Morphometric analyses revealed largely asymmetric changes. Statistically significant right posterolateral atrophy was observed in C9 negative ALS compared to healthy controls at $p < 0.05$ FWE. C9 negative ALS patients exhibited left ventral lateral pathology in comparison to PLS patients at $p < 0.05$ FWE. PLS patients exhibited bilateral posterior density reductions in contrast to healthy controls. (**Figure 14**)

Figure 14*: Patterns of thalamic atrophy in C9 negative ALS in comparison to healthy controls (1), in C9 negative ALS versus PLS (2) and in PLS compared to healthy controls (3). Morphometric changes are shown on an atlas-defined bi-thalamic grey matter mask (white) with corresponding p-values corrected for age, gender, total intracranial volumes and education. The colour bar indicates probability values less than 0.05.*

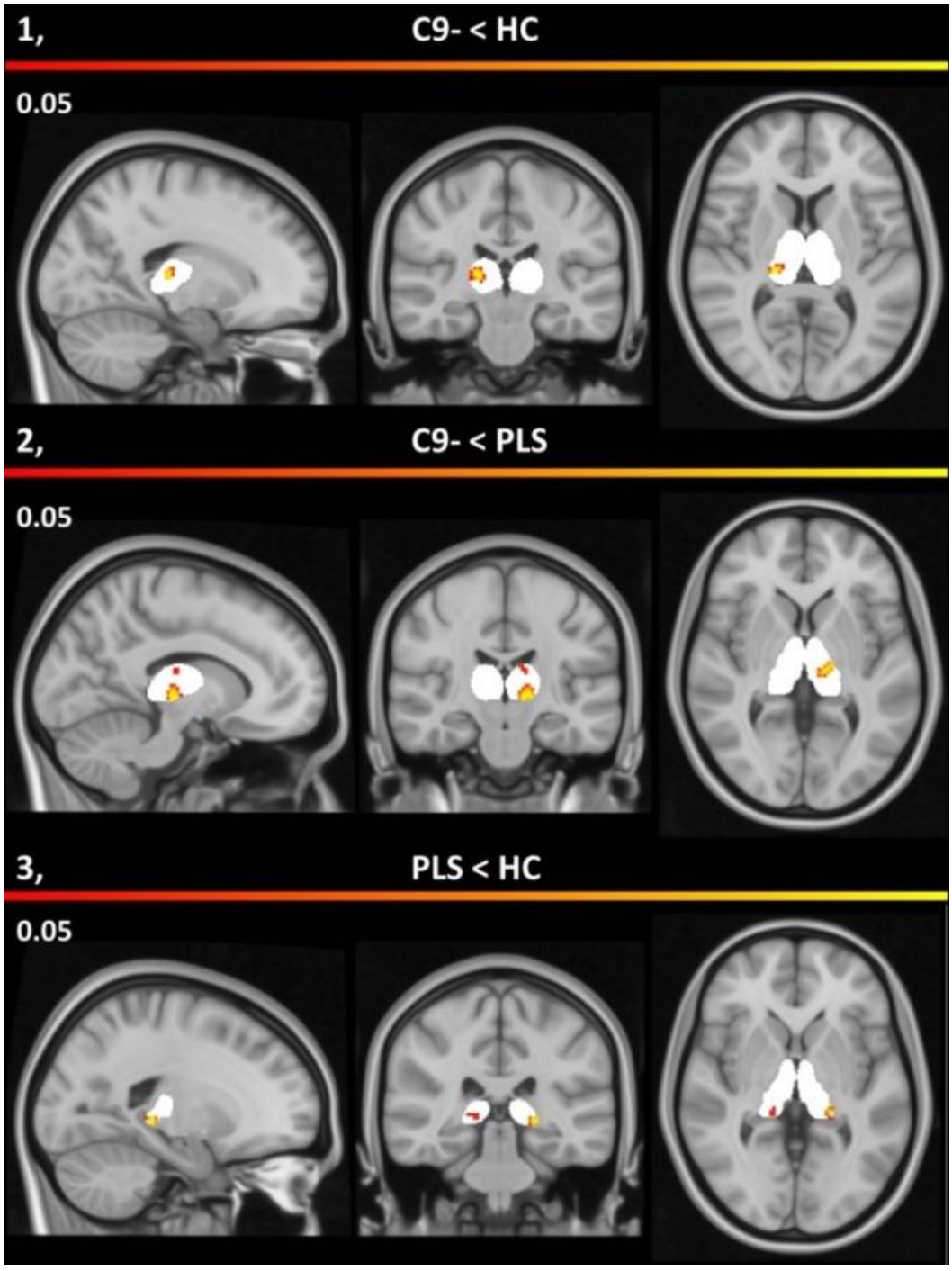

Correlation analyses

Within the patient group (ALS, PLS), we only found a significant association between pulvinar volumes and symptom duration (r = -0.269; p_{FDR} = 0.02). The association between symptom duration and posterior-lateral geniculate volume did not survive correction for multiple comparisons (r = -0.208; p_{unc} = 0.018; p_{FDR} = 0.09). There were no direct associations between the volumes of motor nuclei and ALS functional rating scale values.

Discussion

Our findings indicate phenotype-specific patterns of thalamic degeneration in MND with the preferential involvement of specific nuclei as opposed to global thalamic atrophy. The selective involvement of thalamic nuclei highlights that thalamic pathology in motor neuron diseases is not homogenous; therefore earlier efforts to evaluate the entire structure by volumetric, metabolic, shape or diffusivity measures are likely to have averaged biophysical indices across affected and unaffected regions.

One of the key objectives of the study was to assess thalamic motor nuclei in ALS. The ventral anterior nucleus contributes to planning and initiating movement, while the ventral lateral nucleus plays a role in movement modulation and coordination (623). The majority of ALS imaging studies focus on pyramidal weakness and evaluate motor cortex, corticospinal tract and spinal cord metrics (624). Extrapyramidal motor deficits have been sporadically reported in ALS (600, 625), but ascertaining extra-pyramidal

signs clinically is challenging in the presence of combined upper and lower motor neuron degeneration. In this study, both *C9orf72* negative ALS patients and PLS patients exhibited significant volume reductions in thalamic motor nuclei. Extrapyramidal features of ALS are relatively under recognised despite case series (600, 625, 626), gait analyses (459), and nuclear medicine studies in both sporadic (627) and familial cases (628, 629). Occupational therapy and physiotherapy interventions in ALS typically focus on pyramidal weakness; spasticity management for UMN dysfunction and fitting orthoses to limbs affected by LMN dysfunction. Impaired gait initiation and impaired postural reflexes however are also likely to contribute to poor mobility and increased fall risk in ALS and may benefit from targeted interventions. (630, 631) We have not identified direct correlations between ALSFRS-r and motor nucleus volumes in ALS or PLS. This is not unexpected, as ALSFR-r is thought to be disproportionately representative of lower motor neuron degeneration in ALS and may be suboptimal to assess motor disability in PLS. (632, 633)

We have also identified significant volume reductions in sensory nuclei in both the *C9orf72* negative ALS cohort and in the PLS group. Sensory deficits are seldom evaluated routinely in established ALS and PLS patients, as clinical disability is dominated by relentlessly progressive limb weakness, bulbar impairment and eventually respiratory weakness. Paraesthesiae are occasionally reported by patients but frank nociceptive, proprioceptive or thermoceptive deficits are not characteristic of ALS. Cortical imaging in ALS does not typically identify post central gyrus involvement (131), but posterior column degeneration has been previously captured

on spinal imaging (339) . Spinal dorsal column degeneration have been reported based on DTI and MT data (339, 340) and combined spinal DTI and neurophysiology studies suggest subclinical sensory dysfunction in ALS patients without frank sensory symptoms (174). There is also growing neurophysiological evidence that cerebral sensory processing may be affected in ALS. (316) Our finding of ventral posterolateral and ventral medial thalamus degeneration indicates that ALS pathology does not spare the somatosensory nuclei and sub-clinical sensory deficits are likely to add to the clinical heterogeneity of the condition. Similarly to the growing evidence of extra-pyramidal motor deficits in ALS, multidisciplinary rehabilitation efforts in ALS should take posterior column and sensory thalamus degeneration into account when assessing gait and fall risks. (630, 631)

In our study, we identified significant mediodorsal-paratenial-reuniens pathology in both PLS and ALS. Our results suggest that this group of nuclei are affected in ALS irrespective of *C9orf72* status. These nuclei play a physiological role in executive function (634-636), memory consolidation (637, 638), recall (638, 639). The involvement of thalamic nuclei which mediate cognitive functions mirrors previous observations of extra-motor cortical involvement in ALS. Both ALS and FTD studies provide ample evidence that thalamic pathology is not unique to *C9orf72* (527, 603), and it is also clear that a proportion of *C9orf72* negative sporadic ALS patients fulfil diagnostic criteria for comorbid FTD (612). In our C9- cohort 8% of patients had comorbid FTD and 21% had cognitive impairment based on a disease-specific screening instrument. Our findings support the notion that *C9orf72* is not the sole cause of ALS-

associated cognitive impairment and that sporadic cases also exhibit extra-motor grey matter changes and cognitive impairment despite testing negative for a large panel of established mutations. Cognitive deficits in ALS are typically linked to extra-motor cortical pathology and frontotemporal white matter alterations, and the contribution of subcortical grey matter degeneration to neuropsychological manifestations is seldom evaluated specifically. Neuropsychological deficits in ALS are thought to be dominated by executive (640, 641) and behavioural dysfunction (642), but memory deficits are also increasingly recognised (643, 644). Characterising the anatomical substrate of cognitive deficits in familial and sporadic ALS is clinically relevant as non-motor manifestations in ALS impact on adherence to therapy, caregiver burden, compliance with assistive devices, decision to participate in clinical trials, and quality of life (645, 646). Intergroup volumetric differences between hexanucleotide carriers and sporadic ALS patients did not reach significance following FDR corrections in our study, but reduced ($p = 0.085$ FDR) mediodorsal-paratenial-reuniens volumes were observed in hexanucleotide carriers compared to *C9orf72* negative ALS patients. On vertex analyses however *C9orf72* positive patients exhibited significant superior–inferior shape deformations compared to C9negative patients. GGGGCC hexanucleotide expansions have been consistently linked to pulvinar atrophy in FTD both on imaging (24, 602, 647) and post mortem (648, 649). In contrast to observations in FTD, we have not observed preferential pulvinar involvement in our sample of *C9orf72* positive ALS cohort. While the sample size of our *C9orf72* positive cohort is limited, we have observed marked pulvinar atrophy in our PLS cohort who tested negative for repeat expansions. The thalamic profile of our PLS group suggest that pulvinar atrophy is not unique to hexanucleotide repeat expansions carriers in motor neuron diseases.

C9orf72 negative ALS patients showed additional anteroventral changes compared to healthy controls. The physiological role of the anteroventral nucleus is primarily associated with learning (650) and memory encoding (651). It plays a role in episodic memory; encoding content and recollection, (652) but has also been linked to emotional processing (653) and executive functions (654). It's involvement in *C9orf72* negative ALS is consistent with the notion that pathology in sporadic ALS is not confined to primary motor regions; it is a multisystem degenerative process involving motor and extra-motor regions.

Our findings suggest that PLS has a distinctive thalamic signature with preferential pulvinar and lateral geniculate compared to healthy controls but also in contrast to *C9orf72* negative ALS patients. The lateral geniculate not only relays retinofugal information to the visual cortex (655) it is thought to contribute to visuospatial filtering and perception. (656) Pulvinar-limitans volume reductions were more marked than those observed in *C9orf72* negative ALS. Posterior pulvinar thalamic regions play a role in maintaining attention to visual stimuli (657, 658), and pulvino-cortical projections are associated with attention modulation, working memory, and decision making. (659, 660) These observations are consistent with the view that PLS has a number of unique, phenotype-specific imaging features, distinct from ALS. The involvement of the motor nuclei, sensory nuclei and the mediodorsal-paratenial-reuniens region in PLS are comparable to the sub-thalamic profile of *C9orf72* negative ALS. Focal pathological

changes in sensory thalamus regions have not been previously reported in PLS. The involvement of ventral anterior and ventral lateral nuclei in PLS, which mediate movement initiation and modulation, are relatively novel findings as extrapyramidal dysfunction is not well established in PLS. It is noteworthy that thalamic pathology is thought to contribute to the development pseudobulbar affect (pathological crying and laughing) (661) which has a particularly high incidence in PLS. The comprehensive characterisation of regional thalamic pathology in PLS complements the emerging literature on subcortical grey matter degeneration, extra-motor involvement and neuropsychological deficits. (118, 607, 662)

As our *C9orf72* negative ALS group is a sporadic ALS cohort, which tested negative for a large panel of established ALS-associated mutations. The characterisation of the imaging features of this group is clinically relevant, as they represent approximately 90% of ALS patients. These patients represent the majority of our patients presenting to clinics for diagnostic clarification, clinical follow-up and multidisciplinary management. C9negative sporadic patients exhibit the same stereotyped disease trajectory of relentless motor decline as other ALS patients and succumb to respiratory compromise within 3-5 years of their diagnosis despite testing negative for established mutations.

Histopathological considerations

Postmortem findings are seldom reported in conjunction with neuroimaging results (353, 526, 603) and existing imaging studies have not elaborated on post-mortem

thalamus pathology. Studies of pathological TDP-43 patterns in ALS have consistently reported thalamic involvement, (489) but the vulnerability of specific thalamic nuclei are poorly characterised. Data from large case series (404) suggest the preferential involvement of large thalamic relay neurons projecting to layer IV of the neocortex which is associated with Stage 2 of a corticofugal pTDP-43 model. (398) Few post-mortem studies have specifically evaluated thalamic changes in the ALS-FTD spectrum and many of these are case reports or case-series. (663) A large post-mortem study identified increased thalamic iron load in FTD in comparison to the other neurodegenerative conditions (664).

Study limitations

This study has a number of limitations. Consistent with the population-based incidence of *C9orf72* in ALS, the cohort size of C9+ ALS group is limited and precludes conclusive genotype-associated observations. The inclusion of a non-MND disease-control group with an alternative neurodegenerative diagnosis, such as AD or FTD would have supported the specificity of our thalamic findings to ALS and PLS. We have focused on descriptive analyses and not explored direct clinico-radiological correlations between neuropsychological measures and imaging findings (456). Cognitive functions and behavioural regulation are mediated through function-specific multi-synaptic cortico-basal circuits (665) and therefore seeking direct associations between clinical measures and focal thalamic indices would overlook the contribution of other white and grey matter components to clinical performance. Post mortem histopathology data or ex-vivo MRI would have provided important validation for the radiological

observations made in vivo. Finally, while our data provides a snapshot of thalamic alterations in ALS, a robust multi-timepoint design would have provided crucial longitudinal insights. Notwithstanding these limitations our data provide evidence of focal thalamic involvement in ALS and PLS and demonstrate the utility of appraising thalamic nuclei individually instead of evaluating overall thalamic changes.

Conclusions

We have detected phenotype-specific patterns of focal thalamic pathology in ALS and PLS. The characterisation of thalamic pathology allows the identification of the most vulnerable group of nuclei, the measures of which are superior biomarkers candidates than indices of the entire structure. The characterisation of thalamic nuclei implicated in sensory, cognitive and behavioural functions support the conceptualisation of ALS and PLS as multi-system conditions and confirms that extra-motor involvement is not confined to cortical grey matter pathology.

Chapter 7: Amygdala pathology in ALS and PLS

Introduction

While ALS is primarily associated with motor cortex (122, 666) and spinal cord degeneration (120, 121), it has gradually been recognised as a multi-system disorder with widespread frontotemporal (131, 138), extra-pyramidal (459), cerebellar involvement (128, 468) and a variety of extra-motor manifestations (641).

Imaging studies in ALS have consistently captured some degree of temporal lobe pathology, but significant inconsistencies exist due to differences in imaging methods, sample sizes, recruitment strategies, inclusion criteria and patient stratification (146). Early temporal lobe studies in ALS primarily focused on cortical grey matter involvement (667) before white matter alterations were also gradually characterised (461, 668). Dedicated hippocampus studies have been recently published both in ALS (509, 669) and PLS (367, 538) confirming that mesial temporal lobe pathology in an important feature of the motor neuron disease spectrum. The amygdala however is surprisingly understudied in ALS in vivo, despite reports of deficits in social cognition (577, 670), memory impairment (644), behavioural changes (4, 642), and evidence of amygdala pathology on post mortem examination (671-673). The amygdala is a key structure of the limbic system which mediates a number of cognitive and behavioural functions and has direct connections to brain regions affected in ALS such as the thalamus (321), hypothalamus (674), and the accumbens nucleus (601). It plays a key

role in memory modulation, reward processing, emotional learning, and the regulation of aggression, fear, and anxiety.

Dedicated amygdala studies are not only sparse in the ALS imaging literature but their findings are strikingly inconsistent. Some of the inconsistency may be explained by differences in imaging methodology and patient selection, but the most likely cause of the inconsistency is that the amygdala is typically evaluated as a single structure in ALS. Metabolic, diffusivity, morphometric, volumetric and vertex-based approaches have previously been utilised to characterise overall amygdala pathology in vivo (3, 123, 140, 154, 156, 327, 328, 461, 538, 589, 601, 675, 676) but the involvement of specific nuclei has not been systematically assessed to date. The obvious risk of assessing the amygdala as a single structure is that pathology in affected and unaffected regions is likely to be averaged. Evidence from histopathology studies suggests that amygdala pathology in ALS in not global, but selectively involves specific nuclei (671, 672, 677, 678). Many of the seminal histology reports on selective amygdala pathology in ALS however predate the discovery of *C9orf72* GGGGCC hexanucleotide repeats.

Accordingly, our objective was the systematic evaluation of amygdala pathology in vivo in a large cohort of genetically and phenotypically characterised motor neuron disease patients using both measures of the entire amygdala and evaluating alterations in specific nuclei. Based on the available histopathology literature we hypothesised that selective nuclear degeneration may be captured in the amygdala of ALS patients using

high-resolution structural imaging, in-depth genetic and clinical profiling and conservative structural analysis pipelines. Based on the clinical phenotype of GGGGCC hexanucleotide carriers (7, 604) we additionally hypothesised that genotype-specific amygdalar signatures may be captured.

Methods

Ethics statement

This study was approved by the institutional ethics committee (Beaumont Hospital, Dublin, Ireland), in accordance with the 1964 Helsinki declaration and its later amendments. All participants provided informed consent prior to inclusion. Recruitment, data management, consent forms and information leaflets were specifically approved by the institutional ethics committee.

Participants

ALS patients had 'probable' or 'definite' ALS according to the El Escorial criteria (609) and PLS patients were diagnosed based on the Gordon criteria (605). To aid the interpretation of the radiological profile of the patient groups, healthy controls were also included in this study. Exclusion criteria for all participants included known cerebrovascular events, head injuries, neoplastic conditions, neuroinflammatory conditions and inability to undergo MRI scanning due to implanted metallic devices such as pacemakers, dental plates or baclofen pumps. A total of 5 patients and 7 controls could not be included due to claustrophobia, orthopnoea or unexpected

incidental intracranial findings. The final analysis included data from 100 ALS patients, 33 PLS patients and 117 healthy controls. The demographic and clinical profile of each participant was carefully recorded; motor disability was appraised by the revised ALS functional rating scale (ALSFRS-r) (610), the Edinburgh Cognitive ALS Screen (ECAS) (397) was administered for cognitive screening using population-based normative values (611) and co-morbid FTD was established based on the revised Strong criteria (612). The healthy controls of the study had no known neurological or psychiatric conditions, previous head injuries or a family history of neurodegenerative conditions. Healthy controls were unrelated to the participating patients.

Neuroimaging methods

MRI data were acquired in a dedicated research facility on a 3 Tesla Philips Achieva system using an 8-channel receive-only head coil. T_1-weighted images were acquired with a 3D Inversion Recovery prepared Spoiled Gradient Recalled echo (IR-SPGR) pulse sequence with a field-of-view (FOV): 256 x 256 x 160 mm, spatial resolution: 1 mm^3, TR/TE = 8.5/3.9 ms, TI =1060 ms, flip angle = 8°, SENSE factor = 1.5.

TIV volumes

For the comparisons of amygdala volumes, total intracranial volume (TIV) was used as a covariate in addition to age, gender and education. TIV was calculated for each participant by adding grey matter, white matter and cerebrospinal fluid volume estimates. Subsequent to skull-removal (613) and quality control, each participant's T1-weighted image was linearly aligned to MNI152 standard space using FMRIB's

Linear Image Registration Tool (FLIRT)(614). FMRIB's Automated Segmentation Tool (FAST) (615) was utilised for tissue-type segmentation which accounts for spatial intensity variations. The inverse of the determinant of the affine registration matrix was calculated and multiplied by the size of the template for tissue-type volume estimations.

Amygdala segmentation

A Bayesian inference was used to segment the amygdala into 9 sub-regions using a probabilistic atlas developed based on histological data in the FreeSurfer analysis suite (598, 679) (**Figure 15**.). The amygdala was parcellated into the following nuclei in each hemisphere: Lateral nucleus (LN), Basal nucleus (BN), Accessory basal nucleus (ABN), Anterior amygdaloid area (AAA), Central nucleus (CN), Medial nucleus (MN), Cortical nucleus (CN), Cortico-amygdaloid transition (CAT), and Paralaminar nucleus (PN). The raw volume estimates of the above nuclei were averaged between left and right. "Total amygdala volume" was defined as the mean of the left and right total amygdala volume estimates.

Figure 15*: Atlas-based segmentation of the amygdala; Lateral nucleus (LN), Basal nucleus (BN), Accessory basal nucleus (ABN), Anterior amygdaloid area (AAA), Central nucleus (CN), Medial nucleus (MN), Cortical nucleus (CN), Cortico-amygdaloid transition (CAT), Paralaminar nucleus (PN)*

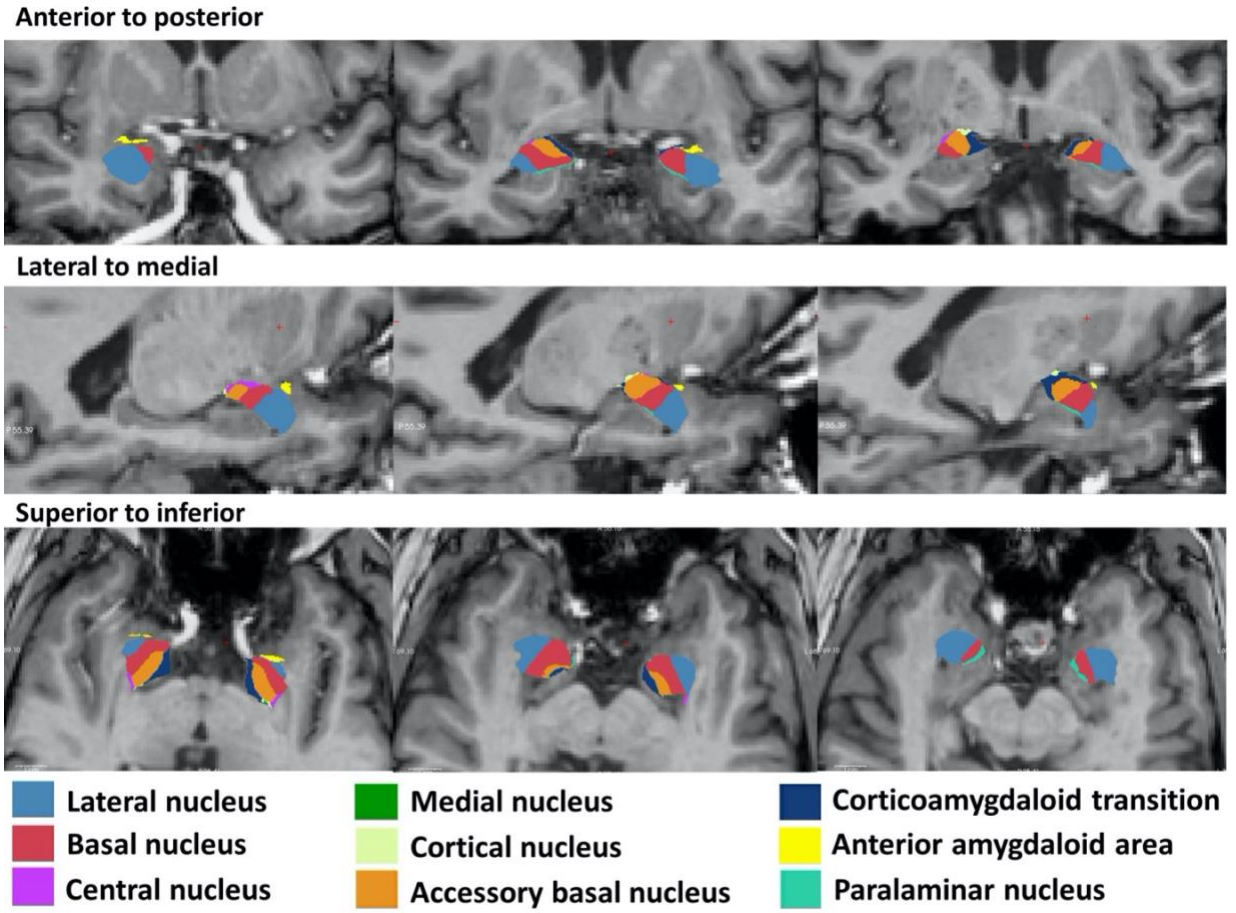

Vertex analyses

Patterns of amygdala atrophy were further evaluated using vertex analyses. Focal amygdala shape deformations were explored using FMRIB's subcortical segmentation and registration tool FIRST (616). An average amygdala shape was generated from all participants. Vertex locations of each subject were projected on the surface of the average amygdala shape template as scalar values, positive value being outside the surface and negative values inside. Group differences were explored using permutation based non-parametric inference as implemented by FMRIB's 'RANDOMISE' module (617). Design matrices included demeaned total intracranial volume, age, education, and gender as covariates (617).

Genetics

All patients were tested for pathogenic GGGGCC hexanucleotide repeat expansions by repeat-primed PCR using the Applied Biosystems (Foster City, CA, USA) 3130xl Genetic Analyser and visualised using GeneMapper version 4.0. More than 30 hexanucleotide repeats were considered pathological. Additionally, ALS and PLS patients were tested for a panel of motor neuron disease associated mutations including *SOD1, TARDBP, FUS, OPTN, ATXN2, VCP, ANG, ALS2, SETX, SPG11, VAPB, FIG4, UBQLN2, SIGMAR1, CHMP2B, PFN1, ERBB4, HNRNPA1, MATR3, CHCHD10, UNC13A, DAO, DCTN1, NEFH, PRPH, SQSTM1, TAF15, SPAST, ELP3, LMNB1, SARM1, C21orf2, NEK1, FUS, CHMP2B, GRN, MAPT, PSEN1, PSEN2, TBK1*. Sixty-seven ALS patients underwent whole genome sequencing (620) and 33 ALS patients underwent target next –generation targeted

sequencing. (621) All 33 PLS patients underwent whole genome sequencing. In addition to *C9orf72* testing and genetic screening for established ALS-causing mutations, PLS patients were also screened for 70 genes implicated in hereditary spastic paraplegia (HSP) (116, 622).

Statistical analysis

Volumetric and demographic data were interpreted using IBM SPSS v. 20. Assumptions of normality were examined using the Kolmogorov-Smirnov test. Skewness and kurtosis were assessed separately for each study group. Since all variables followed a normal distribution, parametric statistics were applied. Group differences (HC, ALS-C9+, ALS-C9-, PLS) in demographic variables were examined using multivariate analysis of variance (MANOVA) followed by post-hoc comparisons (age, education) and chi-square test (gender, handedness, site of onset). Group differences in amygdala nuclei volumes were examined using multivariate analysis of covariance (MANCOVA) with total intracranial volume (TIV), age, gender and education as covariates. $p < 0.05$ was considered significant in post-hoc comparisons following Bonferroni corrections for multiple comparisons to reduce Type I error. The association between symptom duration and nuclear volumes was examined with partial correlation, using age, gender, education and TIV as covariates.

Results

The four study groups were matched for age, gender, education and handedness (**Tables 40 and 41**.) ALS patients were categorised based on their *C9orf72* hexanucleotide expansion status. All ALS patients and PLS patients tested negative for other established mutations associated with ALS.

Table 40*: The clinical and demographic profile of study participants: C9orf72 positive ALS patients (ALS C9+), C9orf72 negative ALS patients (ALS C9-), primary lateral sclerosis patients (PLS), and healthy controls (HC)*

Study Group	***ALS C9+ n=12***	***ALS C9- n=88***	***PLS n=33***	***HC n=117***	***p value***
Age (years)	57.25 (16.45)	60.18 (10.31)	60.48 (10.49)	57.38 (11.91)	0.263
Gender (Male)	6 (50%)	56 (63.6%)	19 (57.6%)	56 (47.9%)	0.598
Education (years)	12.50 (3.21)	13.58 (3.17)	12.88 (3.38)	14.31 (3.29)	0.053
Handedness (right)	9 (75%)	81 (92%)	29 (87.9%)	109 (93.2%)	0.185
Onset (Bulbar)	2 (16.66%)	16 (18.18%)	1 (3.03%)	n/a	.102
Onset (Limb)	10 (83.33%)	72 (81.81%)	32 (96.96%)	n/a	.102
ALSFRS-R	36.08 (7.585)	36.69 (7.495)	34.36 (5.337)	n/a	.272
Cognitive impairment on ECAS	7 (58.3%)	19 (21.5%)	8 (24.2%)	n/a	.023
Comorbid FTD as per the Strong criteria	8 (66.66%)	7 (7.95%)	1 (3.03%)	n/a	< .01

Table 41. *Effect sizes for intergroup differences using Cohen's |d|. A '|d|' value over 0.80 is considered a large effect size and is shown in red; 0.50-0.79 signifies a medium effect size and is highlighted in green, 0.20-0.49 is regarded as a small effect size and is shown in yellow, |d| < 0.19 is a negligible effect size and is presented in grey.*

Amygdala nuclei	C9+ALS versus HC	C9-ALS versus HC	PLS Versus HC	C9+ALS versus C9-ALS	C9+ALS versus PLS	C9-ALS versus PLS
Whole amygdala	-0.8	-0.32	-0	-0.47	-0.77	-0.3
Lateral nucleus	-0.8	-0.24	-0.1	-0.59	-0.73	-0.14
Basal nucleus	-0.7	-0.28	0	-0.45	-0.72	-0.28
Accessory basal nucleus	-0.8	-0.42	-0	-0.39	-0.77	-0.39
Anterior amygdaloid area	-0.6	-0.29	0.29	-0.29	-0.86	-0.57
Central nucleus	-0.29	-0.29	0.00	0.00	-0.29	-0.29
Medial nucleus	-0.25	-0.50	0.25	0.25	-0.50	-0.75
Cortical nucleus	-0.67	-0.33	0.33	-0.33	-1.00	-0.67
Cortico-amygdaloid transition	-0.90	-0.35	0.00	-0.55	-0.90	-0.35
Paralaminar nuclues	-0.40	-0.20	0.00	-0.20	-0.40	-0.20

Volumetric profile

Differences in total amygdala volumes did not reach statistical significance following corrections for multiple comparisons, but an important trend of volume reduction was detected in *C9orf72* positive ALS patients compared to healthy controls (p_{cor}=0.055). In *C9orf72* negative ALS patients, accessory basal nucleus (p_{cor}=0.021) and the cortical nucleus (p_{cor}=0.022) volumes were significantly lower than in healthy controls. A trend of volume reduction was also observed in the anterior amygdaloid area (p_{cor}=0.057). *C9orf72* negative patients also had significantly lower cortical nucleus (p_{cor}=0.034) and anterior amygdaloid area (p_{cor}=0.042) volumes compared to PLS patients. *C9orf72* hexanucleotide carriers exhibited preferential volume reductions in the lateral nucleus (p_{cor}=0.043), the cortico-amygdaloid transition area (p_{cor}=0.024) and a trend of volume reduction in the accessory basal nucleus (p_{cor}=0.057) with reference to healthy controls. PLS patients did not show overall amygdala atrophy or volume reductions in specific nuclei. (**Table 42, Figures 16-18**.) Furthermore, no direct association was identified between symptom duration and nuclear volumes in any of the patient groups.

Table 42*: Estimated marginal means (Mean ± S.E.) are adjusted for age (58.77), gender (1.45), education (13.78) and TIV (1429036.83). Bold p-values are significant at p < 0.05 following Bonferroni correction for multiple comparisons. Partial η^2 effect size is interpreted as small ($\eta^2p = 0.01$), medium ($\eta^2p = 0.06$) and large ($\eta^2p = 0.14$). ^{t} indicates a statistical trend of 0.05 < p_{cor} < 0.06*

	Study Group				Post-hoc comparisons						
	ALS C9+	ALS C9-	PLS	HC	ALS C9+ vs HC	ALS C9- vs HC	PLS vs HC	ALS C9+ vs ALS C9-	ALS C9+ vs PLS	ALS C9- vs PLS	Effect size
Whole amygdala	1672.88 ±50.03	1754.97 ±18.50	1806.97 ±30.15	1811.23 ±16.12	**0.055^t**	0.144	1.000	0.753	0.134	0.847	η^2p=0.043
Lateral nucleus	632.39 ±18.34	669.41 ±6.78	678.01 ±11.05	684.74 ±5.91	**0.043**	0.555	1.000	0.358	0.203	1.000	η^2p=0.035
Basal nucleus	428.78 ±13.74	449.06 ±5.08	462.37 ±8.28	462.62 ±4.43	0.120	0.284	1.000	1.000	0.222	1.000	η^2p=0.034
Accessory basal nucleus	251.83 ±9.04	263.48 ±3.34	275.43 ±5.45	276.68 ±2.91	**0.057^t**	**0.021**	1.000	1.000	0.156	0.371	η^2p=0.054
Anterior amygdaloid area	52.50 ±2.11	54.09 ±0.78	58.13 ±1.27	56.82 ±0.68	0.317	**0.057^t**	1.000	1.000	0.137	**0.042**	η^2p=0.051
Central nucleus	45.86 ±2.07	45.70 ±0.77	47.77 ±1.25	47.17 ±0.67	1.000	0.922	1.000	1.000	1.000	0.946	η^2p=0.013
Medial nucleus	20.96 ±1.35	19.93 ±0.50	22.34 ±0.82	21.07 ±0.44	1.000	0.547	1.000	1.000	1.000	0.074	η^2p=0.028
Cortical nucleus	24.95 ±1.13	25.06 ±0.42	27.27 ±0.68	26.70 ±0.36	0.856	**0.022**	1.000	1.000	0.470	**0.034**	η^2p=0.051
Cortico-amygdaloid transition	165.04 ±5.95	176.66 ±2.20	183.45 ±3.58	183.26 ±1.92	**0.024**	0.155	1.000	0.410	**0.050**	0.635	η^2p=0.049
Paralaminar nucleus	50.56 ±1.51	51.56 ±0.56	52.12 ±0.91	52.19 ±0.49	1.000	1.000	1.000	1.000	1.000	1.000	η^2p=0.006

Figure 16: *The volumetric profile of the amygdala in healthy controls (HC), primary lateral sclerosis (PLS), C9orf72 positive ALS (ALS-C9+), C9orf72 negative ALS (ALS-C9-) based on estimated marginal means adjusted for age, gender, education and total intracranial volumes. Error bars represent 95% confidence intervals.*

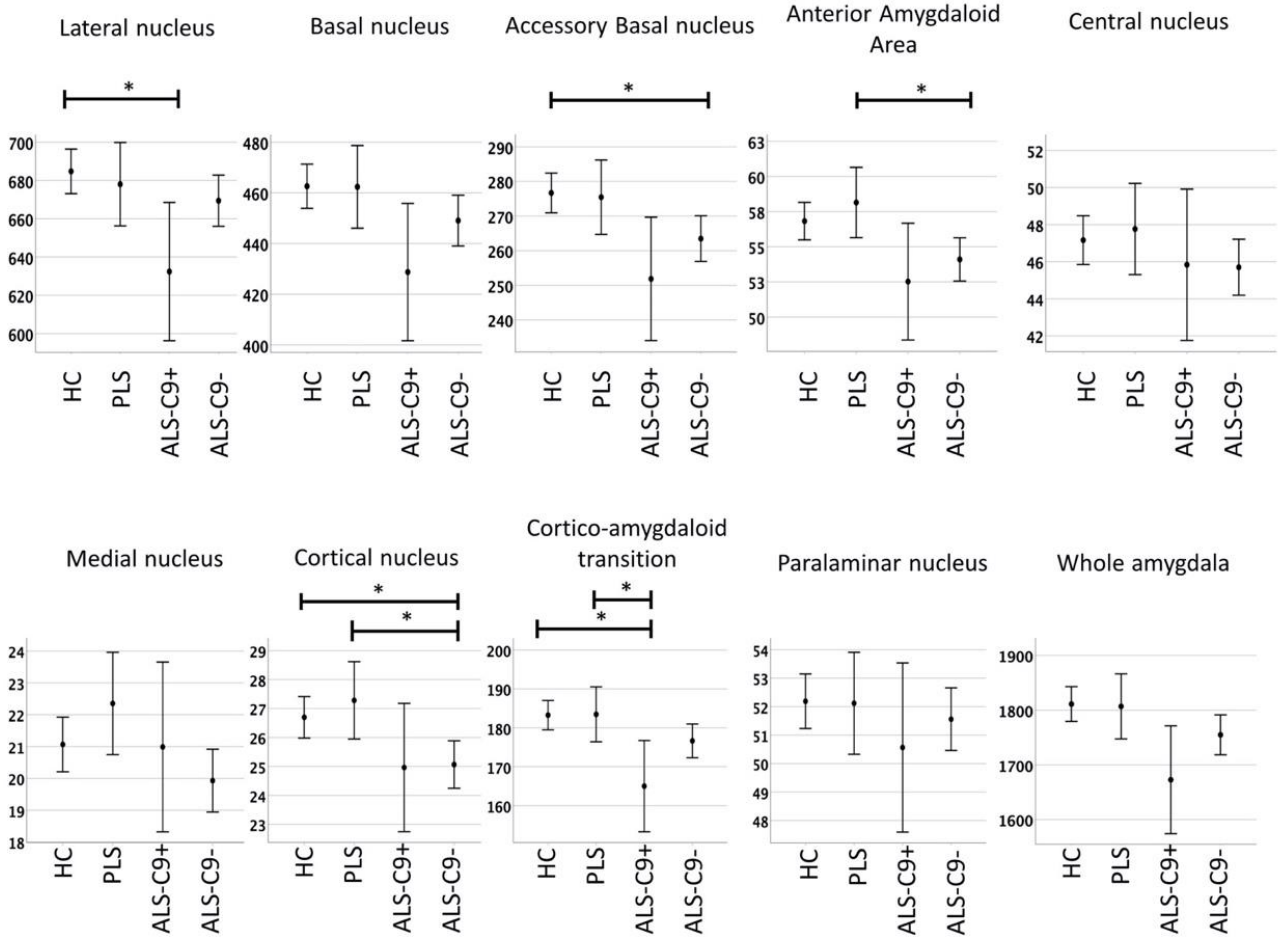

Figure 17*: The raw volumetric profile of amygdalar nuclei in C9orf72 hexanucleotide carrying ALS patients (ALS-C9+), C9orf72 negative amyotrophic lateral sclerosis patients (ALS-C9-), primary lateral sclerosis patients (PLS) and healthy controls (HC). Statistically significant intergroup differences following corrections for age, gender, intracranial volumes and multiple comparisons are indicated with asterisks. * p < 0.05*

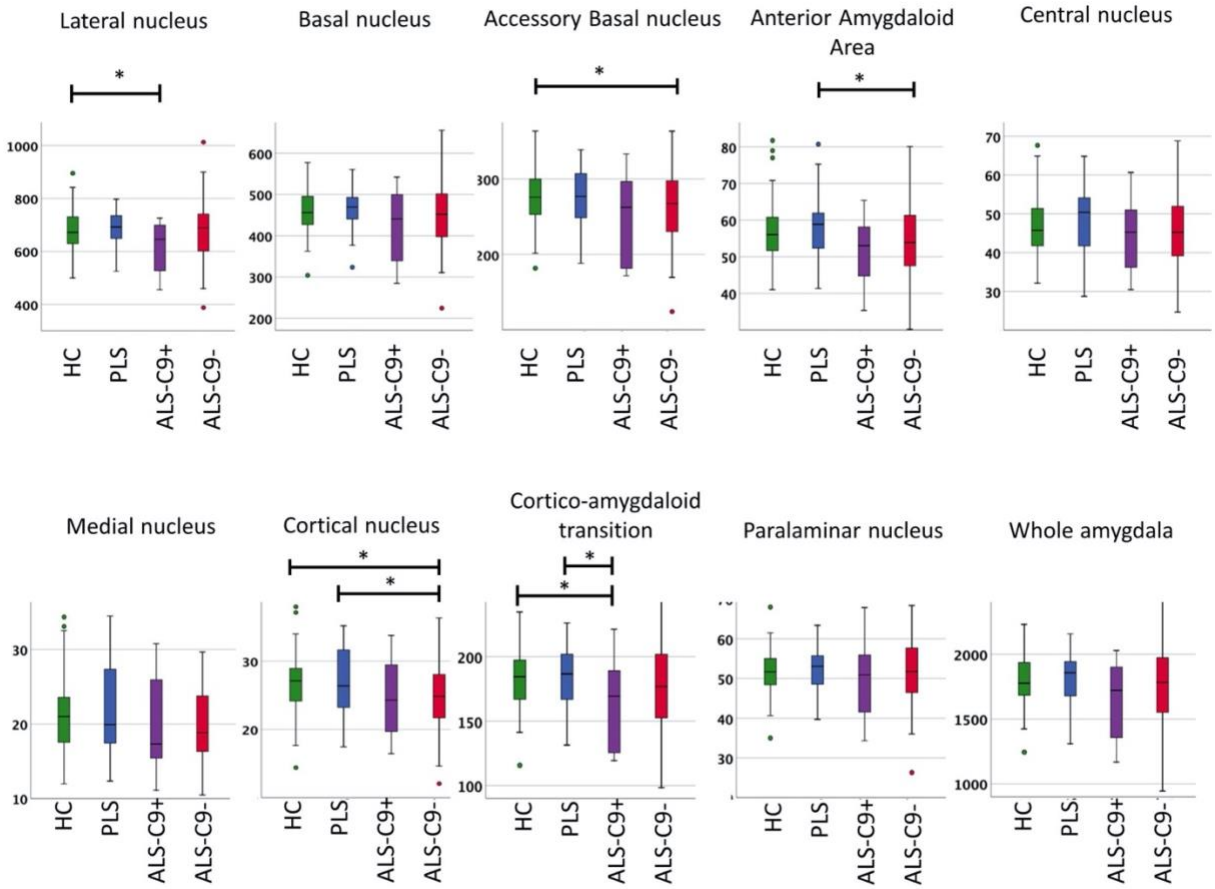

Figure 18. *The segmental amygdala profile of C9+ ALS, C9- ALS, and PLS with reference to healthy controls. 100% represents the estimated marginal mean of healthy controls for each structure. Estimated marginal means of volumes were calculated with the following values age = 58.77, gender = 1.45, Education = 13.78, total intracranial volume = 1429036.83.*

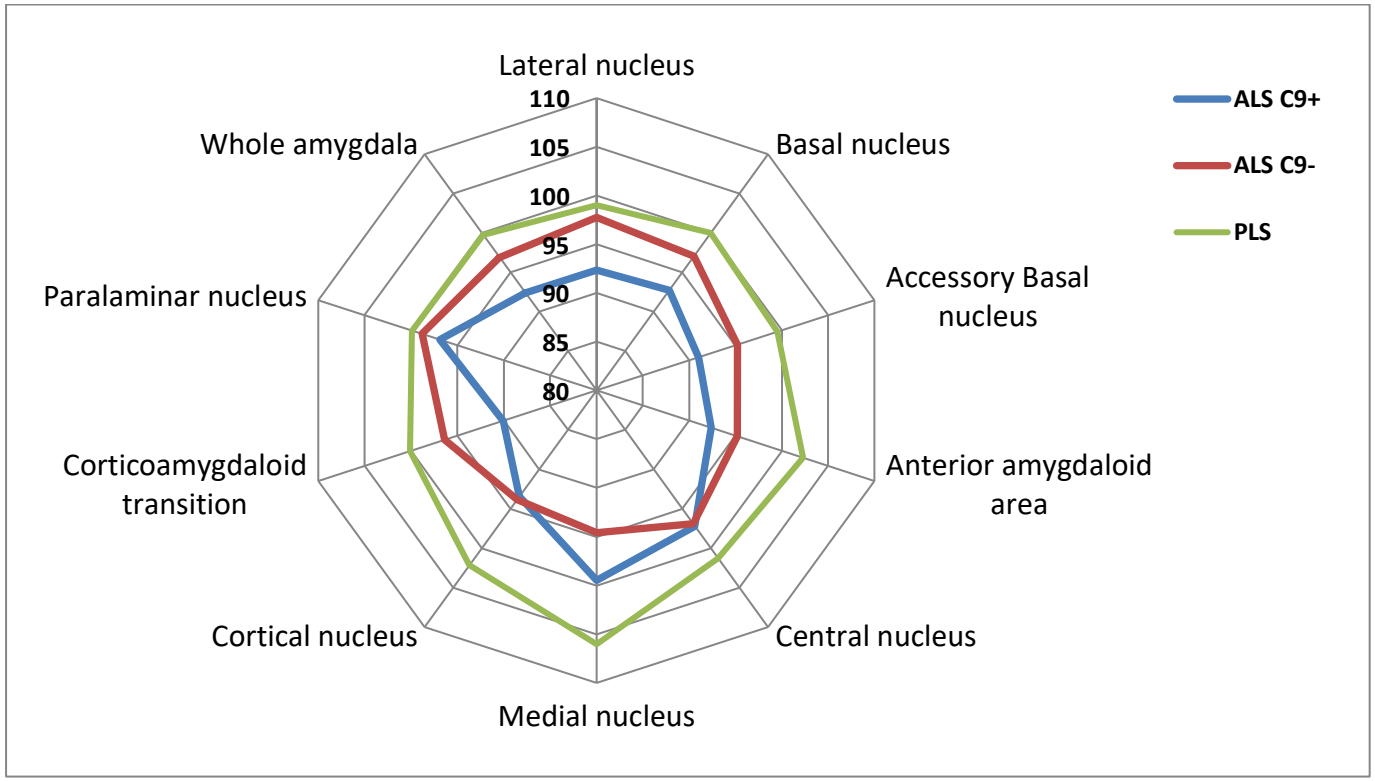

Vertex changes

Surface projected shape deformation only reached significance in the *C9orf72* positive ALS versus healthy control contrast, highlighting a unilateral pattern of inferior medial atrophy in the left amygdala (**Figure 19**.).

Figure 19*: Shape deformation in C9orf72 positive ALS patients compared to healthy controls (HC) based on vertex analyses at p < 0.05 corrected for age, gender, education and total intracranial volumes. Blue colour indicates the 3 dimensional amygdalal mesh and orange highlights surface projected atrophy at p < 0.05 FWE.*

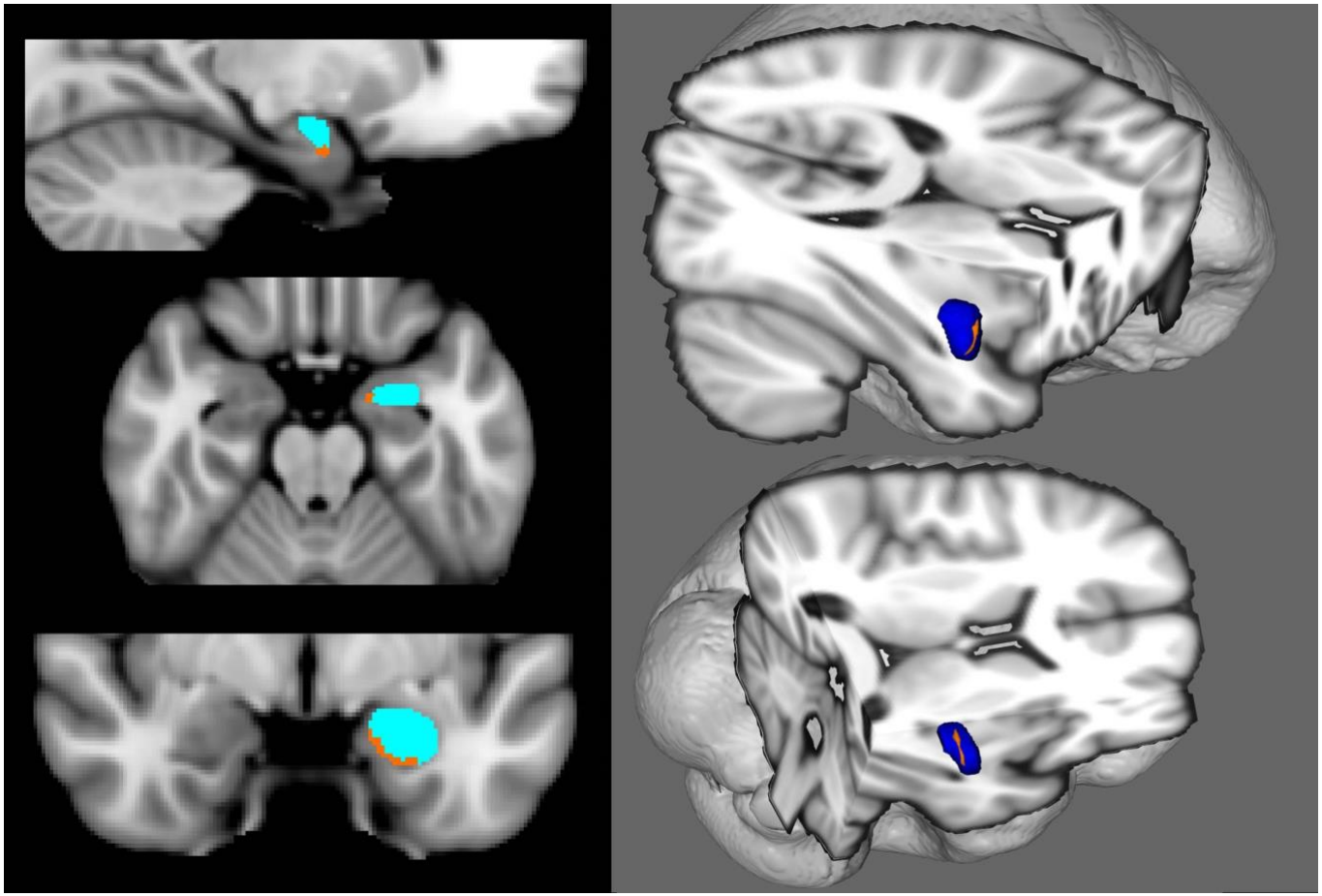

Discussion

Our findings highlight the selective degeneration of amygdalar nuclei as opposed to global amygdala pathology in ALS. Furthermore, our data suggest genotype-specific patterns of amygdala pathology.

Global amygdala involvement in ALS has been observed qualitatively (680) and investigated in dedicated cross-sectional (123, 327, 675) and longitudinal imaging studies (156, 589). Imaging modalities of existing amygdala studies in ALS include PET (328, 681), volumetry (327, 601, 675), fMRI (676), voxel-based morphometry (140, 154), ROI morphometry (327), vertex analyses (327, 601), diffusion tensor imaging (156, 601) and the assessment of peri-amygdalar white matter alterations (461). The findings of these reports are strikingly inconsistent; some studies did not detect significant amygdala atrophy (154, 327, 589, 601) while others identified considerable pathological changes (156, 328, 675, 676). Interestingly, some studies found no volume reductions, but identified focal shape deformation in the same cohort (327), which highlights the differing detection sensitivity of the various methodological approaches. A PET study identified a cluster of relative hypermetabolism in the medial temporal lobe including the amygdala which was putatively interpreted as astrocytosis or microglial activation (328). The majority of ALS imaging studies which comment on the amygdala are cross-sectional and the few longitudinal studies arrive to different conclusions. Some studies detect progressive amygdala atrophy over time (156), while others don't detect progressive change longitudinally (589). Patient selection and the

choice of image analysis are the two most likely factors in the inconsistency. ALS is a clinically heterogeneous condition with considerable differences in motor disability and neuropsychological performance. Compared to other neurodegenerative conditions, imaging studies of ALS typically include relatively small patient samples (129) and patients tend to only tolerate MRI scanning for a limited period of time after the diagnosis which leads to a considerable selection bias. Small patient samples coupled with clinical heterogeneity are likely to contribute to the inconsistency of mesial temporal lobe findings in ALS. Clinical heterogeneity in motor neuron disease (MND) is multidimensional and include variance in relative upper motor neuron / lower motor neuron (LMN) involvement, differing motor disability profiles, varying progression rates, inconsistencies in neuropsychological manifestations and considerable differences in survival (124). While clinical heterogeneity is regarded as a barrier to drug development by some (682) and a key contributor to diagnostic delay by others (683), it highlights the need for individualised management strategies and interventions tailored to individual clinical, genetic and radiological profiles. To circumvent disease heterogeneity and sample size limitations, extra-motor studies in ALS typically use one of the two main stratification strategies (510, 523); patient categorisation based on neuropsychological profile (154, 327) or based on genotype (601). Our findings illustrate the importance of patient stratification based on objective criteria which in our case allows the description of genotype-specific signatures. Our findings also showcase the limitation of measuring total volumes in a cytologically and functionally heterogeneous structure; total volumes were not significantly different between the study groups but the volumes of individual nuclei were.

Our cohort of *C9orf72* negative ALS patients exhibited focal changes in the accessory basal nucleus, cortical nucleus and anterior amygdaloid area compared to healthy controls. The accessory basal nucleus forms the connection between the central and lateral nuclei (684, 685), and its activation has been shown to subdue high-anxiety states and fear-related freezing (685, 686). The cortical nucleus of the amygdala mediates ingestive, defensive and reproductive behaviours and is also thought to be involved in the processing of pheromonal information (687). The corticomedial nuclei are involved in olfaction and appetite regulation. The relevance of characterising the extra-motor profile of *C9orf72* negative sporadic ALS patients is that these patients represent the majority of patients presenting to ALS clinics. Following the discovery of GGGGCC repeats, there was a notion that frontotemporal changes are unique to hexanucleotide repeat carriers and *C9orf72* negative ALS patients may represent a relatively pure or 'classical' motor variant of ALS with limited extra-motor involvement (604). This concept has been gradually challenged by the detection of considerable temporal, frontal and subcortical pathology in *C9orf72* negative cohorts (3, 527). Our findings also indicate that mesial temporal lobe involvement is not unique to the *C9orf72*.

Degeneration of the amygdala has been previously linked to *C9orf72* repeat expansions based on both post mortem (648) and imaging observations (688). Presymptomatic studies of *C9orf72* hexanucleotide repeat carriers seldom comment specifically on amygdala involvement (24) despite description of extensive temporal lobe changes long before symptom manifestation (7, 26). We have identified a

statistical trend of total amygdala volume reduction in hexanucleotide repeat carriers compared to controls (p=0.055) and significant shape deformation. In our study, *C9orf72* hexanucleotide carriers exhibited preferential volume reductions in the lateral nucleus, cortico-amygdaloid transition area and accessory basal nucleus. The lateral, basal and accessory basal nuclei all form part of the basolateral group of nuclei which has reciprocal connections to sensory association areas of the cortex and direct projections to the thalamus (689). The lateral nucleus has an established role in fear-related processes, a key component of Pavlovian fear-conditioning (690), involved in short-term (691), and long-term fear-memory (692-694). The corticoamygdaloid transition zone is a zone of confluence between the medial parvicellular basal nucleus, paralaminar nucleus, and the sulcal periamygdaloid cortex and provides the main input to the lateral core subdivision (695). Our findings indicate relatively divergent amygdalar profiles in hexanucleotide repeat carriers and sporadic ALS patients. The only shared area affected in both patient groups irrespective of *C9orf72* hexanucleotide status is the accessory basal nucleus. The characterisation of *C9orf72*-associated amygdalar changes in ALS complements previous reports of unique radiological features, progression patterns, and clinical manifestations associated with the genotype (23, 604, 696).

PLS patients showed no volume reductions in any of the amygdalar nuclei. PLS is still widely regarded as 'pure' motor system disorder despite recent reports of cognitive and behavioural deficits (607, 662, 697). PLS is considered a separate entity by some and the UMN-dominant extreme of the ALS spectrum by others (5). From a clinical

perspective, PLS has a number of unique features and a relatively stereotyped disease trajectory which justify the assessment of cerebral pathology as a distinct group separate from ALS. PLS patients typically have longer survival than ALS patients, present with relatively symmetric limb spasticity, and despite frequent bulbar involvement, they rarely require feeding tube placement or respiratory support. Given the predominance of upper motor neuron signs on clinical assessment, PLS imaging studies typically focus on precentral gyrus pathology. From a radiological perspective PLS is classically associated with motor cortex atrophy (116, 666, 698), corpus callosum (699, 700) and corticospinal tract degeneration(701-703), but more recently, brainstem (537), temporal lobe (116), cerebellar (116) and subcortical grey matter changes have also been described (367, 538). Consistent with the expanding literature of extra-motor changes in PLS white matter alterations have been described in the superior and inferior longitudinal fasciculi, fornix, thalamic radiations, and parietal lobes based on diffusivity metrics (134, 704). Emerging evidence of neuropsychological deficits (607, 662) provide the rational for the targeted assessment of temporal lobe changes in PLS.

Post mortem studies consistently describe amygdala changes in amyotrophic lateral sclerosis (489, 705-707). Histopathological changes in the amygdala include focal TDP-43 burden (496, 706-708), neuronal loss (496, 671, 677, 709-711) and gliosis (709, 710, 712, 713). Pathological TDP-43 accumulation in the anteromedial portions of the temporal lobe is regarded as stage 4 of the recently proposed pathological staging system (404). Amygdalar changes have also been linked to clinical stages on imaging.

Peri-amygdalar white matter alterations were identified in patients with stage 2 disease based on the King's staging system (461). Focal amygdalar changes have been previously described in ALS with the preferential involvement of the basolateral nuclei showing heavy gliosis (672) and neuronal loss (671). With few exceptions (133), the majority of large ALS imaging studies lack post mortem assessment which precludes the histological validation of ante mortem imaging findings and the appraisal of the sensitivity profile of specific imaging techniques. From a biological perspective, there is considerable concordance among post mortem, clinical and imaging studies in ALS that interconnected brain regions exhibit concomitant degeneration (714-716). This is commonly interpreted as evidence of connectivity-based (715), trans-synaptic (717) or prion-like (398) disease propagation. The amygdalar changes identified in this study are consistent with this notion, as other components of the limbic system and key projections of the amygdala such as the hypothalamus, dorsomedial thalamus, facial nerve nuclei, and the nucleus accumbens are also established foci of ALS pathology (509, 601).

The post mortem literature of PLS is sparse compared to the number of studies published in ALS. The commonest post mortem findings in PLS include Betz cell depletion in the motor cortex, demyelination and the degeneration of the corticospinal tracts (495, 718-722). Extra-motor involvement has also been described in PLS (723-726), but many of these reports include clinically diverse patients. Very few post mortem studies specifically highlight amygdala pathology in primary lateral sclerosis (496, 727). Our imaging study did not identify amygdala atrophy in PLS which is in

contrast to our findings in the ALS cohort and supports the conceptualisation of PLS as a separate entity, distinct from ALS (5).

Neuropsychological deficits in ALS are thought to be dominated by executive dysfunction (641) and behavioural impairment (4), but memory impairment and deficits in social cognition are increasingly recognised (577, 670, 728, 729). Amygdala-mediated limbic dysfunction has been specifically suggested in ALS based on impaired recognition of threat in fear-inducing situations (730). Altered cerebral activation to emotional stimuli has also been repeatedly reported in ALS (731, 732). Abnormal anxiety-mediated amygdala activation patterns were previously described in ALS based on emotional processing paradigms (676). The neural underpinnings of Theory of Mind (ToM) deficits have also been investigated by resting-state fMRI studies in ALS and recent data suggest a divergent longitudinal course in limb-onset and bulbar onset patients (733). Anxiety is seldom studied specifically in ALS, but a recent large study which included 159 patients demonstrated the important quality-of-life ramification of anxiety in ALS (734). Impaired emotional regulation is hugely relevant clinically as it may impact on engagement with multidisciplinary management, decisions to participate in clinical trials and adherence to therapy. Reduced fear or anxiety may affect safety awareness, usage of assistive devices and compliance with and rehabilitation efforts (735). Deficits in social cognition may affect caregiver burden (736). ALS patients make a series of emotional adjustments as they face difficult decisions around finances, continuation of employment, feeding tube placement, and ventilation all of which require the careful consideration of individual preferences,

caregiver views, and personal values (737). Subtle autonomic (480, 738), sensory (169), and olfactory (187, 739) dysfunction have also been documented in ALS (15, 740) as well as changes in appetite (741) implicating the involvement of amygdala-mediated circuits. Cerebral sexual dimorphism is well established based on neuroimaging data form healthy cohorts (742, 743), but also in ALS (164, 744). Developmental gender differences are thought to be particularly important with regards to amygdala volumes (745-747) which are often linked to gender-specific stress response profiles (734, 748). In our study we did not identify gender-specific volumetric traits, but the emerging literature of gene-gender interactions in ALS (744, 749, 750) underline the importance of examining gender effects in neuroimaging studies.

This study is not without limitations. The size of our *C9orf72* positive ALS cohort is relatively small to make conclusive observations about genotype-specific amygdalar signatures. We have no post mortem data to validate the selective degeneration of amygdalar nuclei observed in vivo. Our study is cross-sectional and merely provides a snapshot of structural degeneration instead of characterising the longitudinal trajectory of accruing amygdala pathology over time. A multi-time point longitudinal study design with presymptomatic mutation carriers would provide important additional insights (119, 151). The assessment of additional metabolic, functional or diffusivity metrics would have complemented our structural findings (153, 568, 578, 751). Notwithstanding these limitations, our study confirms considerable amygdala degeneration in ALS and highlights the importance of screening for limbic system-mediated cognitive functions. Our findings showcase the importance of evaluating

non-motor brain regions in ALS radiologically and demonstrate that routine T1-weighted sequences can be utilised for the detailed characterisation of mesial temporal lobe structures. The heterogeneity of extra-motor involvement across motor neuron disease phenotypes (ALS/PLS) and genotypes (sporadic/*C9orf72*) underscores the importance of individualised management strategies. Our findings need to be validated in larger cohorts, possibly pooled from multiple centres and replicated in longitudinal studies.

Conclusions

Amygdala pathology is a consistent feature of both sporadic and *C9orf72*-associated ALS. The selective pathology of amygdalar nuclei detected in vivo is consistent with previous post mortem reports. The assessment of total amygdala volumes and shape deformations is insufficient to capture focal alterations in the structure. The involvement of the amygdala in ALS is likely to contribute to the heterogeneity of extra-motor manifestations including deficits in social cognition, emotional processing and memory impairment. Our findings confirm that mesial temporal lobe pathology is not unique to the *C9orf72* genotype and underscore the importance for screening for neuropsychological deficits in sporadic patients.

REFERENCES

1. Miller T, Cudkowicz M, Shaw PJ, Andersen PM, Atassi N, Bucelli RC, et al. Phase 1-2 Trial of Antisense Oligonucleotide Tofersen for SOD1 ALS. The New England journal of medicine. 2020;383(2):109-19.
2. Mueller C, Berry JD, McKenna-Yasek DM, Gernoux G, Owegi MA, Pothier LM, et al. SOD1 Suppression with Adeno-Associated Virus and MicroRNA in Familial ALS. The New England journal of medicine. 2020;383(2):151-8.
3. Omer T, Finegan E, Hutchinson S, Doherty M, Vajda A, McLaughlin RL, et al. Neuroimaging patterns along the ALS-FTD spectrum: a multiparametric imaging study. Amyotrophic lateral sclerosis & frontotemporal degeneration. 2017;18(7-8):611-23.
4. Burke T, Pinto-Grau M, Lonergan K, Bede P, O'Sullivan M, Heverin M, et al. A Cross-sectional population-based investigation into behavioral change in amyotrophic lateral sclerosis: subphenotypes, staging, cognitive predictors, and survival. Ann Clin Transl Neurol. 2017;4(5):305-17.
5. Finegan E, Chipika RH, Shing SLH, Hardiman O, Bede P. Primary lateral sclerosis: a distinct entity or part of the ALS spectrum? Amyotrophic lateral sclerosis & frontotemporal degeneration. 2019;20(3-4):133-45.
6. Kiernan MC, Ziemann U, Eisen A. Amyotrophic lateral sclerosis: Origins traced to impaired balance between neural excitation and inhibition in the neonatal period. Muscle & nerve. 2019;60(3):232-5.
7. Bertrand A, Wen J, Rinaldi D, Houot M, Sayah S, Camuzat A, et al. Early Cognitive, Structural, and Microstructural Changes in Presymptomatic C9orf72 Carriers Younger Than 40 Years. JAMA neurology. 2018;75(2):236-45.
8. Querin G, Bede P, El Mendili MM, Li M, Pelegrini-Issac M, Rinaldi D, et al. Presymptomatic spinal cord pathology in c9orf72 mutation carriers: A longitudinal neuroimaging study. Annals of neurology. 2019;86(2):158-67.
9. Benatar M, Turner MR, Wuu J. Defining pre-symptomatic amyotrophic lateral sclerosis. Amyotrophic lateral sclerosis & frontotemporal degeneration. 2019;20(5-6):303-9.
10. Carew JD, Nair G, Andersen PM, Wuu J, Gronka S, Hu X, et al. Presymptomatic spinal cord neurometabolic findings in SOD1-positive people at risk for familial ALS. Neurology. 2011;77(14):1370-5.
11. Cirak S, Arechavala-Gomeza V, Guglieri M, Feng L, Torelli S, Anthony K, et al. Exon skipping and dystrophin restoration in patients with Duchenne muscular dystrophy after systemic phosphorodiamidate morpholino oligomer treatment: an open-label, phase 2, dose-escalation study. Lancet (London, England). 2011;378(9791):595-605.
12. Mendell JR, Rodino-Klapac LR, Sahenk Z, Roush K, Bird L, Lowes LP, et al. Eteplirsen for the treatment of Duchenne muscular dystrophy. Ann Neurol. 2013;74(5):637-47.
13. Mendell JR, Goemans N, Lowes LP, Alfano LN, Berry K, Shao J, et al. Longitudinal effect of eteplirsen versus historical control on ambulation in Duchenne muscular dystrophy. Ann Neurol. 2016;79(2):257-71.
14. Kanouchi T, Ohkubo T, Yokota T. Can regional spreading of amyotrophic lateral sclerosis motor symptoms be explained by prion-like propagation? J Neurol Neurosurg Psychiatry. 2012;83(7):739-45.
15. Bede P, Iyer PM, Schuster C, Elamin M, McLaughlin RL, Kenna K, et al. The selective anatomical vulnerability of ALS: 'disease-defining' and 'disease-defying' brain regions. Amyotrophic lateral sclerosis & frontotemporal degeneration. 2016;17(7-8):561-70.
16. Eisen A. The real onset of amyotrophic lateral sclerosis. J Neurol Neurosurg Psychiatry. 2011;82(6):593.

17. Benatar M, Wuu J. Presymptomatic studies in ALS: rationale, challenges, and approach. Neurology. 2012;79(16):1732-9.
18. Swash M, Ingram D. Preclinical and subclinical events in motor neuron disease. J Neurol Neurosurg Psychiatry. 1988;51(2):165-8.
19. Eisen A, Kiernan M, Mitsumoto H, Swash M. Amyotrophic lateral sclerosis: a long preclinical period? J Neurol Neurosurg Psychiatry. 2014;85(11):1232-8.
20. Aggarwal A, Nicholson G. Detection of preclinical motor neurone loss in SOD1 mutation carriers using motor unit number estimation. J Neurol Neurosurg Psychiatry. 2002;73(2):199-201.
21. Aggarwal A, Nicholson G. Normal complement of motor units in asymptomatic familial (SOD1 mutation) amyotrophic lateral sclerosis carriers. J Neurol Neurosurg Psychiatry. 2001;71(4):478-81.
22. Walhout R, Schmidt R, Westeneng HJ, Verstraete E, Seelen M, van Rheenen W, et al. Brain morphologic changes in asymptomatic C9orf72 repeat expansion carriers. Neurology. 2015;85(20):1780-8.
23. Floeter MK, Bageac D, Danielian LE, Braun LE, Traynor BJ, Kwan JY. Longitudinal imaging in C9orf72 mutation carriers: Relationship to phenotype. Neuroimage Clin. 2016;12:1035-43.
24. Lee SE, Sias AC, Mandelli ML, Brown JA, Brown AB, Khazenzon AM, et al. Network degeneration and dysfunction in presymptomatic C9ORF72 expansion carriers. Neuroimage Clin. 2017;14:286-97.
25. Papma JM, Jiskoot LC, Panman JL, Dopper EG, den Heijer T, Donker Kaat L, et al. Cognition and gray and white matter characteristics of presymptomatic C9orf72 repeat expansion. Neurology. 2017;89(12):1256-64.
26. Wen J, Zhang H, Alexander DC, Durrleman S, Routier A, Rinaldi D, et al. Neurite density is reduced in the presymptomatic phase of C9orf72 disease. J Neurol Neurosurg Psychiatry. 2019;90(4):387-94.
27. Le Blanc G, Jetté Pomerleau V, McCarthy J, Borroni B, van Swieten J, Galimberti D, et al. Faster Cortical Thinning and Surface Area Loss in Presymptomatic and Symptomatic C9orf72 Repeat Expansion Adult Carriers. Ann Neurol. 2020.
28. De Vocht J, Blommaert J, Devrome M, Radwan A, Van Weehaeghe D, De Schaepdryver M, et al. Use of Multimodal Imaging and Clinical Biomarkers in Presymptomatic Carriers of C9orf72 Repeat Expansion. JAMA Neurol. 2020.
29. Gorges M, Vercruysse P, Müller HP, Huppertz HJ, Rosenbohm A, Nagel G, et al. Hypothalamic atrophy is related to body mass index and age at onset in amyotrophic lateral sclerosis. J Neurol Neurosurg Psychiatry. 2017;88(12):1033-41.
30. Menke RA, Proudfoot M, Wuu J, Andersen PM, Talbot K, Benatar M, et al. Increased functional connectivity common to symptomatic amyotrophic lateral sclerosis and those at genetic risk. J Neurol Neurosurg Psychiatry. 2016;87(6):580-8.
31. Vucic S, Winhammar JM, Rowe DB, Kiernan MC. Corticomotoneuronal function in asymptomatic SOD-1 mutation carriers. Clinical neurophysiology : official journal of the International Federation of Clinical Neurophysiology. 2010;121(10):1781-5.
32. Ng MC, Ho JT, Ho SL, Lee R, Li G, Cheng TS, et al. Abnormal diffusion tensor in nonsymptomatic familial amyotrophic lateral sclerosis with a causative superoxide dismutase 1 mutation. Journal of magnetic resonance imaging : JMRI. 2008;27(1):8-13.
33. Turner MR, Hammers A, Al-Chalabi A, Shaw CE, Andersen PM, Brooks DJ, et al. Distinct cerebral lesions in sporadic and 'D90A' SOD1 ALS: studies with [11C]flumazenil PET. Brain. 2005;128(Pt 6):1323-9.
34. Premi E, Calhoun VD, Diano M, Gazzina S, Cosseddu M, Alberici A, et al. The inner fluctuations of the brain in presymptomatic Frontotemporal Dementia: The chronnectome fingerprint. Neuroimage. 2019;189:645-54.

35. Staffaroni AM, Cobigo Y, Goh SM, Kornak J, Bajorek L, Chiang K, et al. Individualized atrophy scores predict dementia onset in familial frontotemporal lobar degeneration. Alzheimer's & dementia : the journal of the Alzheimer's Association. 2020;16(1):37-48.
36. Gazzina S, Grassi M, Premi E, Cosseddu M, Alberici A, Archetti S, et al. Education modulates brain maintenance in presymptomatic frontotemporal dementia. J Neurol Neurosurg Psychiatry. 2019;90(10):1124-30.
37. Mutsaerts H, Mirza SS, Petr J, Thomas DL, Cash DM, Bocchetta M, et al. Cerebral perfusion changes in presymptomatic genetic frontotemporal dementia: a GENFI study. Brain. 2019;142(4):1108-20.
38. Fumagalli GG, Basilico P, Arighi A, Bocchetta M, Dick KM, Cash DM, et al. Distinct patterns of brain atrophy in Genetic Frontotemporal Dementia Initiative (GENFI) cohort revealed by visual rating scales. Alzheimer's research & therapy. 2018;10(1):46.
39. Cash DM, Bocchetta M, Thomas DL, Dick KM, van Swieten JC, Borroni B, et al. Patterns of gray matter atrophy in genetic frontotemporal dementia: results from the GENFI study. Neurobiol Aging. 2018;62:191-6.
40. Premi E, Grassi M, van Swieten J, Galimberti D, Graff C, Masellis M, et al. Cognitive reserve and TMEM106B genotype modulate brain damage in presymptomatic frontotemporal dementia: a GENFI study. Brain. 2017;140(6):1784-91.
41. Tavares TP, Mitchell DGV, Coleman K, Shoesmith C, Bartha R, Cash DM, et al. Ventricular volume expansion in presymptomatic genetic frontotemporal dementia. Neurology. 2019;93(18):e1699-e706.
42. Rittman T, Borchert R, Jones S, van Swieten J, Borroni B, Galimberti D, et al. Functional network resilience to pathology in presymptomatic genetic frontotemporal dementia. Neurobiol Aging. 2019;77:169-77.
43. Cury C, Durrleman S, Cash DM, Lorenzi M, Nicholas JM, Bocchetta M, et al. Spatiotemporal analysis for detection of pre-symptomatic shape changes in neurodegenerative diseases: Initial application to the GENFI cohort. Neuroimage. 2019;188:282-90.
44. Sudre CH, Bocchetta M, Cash D, Thomas DL, Woollacott I, Dick KM, et al. White matter hyperintensities are seen only in GRN mutation carriers in the GENFI cohort. Neuroimage Clin. 2017;15:171-80.
45. Staffaroni AM, Bajorek L, Casaletto KB, Cobigo Y, Goh SM, Wolf A, et al. Assessment of executive function declines in presymptomatic and mildly symptomatic familial frontotemporal dementia: NIH-EXAMINER as a potential clinical trial endpoint. Alzheimer's & dementia : the journal of the Alzheimer's Association. 2020;16(1):11-21.
46. Lulé DE, Müller HP, Finsel J, Weydt P, Knehr A, Winroth I, et al. Deficits in verbal fluency in presymptomatic C9orf72 mutation gene carriers-a developmental disorder. J Neurol Neurosurg Psychiatry. 2020.
47. Popuri K, Dowds E, Beg MF, Balachandar R, Bhalla M, Jacova C, et al. Gray matter changes in asymptomatic C9orf72 and GRN mutation carriers. NeuroImage Clinical. 2018;18:591-8.
48. Feis RA, Bouts M, Panman JL, Jiskoot LC, Dopper EGP, Schouten TM, et al. Single-subject classification of presymptomatic frontotemporal dementia mutation carriers using multimodal MRI. Neuroimage Clin. 2019;22:101718.
49. Panman JL, Jiskoot LC, Bouts M, Meeter LHH, van der Ende EL, Poos JM, et al. Gray and white matter changes in presymptomatic genetic frontotemporal dementia: a longitudinal MRI study. Neurobiol Aging. 2019;76:115-24.
50. Feis RA, Bouts M, de Vos F, Schouten TM, Panman JL, Jiskoot LC, et al. A multimodal MRI-based classification signature emerges just prior to symptom onset in frontotemporal dementia mutation carriers. J Neurol Neurosurg Psychiatry. 2019;90(11):1207-14.
51. Rohrer JD, Nicholas JM, Cash DM, van Swieten J, Dopper E, Jiskoot L, et al. Presymptomatic cognitive and neuroanatomical changes in genetic frontotemporal dementia

in the Genetic Frontotemporal dementia Initiative (GENFI) study: a cross-sectional analysis. The Lancet Neurology. 2015;14(3):253-62.
52. Aggarwal A. Handgrip maximal voluntary isometric contraction does not correlate with thenar motor unit number estimation. Neurology research international. 2012;2012:187947.
53. Proudfoot M, Rohenkohl G, Quinn A, Colclough GL, Wuu J, Talbot K, et al. Altered cortical beta-band oscillations reflect motor system degeneration in amyotrophic lateral sclerosis. Hum Brain Mapp. 2017;38(1):237-54.
54. Geevasinga N, Menon P, Nicholson GA, Ng K, Howells J, Kril JJ, et al. Cortical Function in Asymptomatic Carriers and Patients With C9orf72 Amyotrophic Lateral Sclerosis. JAMA Neurol. 2015;72(11):1268-74.
55. Vucic S, Nicholson GA, Kiernan MC. Cortical hyperexcitability may precede the onset of familial amyotrophic lateral sclerosis. Brain. 2008;131(Pt 6):1540-50.
56. Benussi A, Gazzina S, Premi E, Cosseddu M, Archetti S, Dell'Era V, et al. Clinical and biomarker changes in presymptomatic genetic frontotemporal dementia. Neurobiol Aging. 2019;76:133-40.
57. Benatar M, Wuu J, Andersen PM, Lombardi V, Malaspina A. Neurofilament light: A candidate biomarker of presymptomatic amyotrophic lateral sclerosis and phenoconversion. Ann Neurol. 2018;84(1):130-9.
58. Benatar M, Wuu J, Lombardi V, Jeromin A, Bowser R, Andersen PM, et al. Neurofilaments in pre-symptomatic ALS and the impact of genotype. Amyotrophic lateral sclerosis & frontotemporal degeneration. 2019;20(7-8):538-48.
59. Weydt P, Oeckl P, Huss A, Müller K, Volk AE, Kuhle J, et al. Neurofilament levels as biomarkers in asymptomatic and symptomatic familial amyotrophic lateral sclerosis. Ann Neurol. 2016;79(1):152-8.
60. Oeckl P, Weydt P, Thal DR, Weishaupt JH, Ludolph AC, Otto M. Proteomics in cerebrospinal fluid and spinal cord suggests UCHL1, MAP2 and GPNMB as biomarkers and underpins importance of transcriptional pathways in amyotrophic lateral sclerosis. Acta neuropathologica. 2020;139(1):119-34.
61. Thompson AG, Gray E, Bampton A, Raciborska D, Talbot K, Turner MR. CSF chitinase proteins in amyotrophic lateral sclerosis. J Neurol Neurosurg Psychiatry. 2019;90(11):1215-20.
62. Gendron TF, Chew J, Stankowski JN, Hayes LR, Zhang YJ, Prudencio M, et al. Poly(GP) proteins are a useful pharmacodynamic marker for C9ORF72-associated amyotrophic lateral sclerosis. Science translational medicine. 2017;9(383).
63. Lehmer C, Oeckl P, Weishaupt JH, Volk AE, Diehl-Schmid J, Schroeter ML, et al. Poly-GP in cerebrospinal fluid links C9orf72-associated dipeptide repeat expression to the asymptomatic phase of ALS/FTD. EMBO molecular medicine. 2017;9(7):859-68.
64. Barschke P, Oeckl P, Steinacker P, Al Shweiki MR, Weishaupt JH, Landwehrmeyer GB, et al. Different CSF protein profiles in amyotrophic lateral sclerosis and frontotemporal dementia with C9orf72 hexanucleotide repeat expansion. J Neurol Neurosurg Psychiatry. 2020;91(5):503-11.
65. Stoccoro A, Mosca L, Carnicelli V, Cavallari U, Lunetta C, Marocchi A, et al. Mitochondrial DNA copy number and D-loop region methylation in carriers of amyotrophic lateral sclerosis gene mutations. Epigenomics. 2018;10(11):1431-43.
66. Chen Q, Boeve BF, Senjem M, Tosakulwong N, Lesnick T, Brushaber D, et al. Trajectory of lobar atrophy in asymptomatic and symptomatic GRN mutation carriers: a longitudinal MRI study. Neurobiol Aging. 2020;88:42-50.
67. Lee SE, Sias AC, Kosik EL, Flagan TM, Deng J, Chu SA, et al. Thalamo-cortical network hyperconnectivity in preclinical progranulin mutation carriers. Neuroimage Clin. 2019;22:101751.
68. Olm CA, McMillan CT, Irwin DJ, Van Deerlin VM, Cook PA, Gee JC, et al. Longitudinal structural gray matter and white matter MRI changes in presymptomatic progranulin mutation carriers. Neuroimage Clin. 2018;19:497-506.

69. Dopper EG, Rombouts SA, Jiskoot LC, den Heijer T, de Graaf JR, de Koning I, et al. Structural and functional brain connectivity in presymptomatic familial frontotemporal dementia. Neurology. 2014;83(2):e19-26.
70. Caroppo P, Habert MO, Durrleman S, Funkiewiez A, Perlbarg V, Hahn V, et al. Lateral Temporal Lobe: An Early Imaging Marker of the Presymptomatic GRN Disease? Journal of Alzheimer's disease : JAD. 2015;47(3):751-9.
71. Premi E, Cauda F, Costa T, Diano M, Gazzina S, Gualeni V, et al. Looking for Neuroimaging Markers in Frontotemporal Lobar Degeneration Clinical Trials: A Multi-Voxel Pattern Analysis Study in Granulin Disease. Journal of Alzheimer's disease : JAD. 2016;51(1):249-62.
72. Jacova C, Hsiung GY, Tawankanjanachot I, Dinelle K, McCormick S, Gonzalez M, et al. Anterior brain glucose hypometabolism predates dementia in progranulin mutation carriers. Neurology. 2013;81(15):1322-31.
73. Premi E, Gazzina S, Bozzali M, Archetti S, Alberici A, Cercignani M, et al. Cognitive reserve in granulin-related frontotemporal dementia: from preclinical to clinical stages. PLoS One. 2013;8(9):e74762.
74. Milanesi E, Bonvicini C, Alberici A, Pilotto A, Cattane N, Premi E, et al. Molecular signature of disease onset in granulin mutation carriers: a gene expression analysis study. Neurobiol Aging. 2013;34(7):1837-45.
75. Premi E, Cauda F, Gasparotti R, Diano M, Archetti S, Padovani A, et al. Multimodal FMRI resting-state functional connectivity in granulin mutations: the case of fronto-parietal dementia. PLoS One. 2014;9(9):e106500.
76. Borroni B, Alberici A, Cercignani M, Premi E, Serra L, Cerini C, et al. Granulin mutation drives brain damage and reorganization from preclinical to symptomatic FTLD. Neurobiol Aging. 2012;33(10):2506-20.
77. Pietroboni AM, Fumagalli GG, Ghezzi L, Fenoglio C, Cortini F, Serpente M, et al. Phenotypic heterogeneity of the GRN Asp22fs mutation in a large Italian kindred. Journal of Alzheimer's disease : JAD. 2011;24(2):253-9.
78. Borroni B, Alberici A, Premi E, Archetti S, Garibotto V, Agosti C, et al. Brain magnetic resonance imaging structural changes in a pedigree of asymptomatic progranulin mutation carriers. Rejuvenation research. 2008;11(3):585-95.
79. Wu L, Liu J, Feng X, Dong J, Qin W, Liu Y, et al. 11C-CFT-PET in Presymptomatic FTDP-17: A Potential Biomarker Predicting Onset. Journal of Alzheimer's disease : JAD. 2018;61(2):613-8.
80. Domínguez-Vivero C, Wu L, Lee S, Manoochehri M, Cines S, Brickman AM, et al. Structural Brain Changes in Pre-Clinical FTD MAPT Mutation Carriers. Journal of Alzheimer's disease : JAD. 2020;75(2):595-606.
81. Dopper EG, Chalos V, Ghariq E, den Heijer T, Hafkemeijer A, Jiskoot LC, et al. Cerebral blood flow in presymptomatic MAPT and GRN mutation carriers: A longitudinal arterial spin labeling study. Neuroimage Clin. 2016;12:460-5.
82. Chen Q, Boeve BF, Senjem M, Tosakulwong N, Lesnick TG, Brushaber D, et al. Rates of lobar atrophy in asymptomatic MAPT mutation carriers. Alzheimer's & dementia (New York, N Y). 2019;5:338-46.
83. Eskildsen SF, Østergaard LR, Rodell AB, Østergaard L, Nielsen JE, Isaacs AM, et al. Cortical volumes and atrophy rates in FTD-3 CHMP2B mutation carriers and related non-carriers. Neuroimage. 2009;45(3):713-21.
84. Rohrer JD, Ahsan RL, Isaacs AM, Nielsen JE, Ostergaard L, Scahill R, et al. Presymptomatic generalized brain atrophy in frontotemporal dementia caused by CHMP2B mutation. Dementia and geriatric cognitive disorders. 2009;27(2):182-6.
85. Lunau L, Mouridsen K, Rodell A, Ostergaard L, Nielsen JE, Isaacs A, et al. Presymptomatic cerebral blood flow changes in CHMP2B mutation carriers of familial frontotemporal dementia (FTD-3), measured with MRI. BMJ open. 2012;2(2):e000368.

86. Wijeratne PA, Johnson EB, Eshaghi A, Aksman L, Gregory S, Johnson HJ, et al. Robust Markers and Sample Sizes for Multicenter Trials of Huntington Disease. Ann Neurol. 2020;87(5):751-62.
87. Wilkes FA, Abaryan Z, Ching CRK, Gutman BA, Madsen SK, Walterfang M, et al. Striatal morphology and neurocognitive dysfunction in Huntington disease: The IMAGE-HD study. Psychiatry research Neuroimaging. 2019;291:1-8.
88. Tang X, Ross CA, Johnson H, Paulsen JS, Younes L, Albin RL, et al. Regional subcortical shape analysis in premanifest Huntington's disease. Hum Brain Mapp. 2019;40(5):1419-33.
89. McColgan P, Gregory S, Seunarine KK, Razi A, Papoutsi M, Johnson E, et al. Brain Regions Showing White Matter Loss in Huntington's Disease Are Enriched for Synaptic and Metabolic Genes. Biol Psychiatry. 2018;83(5):456-65.
90. Castro E, Polosecki P, Rish I, Pustina D, Warner JH, Wood A, et al. Baseline multimodal information predicts future motor impairment in premanifest Huntington's disease. Neuroimage Clin. 2018;19:443-53.
91. McColgan P, Gregory S, Razi A, Seunarine KK, Gargouri F, Durr A, et al. White matter predicts functional connectivity in premanifest Huntington's disease. Ann Clin Transl Neurol. 2017;4(2):106-18.
92. Ahveninen LM, Stout JC, Georgiou-Karistianis N, Lorenzetti V, Glikmann-Johnston Y. Reduced amygdala volumes are related to motor and cognitive signs in Huntington's disease: The IMAGE-HD study. Neuroimage Clin. 2018;18:881-7.
93. Rosas HD, Wilkens P, Salat DH, Mercaldo ND, Vangel M, Yendiki AY, et al. Complex spatial and temporally defined myelin and axonal degeneration in Huntington disease. Neuroimage Clin. 2018;20:236-42.
94. Lahr J, Minkova L, Tabrizi SJ, Stout JC, Kloppel S, Scheller E. Working Memory-Related Effective Connectivity in Huntington's Disease Patients. Front Neurol. 2018;9:370.
95. Gordon BA, Blazey TM, Christensen J, Dincer A, Flores S, Keefe S, et al. Tau PET in autosomal dominant Alzheimer's disease: relationship with cognition, dementia and other biomarkers. Brain. 2019;142(4):1063-76.
96. Preische O, Schultz SA, Apel A, Kuhle J, Kaeser SA, Barro C, et al. Serum neurofilament dynamics predicts neurodegeneration and clinical progression in presymptomatic Alzheimer's disease. Nature medicine. 2019;25(2):277-83.
97. Gordon BA, Blazey TM, Su Y, Hari-Raj A, Dincer A, Flores S, et al. Spatial patterns of neuroimaging biomarker change in individuals from families with autosomal dominant Alzheimer's disease: a longitudinal study. The Lancet Neurology. 2018;17(3):241-50.
98. Kinnunen KM, Cash DM, Poole T, Frost C, Benzinger TLS, Ahsan RL, et al. Presymptomatic atrophy in autosomal dominant Alzheimer's disease: A serial magnetic resonance imaging study. Alzheimer's & dementia : the journal of the Alzheimer's Association. 2018;14(1):43-53.
99. Lee S, Zimmerman ME, Narkhede A, Nasrabady SE, Tosto G, Meier IB, et al. White matter hyperintensities and the mediating role of cerebral amyloid angiopathy in dominantly-inherited Alzheimer's disease. PLoS One. 2018;13(5):e0195838.
100. Sala-Llonch R, Falgàs N, Bosch B, Fernández-Villullas G, Balasa M, Antonell A, et al. Regional patterns of 18F-florbetaben uptake in presenilin 1 mutation carriers. Neurobiol Aging. 2019;81:1-8.
101. Ryan NS, Keihaninejad S, Shakespeare TJ, Lehmann M, Crutch SJ, Malone IB, et al. Magnetic resonance imaging evidence for presymptomatic change in thalamus and caudate in familial Alzheimer's disease. Brain. 2013;136(Pt 5):1399-414.
102. Dean DC, 3rd, Hurley SA, Kecskemeti SR, O'Grady JP, Canda C, Davenport-Sis NJ, et al. Association of Amyloid Pathology With Myelin Alteration in Preclinical Alzheimer Disease. JAMA Neurol. 2017;74(1):41-9.

103. Donix M, Burggren AC, Suthana NA, Siddarth P, Ekstrom AD, Krupa AK, et al. Family history of Alzheimer's disease and hippocampal structure in healthy people. The American journal of psychiatry. 2010;167(11):1399-406.
104. Verfaillie SCJ, Pichet Binette A, Vachon-Presseau E, Tabrizi S, Savard M, Bellec P, et al. Subjective Cognitive Decline Is Associated With Altered Default Mode Network Connectivity in Individuals With a Family History of Alzheimer's Disease. Biological psychiatry Cognitive neuroscience and neuroimaging. 2018;3(5):463-72.
105. Liu SY, Wile DJ, Fu JF, Valerio J, Shahinfard E, McCormick S, et al. The effect of LRRK2 mutations on the cholinergic system in manifest and premanifest stages of Parkinson's disease: a cross-sectional PET study. The Lancet Neurology. 2018;17(4):309-16.
106. Vilas D, Segura B, Baggio HC, Pont-Sunyer C, Compta Y, Valldeoriola F, et al. Nigral and striatal connectivity alterations in asymptomatic LRRK2 mutation carriers: A magnetic resonance imaging study. Mov Disord. 2016;31(12):1820-8.
107. Helmich RC, Thaler A, van Nuenen BF, Gurevich T, Mirelman A, Marder KS, et al. Reorganization of corticostriatal circuits in healthy G2019S LRRK2 carriers. Neurology. 2015;84(4):399-406.
108. Pyatigorskaya N, Sharman M, Corvol JC, Valabregue R, Yahia-Cherif L, Poupon F, et al. High nigral iron deposition in LRRK2 and Parkin mutation carriers using R2* relaxometry. Mov Disord. 2015;30(8):1077-84.
109. Thaler A, Artzi M, Mirelman A, Jacob Y, Helmich RC, van Nuenen BF, et al. A voxel-based morphometry and diffusion tensor imaging analysis of asymptomatic Parkinson's disease-related G2019S LRRK2 mutation carriers. Mov Disord. 2014;29(6):823-7.
110. Thaler A, Mirelman A, Helmich RC, van Nuenen BF, Rosenberg-Katz K, Gurevich T, et al. Neural correlates of executive functions in healthy G2019S LRRK2 mutation carriers. Cortex. 2013;49(9):2501-11.
111. Brockmann K, Gröger A, Di Santo A, Liepelt I, Schulte C, Klose U, et al. Clinical and brain imaging characteristics in leucine-rich repeat kinase 2-associated PD and asymptomatic mutation carriers. Mov Disord. 2011;26(13):2335-42.
112. Reetz K, Tadic V, Kasten M, Brüggemann N, Schmidt A, Hagenah J, et al. Structural imaging in the presymptomatic stage of genetically determined parkinsonism. Neurobiol Dis. 2010;39(3):402-8.
113. Anders S, Sack B, Pohl A, Münte T, Pramstaller P, Klein C, et al. Compensatory premotor activity during affective face processing in subclinical carriers of a single mutant Parkin allele. Brain. 2012;135(Pt 4):1128-40.
114. Buhmann C, Binkofski F, Klein C, Büchel C, van Eimeren T, Erdmann C, et al. Motor reorganization in asymptomatic carriers of a single mutant Parkin allele: a human model for presymptomatic parkinsonism. Brain. 2005;128(Pt 10):2281-90.
115. Szamosi A, Nagy H, Kéri S. Delay discounting of reward and caudate nucleus volume in individuals with α-synuclein gene duplication before and after the development of Parkinson's disease. Neurodegener Dis. 2013;11(2):72-8.
116. Finegan E, Chipika RH, Li Hi Shing S, Doherty MA, Hengeveld JC, Vajda A, et al. The clinical and radiological profile of primary lateral sclerosis: a population-based study. Journal of neurology. 2019;266(11):2718-33.
117. Finegan E, Li Hi Shing S, Siah WF, Chipika RH, Chang KM, McKenna MC, et al. Evolving diagnostic criteria in primary lateral sclerosis: The clinical and radiological basis of “probable PLS”. Journal of the Neurological Sciences. 2020;417:117052.
118. Clark MG, Smallwood Shoukry R, Huang CJ, Danielian LE, Bageac D, Floeter MK. Loss of functional connectivity is an early imaging marker in primary lateral sclerosis. Amyotrophic lateral sclerosis & frontotemporal degeneration. 2018;19(7-8):562-9.
119. Schuster C, Elamin M, Hardiman O, Bede P. Presymptomatic and longitudinal neuroimaging in neurodegeneration--from snapshots to motion picture: a systematic review. J Neurol Neurosurg Psychiatry. 2015;86(10):1089-96.

120. El Mendili MM, Querin G, Bede P, Pradat PF. Spinal Cord Imaging in Amyotrophic Lateral Sclerosis: Historical Concepts-Novel Techniques. Front Neurol. 2019;10:350.
121. Querin G, El Mendili MM, Bede P, Delphine S, Lenglet T, Marchand-Pauvert V, et al. Multimodal spinal cord MRI offers accurate diagnostic classification in ALS. Journal of neurology, neurosurgery, and psychiatry. 2018;89(11):1220-1.
122. Schuster C, Hardiman O, Bede P. Development of an Automated MRI-Based Diagnostic Protocol for Amyotrophic Lateral Sclerosis Using Disease-Specific Pathognomonic Features: A Quantitative Disease-State Classification Study. PLoS One. 2016;11(12):e0167331.
123. Bede P, Iyer PM, Finegan E, Omer T, Hardiman O. Virtual brain biopsies in amyotrophic lateral sclerosis: Diagnostic classification based on in vivo pathological patterns. NeuroImage Clinical. 2017;15:653-8.
124. Chipika RH, Finegan E, Li Hi Shing S, Hardiman O, Bede P. Tracking a Fast-Moving Disease: Longitudinal Markers, Monitoring, and Clinical Trial Endpoints in ALS. Frontiers in neurology. 2019;10:229.
125. Smith MC. Nerve fibre degeneration in the brain in amiotrophyc lateral sclerosis. Journal of neurology, neurosurgery, and psychiatry. 1960;23(4):269-82.
126. Metwalli NS, Benatar M, Nair G, Usher S, Hu X, Carew JD. Utility of axial and radial diffusivity from diffusion tensor MRI as markers of neurodegeneration in amyotrophic lateral sclerosis. Brain research. 2010;1348:156-64.
127. Filippini N, Douaud G, Mackay CE, Knight S, Talbot K, Turner MR. Corpus callosum involvement is a consistent feature of amyotrophic lateral sclerosis. Neurology. 2010;75(18):1645-52.
128. Bede P, Elamin M, Byrne S, McLaughlin RL, Kenna K, Vajda A, et al. Patterns of cerebral and cerebellar white matter degeneration in ALS. J Neurol Neurosurg Psychiatry. 2015;86(4):468-70.
129. Bede P, Hardiman O. Lessons of ALS imaging: Pitfalls and future directions - A critical review. NeuroImage Clinical. 2014;4:436-43.
130. Chapman MC, Jelsone-Swain L, Fling BW, Johnson TD, Gruis K, Welsh RC. Corpus callosum area in amyotrophic lateral sclerosis. Amyotrophic lateral sclerosis : official publication of the World Federation of Neurology Research Group on Motor Neuron Diseases. 2012;13(6):589-91.
131. Schuster C, Elamin M, Hardiman O, Bede P. The segmental diffusivity profile of amyotrophic lateral sclerosis associated white matter degeneration. Eur J Neurol. 2016;23(8):1361-71.
132. Floeter MK, Danielian LE, Braun LE, Wu T. Longitudinal diffusion imaging across the C9orf72 clinical spectrum. J Neurol Neurosurg Psychiatry. 2018;89(1):53-60.
133. Cardenas AM, Sarlls JE, Kwan JY, Bageac D, Gala ZS, Danielian LE, et al. Pathology of callosal damage in ALS: An ex-vivo, 7 T diffusion tensor MRI study. NeuroImage Clinical. 2017;15:200-8.
134. Meoded A, Kwan JY, Peters TL, Huey ED, Danielian LE, Wiggs E, et al. Imaging Findings Associated with Cognitive Performance in Primary Lateral Sclerosis and Amyotrophic Lateral Sclerosis. Dementia and geriatric cognitive disorders extra. 2013;3(1):233-50.
135. Chapman MC, Jelsone-Swain L, Johnson TD, Gruis KL, Welsh RC. Diffusion tensor MRI of the corpus callosum in amyotrophic lateral sclerosis. J Magn Reson Imaging. 2013.
136. Agosta F, Pagani E, Rocca MA, Caputo D, Perini M, Salvi F, et al. Voxel-based morphometry study of brain volumetry and diffusivity in amyotrophic lateral sclerosis patients with mild disability. Hum Brain Mapp. 2007;28(12):1430-8.
137. Omer T, Finegan E, Hutchinson S, Doherty M, Vajda A, McLaughlin RL, et al. Neuroimaging patterns along the ALS-FTD spectrum: a multiparametric imaging study. Amyotrophic lateral sclerosis & frontotemporal degeneration. 2017:1-13.
138. Bede P, Bokde AL, Byrne S, Elamin M, McLaughlin RL, Kenna K, et al. Multiparametric MRI study of ALS stratified for the C9orf72 genotype. Neurology. 2013;81(4):361-9.

139. Yamauchi H, Fukuyama H, Ouchi Y, Nagahama Y, Kimura J, Asato R, et al. Corpus callosum atrophy in amyotrophic lateral sclerosis. J Neurol Sci. 1995;134(1-2):189-96.
140. Kassubek J, Unrath A, Huppertz HJ, Lule D, Ethofer T, Sperfeld AD, et al. Global brain atrophy and corticospinal tract alterations in ALS, as investigated by voxel-based morphometry of 3-D MRI. Amyotroph Lateral Sc. 2005;6(4):213-20.
141. Zhang J, Ji B, Hu J, Zhou C, Li L, Li Z, et al. Aberrant interhemispheric homotopic functional and structural connectivity in amyotrophic lateral sclerosis. J Neurol Neurosurg Psychiatry. 2017;88(5):369-70.
142. Wittstock M, Wolters A, Benecke R. Transcallosal inhibition in amyotrophic lateral sclerosis. Clin Neurophysiol. 2007;118(2):301-7.
143. Bede P. The histological correlates of imaging metrics: postmortem validation of in vivo findings. Amyotrophic lateral sclerosis & frontotemporal degeneration. 2019:1-4.
144. Broad RJ, Gabel MC, Dowell NG, Schwartzman DJ, Seth AK, Zhang H, et al. Neurite orientation and dispersion density imaging (NODDI) detects cortical and corticospinal tract degeneration in ALS. Journal of neurology, neurosurgery, and psychiatry. 2018.
145. Barritt AW, Gabel MC, Cercignani M, Leigh PN. Emerging Magnetic Resonance Imaging Techniques and Analysis Methods in Amyotrophic Lateral Sclerosis. Front Neurol. 2018;9:1065.
146. Bede P, Querin G, Pradat PF. The changing landscape of motor neuron disease imaging: the transition from descriptive studies to precision clinical tools. Curr Opin Neurol. 2018;31(4):431-8.
147. Querin G, El Mendili MM, Bede P, Delphine S, Lenglet T, Marchand-Pauvert V, et al. Multimodal spinal cord MRI offers accurate diagnostic classification in ALS. Journal of neurology, neurosurgery, and psychiatry. 2018.
148. Schuster C, Hardiman O, Bede P. Survival prediction in Amyotrophic lateral sclerosis based on MRI measures and clinical characteristics. BMC Neurol. 2017;17(1):73.
149. Grollemund V, Pradat PF, Querin G, Delbot F, Le Chat G, Pradat-Peyre JF, et al. Machine Learning in Amyotrophic Lateral Sclerosis: Achievements, Pitfalls, and Future Directions. Frontiers in neuroscience. 2019;13:135.
150. Menke RA, Korner S, Filippini N, Douaud G, Knight S, Talbot K, et al. Widespread grey matter pathology dominates the longitudinal cerebral MRI and clinical landscape of amyotrophic lateral sclerosis. Brain : a journal of neurology. 2014;137(Pt 9):2546-55.
151. Bede P, Hardiman O. Longitudinal structural changes in ALS: a three time-point imaging study of white and gray matter degeneration. Amyotrophic lateral sclerosis & frontotemporal degeneration. 2018;19(3-4):232-41.
152. Fortanier E, Grapperon AM, Le Troter A, Verschueren A, Ridley B, Guye M, et al. Structural Connectivity Alterations in Amyotrophic Lateral Sclerosis: A Graph Theory Based Imaging Study. Frontiers in neuroscience. 2019;13:1044.
153. Bede P. Deciphering neurodegeneration: A paradigm shift from focality to connectivity. Neurology. 2017.
154. Bede P, Omer T, Finegan E, Chipika RH, Iyer PM, Doherty MA, et al. Connectivity-based characterisation of subcortical grey matter pathology in frontotemporal dementia and ALS: a multimodal neuroimaging study. Brain Imaging Behav. 2018;12(6):1696-707.
155. Nasseroleslami B, Dukic S, Broderick M, Mohr K, Schuster C, Gavin B, et al. Characteristic Increases in EEG Connectivity Correlate With Changes of Structural MRI in Amyotrophic Lateral Sclerosis. Cereb Cortex. 2017:1-15.
156. Menke RAL, Proudfoot M, Talbot K, Turner MR. The two-year progression of structural and functional cerebral MRI in amyotrophic lateral sclerosis. NeuroImage: Clinical. 2018;17:953-61.
157. Wittstock M, Meister S, Walter U, Benecke R, Wolters A. Mirror movements in amyotrophic lateral sclerosis. Amyotrophic lateral sclerosis : official publication of the World Federation of Neurology Research Group on Motor Neuron Diseases. 2011;12(6):393-7.

158. Di Paola M, Di Iulio F, Cherubini A, Blundo C, Casini AR, Sancesario G, et al. When, where, and how the corpus callosum changes in MCI and AD: a multimodal MRI study. Neurology. 2010;74(14):1136-42.
159. Qiu Y, Liu S, Hilal S, Loke YM, Ikram MK, Xu X, et al. Inter-hemispheric functional dysconnectivity mediates the association of corpus callosum degeneration with memory impairment in AD and amnestic MCI. Scientific reports. 2016;6:32573.
160. Goldman JG, Bledsoe IO, Merkitch D, Dinh V, Bernard B, Stebbins GT. Corpus callosal atrophy and associations with cognitive impairment in Parkinson disease. Neurology. 2017;88(13):1265-72.
161. Elahi FM, Marx G, Cobigo Y, Staffaroni AM, Kornak J, Tosun D, et al. Longitudinal white matter change in frontotemporal dementia subtypes and sporadic late onset Alzheimer's disease. NeuroImage Clinical. 2017;16:595-603.
162. Unrath A, Muller HP, Riecker A, Ludolph AC, Sperfeld AD, Kassubek J. Whole brain-based analysis of regional white matter tract alterations in rare motor neuron diseases by diffusion tensor imaging. Hum Brain Mapp. 2010;31(11):1727-40.
163. Prendergast DM, Ardekani B, Ikuta T, John M, Peters B, DeRosse P, et al. Age and sex effects on corpus callosum morphology across the lifespan. Hum Brain Mapp. 2015;36(7):2691-702.
164. Bede P, Elamin M, Byrne S, Hardiman O. Sexual dimorphism in ALS: exploring gender-specific neuroimaging signatures. Amyotrophic lateral sclerosis & frontotemporal degeneration. 2014;15(3-4):235-43.
165. Sábado J, Casanovas A, Tarabal O, Hereu M, Piedrafita L, Calderó J, et al. Accumulation of misfolded SOD1 in dorsal root ganglion degenerating proprioceptive sensory neurons of transgenic mice with amyotrophic lateral sclerosis. BioMed research international. 2014;2014:852163.
166. Tao QQ, Wei Q, Wu ZY. Sensory nerve disturbance in amyotrophic lateral sclerosis. Life sciences. 2018;203:242-5.
167. Sassone J, Taiana M, Lombardi R, Porretta-Serapiglia C, Freschi M, Bonanno S, et al. ALS mouse model SOD1G93A displays early pathology of sensory small fibers associated to accumulation of a neurotoxic splice variant of peripherin. Hum Mol Genet. 2016;25(8):1588-99.
168. Swinnen B, Robberecht W. The phenotypic variability of amyotrophic lateral sclerosis. Nature reviews Neurology. 2014;10(11):661-70.
169. Hammad M, Silva A, Glass J, Sladky JT, Benatar M. Clinical, electrophysiologic, and pathologic evidence for sensory abnormalities in ALS. Neurology. 2007;69(24):2236-42.
170. Gubbay SS, Kahana E, Zilber N, Cooper G, Pintov S, Leibowitz Y. Amyotrophic lateral sclerosis. A study of its presentation and prognosis. J Neurol. 1985;232(5):295-300.
171. Isaacs JD, Dean AF, Shaw CE, Al-Chalabi A, Mills KR, Leigh PN. Amyotrophic lateral sclerosis with sensory neuropathy: part of a multisystem disorder? J Neurol Neurosurg Psychiatry. 2007;78(7):750-3.
172. Gregory R, Mills K, Donaghy M. Progressive sensory nerve dysfunction in amyotrophic lateral sclerosis: a prospective clinical and neurophysiological study. J Neurol. 1993;240(5):309-14.
173. Radtke RA, Erwin A, Erwin CW. Abnormal sensory evoked potentials in amyotrophic lateral sclerosis. Neurology. 1986;36(6):796-801.
174. Iglesias C, Sangari S, El Mendili MM, Benali H, Marchand-Pauvert V, Pradat PF. Electrophysiological and spinal imaging evidences for sensory dysfunction in amyotrophic lateral sclerosis. BMJ open. 2015;5(2):e007659.
175. Pugdahl K, Fuglsang-Frederiksen A, de Carvalho M, Johnsen B, Fawcett PR, Labarre-Vila A, et al. Generalised sensory system abnormalities in amyotrophic lateral sclerosis: a European multicentre study. J Neurol Neurosurg Psychiatry. 2007;78(7):746-9.

176. Pugdahl K, Fuglsang-Frederiksen A, Johnsen B, de Carvalho M, Fawcett PR, Labarre-Vila A, et al. A prospective multicentre study on sural nerve action potentials in ALS. Clinical neurophysiology : official journal of the International Federation of Clinical Neurophysiology. 2008;119(5):1106-10.
177. Zhou C, Hu X, Hu J, Liang M, Yin X, Chen L, et al. Altered Brain Network in Amyotrophic Lateral Sclerosis: A Resting Graph Theory-Based Network Study at Voxel-Wise Level. Front Neurosci. 2016;10:204.
178. Devine MS, Pannek K, Coulthard A, McCombe PA, Rose SE, Henderson RD. Exposing asymmetric gray matter vulnerability in amyotrophic lateral sclerosis. Neuroimage Clin. 2015;7:782-7.
179. Dalla Bella E, Lombardi R, Porretta-Serapiglia C, Ciano C, Gellera C, Pensato V, et al. Amyotrophic lateral sclerosis causes small fiber pathology. Eur J Neurol. 2016;23(2):416-20.
180. Isak B, Pugdahl K, Karlsson P, Tankisi H, Finnerup NB, Furtula J, et al. Quantitative sensory testing and structural assessment of sensory nerve fibres in amyotrophic lateral sclerosis. J Neurol Sci. 2017;373:329-34.
181. Nolano M, Provitera V, Manganelli F, Iodice R, Caporaso G, Stancanelli A, et al. Non-motor involvement in amyotrophic lateral sclerosis: new insight from nerve and vessel analysis in skin biopsy. Neuropathol Appl Neurobiol. 2017;43(2):119-32.
182. Weis J, Katona I, Müller-Newen G, Sommer C, Necula G, Hendrich C, et al. Small-fiber neuropathy in patients with ALS. Neurology. 2011;76(23):2024-9.
183. Moisset X, Cornut-Chauvinc C, Clavelou P, Pereira B, Dallel R, Guy N. Is there pain with neuropathic characteristics in patients with amyotrophic lateral sclerosis? A cross-sectional study. Palliative medicine. 2016;30(5):486-94.
184. Camu W, Khoris J, Moulard B, Salachas F, Briolotti V, Rouleau GA, et al. Genetics of familial ALS and consequences for diagnosis. French ALS Research Group. J Neurol Sci. 1999;165 Suppl 1:S21-6.
185. Dyck PJ, Stevens JC, Mulder DW, Espinosa RE. Frequency of nerve fiber degeneration of peripheral motor and sensory neurons in amyotrophic lateral sclerosis. Morphometry of deep and superficial peroneal nerves. Neurology. 1975;25(8):781-5.
186. Khoris J, Moulard B, Briolotti V, Hayer M, Durieux A, Clavelou P, et al. Coexistence of dominant and recessive familial amyotrophic lateral sclerosis with the D90A Cu,Zn superoxide dismutase mutation within the same country. Eur J Neurol. 2000;7(2):207-11.
187. Elian M. Olfactory impairment in motor neuron disease: a pilot study. J Neurol Neurosurg Psychiatry. 1991;54(10):927-8.
188. Hawkes CH, Shephard BC, Geddes JF, Body GD, Martin JE. Olfactory disorder in motor neuron disease. Exp Neurol. 1998;150(2):248-53.
189. Gunther R, Schrempf W, Hahner A, Hummel T, Wolz M, Storch A, et al. Impairment in Respiratory Function Contributes to Olfactory Impairment in Amyotrophic Lateral Sclerosis. Front Neurol. 2018;9:79.
190. Gunther R, Richter N, Sauerbier A, Chaudhuri KR, Martinez-Martin P, Storch A, et al. Non-Motor Symptoms in Patients Suffering from Motor Neuron Diseases. Front Neurol. 2016;7:117.
191. Tarlarini C, Greco LC, Lizio A, Gerardi F, Sansone VA, Lunetta C. Taste changes in amyotrophic lateral sclerosis and effects on quality of life. Neurological sciences : official journal of the Italian Neurological Society and of the Italian Society of Clinical Neurophysiology. 2019;40(2):399-404.
192. Simmatis L, Atallah G, Scott SH, Taylor S. The feasibility of using robotic technology to quantify sensory, motor, and cognitive impairments associated with ALS. Amyotrophic lateral sclerosis & frontotemporal degeneration. 2019;20(1-2):43-52.
193. Tabor-Gray L, Vasilopoulos T, Wheeler-Hegland K, Wymer J, Plowman EK. Reflexive Airway Sensorimotor Responses in Individuals with Amyotrophic Lateral Sclerosis. Dysphagia. 2021;36(4):574-82.

194. Ruoppolo G, Onesti E, Gori MC, Schettino I, Frasca V, Biasiotta A, et al. Laryngeal Sensitivity in Patients with Amyotrophic Lateral Sclerosis. Front Neurol. 2016;7:212.
195. Amin MR, Harris D, Cassel SG, Grimes E, Heiman-Patterson T. Sensory testing in the assessment of laryngeal sensation in patients with amyotrophic lateral sclerosis. The Annals of otology, rhinology, and laryngology. 2006;115(7):528-34.
196. Santos-Bento M, de Carvalho M, Evangelista T, Sales Luís ML. Sympathetic sudomotor function and amyotrophic lateral sclerosis. Amyotrophic lateral sclerosis and other motor neuron disorders : official publication of the World Federation of Neurology, Research Group on Motor Neuron Diseases. 2001;2(2):105-8.
197. Deepika J, Manvir B, Sumit S, Vinay G, Trilochan S, Garima S, et al. Quantitative thermal sensory testing in patients with amyotrophic lateral sclerosis using reaction time exclusive method of levels (MLE). Electromyography and clinical neurophysiology. 2006;46(3):145-8.
198. Xu YS, Zhang J, Zheng JY, Zhang S, Kang DX, Fan DS. Fully intact contact heat evoked potentials in patients with amyotrophic lateral sclerosis. Muscle & nerve. 2009;39(6):735-8.
199. Argyriou AA, Polychronopoulos P, Talelli P, Chroni E. F wave study in amyotrophic lateral sclerosis: assessment of balance between upper and lower motor neuron involvement. Clinical neurophysiology : official journal of the International Federation of Clinical Neurophysiology. 2006;117(6):1260-5.
200. Pouget J. [Electroneuromyographic criteria of amyotrophic lateral sclerosis]. Revue neurologique. 2006;162 Spec No 2:4s34-4s42.
201. Underwood CK, Kurniawan ND, Butler TJ, Cowin GJ, Wallace RH. Non-invasive diffusion tensor imaging detects white matter degeneration in the spinal cord of a mouse model of amyotrophic lateral sclerosis. Neuroimage. 2011;55(2):455-61.
202. Rabin BA, Griffin JW, Crain BJ, Scavina M, Chance PF, Cornblath DR. Autosomal dominant juvenile amyotrophic lateral sclerosis. Brain. 1999;122 (Pt 8):1539-50.
203. Agosta F, Canu E, Inuggi A, Chio A, Riva N, Silani V, et al. Resting state functional connectivity alterations in primary lateral sclerosis. Neurobiol Aging. 2014;35(4):916-25.
204. Anagnostou E, Zachou A, Breza M, Kladi A, Karadima G, Koutsis G. Disentangling balance impairments in spinal and bulbar muscular atrophy. Neurosci Lett. 2019;705:94-8.
205. Yang J, Wang Q, Lin L, Wang D, Zheng H, Guan Y. [Comparison of clinical and physiological characteristics between Kennedy disease and amyotrophic lateral sclerosis]. Nan fang yi ke da xue xue bao = Journal of Southern Medical University. 2014;34(11):1688-92.
206. Li TM, Alberman E, Swash M. Comparison of sporadic and familial disease amongst 580 cases of motor neuron disease. J Neurol Neurosurg Psychiatry. 1988;51(6):778-84.
207. Siniscalchi A. [Tolerability of riluzole: a review of the literature]. La Clinica terapeutica. 2004;155(1):25-8.
208. Wagner ML, Landis BE. Riluzole: a new agent for amyotrophic lateral sclerosis. The Annals of pharmacotherapy. 1997;31(6):738-44.
209. Bryson HM, Fulton B, Benfield P. Riluzole. A review of its pharmacodynamic and pharmacokinetic properties and therapeutic potential in amyotrophic lateral sclerosis. Drugs. 1996;52(4):549-63.
210. Jamal GA, Weir AI, Hansen S, Ballantyne JP. Sensory involvement in motor neuron disease: further evidence from automated thermal threshold determination. J Neurol Neurosurg Psychiatry. 1985;48(9):906-10.
211. Krieg I, Dalin D, Heimbach B, Wiesmeier IK, Maurer C. Abnormal trunk control determines postural abnormalities in Amyotrophic Lateral Sclerosis. NeuroRehabilitation. 2019;44(4):599-608.
212. Radovanovic S, Milicev M, Peric S, Basta I, Kostic V, Stevic Z. Gait in amyotrophic lateral sclerosis: Is gait pattern differently affected in spinal and bulbar onset of the disease during dual task walking? Amyotrophic lateral sclerosis & frontotemporal degeneration. 2014;15(7-8):488-93.

213. Liao F, Wang J, He P. Multi-resolution entropy analysis of gait symmetry in neurological degenerative diseases and amyotrophic lateral sclerosis. Medical engineering & physics. 2008;30(3):299-310.
214. Pradat PF, Bruneteau G, Munerati E, Salachas F, Le Forestier N, Lacomblez L, et al. Extrapyramidal stiffness in patients with amyotrophic lateral sclerosis. Mov Disord. 2009;24(14):2143-8.
215. Sanjak M, Hirsch MA, Bravver EK, Bockenek WL, Norton HJ, Brooks BR. Vestibular deficits leading to disequilibrium and falls in ambulatory amyotrophic lateral sclerosis. Archives of physical medicine and rehabilitation. 2014;95(10):1933-9.
216. Lukomski M, Klimek A. [Electronystagmographic examination in patients with amyotrophic lateral sclerosis (ALS)]. Neurologia i neurochirurgia polska. 1993;27(4):493-8.
217. Pelletier C, Abou-Zeid E, Bartoshuk L, Rudnicki S. Is Taste Altered in Patients with ALS? Chemosensory Perception. 2013;6.
218. Lang CJ, Schwandner K, Hecht M. Do patients with motor neuron disease suffer from disorders of taste or smell? Amyotrophic lateral sclerosis : official publication of the World Federation of Neurology Research Group on Motor Neuron Diseases. 2011;12(5):368-71.
219. Jesus P, Massoulard A, Marin B, Nicol M, Laplagne O, Baptiste A, et al. First assessment at home of amyotrophic lateral sclerosis (ALS) patients by a nutrition network in the French region of Limousin. Amyotrophic lateral sclerosis : official publication of the World Federation of Neurology Research Group on Motor Neuron Diseases. 2012;13(6):538-43.
220. Shimizu T, Kawata A, Kato S, Hayashi M, Takamoto K, Hayashi H, et al. Autonomic failure in ALS with a novel SOD1 gene mutation. Neurology. 2000;54(7):1534-7.
221. Pavlovic S, Stevic Z, Milovanovic B, Milicic B, Rakocevic-Stojanovic V, Lavrnic D, et al. Impairment of cardiac autonomic control in patients with amyotrophic lateral sclerosis. Amyotrophic lateral sclerosis : official publication of the World Federation of Neurology Research Group on Motor Neuron Diseases. 2010;11(3):272-6.
222. Shemisa K, Kaelber D, Parikh SA, Mackall JA. Autonomic etiology of heart block in amyotrophic lateral sclerosis: a case report. Journal of medical case reports. 2014;8:224.
223. Kawata A, Kato S, Hayashi H, Hirai S. Prominent sensory and autonomic disturbances in familial amyotrophic lateral sclerosis with a Gly93Ser mutation in the SOD1 gene. J Neurol Sci. 1997;153(1):82-5.
224. Hineno A, Nakamura A, Shimojima Y, Yoshida K, Oyanagai K, Ikeda S. Distinctive clinicopathological features of 2 large families with amyotrophic lateral sclerosis having L106V mutation in SOD1 gene. J Neurol Sci. 2012;319(1-2):63-74.
225. Marjanović IV, Selak-Djokić B, Perić S, Janković M, Arsenijević V, Basta I, et al. Comparison of the clinical and cognitive features of genetically positive ALS patients from the largest tertiary center in Serbia. J Neurol. 2017;264(6):1091-8.
226. Beck M, Giess R, Magnus T, Puls I, Reiners K, Toyka KV, et al. Progressive sudomotor dysfunction in amyotrophic lateral sclerosis. J Neurol Neurosurg Psychiatry. 2002;73(1):68-70.
227. Dalla Vecchia L, De Maria B, Marinou K, Sideri R, Lucini A, Porta A, et al. Cardiovascular neural regulation is impaired in amyotrophic lateral sclerosis patients. A study by spectral and complexity analysis of cardiovascular oscillations. Physiological measurement. 2015;36(4):659-70.
228. Vucic S. Sensory and autonomic nervous system dysfunction in amyotrophic lateral sclerosis. Neuropathol Appl Neurobiol. 2017;43(2):99-101.
229. Mogyoros I, Kiernan MC, Burke D, Bostock H. Ischemic resistance of cutaneous afferents and motor axons in patients with amyotrophic lateral sclerosis. Muscle & nerve. 1998;21(12):1692-700.
230. Lopes LCG, Galhardoni R, Silva V, Jorge FMH, Yeng LT, Callegaro D, et al. Beyond weakness: Characterization of pain, sensory profile and conditioned pain modulation in patients with motor neuron disease: A controlled study. European journal of pain (London, England). 2018;22(1):72-83.

231. Truini A, Biasiotta A, Onesti E, Di Stefano G, Ceccanti M, La Cesa S, et al. Small-fibre neuropathy related to bulbar and spinal-onset in patients with ALS. J Neurol. 2015;262(4):1014-8.
232. Ferrari G, Grisan E, Scarpa F, Fazio R, Comola M, Quattrini A, et al. Corneal confocal microscopy reveals trigeminal small sensory fiber neuropathy in amyotrophic lateral sclerosis. Frontiers in aging neuroscience. 2014;6:278.
233. Rothstein JD, Martin LJ, Kuncl RW. Decreased glutamate transport by the brain and spinal cord in amyotrophic lateral sclerosis. The New England journal of medicine. 1992;326(22):1464-8.
234. Wirguin I, Brenner T, Argov Z, Steiner I. Multifocal motor nerve conduction abnormalities in amyotrophic lateral sclerosis. J Neurol Sci. 1992;112(1-2):199-203.
235. Ben Hamida M, Hentati F. [Charcot's disease and juvenile amyotrophic lateral sclerosis]. Revue neurologique. 1984;140(3):202-6.
236. Jokelainen M. Amyotrophic lateral sclerosis in Finland. II: Clinical characteristics. Acta neurologica Scandinavica. 1977;56(3):194-204.
237. Alter M, Schaumann B. Hereditary Amyotrophic Lateral Sclerosis. A report of two families. European neurology. 1976;14(4):250-65.
238. Ross MA. Acquired motor neuron disorders. Neurologic clinics. 1997;15(3):481-500.
239. Charles T, Swash M. Amyotrophic lateral sclerosis: current understanding. The Journal of neuroscience nursing : journal of the American Association of Neuroscience Nurses. 2001;33(5):245-53.
240. Akaishi T, Takahashi T, Abe M, Aoki M, Ishii T. Consideration of gravity as a possible etiological factor in amyotrophic lateral sclerosis. Medical hypotheses. 2019;132:109369.
241. van der Graaff MM, de Jong JM, Baas F, de Visser M. Upper motor neuron and extra-motor neuron involvement in amyotrophic lateral sclerosis: a clinical and brain imaging review. Neuromuscular disorders : NMD. 2009;19(1):53-8.
242. Liu J, Zhang X, Ding X, Song M, Sui K. Analysis of clinical and electrophysiological characteristics of 150 patients with amyotrophic lateral sclerosis in China. Neurological sciences : official journal of the Italian Neurological Society and of the Italian Society of Clinical Neurophysiology. 2019;40(2):363-9.
243. Isak B, Tankisi H, Johnsen B, Pugdahl K, Torvin MØLler A, Finnerup NB, et al. Involvement of distal sensory nerves in amyotrophic lateral sclerosis. Muscle & nerve. 2016;54(6):1086-92.
244. Kulkantrakorn K, Suksasunee D. Clinical, electrodiagnostic, and outcome correlation in ALS patients in Thailand. Journal of clinical neuroscience : official journal of the Neurosurgical Society of Australasia. 2017;43:165-9.
245. Ren YT, Cui F, Yang F, Chen ZH, Ling L, Huang XS. [An analysis of characteristics of nerve conduction in 154 cases of amyotrophic lateral sclerosis]. Zhonghua nei ke za zhi. 2016;55(10):755-8.
246. Shefner JM, Tyler HR, Krarup C. Abnormalities in the sensory action potential in patients with amyotrophic lateral sclerosis. Muscle & nerve. 1991;14(12):1242-6.
247. Theys PA, Peeters E, Robberecht W. Evolution of motor and sensory deficits in amyotrophic lateral sclerosis estimated by neurophysiological techniques. J Neurol. 1999;246(6):438-42.
248. Pegat A, Bouhour F, Mouzat K, Vial C, Pegat B, Leblanc P, et al. Electrophysiological Characterization of C9ORF72-Associated Amyotrophic Lateral Sclerosis: A Retrospective Study. European neurology. 2019;82(4-6):106-12.
249. Behnia M, Kelly JJ. Role of electromyography in amyotrophic lateral sclerosis. Muscle & nerve. 1991;14(12):1236-41.
250. Imai E, Nakamura T, Atsuta N, Nakatochi M, Suzuki M, Harada Y, et al. A nerve conduction study predicts the prognosis of sporadic amyotrophic lateral sclerosis. J Neurol. 2020.

251. Dasheiff RM, Drake ME, Brendle A, Erwin CW. Abnormal somatosensory evoked potentials in amyotrophic lateral sclerosis. Electroencephalography and clinical neurophysiology. 1985;60(4):306-11.
252. Sangari S, Giron A, Marrelec G, Pradat PF, Marchand-Pauvert V. Abnormal cortical brain integration of somatosensory afferents in ALS. Clinical neurophysiology : official journal of the International Federation of Clinical Neurophysiology. 2018;129(4):874-84.
253. Shimizu T, Bokuda K, Kimura H, Kamiyama T, Nakayama Y, Kawata A, et al. Sensory cortex hyperexcitability predicts short survival in amyotrophic lateral sclerosis. Neurology. 2018;90(18):e1578-e87.
254. Isak B, Tankisi H, Johnsen B, Pugdahl K, Finnerup NB, Fuglsang-Frederiksen A. Laser and somatosensory evoked potentials in amyotrophic lateral sclerosis. Clinical neurophysiology : official journal of the International Federation of Clinical Neurophysiology. 2016;127(10):3322-8.
255. Subramaniam JS, Yiannikas C. Multimodality evoked potentials in motor neuron disease. Arch Neurol. 1990;47(9):989-94.
256. Georgesco M, Salerno A, Carlander B, Léger JJ, Camu W, Billiard M, et al. [Somatosensory evoked potentials in amyotrophic lateral sclerosis and primary lateral sclerosis]. Revue neurologique. 1994;150(4):292-8.
257. Constantinovici A. Abnormal somatosensory evoked potentials in amyotrophic lateral sclerosis. Romanian journal of neurology and psychiatry = Revue roumaine de neurologie et psychiatrie. 1993;31(3-4):273-8.
258. Swash M. Sensorimotor integration is problematic in amyotrophic lateral sclerosis. Clinical neurophysiology : official journal of the International Federation of Clinical Neurophysiology. 2018;129(4):849-50.
259. Mondelli M, Rossi A, Passero S, Guazzi GC. Involvement of peripheral sensory fibers in amyotrophic lateral sclerosis: electrophysiological study of 64 cases. Muscle & nerve. 1993;16(2):166-72.
260. Koszewicz M, Bilińska M, Podemski R. [Electrophysiological estimation of the peripheral nerves conduction parameters and the autonomic nervous system function in the course of amyotrophic lateral sclerosis]. Neurologia i neurochirurgia polska. 2005;39(5):351-7.
261. de Carvalho M, Swash M. Nerve conduction studies in amyotrophic lateral sclerosis. Muscle & nerve. 2000;23(3):344-52.
262. Berardelli A, Inghilleri M, Formisano R, Accornero N, Manfredi M. Stimulation of motor tracts in motor neuron disease. J Neurol Neurosurg Psychiatry. 1987;50(6):732-7.
263. Harada Y, Nakamura T, Suzuki M, Ueda M, Hirayama M, Katsuno M. Impaired pain processing and its association with attention disturbance in patients with amyotrophic lateral sclerosis. Neurological sciences : official journal of the Italian Neurological Society and of the Italian Society of Clinical Neurophysiology. 2021;42(8):3327-35.
264. Norioka R, Shimizu T, Bokuda K, Morishima R, Kawazoe T, Kimura H, et al. Enlarged high frequency oscillations of the median nerve somatosensory evoked potential and survival in amyotrophic lateral sclerosis. Clinical neurophysiology : official journal of the International Federation of Clinical Neurophysiology. 2021;132(9):2003-11.
265. Nardone R, Golaszewski S, Thomschewski A, Sebastianelli L, Versace V, Brigo F, et al. Disinhibition of sensory cortex in patients with amyotrophic lateral sclerosis. Neurosci Lett. 2020;722:134860.
266. Höffken O, Schmelz A, Lenz M, Gruhn K, Grehl T, Tegenthoff M, et al. Excitability in somatosensory cortex correlates with motoric impairment in amyotrophic lateral sclerosis. Amyotrophic lateral sclerosis & frontotemporal degeneration. 2019;20(3-4):192-8.
267. Matamala JM, Howells J, Dharmadasa T, Huynh W, Park SB, Burke D, et al. Excitability of sensory axons in amyotrophic lateral sclerosis. Clinical neurophysiology : official journal of the International Federation of Clinical Neurophysiology. 2018;129(7):1472-8.

268. Jin X, Jiang JY, Lu FZ, Xia XL, Wang LX, Zheng CJ. Electrophysiological differences between Hirayama disease, amyotrophic lateral sclerosis and cervical spondylotic amyotrophy. BMC musculoskeletal disorders. 2014;15:349.
269. Simone IL, Tortelli R, Samarelli V, D'Errico E, Sardaro M, Difruscolo O, et al. Laser evoked potentials in amyotrophic lateral sclerosis. J Neurol Sci. 2010;288(1-2):106-11.
270. Hamada M, Hanajima R, Terao Y, Sato F, Okano T, Yuasa K, et al. Median nerve somatosensory evoked potentials and their high-frequency oscillations in amyotrophic lateral sclerosis. Clinical neurophysiology : official journal of the International Federation of Clinical Neurophysiology. 2007;118(4):877-86.
271. Ogata K, Tobimatsu S, Furuya H, Kira J. Sporadic amyotrophic lateral sclerosis showing abnormal somatosensory evoked potentials: a report of three cases. Fukuoka igaku zasshi = Hukuoka acta medica. 2001;92(6):242-50.
272. Matsumoto A, Kawashima A, Doi S, Moriwaka F, Tashiro K. [The spinal somatosensory evoked potentials in amyotrophic lateral sclerosis in relation to the spinal cord conduction velocities]. No to shinkei = Brain and nerve. 1999;51(1):41-7.
273. Schulte-Mattler WJ, Jakob M, Zierz S. Focal sensory nerve abnormalities in patients with amyotrophic lateral sclerosis. J Neurol Sci. 1999;162(2):189-93.
274. Emeryk-Szajewska B, Kostera-Pruszczyk A, Rowińska-Marcińska K, Karwańska A. [Median nerve electrophysiological assessment in amyotrophic lateral sclerosis]. Neurologia i neurochirurgia polska. 1998;32(1):39-49.
275. Mogyoros I, Kiernan MC, Burke D, Bostock H. Strength-duration properties of sensory and motor axons in amyotrophic lateral sclerosis. Brain. 1998;121 (Pt 5):851-9.
276. Georgesco M, Salerno A, Camu W. Somatosensory evoked potentials elicited by stimulation of lower-limb nerves in amyotrophic lateral sclerosis. Electroencephalography and clinical neurophysiology. 1997;104(4):333-42.
277. Zanette G, Tinazzi M, Polo A, Rizzuto N. Motor neuron disease with pyramidal tract dysfunction involves the cortical generators of the early somatosensory evoked potential to tibial nerve stimulation. Neurology. 1996;47(4):932-8.
278. Palma V, Guadagnino M, Brescia Morra V, Nolfe G. Multimodality evoked potentials in sporadic amyotrophic lateral sclerosis: a statistical approach. Electromyography and clinical neurophysiology. 1993;33(3):167-71.
279. Gao XX, Tang X. [Relation between the clinical manifestations and electromyographic findings in motor neurone disease]. Zhonghua shen jing jing shen ke za zhi = Chinese journal of neurology and psychiatry. 1991;24(2):98-100, 25.
280. Zanette G, Polo A, Gasperini M, Bertolasi L, De Grandis D. Far-field and cortical somatosensory evoked potentials in motor neuron disease. Muscle & nerve. 1990;13(1):47-55.
281. Facco E, Micaglio G, Liviero MC, Ceccato MB, Toffoletto F, Martinuzzi A, et al. Sensory-motor conduction time in amyotrophic lateral sclerosis. Rivista di neurologia. 1989;59(3):108-12.
282. Cosi V, Poloni M, Mazzini L, Callieco R. Somatosensory evoked potentials in amyotrophic lateral sclerosis. J Neurol Neurosurg Psychiatry. 1984;47(8):857-61.
283. Verde F, Del Tredici K, Braak H, Ludolph A. The multisystem degeneration amyotrophic lateral sclerosis - neuropathological staging and clinical translation. Archives italiennes de biologie. 2017;155(4):118-30.
284. Fatima M, Tan R, Halliday GM, Kril JJ. Spread of pathology in amyotrophic lateral sclerosis: assessment of phosphorylated TDP-43 along axonal pathways. Acta neuropathologica communications. 2015;3:47.
285. Kawamura Y, Dyck PJ, Shimono M, Okazaki H, Tateishi J, Doi H. Morphometric comparison of the vulnerability of peripheral motor and sensory neurons in amyotrophic lateral sclerosis. Journal of neuropathology and experimental neurology. 1981;40(6):667-75.
286. De Reuck J, Devos D, Moreau C, Auger F, Durieux N, Deramecourt V, et al. Topographic distribution of brain iron deposition and small cerebrovascular lesions in amyotrophic lateral

sclerosis and in frontotemporal lobar degeneration: a post-mortem 7.0-tesla magnetic resonance imaging study with neuropathological correlates. Acta neurologica Belgica. 2017;117(4):873-8.
287. Oyanagi K, Mochizuki Y, Nakayama Y, Hayashi K, Shimizu T, Nagao M, et al. Marked preservation of the visual and olfactory pathways in ALS patients in a totally locked-in state. Clinical neuropathology. 2015;34(5):267-74.
288. Devigili G, Uçeyler N, Beck M, Reiners K, Stoll G, Toyka KV, et al. Vasculitis-like neuropathy in amyotrophic lateral sclerosis unresponsive to treatment. Acta neuropathologica. 2011;122(3):343-52.
289. Sawa N, Kataoka H, Sugie K, Kawahara M, Horikawa H, Kusunoki S, et al. Clinical analysis and outcomes of amyotrophic lateral sclerosis with demyelinating polyneuropathy. Amyotrophic lateral sclerosis : official publication of the World Federation of Neurology Research Group on Motor Neuron Diseases. 2012;13(1):125-31.
290. Luigetti M, Conte A, Del Grande A, Bisogni G, Romano A, Sabatelli M. Sural nerve pathology in ALS patients: a single-centre experience. Neurological sciences : official journal of the Italian Neurological Society and of the Italian Society of Clinical Neurophysiology. 2012;33(5):1095-9.
291. Ben Hamida M, Letaief F, Hentati F, Ben Hamida C. Morphometric study of the sensory nerve in classical (or Charcot disease) and juvenile amyotrophic lateral sclerosis. J Neurol Sci. 1987;78(3):313-29.
292. Bradley WG, Good P, Rasool CG, Adelman LS. Morphometric and biochemical studies of peripheral nerves in amyotrophic lateral sclerosis. Ann Neurol. 1983;14(3):267-77.
293. Heads T, Pollock M, Robertson A, Sutherland WH, Allpress S. Sensory nerve pathology in amyotrophic lateral sclerosis. Acta neuropathologica. 1991;82(4):316-20.
294. Vaughan SK, Sutherland NM, Zhang S, Hatzipetros T, Vieira F, Valdez G. The ALS-inducing factors, TDP43(A315T) and SOD1(G93A), directly affect and sensitize sensory neurons to stress. Sci Rep. 2018;8(1):16582.
295. Vaughan SK, Kemp Z, Hatzipetros T, Vieira F, Valdez G. Degeneration of proprioceptive sensory nerve endings in mice harboring amyotrophic lateral sclerosis-causing mutations. The Journal of comparative neurology. 2015;523(17):2477-94.
296. Marcuzzo S, Bonanno S, Figini M, Scotti A, Zucca I, Minati L, et al. A longitudinal DTI and histological study of the spinal cord reveals early pathological alterations in G93A-SOD1 mouse model of amyotrophic lateral sclerosis. Exp Neurol. 2017;293:43-52.
297. Filali M, Lalonde R, Rivest S. Sensorimotor and cognitive functions in a SOD1(G37R) transgenic mouse model of amyotrophic lateral sclerosis. Behav Brain Res. 2011;225(1):215-21.
298. Izquierdo A, Murray EA. Functional interaction of medial mediodorsal thalamic nucleus but not nucleus accumbens with amygdala and orbital prefrontal cortex is essential for adaptive response selection after reinforcer devaluation. J Neurosci. 2010;30(2):661-9.
299. Fischer LR, Culver DG, Davis AA, Tennant P, Wang M, Coleman M, et al. The WldS gene modestly prolongs survival in the SOD1G93A fALS mouse. Neurobiol Dis. 2005;19(1-2):293-300.
300. Guo YS, Wu DX, Wu HR, Wu SY, Yang C, Li B, et al. Sensory involvement in the SOD1-G93A mouse model of amyotrophic lateral sclerosis. Experimental & molecular medicine. 2009;41(3):140-50.
301. Rubio MA, Herrando-Grabulosa M, Vilches JJ, Navarro X. Involvement of sensory innervation in the skin of SOD1(G93A) ALS mice. Journal of the peripheral nervous system : JPNS. 2016;21(2):88-95.
302. Jiang M, Schuster JE, Fu R, Siddique T, Heckman CJ. Progressive changes in synaptic inputs to motoneurons in adult sacral spinal cord of a mouse model of amyotrophic lateral sclerosis. J Neurosci. 2009;29(48):15031-8.

303. Cowin GJ, Butler TJ, Kurniawan ND, Watson C, Wallace RH. Magnetic resonance microimaging of the spinal cord in the SOD1 mouse model of amyotrophic lateral sclerosis detects motor nerve root degeneration. Neuroimage. 2011;58(1):69-74.
304. Bernard-Marissal N, Médard JJ, Azzedine H, Chrast R. Dysfunction in endoplasmic reticulum-mitochondria crosstalk underlies SIGMAR1 loss of function mediated motor neuron degeneration. Brain. 2015;138(Pt 4):875-90.
305. Mehta AR, Gregory JM, Dando O, Carter RN, Burr K, Nanda J, et al. Mitochondrial bioenergetic deficits in C9orf72 amyotrophic lateral sclerosis motor neurons cause dysfunctional axonal homeostasis. Acta neuropathologica. 2021;141(2):257-79.
306. Shankar L, Shankar SK, Santosh V, Taly AB, Nagaraja D, Devi G, et al. Light and ultrastructural pathology of spinal cords in sporadic forms of amyotrophic lateral sclerosis from South Asia. Neurology India. 1995;43(2):83-90.
307. Bączyk M, Alami NO, Delestrée N, Martinot C, Tang L, Commisso B, et al. Synaptic restoration by cAMP/PKA drives activity-dependent neuroprotection to motoneurons in ALS. The Journal of experimental medicine. 2020;217(8).
308. Peng AYT, Agrawal I, Ho WY, Yen YC, Pinter AJ, Liu J, et al. Loss of TDP-43 in astrocytes leads to motor deficits by triggering A1-like reactive phenotype and triglial dysfunction. Proceedings of the National Academy of Sciences of the United States of America. 2020;117(46):29101-12.
309. Ruiz-Soto M, Riancho J, Tapia O, Lafarga M, Berciano MT. Satellite Glial Cells of the Dorsal Root Ganglion: A New "Guest/Physiopathological Target" in ALS. Frontiers in aging neuroscience. 2020;12:595751.
310. Weerasekera A, Crabbé M, Tomé SO, Gsell W, Sima D, Casteels C, et al. Non-invasive characterization of amyotrophic lateral sclerosis in a hTDP-43(A315T) mouse model: A PET-MR study. Neuroimage Clin. 2020;27:102327.
311. Seki S, Yamamoto T, Quinn K, Spigelman I, Pantazis A, Olcese R, et al. Circuit-Specific Early Impairment of Proprioceptive Sensory Neurons in the SOD1(G93A) Mouse Model for ALS. J Neurosci. 2019;39(44):8798-815.
312. Chiò A, Pagani M, Agosta F, Calvo A, Cistaro A, Filippi M. Neuroimaging in amyotrophic lateral sclerosis: insights into structural and functional changes. The Lancet Neurology. 2014;13(12):1228-40.
313. Poujois A, Schneider FC, Faillenot I, Camdessanche JP, Vandenberghe N, Thomas-Anterion C, et al. Brain plasticity in the motor network is correlated with disease progression in amyotrophic lateral sclerosis. Hum Brain Mapp. 2013;34(10):2391-401.
314. Mohammadi B, Kollewe K, Samii A, Dengler R, Munte TF. Functional neuroimaging at different disease stages reveals distinct phases of neuroplastic changes in amyotrophic lateral sclerosis. Hum Brain Mapp. 2011;32(5):750-8.
315. Grosskreutz J, Kaufmann J, Fradrich J, Dengler R, Heinze HJ, Peschel T. Widespread sensorimotor and frontal cortical atrophy in Amyotrophic Lateral Sclerosis. BMC neurology. 2006;6:17.
316. Lule D, Diekmann V, Muller HP, Kassubek J, Ludolph AC, Birbaumer N. Neuroimaging of multimodal sensory stimulation in amyotrophic lateral sclerosis. J Neurol Neurosurg Psychiatry. 2010;81(8):899-906.
317. Zhou F, Xu R, Dowd E, Zang Y, Gong H, Wang Z. Alterations in regional functional coherence within the sensory-motor network in amyotrophic lateral sclerosis. Neurosci Lett. 2014;558:192-6.
318. Rose S, Pannek K, Bell C, Baumann F, Hutchinson N, Coulthard A, et al. Direct evidence of intra- and interhemispheric corticomotor network degeneration in amyotrophic lateral sclerosis: an automated MRI structural connectivity study. Neuroimage. 2012;59(3):2661-9.
319. Luo C, Chen Q, Huang R, Chen X, Chen K, Huang X, et al. Patterns of spontaneous brain activity in amyotrophic lateral sclerosis: a resting-state FMRI study. PLoS One. 2012;7(9):e45470.

320. Cosottini M, Pesaresi I, Piazza S, Diciotti S, Cecchi P, Fabbri S, et al. Structural and functional evaluation of cortical motor areas in Amyotrophic Lateral Sclerosis. Exp Neurol. 2012;234(1):169-80.
321. Tu S, Menke RAL, Talbot K, Kiernan MC, Turner MR. Regional thalamic MRI as a marker of widespread cortical pathology and progressive frontotemporal involvement in amyotrophic lateral sclerosis. J Neurol Neurosurg Psychiatry. 2018;89(12):1250-8.
322. Menke RAL, Proudfoot M, Talbot K, Turner MR. The two-year progression of structural and functional cerebral MRI in amyotrophic lateral sclerosis. NeuroImage Clinical. 2018;17:953-61.
323. Xu J, Li H, Li C, Yao JC, Hu J, Wang J, et al. Abnormal cortical-basal ganglia network in amyotrophic lateral sclerosis: A voxel-wise network efficiency analysis. Behav Brain Res. 2017;333:123-8.
324. Buhour MS, Doidy F, Mondou A, Pelerin A, Carluer L, Eustache F, et al. Voxel-based mapping of grey matter volume and glucose metabolism profiles in amyotrophic lateral sclerosis. EJNMMI research. 2017;7(1):21.
325. Zhang JQ, Ji B, Zhou CY, Li LC, Li ZH, Hu XP, et al. Differential Impairment of Thalamocortical Structural Connectivity in Amyotrophic Lateral Sclerosis. CNS Neurosci Ther. 2017;23(2):155-61.
326. Masuda M, Senda J, Watanabe H, Epifanio B, Tanaka Y, Imai K, et al. Involvement of the caudate nucleus head and its networks in sporadic amyotrophic lateral sclerosis-frontotemporal dementia continuum. Amyotrophic lateral sclerosis & frontotemporal degeneration. 2016;17(7-8):571-9.
327. Machts J, Loewe K, Kaufmann J, Jakubiczka S, Abdulla S, Petri S, et al. Basal ganglia pathology in ALS is associated with neuropsychological deficits. Neurology. 2015;85(15):1301-9.
328. Van Laere K, Vanhee A, Verschueren J, De Coster L, Driesen A, Dupont P, et al. Value of 18fluorodeoxyglucose-positron-emission tomography in amyotrophic lateral sclerosis: a prospective study. JAMA Neurol. 2014;71(5):553-61.
329. Barbagallo G, Nicoletti G, Cherubini A, Trotta M, Tallarico T, Chiriaco C, et al. Diffusion tensor MRI changes in gray structures of the frontal-subcortical circuits in amyotrophic lateral sclerosis. Neurological sciences : official journal of the Italian Neurological Society and of the Italian Society of Clinical Neurophysiology. 2014;35(6):911-8.
330. Sato K, Aoki S, Iwata NK, Abe O, Mori H, Ohtomo K. [Magnetic resonance imaging in patients of amyotrophic lateral sclerosis with and without dementia]. Brain and nerve = Shinkei kenkyu no shinpo. 2009;61(11):1259-68.
331. Li S, Chen Q, Yu B, Xue K, Luo C, Xu Y, et al. Structural and functional changes mapped in the brains of amyotrophic lateral sclerosis patients with/without dysphagia: a pilot study. Amyotrophic lateral sclerosis : official publication of the World Federation of Neurology Research Group on Motor Neuron Diseases. 2009;10(5-6):280-7.
332. Thivard L, Pradat PF, Lehericy S, Lacomblez L, Dormont D, Chiras J, et al. Diffusion tensor imaging and voxel based morphometry study in amyotrophic lateral sclerosis: relationships with motor disability. J Neurol Neurosurg Psychiatry. 2007;78(8):889-92.
333. Turner MR, Cagnin A, Turkheimer FE, Miller CC, Shaw CE, Brooks DJ, et al. Evidence of widespread cerebral microglial activation in amyotrophic lateral sclerosis: an [11C](R)-PK11195 positron emission tomography study. Neurobiol Dis. 2004;15(3):601-9.
334. Sach M, Winkler G, Glauche V, Liepert J, Heimbach B, Koch MA, et al. Diffusion tensor MRI of early upper motor neuron involvement in amyotrophic lateral sclerosis. Brain. 2004;127(Pt 2):340-50.
335. Sharma KR, Sheriff S, Maudsley A, Govind V. Diffusion tensor imaging of basal ganglia and thalamus in amyotrophic lateral sclerosis. Journal of neuroimaging : official journal of the American Society of Neuroimaging. 2013;23(3):368-74.

336. Chang JL, Lomen-Hoerth C, Murphy J, Henry RG, Kramer JH, Miller BL, et al. A voxel-based morphometry study of patterns of brain atrophy in ALS and ALS/FTLD. Neurology. 2005;65(1):75-80.
337. Ahmed RM, Bocchetta M, Todd EG, Tse NY, Devenney EM, Tu S, et al. Tackling clinical heterogeneity across the amyotrophic lateral sclerosis-frontotemporal dementia spectrum using a transdiagnostic approach. Brain communications. 2021;3(4):fcab257.
338. Barry RL, Babu S, Anteraper SA, Triantafyllou C, Keil B, Rowe OE, et al. Ultra-high field (7T) functional magnetic resonance imaging in amyotrophic lateral sclerosis: a pilot study. Neuroimage Clin. 2021;30:102648.
339. Cohen-Adad J, El Mendili MM, Morizot-Koutlidis R, Lehericy S, Meininger V, Blancho S, et al. Involvement of spinal sensory pathway in ALS and specificity of cord atrophy to lower motor neuron degeneration. Amyotrophic lateral sclerosis & frontotemporal degeneration. 2013;14(1):30-8.
340. Rasoanandrianina H, Grapperon AM, Taso M, Girard OM, Duhamel G, Guye M, et al. Region-specific impairment of the cervical spinal cord (SC) in amyotrophic lateral sclerosis: A preliminary study using SC templates and quantitative MRI (diffusion tensor imaging/inhomogeneous magnetization transfer). NMR in biomedicine. 2017;30(12).
341. Rajagopalan V, Pioro EP. Corticospinal Tract and Related Grey Matter Morphometric Shape Analysis in ALS Phenotypes: A Fractal Dimension Study. Brain sciences. 2021;11(3).
342. Kalra S, Tai P, Genge A, Arnold DL. Rapid improvement in cortical neuronal integrity in amyotrophic lateral sclerosis detected by proton magnetic resonance spectroscopic imaging. J Neurol. 2006;253(8):1060-3.
343. Pioro EP, Antel JP, Cashman NR, Arnold DL. Detection of cortical neuron loss in motor neuron disease by proton magnetic resonance spectroscopic imaging in vivo. Neurology. 1994;44(10):1933-8.
344. Chipika RH, Finegan E, Li Hi Shing S, McKenna MC, Christidi F, Chang KM, et al. "Switchboard" malfunction in motor neuron diseases: Selective pathology of thalamic nuclei in amyotrophic lateral sclerosis and primary lateral sclerosis. Neuroimage Clin. 2020;27:102300.
345. Fang X, Zhang Y, Wang Y, Zhang Y, Hu J, Wang J, et al. Disrupted effective connectivity of the sensorimotor network in amyotrophic lateral sclerosis. J Neurol. 2016;263(3):508-16.
346. Sheelakumari R, Madhusoodanan M, Radhakrishnan A, Ranjith G, Thomas B. A Potential Biomarker in Amyotrophic Lateral Sclerosis: Can Assessment of Brain Iron Deposition with SWI and Corticospinal Tract Degeneration with DTI Help? AJNR Am J Neuroradiol. 2016;37(2):252-8.
347. Rajagopalan V, Pioro EP. Differential involvement of corticospinal tract (CST) fibers in UMN-predominant ALS patients with or without CST hyperintensity: A diffusion tensor tractography study. Neuroimage Clin. 2017;14:574-9.
348. Chen JH, Huang NX, Zou TX, Chen HJ. Brain Cortical Complexity Alteration in Amyotrophic Lateral Sclerosis: A Preliminary Fractal Dimensionality Study. BioMed research international. 2020;2020:1521679.
349. Bueno APA, Pinaya WHL, Moura LM, Bertoux M, Radakovic R, Kiernan MC, et al. Structural and functional papez circuit integrity in amyotrophic lateral sclerosis. Brain Imaging Behav. 2018;12(6):1622-30.
350. Chen ZY, Liu MQ, Ma L. Gray Matter Volume Changes over the Whole Brain in the Bulbar- and Spinal-onset Amyotrophic Lateral Sclerosis: a Voxel-based Morphometry Study. Chinese medical sciences journal = Chung-kuo i hsueh k'o hsueh tsa chih. 2018;33(1):20-8.
351. Kim HJ, de Leon M, Wang X, Kim HY, Lee YJ, Kim YH, et al. Relationship between Clinical Parameters and Brain Structure in Sporadic Amyotrophic Lateral Sclerosis Patients According to Onset Type: A Voxel-Based Morphometric Study. PLoS One. 2017;12(1):e0168424.
352. de Albuquerque M, Anjos LG, Maia Tavares de Andrade H, de Oliveira MS, Castellano G, Junqueira Ribeiro de Rezende T, et al. MRI Texture Analysis Reveals Deep Gray Nuclei

Damage in Amyotrophic Lateral Sclerosis. Journal of neuroimaging : official journal of the American Society of Neuroimaging. 2016;26(2):201-6.
353. Irwin DJ, McMillan CT, Brettschneider J, Libon DJ, Powers J, Rascovsky K, et al. Cognitive decline and reduced survival in C9orf72 expansion frontotemporal degeneration and amyotrophic lateral sclerosis. J Neurol Neurosurg Psychiatry. 2013;84(2):163-9.
354. Mioshi E, Lillo P, Yew B, Hsieh S, Savage S, Hodges JR, et al. Cortical atrophy in ALS is critically associated with neuropsychiatric and cognitive changes. Neurology. 2013;80(12):1117-23.
355. Thorns J, Jansma H, Peschel T, Grosskreutz J, Mohammadi B, Dengler R, et al. Extent of cortical involvement in amyotrophic lateral sclerosis--an analysis based on cortical thickness. BMC neurology. 2013;13:148.
356. Mohammadi B, Kollewe K, Samii A, Krampfl K, Dengler R, Munte TF. Decreased brain activation to tongue movements in amyotrophic lateral sclerosis with bulbar involvement but not Kennedy syndrome. J Neurol. 2009;256(8):1263-9.
357. Kato S, Hayashi H, Yagishita A. Involvement of the frontotemporal lobe and limbic system in amyotrophic lateral sclerosis: as assessed by serial computed tomography and magnetic resonance imaging. J Neurol Sci. 1993;116(1):52-8.
358. Trojsi F, Caiazzo G, Corbo D, Piccirillo G, Cristillo V, Femiano C, et al. Microstructural changes across different clinical milestones of disease in amyotrophic lateral sclerosis. PLoS One. 2015;10(3):e0119045.
359. Kim JE, Oh JS, Sung JJ, Lee KW, Song IC, Hong YH. Diffusion tensor tractography analysis of the corpus callosum fibers in amyotrophic lateral sclerosis. Journal of clinical neurology (Seoul, Korea). 2014;10(3):249-56.
360. Agosta F, Valsasina P, Absinta M, Riva N, Sala S, Prelle A, et al. Sensorimotor functional connectivity changes in amyotrophic lateral sclerosis. Cereb Cortex. 2011;21(10):2291-8.
361. Wei J, Lin JH, Cai LM, Shi JY, Zhang XH, Zou ZY, et al. Abnormal Stability of Dynamic Functional Architecture in Amyotrophic Lateral Sclerosis: A Preliminary Resting-State fMRI Study. Front Neurol. 2021;12:744688.
362. Qiu T, Zhang Y, Tang X, Liu X, Wang Y, Zhou C, et al. Precentral degeneration and cerebellar compensation in amyotrophic lateral sclerosis: A multimodal MRI analysis. Hum Brain Mapp. 2019;40(12):3464-74.
363. Pisharady PK, Eberly LE, Cheong I, Manousakis G, Guliani G, Clark HB, et al. Tract-specific analysis improves sensitivity of spinal cord diffusion MRI to cross-sectional and longitudinal changes in amyotrophic lateral sclerosis. Communications biology. 2020;3(1):370.
364. Olney NT, Bischof A, Rosen H, Caverzasi E, Stern WA, Lomen-Hoerth C, et al. Measurement of spinal cord atrophy using phase sensitive inversion recovery (PSIR) imaging in motor neuron disease. PLoS One. 2018;13(11):e0208255.
365. Wang Y, Li X, Chen W, Wang Z, Xu Y, Luo J, et al. Detecting neuronal dysfunction of hand motor cortex in ALS: A MRSI study. Somatosensory & motor research. 2017;34(1):15-20.
366. Wang Y, Liu L, Ma L, Huang X, Lou X, Wang Y, et al. Preliminary study on cervical spinal cord in patients with amyotrophic lateral sclerosis using MR diffusion tensor imaging. Academic radiology. 2014;21(5):590-6.
367. Finegan E, Hi Shing SL, Chipika RH, McKenna MC, Doherty MA, Hengeveld JC, et al. Thalamic, hippocampal and basal ganglia pathology in primary lateral sclerosis and amyotrophic lateral sclerosis: Evidence from quantitative imaging data. Data in brief. 2020;29:105115.
368. Finegan E, Shing SLH, Chipika RH, Chang KM, McKenna MC, Doherty MA, et al. Extra-motor cerebral changes and manifestations in primary lateral sclerosis. Brain Imaging Behav. 2021.
369. Tartaglia MC, Laluz V, Rowe A, Findlater K, Lee DH, Kennedy K, et al. Brain atrophy in primary lateral sclerosis. Neurology. 2009;72(14):1236-41.

370. Butman JA, Floeter MK. Decreased thickness of primary motor cortex in primary lateral sclerosis. AJNR Am J Neuroradiol. 2007;28(1):87-91.
371. Russo LS, Jr. Clinical and electrophysiological studies in primary lateral sclerosis. Arch Neurol. 1982;39(10):662-4.
372. Ni W, Chen S, Qiao K, Wang N, Wu ZY. Genotype-phenotype correlation in Chinese patients with spinal and bulbar muscular atrophy. PLoS One. 2015;10(3):e0122279.
373. Rhodes LE, Freeman BK, Auh S, Kokkinis AD, La Pean A, Chen C, et al. Clinical features of spinal and bulbar muscular atrophy. Brain. 2009;132(Pt 12):3242-51.
374. Hama T, Hirayama M, Hara T, Nakamura T, Atsuta N, Banno H, et al. Discrimination of spinal and bulbar muscular atrophy from amyotrophic lateral sclerosis using sensory nerve action potentials. Muscle & nerve. 2012;45(2):169-74.
375. Xu Y, Zhang S, Fan D. [Upper motor neuron involvement in Kennedy disease evaluated by triple stimulation technique]. Zhonghua yi xue za zhi. 2015;95(19):1522-5.
376. Ferrante MA, Wilbourn AJ. The characteristic electrodiagnostic features of Kennedy's disease. Muscle & nerve. 1997;20(3):323-9.
377. Xu YS, Zhang J, Lu M, Zheng JY, Zhang S, Kang DX, et al. [Test of sensory nerve in patients with Kennedy disease]. Zhonghua yi xue za zhi. 2008;88(39):2771-4.
378. Fu SC, Kuo HC, Chu CC, Wu YR, Ro LS, Liu CS, et al. Long-term follow-up of spinal and bulbar muscular atrophy in Taiwan. Journal of the Formosan Medical Association = Taiwan yi zhi. 2013;112(6):326-31.
379. Nishiyama A, Sugeno N, Tateyama M, Nishiyama S, Kato M, Aoki M. Postural leg tremor in X-linked spinal and bulbar muscular atrophy. Journal of clinical neuroscience : official journal of the Neurosurgical Society of Australasia. 2014;21(5):799-802.
380. Kim H, Lim YM, Lee EJ, Oh YJ, Kim KK. Correlation between the CAG repeat size and electrophysiological findings in patients with spinal and bulbar muscular atrophy. Muscle & nerve. 2018;57(4):683-6.
381. Meng L, Liu J, Liu X, Wang Z, Yuan Y, Zhang W. [Pathological features of muscles and peripheral nerves of Kennedy's disease: a report of 12 cases]. Zhonghua yi xue za zhi. 2015;95(21):1681-5.
382. Lai TH, Soong BW, Chen JT, Chen YY, Lai KL, Wu ZA, et al. Multimodal evoked potentials of Kennedy's disease. The Canadian journal of neurological sciences Le journal canadien des sciences neurologiques. 2007;34(3):328-32.
383. Suntrup S, Kristina Teismann I, Steinstraeter O, Bernd Ringelstein E, Pantev C, Dziewas R. Decreased cortical somatosensory finger representation in X-linked recessive bulbospinal neuronopathy (Kennedy disease): a magnetoencephalographic study. Journal of neuroimaging : official journal of the American Society of Neuroimaging. 2010;20(1):16-21.
384. Prokhorenko OA, Vasconcelos OM, Lupu VD, Campbell WW, Jabbari B. Sensory physiology assessed by evoked potentials in survivors of poliomyelitis. Muscle & nerve. 2008;38(4):1266-71.
385. Li Hi Shing S, Lope J, Chipika RH, Hardiman O, Bede P. Extra-motor manifestations in post-polio syndrome (PPS): fatigue, cognitive symptoms and radiological features. Neurological sciences : official journal of the Italian Neurological Society and of the Italian Society of Clinical Neurophysiology. 2021.
386. Phukan J, Pender NP, Hardiman O. Cognitive impairment in amyotrophic lateral sclerosis. The Lancet Neurology. 2007;6(11):994-1003.
387. Joyce NC, Carter GT. Electrodiagnosis in persons with amyotrophic lateral sclerosis. PM & R : the journal of injury, function, and rehabilitation. 2013;5(5 Suppl):S89-95.
388. Nishiyama A, Warita H, Takahashi T, Suzuki N, Nishiyama S, Tano O, et al. Prominent sensory involvement in a case of familial amyotrophic lateral sclerosis carrying the L8V SOD1 mutation. Clin Neurol Neurosurg. 2016;150:194-6.
389. Czell D, Neuwirth C, Weber M, Sartoretti-Schefer S, Gutzeit A, Reischauer C. Nine Hole Peg Test and Transcranial Magnetic Stimulation: Useful to Evaluate Dexterity of the Hand and

Disease Progression in Amyotrophic Lateral Sclerosis. Neurology research international. 2019;2019:7397491.
390. Khoury E, Carment L, Lindberg P, Gaillard R, Krebs MO, Amado I. [Sensorimotor aspects and manual dexterity in autism spectrum disorders: A literature review]. L'Encephale. 2020;46(2):135-45.
391. Sunderland A, Bowers MP, Sluman SM, Wilcock DJ, Ardron ME. Impaired dexterity of the ipsilateral hand after stroke and the relationship to cognitive deficit. Stroke. 1999;30(5):949-55.
392. Térémetz M, Carment L, Brénugat-Herne L, Croca M, Bleton JP, Krebs MO, et al. Manual Dexterity in Schizophrenia-A Neglected Clinical Marker? Frontiers in psychiatry. 2017;8:120.
393. Hammer MJ, Barlow SM. Laryngeal somatosensory deficits in Parkinson's disease: implications for speech respiratory and phonatory control. Experimental brain research. 2010;201(3):401-9.
394. Münte TF, Tröger MC, Nusser I, Wieringa BM, Johannes S, Matzke M, et al. Alteration of early components of the visual evoked potential in amyotrophic lateral sclerosis. J Neurol. 1998;245(4):206-10.
395. Matheson JK, Harrington HJ, Hallett M. Abnormalities of multimodality evoked potentials in amyotrophic lateral sclerosis. Arch Neurol. 1986;43(4):338-40.
396. Rojas P, de Hoz R, Ramírez AI, Ferreras A, Salobrar-Garcia E, Muñoz-Blanco JL, et al. Changes in Retinal OCT and Their Correlations with Neurological Disability in Early ALS Patients, a Follow-Up Study. Brain sciences. 2019;9(12).
397. Abrahams S, Newton J, Niven E, Foley J, Bak TH. Screening for cognition and behaviour changes in ALS. Amyotrophic lateral sclerosis & frontotemporal degeneration. 2014;15(1-2):9-14.
398. Braak H, Brettschneider J, Ludolph AC, Lee VM, Trojanowski JQ, Del Tredici K. Amyotrophic lateral sclerosis--a model of corticofugal axonal spread. Nature reviews Neurology. 2013;9(12):708-14.
399. Scekic-Zahirovic J, Fischer M, Stuart-Lopez G, Burg T, Gilet J, Dirrig-Grosch S, et al. Evidence that corticofugal propagation of ALS pathology is not mediated by prion-like mechanism. Prog Neurobiol. 2021;200:101972.
400. McAlary L, Plotkin SS, Yerbury JJ, Cashman NR. Prion-Like Propagation of Protein Misfolding and Aggregation in Amyotrophic Lateral Sclerosis. Frontiers in molecular neuroscience. 2019;12:262.
401. Prasad A, Bharathi V, Sivalingam V, Girdhar A, Patel BK. Molecular Mechanisms of TDP-43 Misfolding and Pathology in Amyotrophic Lateral Sclerosis. Frontiers in molecular neuroscience. 2019;12:25.
402. Vucic S, Kiernan MC. Transcranial Magnetic Stimulation for the Assessment of Neurodegenerative Disease. Neurotherapeutics : the journal of the American Society for Experimental NeuroTherapeutics. 2017;14(1):91-106.
403. Eisen A, Braak H, Del Tredici K, Lemon R, Ludolph AC, Kiernan MC. Cortical influences drive amyotrophic lateral sclerosis. J Neurol Neurosurg Psychiatry. 2017;88(11):917-24.
404. Brettschneider J, Del Tredici K, Toledo JB, Robinson JL, Irwin DJ, Grossman M, et al. Stages of pTDP-43 pathology in amyotrophic lateral sclerosis. Ann Neurol. 2013;74(1):20-38.
405. Chipika RH, Christidi F, Finegan E, Li Hi Shing S, McKenna MC, Chang KM, et al. Amygdala pathology in amyotrophic lateral sclerosis and primary lateral sclerosis. J Neurol Sci. 2020;417:117039.
406. Bede P, Chipika RH, Christidi F, Hengeveld JC, Karavasilis E, Argyropoulos GD, et al. Genotype-associated cerebellar profiles in ALS: focal cerebellar pathology and cerebro-cerebellar connectivity alterations. J Neurol Neurosurg Psychiatry. 2021.
407. Loeffler JP, Picchiarelli G, Dupuis L, Gonzalez De Aguilar JL. The Role of Skeletal Muscle in Amyotrophic Lateral Sclerosis. Brain pathology (Zurich, Switzerland). 2016;26(2):227-36.

408. Tsitkanou S, Lindsay A, Della Gatta P. The role of skeletal muscle in amyotrophic lateral sclerosis: a 'dying-back' or 'dying-forward' phenomenon? The Journal of physiology. 2019;597(23):5527-8.
409. Prell T, Grosskreutz J. The involvement of the cerebellum in amyotrophic lateral sclerosis. Amyotrophic lateral sclerosis & frontotemporal degeneration. 2013;14(7-8):507-15.
410. Schimke N, Krampfl K, Petri S, Dengler R, Bufler J. [Cerebellar symptoms in motor neuron diseases. Special form of amyotrophic lateral sclerosis plus syndrome]. Der Nervenarzt. 2002;73(8):751-3.
411. Yasser S, Fecto F, Siddique T, Sheikh KA, Athar P. An unusual case of familial ALS and cerebellar ataxia. Amyotrophic lateral sclerosis : official publication of the World Federation of Neurology Research Group on Motor Neuron Diseases. 2010;11(6):568-70.
412. De Marco M, Merico A, Berta G, Segato N, Citton V, Baglione A, et al. Morphometric correlates of dysarthric deficit in amyotrophic lateral sclerosis. Amyotrophic lateral sclerosis & frontotemporal degeneration. 2015;16(7-8):464-72.
413. Machida Y, Tsuchiya K, Anno M, Haga C, Ito T, Shimo Y, et al. Sporadic amyotrophic lateral sclerosis with multiple system degeneration: a report of an autopsy case without respirator administration. Acta neuropathologica. 1999;98(5):512-5.
414. Kushner MJ, Parrish M, Burke A, Behrens M, Hays AP, Frame B, et al. Nystagmus in motor neuron disease: clinicopathological study of two cases. Ann Neurol. 1984;16(1):71-7.
415. Jacobs L, Bozian D, Heffner RR, Jr., Barron SA. An eye movement disorder in amyotrophic lateral sclerosis. Neurology. 1981;31(10):1282-7.
416. Gizzi M, DiRocco A, Sivak M, Cohen B. Ocular motor function in motor neuron disease. Neurology. 1992;42(5):1037-46.
417. Donaghy C, Pinnock R, Abrahams S, Cardwell C, Hardiman O, Patterson V, et al. Slow saccades in bulbar-onset motor neurone disease. J Neurol. 2010;257(7):1134-40.
418. Averbuch-Heller L, Helmchen C, Horn AK, Leigh RJ, Büttner-Ennerver JA. Slow vertical saccades in motor neuron disease: correlation of structure and function. Ann Neurol. 1998;44(4):641-8.
419. Yunusova Y, Plowman EK, Green JR, Barnett C, Bede P. Clinical Measures of Bulbar Dysfunction in ALS. Front Neurol. 2019;10:106.
420. Sasegbon A, Hamdy S. The Role of the Cerebellum in Swallowing. Dysphagia. 2021.
421. Parvizi J, Joseph J, Press DZ, Schmahmann JD. Pathological laughter and crying in patients with multiple system atrophy-cerebellar type. Mov Disord. 2007;22(6):798-803.
422. Floeter MK, Katipally R, Kim MP, Schanz O, Stephen M, Danielian L, et al. Impaired corticopontocerebellar tracts underlie pseudobulbar affect in motor neuron disorders. Neurology. 2014;83(7):620-7.
423. Christidi F, Karavasilis E, Ferentinos P, Xirou S, Velonakis G, Rentzos M, et al. Investigating the neuroanatomical substrate of pathological laughing and crying in amyotrophic lateral sclerosis with multimodal neuroimaging techniques. Amyotrophic lateral sclerosis & frontotemporal degeneration. 2018;19(1-2):12-20.
424. Fitzgerald MJT, Gruener G, Mtui E. Clinical Neuroanatomy and Neuroscience: Saunders/Elsevier; 2012.
425. Buckner RL. The cerebellum and cognitive function: 25 years of insight from anatomy and neuroimaging. Neuron. 2013;80(3):807-15.
426. Schmahmann JD. Dysmetria of thought: clinical consequences of cerebellar dysfunction on cognition and affect. Trends in cognitive sciences. 1998;2(9):362-71.
427. Stoodley CJ, Schmahmann JD. Functional topography in the human cerebellum: a meta-analysis of neuroimaging studies. Neuroimage. 2009;44(2):489-501.
428. Van Overwalle F, D'Aes T, Marien P. Social cognition and the cerebellum: A meta-analytic connectivity analysis. Hum Brain Mapp. 2015;36(12):5137-54.

429. Finegan E, Chipika RH, Li Hi Shing S, Hardiman O, Bede P. Pathological Crying and Laughing in Motor Neuron Disease: Pathobiology, Screening, Intervention. Front Neurol. 2019;10:260.
430. Bede P, Finegan E. Revisiting the pathoanatomy of pseudobulbar affect: mechanisms beyond corticobulbar dysfunction. Amyotrophic lateral sclerosis & frontotemporal degeneration. 2018;19(1-2):4-6.
431. Runnqvist E, Bonnard M, Gauvin HS, Attarian S, Trébuchon A, Hartsuiker RJ, et al. Internal modeling of upcoming speech: A causal role of the right posterior cerebellum in non-motor aspects of language production. Cortex. 2016;81:203-14.
432. Allen G, Courchesne E. Differential effects of developmental cerebellar abnormality on cognitive and motor functions in the cerebellum: an fMRI study of autism. The American journal of psychiatry. 2003;160(2):262-73.
433. Desmond JE, Gabrieli JD, Wagner AD, Ginier BL, Glover GH. Lobular patterns of cerebellar activation in verbal working-memory and finger-tapping tasks as revealed by functional MRI. J Neurosci. 1997;17(24):9675-85.
434. Szpunar KK, Watson JM, McDermott KB. Neural substrates of envisioning the future. Proceedings of the National Academy of Sciences of the United States of America. 2007;104(2):642-7.
435. Malm J, Kristensen B, Karlsson T, Carlberg B, Fagerlund M, Olsson T. Cognitive impairment in young adults with infratentorial infarcts. Neurology. 1998;51(2):433-40.
436. Levisohn L, Cronin-Golomb A, Schmahmann JD. Neuropsychological consequences of cerebellar tumour resection in children: Cerebellar cognitive affective syndrome in a paediatric population. Brain. 2000;123(5):1041-50.
437. Tedesco AM, Chiricozzi FR, Clausi S, Lupo M, Molinari M, Leggio MG. The cerebellar cognitive profile. Brain. 2011;134(12):3672-86.
438. Argyropoulos GPD, van Dun K, Adamaszek M, Leggio M, Manto M, Masciullo M, et al. The Cerebellar Cognitive Affective/Schmahmann Syndrome: a Task Force Paper. Cerebellum (London, England). 2020;19(1):102-25.
439. Abidi M, de Marco G, Grami F, Termoz N, Couillandre A, Querin G, et al. Neural Correlates of Motor Imagery of Gait in Amyotrophic Lateral Sclerosis. Journal of magnetic resonance imaging : JMRI. 2021;53(1):223-33.
440. Abidi M, de Marco G, Couillandre A, Feron M, Mseddi E, Termoz N, et al. Adaptive functional reorganization in amyotrophic lateral sclerosis: coexisting degenerative and compensatory changes. Eur J Neurol. 2020;27(1):121-8.
441. Hu T, Hou Y, Wei Q, Yang J, Luo C, Chen Y, et al. Patterns of brain regional functional coherence in cognitive impaired ALS. The International journal of neuroscience. 2020;130(8):751-8.
442. Schonecker S, Neuhofer C, Otto M, Ludolph A, Kassubek J, Landwehrmeyer B, et al. Atrophy in the Thalamus But Not Cerebellum Is Specific for C9orf72 FTD and ALS Patients - An Atlas-Based Volumetric MRI Study. Frontiers in aging neuroscience. 2018;10:45.
443. Canosa A, Pagani M, Cistaro A, Montuschi A, Iazzolino B, Fania P, et al. 18F-FDG-PET correlates of cognitive impairment in ALS. Neurology. 2016;86(1):44-9.
444. Tanaka M, Kondo S, Hirai S, Sun X, Yamagishi T, Okamoto K. Cerebral blood flow and oxygen metabolism in progressive dementia associated with amyotrophic lateral sclerosis. J Neurol Sci. 1993;120(1):22-8.
445. Agosta F, Ferraro PM, Riva N, Spinelli EG, Domi T, Carrera P, et al. Structural and functional brain signatures of C9orf72 in motor neuron disease. Neurobiol Aging. 2017;57:206-19.
446. Christidi F, Karavasilis E, Riederer F, Zalonis I, Ferentinos P, Velonakis G, et al. Gray matter and white matter changes in non-demented amyotrophic lateral sclerosis patients with or without cognitive impairment: A combined voxel-based morphometry and tract-based spatial statistics whole-brain analysis. Brain Imaging Behav. 2018;12(2):547-63.

447. Calvo A, Chiò A, Pagani M, Cammarosano S, Dematteis F, Moglia C, et al. Parkinsonian traits in amyotrophic lateral sclerosis (ALS): a prospective population-based study. J Neurol. 2019;266(7):1633-42.
448. Keil C, Prell T, Peschel T, Hartung V, Dengler R, Grosskreutz J. Longitudinal diffusion tensor imaging in amyotrophic lateral sclerosis. BMC neuroscience. 2012;13:141.
449. Pagani M, Chiò A, Valentini MC, Öberg J, Nobili F, Calvo A, et al. Functional pattern of brain FDG-PET in amyotrophic lateral sclerosis. Neurology. 2014;83(12):1067-74.
450. Pagani M, Öberg J, De Carli F, Calvo A, Moglia C, Canosa A, et al. Metabolic spatial connectivity in amyotrophic lateral sclerosis as revealed by independent component analysis. Hum Brain Mapp. 2016;37(3):942-53.
451. Canosa A, Moglia C, Manera U, Vasta R, Torrieri MC, Arena V, et al. Metabolic brain changes across different levels of cognitive impairment in ALS: a (18)F-FDG-PET study. J Neurol Neurosurg Psychiatry. 2020.
452. Bede P, Bogdahn U, Lope J, Chang KM, Xirou S, Christidi F. Degenerative and regenerative processes in amyotrophic lateral sclerosis: motor reserve, adaptation and putative compensatory changes. Neural regeneration research. 2021;16(6):1208-9.
453. Consonni M, Dalla Bella E, Nigri A, Pinardi C, Demichelis G, Porcu L, et al. Cognitive Syndromes and C9orf72 Mutation Are Not Related to Cerebellar Degeneration in Amyotrophic Lateral Sclerosis. Front Neurosci. 2019;13:440.
454. Canosa A, Vacchiano V, D'Ovidio F, Calvo A, Moglia C, Manera U, et al. Brain metabolic correlates of apathy in amyotrophic lateral sclerosis: An 18F-FDG-positron emission tomography stud. Eur J Neurol. 2021;28(3):745-53.
455. Sala A, Iaccarino L, Fania P, Vanoli EG, Fallanca F, Pagnini C, et al. Testing the diagnostic accuracy of [18F]FDG-PET in discriminating spinal- and bulbar-onset amyotrophic lateral sclerosis. Eur J Nucl Med Mol Imaging. 2019;46(5):1117-31.
456. Verstraete E, Turner MR, Grosskreutz J, Filippi M, Benatar M. Mind the gap: the mismatch between clinical and imaging metrics in ALS. Amyotrophic lateral sclerosis & frontotemporal degeneration. 2015;16(7-8):524-9.
457. Christidi F, Karavasilis E, Velonakis G, Rentzos M, Zambelis T, Zouvelou V, et al. Motor and extra-motor gray matter integrity may underlie neurophysiologic parameters of motor function in amyotrophic lateral sclerosis: a combined voxel-based morphometry and transcranial stimulation study. Brain Imaging Behav. 2018;12(6):1730-41.
458. Kim HJ, Oh SI, de Leon M, Wang X, Oh KW, Park JS, et al. Structural explanation of poor prognosis of amyotrophic lateral sclerosis in the non-demented state. Eur J Neurol. 2017;24(1):122-9.
459. Feron M, Couillandre A, Mseddi E, Termoz N, Abidi M, Bardinet E, et al. Extrapyramidal deficits in ALS: a combined biomechanical and neuroimaging study. Journal of neurology. 2018;265(9):2125-36.
460. Hartung V, Prell T, Gaser C, Turner MR, Tietz F, Ilse B, et al. Voxel-based MRI intensitometry reveals extent of cerebral white matter pathology in amyotrophic lateral sclerosis. PLoS One. 2014;9(8):e104894.
461. Trojsi F, Caiazzo G, Corbo D, Piccirillo G, Cristillo V, Femiano C, et al. Microstructural changes across different clinical milestones of disease in amyotrophic lateral sclerosis. PLoS One. 2015;10(3):e0119045.
462. Baek SH, Park J, Kim YH, Seok HY, Oh KW, Kim HJ, et al. Usefulness of diffusion tensor imaging findings as biomarkers for amyotrophic lateral sclerosis. Sci Rep. 2020;10(1):5199.
463. Bharti K, Khan M, Beaulieu C, Graham SJ, Briemberg H, Frayne R, et al. Involvement of the dentate nucleus in the pathophysiology of amyotrophic lateral sclerosis: A multi-center and multi-modal neuroimaging study. Neuroimage Clin. 2020;28:102385.
464. De Marchi F, Stecco A, Falaschi Z, Filippone F, Pasché A, Bebeti A, et al. Detection of White Matter Ultrastructural Changes for Amyotrophic Lateral Sclerosis Characterization: A Diagnostic Study from Dti-Derived Data. Brain sciences. 2020;10(12).

465. Minnerop M, Specht K, Ruhlmann J, Grothe C, Wüllner U, Klockgether T. In vivo voxel-based relaxometry in amyotrophic lateral sclerosis. J Neurol. 2009;256(1):28-34.
466. Prudlo J, Bißbort C, Glass A, Grossmann A, Hauenstein K, Benecke R, et al. White matter pathology in ALS and lower motor neuron ALS variants: a diffusion tensor imaging study using tract-based spatial statistics. J Neurol. 2012;259(9):1848-59.
467. Trojsi F, Di Nardo F, Caiazzo G, Siciliano M, D'Alvano G, Ferrantino T, et al. Hippocampal connectivity in Amyotrophic Lateral Sclerosis (ALS): more than Papez circuit impairment. Brain Imaging Behav. 2020.
468. Tu S, Menke RAL, Talbot K, Kiernan MC, Turner MR. Cerebellar tract alterations in PLS and ALS. Amyotrophic lateral sclerosis & frontotemporal degeneration. 2019;20(3-4):281-4.
469. Proudfoot M, Bede P, Turner MR. Imaging Cerebral Activity in Amyotrophic Lateral Sclerosis. Front Neurol. 2018;9:1148.
470. Fekete T, Zach N, Mujica-Parodi LR, Turner MR. Multiple kernel learning captures a systems-level functional connectivity biomarker signature in amyotrophic lateral sclerosis. PLoS One. 2013;8(12):e85190.
471. Zhou F, Gong H, Li F, Zhuang Y, Zang Y, Xu R, et al. Altered motor network functional connectivity in amyotrophic lateral sclerosis: a resting-state functional magnetic resonance imaging study. Neuroreport. 2013;24(12):657-62.
472. Han J, Ma L. Functional magnetic resonance imaging study of the brain in patients with amyotrophic lateral sclerosis. Chinese medical sciences journal = Chung-kuo i hsueh k'o hsueh tsa chih. 2006;21(4):228-33.
473. Konrad C, Jansen A, Henningsen H, Sommer J, Turski PA, Brooks BR, et al. Subcortical reorganization in amyotrophic lateral sclerosis. Experimental brain research. 2006;172(3):361-9.
474. Gredal O, Rosenbaum S, Topp S, Karlsborg M, Strange P, Werdelin L. Quantification of brain metabolites in amyotrophic lateral sclerosis by localized proton magnetic resonance spectroscopy. Neurology. 1997;48(4):878-81.
475. Ludolph AC, Langen KJ, Regard M, Herzog H, Kemper B, Kuwert T, et al. Frontal lobe function in amyotrophic lateral sclerosis: a neuropsychologic and positron emission tomography study. Acta neurologica Scandinavica. 1992;85(2):81-9.
476. Buhour MS, Doidy F, Mondou A, Pélerin A, Carluer L, Eustache F, et al. Voxel-based mapping of grey matter volume and glucose metabolism profiles in amyotrophic lateral sclerosis. EJNMMI research. 2017;7(1):21.
477. Matías-Guiu JA, Pytel V, Cabrera-Martín MN, Galán L, Valles-Salgado M, Guerrero A, et al. Amyloid- and FDG-PET imaging in amyotrophic lateral sclerosis. Eur J Nucl Med Mol Imaging. 2016;43(11):2050-60.
478. Cistaro A, Valentini MC, Chiò A, Nobili F, Calvo A, Moglia C, et al. Brain hypermetabolism in amyotrophic lateral sclerosis: a FDG PET study in ALS of spinal and bulbar onset. Eur J Nucl Med Mol Imaging. 2012;39(2):251-9.
479. Bae JS, Ferguson M, Tan R, Mioshi E, Simon N, Burrell J, et al. Dissociation of Structural and Functional Integrities of the Motor System in Amyotrophic Lateral Sclerosis and Behavioral-Variant Frontotemporal Dementia. Journal of clinical neurology (Seoul, Korea). 2016;12(2):209-17.
480. McCluskey L, Vandriel S, Elman L, Van Deerlin VM, Powers J, Boller A, et al. ALS-Plus syndrome: non-pyramidal features in a large ALS cohort. J Neurol Sci. 2014;345(1-2):118-24.
481. Kassubek J, Unrath A, Huppertz HJ, Lulé D, Ethofer T, Sperfeld AD, et al. Global brain atrophy and corticospinal tract alterations in ALS, as investigated by voxel-based morphometry of 3-D MRI. Amyotrophic lateral sclerosis and other motor neuron disorders : official publication of the World Federation of Neurology, Research Group on Motor Neuron Diseases. 2005;6(4):213-20.
482. Schoenfeld MA, Tempelmann C, Gaul C, Kühnel GR, Düzel E, Hopf JM, et al. Functional motor compensation in amyotrophic lateral sclerosis. J Neurol. 2005;252(8):944-52.

483. Canosa A, Palumbo F, Iazzolino B, Peotta L, Di Pede F, Manera U, et al. The interplay among education, brain metabolism, and cognitive impairment suggests a role of cognitive reserve in Amyotrophic Lateral Sclerosis. Neurobiol Aging. 2021;98:205-13.
484. Dalakas MC, Hatazawa J, Brooks RA, Di Chiro G. Lowered cerebral glucose utilization in amyotrophic lateral sclerosis. Ann Neurol. 1987;22(5):580-6.
485. Ishihara K, Araki S, Ihori N, Shiota J, Kawamura M, Nakano I. An autopsy case of frontotemporal dementia with severe dysarthria and motor neuron disease showing numerous basophilic inclusions. Neuropathology : official journal of the Japanese Society of Neuropathology. 2006;26(5):447-54.
486. Kobayashi Z, Tsuchiya K, Kubodera T, Shibata N, Arai T, Miura H, et al. FALS with Gly72Ser mutation in SOD1 gene: report of a family including the first autopsy case. J Neurol Sci. 2011;300(1-2):9-13.
487. Brettschneider J, Van Deerlin VM, Robinson JL, Kwong L, Lee EB, Ali YO, et al. Pattern of ubiquilin pathology in ALS and FTLD indicates presence of C9ORF72 hexanucleotide expansion. Acta neuropathologica. 2012;123(6):825-39.
488. Yokota O, Tsuchiya K, Oda T, Ishihara T, de Silva R, Lees AJ, et al. Amyotrophic lateral sclerosis with dementia: an autopsy case showing many Bunina bodies, tau-positive neuronal and astrocytic plaque-like pathologies, and pallido-nigral degeneration. Acta neuropathologica. 2006;112(5):633-45.
489. Geser F, Brandmeir NJ, Kwong LK, Martinez-Lage M, Elman L, McCluskey L, et al. Evidence of multisystem disorder in whole-brain map of pathological TDP-43 in amyotrophic lateral sclerosis. Arch Neurol. 2008;65(5):636-41.
490. Shellikeri S, Karthikeyan V, Martino R, Black SE, Zinman L, Keith J, et al. The neuropathological signature of bulbar-onset ALS: A systematic review. Neurosci Biobehav Rev. 2017;75:378-92.
491. Petri S, Kollewe K, Grothe C, Hori A, Dengler R, Bufler J, et al. GABA(A)-receptor mRNA expression in the prefrontal and temporal cortex of ALS patients. J Neurol Sci. 2006;250(1-2):124-32.
492. Przedborski S, Donaldson D, Jakowec M, Kish SJ, Guttman M, Rosoklija G, et al. Brain superoxide dismutase, catalase, and glutathione peroxidase activities in amyotrophic lateral sclerosis. Ann Neurol. 1996;39(2):158-65.
493. Rohrer JD, Lashley T, Schott JM, Warren JE, Mead S, Isaacs AM, et al. Clinical and neuroanatomical signatures of tissue pathology in frontotemporal lobar degeneration. Brain : a journal of neurology. 2011;134(9):2565-81.
494. van Blitterswijk M, DeJesus-Hernandez M, Niemantsverdriet E, Murray ME, Heckman MG, Diehl NN, et al. Association between repeat sizes and clinical and pathological characteristics in carriers of C9ORF72 repeat expansions (Xpansize-72): a cross-sectional cohort study. The Lancet Neurology. 2013;12(10):978-88.
495. Sugihara H, Horiuchi M, Kamo T, Fujisawa K, Abe M, Sakiyama T, et al. A case of primary lateral sclerosis taking a prolonged clinical course with dementia and having an unusual dendritic ballooning. Neuropathology : official journal of the Japanese Society of Neuropathology. 1999;19(1):77-84.
496. Kosaka T, Fu YJ, Shiga A, Ishidaira H, Tan CF, Tani T, et al. Primary lateral sclerosis: upper-motor-predominant amyotrophic lateral sclerosis with frontotemporal lobar degeneration--immunohistochemical and biochemical analyses of TDP-43. Neuropathology : official journal of the Japanese Society of Neuropathology. 2012;32(4):373-84.
497. Engel PA, Grunnet M. Atypical dementia and spastic paraplegia in a patient with primary lateral sclerosis and numerous necortical beta amyloid plaques: new disorder or Alzheimer's disease variant? Journal of geriatric psychiatry and neurology. 2000;13(2):60-4.
498. Aguirre N, Beal MF, Matson WR, Bogdanov MB. Increased oxidative damage to DNA in an animal model of amyotrophic lateral sclerosis. Free radical research. 2005;39(4):383-8.

499. Chung YH, Joo KM, Lee YJ, Shin DH, Cha CI. Reactive astrocytes express PARP in the central nervous system of SOD(G93A) transgenic mice. Brain Res. 2004;1003(1-2):199-204.
500. Chung YH, Joo KM, Lim HC, Cho MH, Kim D, Lee WB, et al. Immunohistochemical study on the distribution of phosphorylated extracellular signal-regulated kinase (ERK) in the central nervous system of SOD1G93A transgenic mice. Brain Res. 2005;1050(1-2):203-9.
501. Barańczyk-Kuźma A, Usarek E, Kuźma-Kozakiewcz M, Kaźmierczak B, Gajewska B, Schwalenstocker B, et al. Age-related changes in tau expression in transgenic mouse model of amyotrophic lateral sclerosis. Neurochem Res. 2007;32(3):415-21.
502. Lee JC, Joo KM, Choe SY, Cha CI. Region-specific changes in the immunoreactivity of TRPV4 expression in the central nervous system of SOD1(G93A) transgenic mice as an in vivo model of amyotrophic lateral sclerosis. Journal of molecular histology. 2012;43(6):625-31.
503. Li PA, He Q, Cao T, Yong G, Szauter KM, Fong KS, et al. Up-regulation and altered distribution of lysyl oxidase in the central nervous system of mutant SOD1 transgenic mouse model of amyotrophic lateral sclerosis. Brain research Molecular brain research. 2004;120(2):115-22.
504. Kao CS, van Bruggen R, Kim JR, Chen XXL, Chan C, Lee J, et al. Selective neuronal degeneration in MATR3 S85C knock-in mouse model of early-stage ALS. Nature communications. 2020;11(1):5304.
505. Chew J, Gendron TF, Prudencio M, Sasaguri H, Zhang YJ, Castanedes-Casey M, et al. Neurodegeneration. C9ORF72 repeat expansions in mice cause TDP-43 pathology, neuronal loss, and behavioral deficits. Science (New York, NY). 2015;348(6239):1151-4.
506. Jones AR, Iacoangeli A, Adey BN, Bowles H, Shatunov A, Troakes C, et al. A HML6 endogenous retrovirus on chromosome 3 is upregulated in amyotrophic lateral sclerosis motor cortex. Sci Rep. 2021;11(1):14283.
507. Yang Y, Halliday GM, Kiernan MC, Tan RH. TDP-43 levels in the brain tissue of ALS cases with and without C9ORF72 or ATXN2 gene expansions. Neurology. 2019;93(19):e1748-e55.
508. Plaitakis A, Constantakakis E, Smith J. The neuroexcitotoxic amino acids glutamate and aspartate are altered in the spinal cord and brain in amyotrophic lateral sclerosis. Ann Neurol. 1988;24(3):446-9.
509. Christidi F, Karavasilis E, Rentzos M, Velonakis G, Zouvelou V, Xirou S, et al. Hippocampal pathology in amyotrophic lateral sclerosis: selective vulnerability of subfields and their associated projections. Neurobiol Aging. 2019;84:178-88.
510. Christidi F, Karavasilis E, Rentzos M, Kelekis N, Evdokimidis I, Bede P. Clinical and Radiological Markers of Extra-Motor Deficits in Amyotrophic Lateral Sclerosis. Front Neurol. 2018;9:1005.
511. Eisen A, Bede P. The strength of corticomotoneuronal drive underlies ALS split phenotypes and reflects early upper motor neuron dysfunction. Brain and behavior. 2021:e2403.
512. Eisen A, Turner MR, Lemon R. Tools and talk: an evolutionary perspective on the functional deficits associated with amyotrophic lateral sclerosis. Muscle Nerve. 2014;49(4):469-77.
513. Pascual-Leone A, Amedi A, Fregni F, Merabet LB. The plastic human brain cortex. Annual review of neuroscience. 2005;28:377-401.
514. Villamar MF, Santos Portilla A, Fregni F, Zafonte R. Noninvasive brain stimulation to modulate neuroplasticity in traumatic brain injury. Neuromodulation : journal of the International Neuromodulation Society. 2012;15(4):326-38.
515. Dimyan MA, Cohen LG. Neuroplasticity in the context of motor rehabilitation after stroke. Nature reviews Neurology. 2011;7(2):76-85.
516. Straudi S, Basaglia N. Neuroplasticity-Based Technologies and Interventions for Restoring Motor Functions in Multiple Sclerosis. Advances in experimental medicine and biology. 2017;958:171-85.

517. Herholz SC, Herholz RS, Herholz K. Non-pharmacological interventions and neuroplasticity in early stage Alzheimer's disease. Expert review of neurotherapeutics. 2013;13(11):1235-45.
518. Hutson TH, Di Giovanni S. The translational landscape in spinal cord injury: focus on neuroplasticity and regeneration. Nature reviews Neurology. 2019;15(12):732-45.
519. Konrad C, Henningsen H, Bremer J, Mock B, Deppe M, Buchinger C, et al. Pattern of cortical reorganization in amyotrophic lateral sclerosis: a functional magnetic resonance imaging study. Experimental brain research. 2002;143(1):51-6.
520. Tessitore A, Esposito F, Monsurrò MR, Graziano S, Panza D, Russo A, et al. Subcortical motor plasticity in patients with sporadic ALS: An fMRI study. Brain Res Bull. 2006;69(5):489-94.
521. Konczak J, Pierscianek D, Hirsiger S, Bultmann U, Schoch B, Gizewski ER, et al. Recovery of upper limb function after cerebellar stroke: lesion symptom mapping and arm kinematics. Stroke. 2010;41(10):2191-200.
522. Mitoma H, Buffo A, Gelfo F, Guell X, Fucà E, Kakei S, et al. Consensus Paper. Cerebellar Reserve: From Cerebellar Physiology to Cerebellar Disorders. Cerebellum. 2020;19(1):131-53.
523. Christidi F, Karavasilis E, Velonakis G, Ferentinos P, Rentzos M, Kelekis N, et al. The Clinical and Radiological Spectrum of Hippocampal Pathology in Amyotrophic Lateral Sclerosis. Frontiers in neurology. 2018;9:523.
524. Rohrer JD, Isaacs AM, Mizlienska S, Mead S, Lashley T, Wray S, et al. C9orf72 expansions in frontotemporal dementia and amyotrophic lateral sclerosis. Lancet neurology. 2015.
525. McKenna MC, Chipika RH, Li Hi Shing S, Christidi F, Lope J, Doherty MA, et al. Infratentorial pathology in frontotemporal dementia: cerebellar grey and white matter alterations in FTD phenotypes. J Neurol. 2021.
526. Mahoney CJ, Beck J, Rohrer JD, Lashley T, Mok K, Shakespeare T, et al. Frontotemporal dementia with the C9ORF72 hexanucleotide repeat expansion: clinical, neuroanatomical and neuropathological features. Brain. 2012;135(Pt 3):736-50.
527. Westeneng HJ, Walhout R, Straathof M, Schmidt R, Hendrikse J, Veldink JH, et al. Widespread structural brain involvement in ALS is not limited to the C9orf72 repeat expansion. Journal of neurology, neurosurgery, and psychiatry. 2016;87(12):1354-60.
528. Bocchetta M, Cardoso MJ, Cash DM, Ourselin S, Warren JD, Rohrer JD. Patterns of regional cerebellar atrophy in genetic frontotemporal dementia. Neuroimage Clin. 2016;11:287-90.
529. Chen Y, Kumfor F, Landin-Romero R, Irish M, Hodges JR, Piguet O. Cerebellar atrophy and its contribution to cognition in frontotemporal dementias. Ann Neurol. 2018;84(1):98-109.
530. Chen Y, Landin-Romero R, Kumfor F, Irish M, Hodges JR, Piguet O. Cerebellar structural connectivity and contributions to cognition in frontotemporal dementias. Cortex. 2020;129:57-67.
531. Gellersen HM, Guo CC, O'Callaghan C, Tan RH, Sami S, Hornberger M. Cerebellar atrophy in neurodegeneration—a meta-analysis. Journal of Neurology, Neurosurgery & Psychiatry. 2017;88(9):780-8.
532. Chen Y, Kumfor F, Landin-Romero R, Irish M, Piguet O. The Cerebellum in Frontotemporal Dementia: a Meta-Analysis of Neuroimaging Studies. Neuropsychol Rev. 2019;29(4):450-64.
533. Cash DM, Bocchetta M, Thomas DL, Dick KM, van Swieten JC, Borroni B, et al. Patterns of gray matter atrophy in genetic frontotemporal dementia: results from the GENFI study. Neurobiology of aging. 2018;62:191-6.
534. Tan RH, Devenney E, Dobson-Stone C, Kwok JB, Hodges JR, Kiernan MC, et al. Cerebellar Integrity in the Amyotrophic Lateral Sclerosis - Frontotemporal Dementia Continuum. PLOS ONE. 2014;9(8):e105632.

535. Pioro EP, Turner MR, Bede P. Neuroimaging in primary lateral sclerosis. Amyotrophic lateral sclerosis & frontotemporal degeneration. 2020;21(sup1):18-27.
536. Bede P, Pradat PF, Lope J, Vourc'h P, Blasco H, Corcia P. Primary Lateral Sclerosis: Clinical, radiological and molecular features. Revue neurologique. 2021.
537. Bede P, Chipika RH, Finegan E, Li Hi Shing S, Doherty MA, Hengeveld JC, et al. Brainstem pathology in amyotrophic lateral sclerosis and primary lateral sclerosis: A longitudinal neuroimaging study. NeuroImage Clinical. 2019;24:102054.
538. Finegan E, Li Hi Shing S, Chipika RH, Doherty MA, Hengeveld JC, Vajda A, et al. Widespread subcortical grey matter degeneration in primary lateral sclerosis: a multimodal imaging study with genetic profiling. Neuroimage Clin. 2019;24:102089.
539. Meoded A, Morrissette AE, Katipally R, Schanz O, Gotts SJ, Floeter MK. Cerebro-cerebellar connectivity is increased in primary lateral sclerosis. Neuroimage Clin. 2015;7:288-96.
540. Canu E, Agosta F, Galantucci S, Chiò A, Riva N, Silani V, et al. Extramotor damage is associated with cognition in primary lateral sclerosis patients. PLoS One. 2013;8(12):e82017.
541. de Borba FC, Querin G, França MC, Jr., Pradat PF. Cerebellar degeneration in adult spinal muscular atrophy patients. J Neurol. 2020;267(9):2625-31.
542. Lindig T, Bender B, Hauser TK, Mang S, Schweikardt D, Klose U, et al. Gray and white matter alterations in hereditary spastic paraplegia type SPG4 and clinical correlations. J Neurol. 2015;262(8):1961-71.
543. Servelhere KR, Rezende TJR, de Lima FD, de Brito MR, de França Nunes RF, Casseb RF, et al. Brain Damage and Gene Expression Across Hereditary Spastic Paraplegia Subtypes. Mov Disord. 2021;36(7):1644-53.
544. Orlacchio A, Kawarai T, Totaro A, Errico A, St George-Hyslop PH, Rugarli EI, et al. Hereditary spastic paraplegia: clinical genetic study of 15 families. Arch Neurol. 2004;61(6):849-55.
545. Olivieri G, Pro S, Diodato D, Di Capua M, Longo D, Martinelli D, et al. Corticospinal tract damage in HHH syndrome: a metabolic cause of hereditary spastic paraplegia. Orphanet journal of rare diseases. 2019;14(1):208.
546. Seidel K, De Vos R, Derksen L, Bauer P, Riess O, den Dunnen W, et al. Widespread thalamic and cerebellar degeneration in a patient with a complicated hereditary spastic paraplegia (HSP). Annals of anatomy = Anatomischer Anzeiger : official organ of the Anatomische Gesellschaft. 2009;191(2):203-11.
547. Thal DR, Züchner S, Gierer S, Schulte C, Schöls L, Schüle R, et al. Abnormal Paraplegin Expression in Swollen Neurites, τ- and α-Synuclein Pathology in a Case of Hereditary Spastic Paraplegia SPG7 with an Ala510Val Mutation. Int J Mol Sci. 2015;16(10):25050-66.
548. Pieper CC, Konrad C, Sommer J, Teismann I, Schiffbauer H. Structural changes of central white matter tracts in Kennedy's disease - a diffusion tensor imaging and voxel-based morphometry study. Acta neurologica Scandinavica. 2013;127(5):323-8.
549. Pradat PF, Bernard E, Corcia P, Couratier P, Jublanc C, Querin G, et al. The French national protocol for Kennedy's disease (SBMA): consensus diagnostic and management recommendations. Orphanet journal of rare diseases. 2020;15(1):90.
550. Li Hi Shing S, Murad A, Lope J, Hardiman O, Bede P. Cerebellar remodelling decades after spinal cord insult: neuroplasticity in poliomyelitis survivors. Journal of Integrative Neuroscience. 2021.
551. Li Hi Shing S, Lope J, Chipika RH, Hardiman O, Bede P. Imaging data indicate cerebral reorganisation in poliomyelitis survivors: Possible compensation for longstanding lower motor neuron pathology. Data in brief. 2021;38:107316.
552. Li Hi Shing S, Lope J, McKenna MC, Chipika RH, Hardiman O, Bede P. Increased cerebral integrity metrics in poliomyelitis survivors: putative adaptation to longstanding lower motor neuron degeneration. J Neurol Sci. 2021;424:117361.

553. Xu F, Frazier DT. Role of the cerebellar deep nuclei in respiratory modulation. Cerebellum (London, England). 2002;1(1):35-40.
554. Jensen K, Beylergil SB, Shaikh AG. Slow saccades in cerebellar disease. Cerebellum & ataxias. 2019;6:1.
555. Schmahmann JD. The cerebellum and cognition. Neurosci Lett. 2019;688:62-75.
556. Guo CC, Tan R, Hodges JR, Hu X, Sami S, Hornberger M. Network-selective vulnerability of the human cerebellum to Alzheimer's disease and frontotemporal dementia. Brain : a journal of neurology. 2016;139(Pt 5):1527-38.
557. Argyropoulos GD, Christidi F, Karavasilis E, Velonakis G, Antoniou A, Bede P, et al. Cerebro-cerebellar white matter connectivity in bipolar disorder and associated polarity subphenotypes. Prog Neuropsychopharmacol Biol Psychiatry. 2021;104:110034.
558. Tahedl M, Li Hi Shing S, Finegan E, Chipika RH, Lope J, Hardiman O, et al. Propagation patterns in motor neuron diseases: Individual and phenotype-associated disease-burden trajectories across the UMN-LMN spectrum of MNDs. Neurobiology of aging. 2021;109:78-87.
559. Van Damme P, Veldink JH, van Blitterswijk M, Corveleyn A, van Vught PW, Thijs V, et al. Expanded ATXN2 CAG repeat size in ALS identifies genetic overlap between ALS and SCA2. Neurology. 2011;76(24):2066-72.
560. Tazelaar GHP, Boeynaems S, De Decker M, van Vugt J, Kool L, Goedee HS, et al. ATXN1 repeat expansions confer risk for amyotrophic lateral sclerosis and contribute to TDP-43 mislocalization. Brain communications. 2020;2(2):fcaa064.
561. Neuenschwander AG, Thai KK, Figueroa KP, Pulst SM. Amyotrophic lateral sclerosis risk for spinocerebellar ataxia type 2 ATXN2 CAG repeat alleles: a meta-analysis. JAMA Neurol. 2014;71(12):1529-34.
562. Morello G, Gentile G, Spataro R, Spampinato AG, Guarnaccia M, Salomone S, et al. Genomic Portrait of a Sporadic Amyotrophic Lateral Sclerosis Case in a Large Spinocerebellar Ataxia Type 1 Family. Journal of personalized medicine. 2020;10(4).
563. Nanetti L, Fancellu R, Tomasello C, Gellera C, Pareyson D, Mariotti C. Rare association of motor neuron disease and spinocerebellar ataxia type 2 (SCA2): a new case and review of the literature. J Neurol. 2009;256(11):1926-8.
564. Antenora A, Rinaldi C, Roca A, Pane C, Lieto M, Saccà F, et al. The Multiple Faces of Spinocerebellar Ataxia type 2. Ann Clin Transl Neurol. 2017;4(9):687-95.
565. Sun YM, Lu C, Wu ZY. Spinocerebellar ataxia: relationship between phenotype and genotype - a review. Clinical genetics. 2016;90(4):305-14.
566. Querin G, El Mendili MM, Lenglet T, Behin A, Stojkovic T, Salachas F, et al. The spinal and cerebral profile of adult spinal-muscular atrophy: A multimodal imaging study. NeuroImage Clinical. 2019;21:101618.
567. Bede P, Murad A, Hardiman O. Pathological neural networks and artificial neural networks in ALS: diagnostic classification based on pathognomonic neuroimaging features. Journal of neurology. 2021.
568. Broad RJ, Gabel MC, Dowell NG, Schwartzman DJ, Seth AK, Zhang H, et al. Neurite orientation and dispersion density imaging (NODDI) detects cortical and corticospinal tract degeneration in ALS. Journal of neurology, neurosurgery, and psychiatry. 2019;90(4):404-11.
569. Tahedl M, Li Hi Shing S, Finegan E, Chipika RH, Lope J, Murad A, et al. Imaging data reveal divergent longitudinal trajectories in PLS, ALS and poliomyelitis survivors: Group-level and single-subject traits. Data in brief. 2021;39:107484.
570. Romero JE, Coupé P, Giraud R, Ta VT, Fonov V, Park MTM, et al. CERES: A new cerebellum lobule segmentation method. Neuroimage. 2017;147:916-24.
571. Diedrichsen J. A spatially unbiased atlas template of the human cerebellum. NeuroImage. 2006;33(1):127-38.
572. Diedrichsen J, Balsters JH, Flavell J, Cussans E, Ramnani N. A probabilistic MR atlas of the human cerebellum. NeuroImage. 2009;46(1):39-46.

573. Diedrichsen J, Zotow E. Surface-Based Display of Volume-Averaged Cerebellar Imaging Data. PLoS One. 2015;10(7):e0133402.
574. Elden AC, Kim HJ, Hart MP, Chen-Plotkin AS, Johnson BS, Fang X, et al. Ataxin-2 intermediate-length polyglutamine expansions are associated with increased risk for ALS. Nature. 2010;466(7310):1069-75.
575. Tan RH, Kril JJ, McGinley C, Hassani M, Masuda-Suzukake M, Hasegawa M, et al. Cerebellar neuronal loss in amyotrophic lateral sclerosis cases with ATXN2 intermediate repeat expansions. Annals of neurology. 2016;79(2):295-305.
576. Al-Sarraj S, King A, Troakes C, Smith B, Maekawa S, Bodi I, et al. p62 positive, TDP-43 negative, neuronal cytoplasmic and intranuclear inclusions in the cerebellum and hippocampus define the pathology of C9orf72-linked FTLD and MND/ALS. Acta neuropathologica. 2011;122(6):691-702.
577. Burke T, Pinto-Grau M, Lonergan K, Elamin M, Bede P, Costello E, et al. Measurement of Social Cognition in Amyotrophic Lateral Sclerosis: A Population Based Study. PLoS One. 2016;11(8):e0160850.
578. Nasseroleslami B, Dukic S, Broderick M, Mohr K, Schuster C, Gavin B, et al. Characteristic Increases in EEG Connectivity Correlate With Changes of Structural MRI in Amyotrophic Lateral Sclerosis. Cereb Cortex. 2019;29(1):27-41.
579. van Blitterswijk M, Dejesus-Hernandez M, Niemantsverdriet E, Murray ME, Heckman MG, Diehl NN, et al. Association between repeat sizes and clinical and pathological characteristics in carriers of C9ORF72 repeat expansions (Xpansize-72): a cross-sectional cohort study. Lancet neurology. 2013.
580. Park MT, Pipitone J, Baer LH, Winterburn JL, Shah Y, Chavez S, et al. Derivation of high-resolution MRI atlases of the human cerebellum at 3T and segmentation using multiple automatically generated templates. Neuroimage. 2014;95:217-31.
581. Iglesias JE, Van Leemput K, Bhatt P, Casillas C, Dutt S, Schuff N, et al. Bayesian segmentation of brainstem structures in MRI. Neuroimage. 2015;113:184-95.
582. Karavasilis E, Christidi F, Velonakis G, Giavri Z, Kelekis NL, Efstathopoulos EP, et al. Ipsilateral and contralateral cerebro-cerebellar white matter connections: A diffusion tensor imaging study in healthy adults. J Neuroradiol. 2019;46(1):52-60.
583. Crawford JR, Garthwaite PH. Comparison of a single case to a control or normative sample in neuropsychology: development of a Bayesian approach. Cogn Neuropsychol. 2007;24(4):343-72.
584. Pulst SM, Nechiporuk A, Nechiporuk T, Gispert S, Chen XN, Lopes-Cendes I, et al. Moderate expansion of a normally biallelic trinucleotide repeat in spinocerebellar ataxia type 2. Nature genetics. 1996;14(3):269-76.
585. Kenna KP, McLaughlin RL, Byrne S, Elamin M, Heverin M, Kenny EM, et al. Delineating the genetic heterogeneity of ALS using targeted high-throughput sequencing. J Med Genet. 2013;50(11):776-83.
586. Rheenen Wv, van der Spek RAA, Bakker MK, Vugt JJFAv, Hop PJ, Zwamborn RAJ, et al. Common and rare variant association analyses in Amyotrophic Lateral Sclerosis identify 15 risk loci with distinct genetic architectures and neuron-specific biology. medRxiv. 2021:2021.03.12.21253159.
587. Stoodley CJ, MacMore JP, Makris N, Sherman JC, Schmahmann JD. Location of lesion determines motor vs. cognitive consequences in patients with cerebellar stroke. NeuroImage: Clinical. 2016;12:765-75.
588. Loureiro JR, Oliveira CL, Silveira I. Unstable repeat expansions in neurodegenerative diseases: nucleocytoplasmic transport emerges on the scene. Neurobiol Aging. 2016;39:174-83.
589. Westeneng HJ, Verstraete E, Walhout R, Schmidt R, Hendrikse J, Veldink JH, et al. Subcortical structures in amyotrophic lateral sclerosis. Neurobiol Aging. 2015;36(2):1075-82.

590. Cistaro A, Pagani M, Montuschi A, Calvo A, Moglia C, Canosa A, et al. The metabolic signature of C9ORF72-related ALS: FDG PET comparison with nonmutated patients. Eur J Nucl Med Mol Imaging. 2014.
591. Sharma KR, Saigal G, Maudsley AA, Govind V. 1H MRS of basal ganglia and thalamus in amyotrophic lateral sclerosis. NMR in biomedicine. 2011;24(10):1270-6.
592. Neumann M, Sampathu DM, Kwong LK, Truax AC, Micsenyi MC, Chou TT, et al. Ubiquitinated TDP-43 in frontotemporal lobar degeneration and amyotrophic lateral sclerosis. Science (New York, NY). 2006;314(5796):130-3.
593. Behrens TE, Johansen-Berg H, Woolrich MW, Smith SM, Wheeler-Kingshott CA, Boulby PA, et al. Non-invasive mapping of connections between human thalamus and cortex using diffusion imaging. Nature neuroscience. 2003;6(7):750-7.
594. Bosch-Bouju C, Hyland BI, Parr-Brownlie LC. Motor thalamus integration of cortical, cerebellar and basal ganglia information: implications for normal and parkinsonian conditions. Frontiers in computational neuroscience. 2013;7:163.
595. Blackshaw S, Scholpp S, Placzek M, Ingraham H, Simerly R, Shimogori T. Molecular pathways controlling development of thalamus and hypothalamus: from neural specification to circuit formation. The Journal of neuroscience : the official journal of the Society for Neuroscience. 2010;30(45):14925-30.
596. Schmahmann JD. Vascular syndromes of the thalamus. Stroke; a journal of cerebral circulation. 2003;34(9):2264-78.
597. Johansen-Berg H, Behrens TE, Sillery E, Ciccarelli O, Thompson AJ, Smith SM, et al. Functional-anatomical validation and individual variation of diffusion tractography-based segmentation of the human thalamus. Cereb Cortex. 2005;15(1):31-9.
598. Iglesias JE, Insausti R, Lerma-Usabiaga G, Bocchetta M, Van Leemput K, Greve DN, et al. A probabilistic atlas of the human thalamic nuclei combining ex vivo MRI and histology. Neuroimage. 2018;183:314-26.
599. Kiernan MC, Vucic S, Cheah BC, Turner MR, Eisen A, Hardiman O, et al. Amyotrophic lateral sclerosis. Lancet. 2011;377(9769):942-55.
600. Pradat P-F, Bruneteau G, Munerati E, Salachas F, Le Forestier N, Lacomblez L, et al. Extrapyramidal stiffness in patients with amyotrophic lateral sclerosis. Mov Disord. 2009;24(14):2143-8.
601. Bede P, Elamin M, Byrne S, McLaughlin RL, Kenna K, Vajda A, et al. Basal ganglia involvement in amyotrophic lateral sclerosis. Neurology. 2013;81(24):2107-15.
602. Bocchetta M, Iglesias JE, Neason M, Cash DM, Warren JD, Rohrer JD. Thalamic nuclei in frontotemporal dementia: Mediodorsal nucleus involvement is universal but pulvinar atrophy is unique to C9orf72. Hum Brain Mapp. 2020;41(4):1006-16.
603. Bocchetta M, Gordon E, Cardoso MJ, Modat M, Ourselin S, Warren JD, et al. Thalamic atrophy in frontotemporal dementia - Not just a C9orf72 problem. Neuroimage Clin. 2018;18:675-81.
604. Byrne S, Elamin M, Bede P, Shatunov A, Walsh C, Corr B, et al. Cognitive and clinical characteristics of patients with amyotrophic lateral sclerosis carrying a C9orf72 repeat expansion: a population-based cohort study. Lancet neurology. 2012;11(3):232-40.
605. Gordon PH, Cheng B, Katz IB, Pinto M, Hays AP, Mitsumoto H, et al. The natural history of primary lateral sclerosis. Neurology. 2006;66(5):647-53.
606. Floeter MK, Mills R. Progression in primary lateral sclerosis: a prospective analysis. Amyotrophic Lateral Sclerosis. 2009;10(5-6):339-46.
607. de Vries BS, Spreij LA, Rustemeijer LMM, Bakker LA, Veldink JH, van den Berg LH, et al. A neuropsychological and behavioral study of PLS. Amyotrophic lateral sclerosis & frontotemporal degeneration. 2019;20(5-6):376-84.
608. Le Forestier N, Meininger V. [Primary lateral sclerosis: the era of international diagnosis criteria]. Revue neurologique. 2009;165(5):415-29.

609. Brooks BR, Miller RG, Swash M, Munsat TL, World Federation of Neurology Research Group on Motor Neuron D. El Escorial revisited: revised criteria for the diagnosis of amyotrophic lateral sclerosis. Amyotrophic lateral sclerosis and other motor neuron disorders : official publication of the World Federation of Neurology, Research Group on Motor Neuron Diseases. 2000;1(5):293-9.
610. Cedarbaum JM, Stambler N, Malta E, Fuller C, Hilt D, Thurmond B, et al. The ALSFRS-R: a revised ALS functional rating scale that incorporates assessments of respiratory function. BDNF ALS Study Group (Phase III). J Neurol Sci. 1999;169(1-2):13-21.
611. Pinto-Grau M, Burke T, Lonergan K, McHugh C, Mays I, Madden C, et al. Screening for cognitive dysfunction in ALS: validation of the Edinburgh Cognitive and Behavioural ALS Screen (ECAS) using age and education adjusted normative data. Amyotrophic lateral sclerosis & frontotemporal degeneration. 2017;18(1-2):99-106.
612. Strong MJ, Abrahams S, Goldstein LH, Woolley S, McLaughlin P, Snowden J, et al. Amyotrophic lateral sclerosis - frontotemporal spectrum disorder (ALS-FTSD): Revised diagnostic criteria. Amyotrophic lateral sclerosis & frontotemporal degeneration. 2017;18(3-4):153-74.
613. Smith SM. Fast robust automated brain extraction. Hum Brain Mapp. 2002;17(3):143-55.
614. Jenkinson M, Bannister P, Brady M, Smith S. Improved optimization for the robust and accurate linear registration and motion correction of brain images. NeuroImage. 2002;17(2):825-41.
615. Zhang Y, Brady M, Smith S. Segmentation of brain MR images through a hidden Markov random field model and the expectation-maximization algorithm. IEEE transactions on medical imaging. 2001;20(1):45-57.
616. Patenaude B, Smith SM, Kennedy DN, Jenkinson M. A Bayesian model of shape and appearance for subcortical brain segmentation. NeuroImage. 2011;56(3):907-22.
617. Winkler AM, Ridgway GR, Webster MA, Smith SM, Nichols TE. Permutation inference for the general linear model. NeuroImage. 2014;92:381-97.
618. Nichols TE, Holmes AP. Nonparametric permutation tests for functional neuroimaging: a primer with examples. Hum Brain Mapp. 2002;15(1):1-25.
619. Desikan RS, Segonne F, Fischl B, Quinn BT, Dickerson BC, Blacker D, et al. An automated labeling system for subdividing the human cerebral cortex on MRI scans into gyral based regions of interest. NeuroImage. 2006;31(3):968-80.
620. Project MinE: study design and pilot analyses of a large-scale whole-genome sequencing study in amyotrophic lateral sclerosis. European journal of human genetics : EJHG. 2018;26(10):1537-46.
621. Kenna KP, McLaughlin RL, Byrne S, Elamin M, Heverin M, Kenny EM, et al. Delineating the genetic heterogeneity of ALS using targeted high-throughput sequencing. Journal of medical genetics. 2013.
622. Klebe S, Stevanin G, Depienne C. Clinical and genetic heterogeneity in hereditary spastic paraplegias: from SPG1 to SPG72 and still counting. Revue neurologique. 2015;171(6-7):505-30.
623. Tlamsa AP, Brumberg JC. Organization and morphology of thalamocortical neurons of mouse ventral lateral thalamus. Somatosensory & motor research. 2010;27(1):34-43.
624. Querin G, El Mendili MM, Lenglet T, Delphine S, Marchand-Pauvert V, Benali H, et al. Spinal cord multi-parametric magnetic resonance imaging for survival prediction in amyotrophic lateral sclerosis. Eur J Neurol. 2017;24(8):1040-6.
625. Desai J, Swash M. Extrapyramidal involvement in amyotrophic lateral sclerosis: backward falls and retropulsion. Journal of neurology, neurosurgery, and psychiatry. 1999;67(2):214-6.
626. Williams TL, Shaw PJ, Lowe J, Bates D, Ince PG. Parkinsonism in motor neuron disease: case report and literature review. Acta neuropathologica. 1995;89(3):275-83.

627. Takahashi H, Snow BJ, Bhatt MH, Peppard R, Eisen A, Calne DB. Evidence for a dopaminergic deficit in sporadic amyotrophic lateral sclerosis on positron emission scanning. Lancet. 1993;342(8878):1016-8.
628. Przedborski S, Dhawan V, Donaldson DM, Murphy PL, McKenna-Yasek D, Mandel FS, et al. Nigrostriatal dopaminergic function in familial amyotrophic lateral sclerosis patients with and without copper/zinc superoxide dismutase mutations. Neurology. 1996;47(6):1546-51.
629. O'Dowd S, Curtin D, Waite AJ, Roberts K, Pender N, Reid V, et al. C9ORF72 expansion in amyotrophic lateral sclerosis/frontotemporal dementia also causes parkinsonism. Mov Disord. 2012;27(8):1072-4.
630. Montes J, Cheng B, Diamond B, Doorish C, Mitsumoto H, Gordon PH. The Timed Up and Go test: predicting falls in ALS. Amyotrophic lateral sclerosis : official publication of the World Federation of Neurology Research Group on Motor Neuron Diseases. 2007;8(5):292-5.
631. Schell WE, Mar VS, Da Silva CP. Correlation of falls in patients with Amyotrophic Lateral Sclerosis with objective measures of balance, strength, and spasticity. NeuroRehabilitation. 2019;44(1):85-93.
632. Gordon PH, Cheng B, Katz IB, Mitsumoto H, Rowland LP. Clinical features that distinguish PLS, upper motor neuron-dominant ALS, and typical ALS. Neurology. 2009;72(22):1948-52.
633. Mitsumoto H, Chiuzan C, Gilmore M, Zhang Y, Simmons Z, Paganoni S, et al. Primary lateral sclerosis (PLS) functional rating scale: PLS-specific clinimetric scale. Muscle Nerve. 2020;61(2):163-72.
634. Piras F, Caltagirone C, Spalletta G. Working memory performance and thalamus microstructure in healthy subjects. Neuroscience. 2010;171(2):496-505.
635. Monchi O, Petrides M, Petre V, Worsley K, Dagher A. Wisconsin Card Sorting revisited: distinct neural circuits participating in different stages of the task identified by event-related functional magnetic resonance imaging. J Neurosci. 2001;21(19):7733-41.
636. Perakyla J, Sun L, Lehtimaki K, Peltola J, Ohman J, Mottonen T, et al. Causal Evidence from Humans for the Role of Mediodorsal Nucleus of the Thalamus in Working Memory. Journal of cognitive neuroscience. 2017;29(12):2090-102.
637. Pergola G, Danet L, Pitel AL, Carlesimo GA, Segobin S, Pariente J, et al. The Regulatory Role of the Human Mediodorsal Thalamus. Trends in cognitive sciences. 2018;22(11):1011-25.
638. Tu S, Miller L, Piguet O, Hornberger M. Accelerated forgetting of contextual details due to focal medio-dorsal thalamic lesion. Frontiers in behavioral neuroscience. 2014;8:320.
639. Pergola G, Ranft A, Mathias K, Suchan B. The role of the thalamic nuclei in recognition memory accompanied by recall during encoding and retrieval: an fMRI study. Neuroimage. 2013;74:195-208.
640. Abrahams S, Goldstein LH, Lloyd CM, Brooks DJ, Leigh PN. Cognitive deficits in non-demented amyotrophic lateral sclerosis patients: a neuropsychological investigation. J Neurol Sci. 1995;129 Suppl:54-5.
641. Elamin M, Phukan J, Bede P, Jordan N, Byrne S, Pender N, et al. Executive dysfunction is a negative prognostic indicator in patients with ALS without dementia. Neurology. 2011;76(14):1263-9.
642. Elamin M, Pinto-Grau M, Burke T, Bede P, Rooney J, O'Sullivan M, et al. Identifying behavioural changes in ALS: Validation of the Beaumont Behavioural Inventory (BBI). Amyotrophic lateral sclerosis & frontotemporal degeneration. 2017;18(1-2):68-73.
643. Beeldman E, Raaphorst J, Klein Twennaar M, de Visser M, Schmand BA, de Haan RJ. The cognitive profile of ALS: a systematic review and meta-analysis update. Journal of neurology, neurosurgery, and psychiatry. 2016;87(6):611-9.
644. Christidi F, Karavasilis E, Zalonis I, Ferentinos P, Giavri Z, Wilde EA, et al. Memory-related white matter tract integrity in amyotrophic lateral sclerosis: an advanced neuroimaging and neuropsychological study. Neurobiology of aging. 2017;49:69-78.

645. Burke T, Lonergan K, Pinto-Grau M, Elamin M, Bede P, Madden C, et al. Visual encoding, consolidation, and retrieval in amyotrophic lateral sclerosis: executive function as a mediator, and predictor of performance. Amyotrophic lateral sclerosis & frontotemporal degeneration. 2017;18(3-4):193-201.
646. Caga J, Hsieh S, Lillo P, Dudley K, Mioshi E. The Impact of Cognitive and Behavioral Symptoms on ALS Patients and Their Caregivers. Frontiers in neurology. 2019;10:192.
647. Lee SE, Khazenzon AM, Trujillo AJ, Guo CC, Yokoyama JS, Sha SJ, et al. Altered network connectivity in frontotemporal dementia with C9orf72 hexanucleotide repeat expansion. Brain. 2014;137(Pt 11):3047-60.
648. Vatsavayai SC, Yoon SJ, Gardner RC, Gendron TF, Vargas JN, Trujillo A, et al. Timing and significance of pathological features in C9orf72 expansion-associated frontotemporal dementia. Brain. 2016;139(Pt 12):3202-16.
649. Yang Y, Halliday GM, Hodges JR, Tan RH. von Economo Neuron Density and Thalamus Volumes in Behavioral Deficits in Frontotemporal Dementia Cases with and without a C9ORF72 Repeat Expansion. Journal of Alzheimer's disease : JAD. 2017;58(3):701-9.
650. Warburton EC, Baird A, Morgan A, Muir JL, Aggleton JP. The conjoint importance of the hippocampus and anterior thalamic nuclei for allocentric spatial learning: evidence from a disconnection study in the rat. J Neurosci. 2001;21(18):7323-30.
651. Stillova K, Jurak P, Chladek J, Chrastina J, Halamek J, Bockova M, et al. The Role of Anterior Nuclei of the Thalamus: A Subcortical Gate in Memory Processing: An Intracerebral Recording Study. PLoS One. 2015;10(11):e0140778.
652. Leszczynski M, Staudigl T. Memory-guided attention in the anterior thalamus. Neurosci Biobehav Rev. 2016;66:163-5.
653. Marchand A, Faugere A, Coutureau E, Wolff M. A role for anterior thalamic nuclei in contextual fear memory. Brain Struct Funct. 2014;219(5):1575-86.
654. Ghika-Schmid F, Bogousslavsky J. The acute behavioral syndrome of anterior thalamic infarction: a prospective study of 12 cases. Ann Neurol. 2000;48(2):220-7.
655. Wang J, Miao W, Li J, Li M, Zhen Z, Sabel B, et al. Automatic segmentation of the lateral geniculate nucleus: Application to control and glaucoma patients. J Neurosci Methods. 2015;255:104-14.
656. Sherman SM. Thalamus plays a central role in ongoing cortical functioning. Nature neuroscience. 2016;19(4):533-41.
657. Zihl J, von Cramon D. The contribution of the 'second' visual system to directed visual attention in man. Brain. 1979;102(4):835-56.
658. Snow JC, Allen HA, Rafal RD, Humphreys GW. Impaired attentional selection following lesions to human pulvinar: evidence for homology between human and monkey. Proceedings of the National Academy of Sciences of the United States of America. 2009;106(10):4054-9.
659. Jaramillo J, Mejias JF, Wang XJ. Engagement of Pulvino-cortical Feedforward and Feedback Pathways in Cognitive Computations. Neuron. 2019;101(2):321-36.e9.
660. Saalmann YB, Pinsk MA, Wang L, Li X, Kastner S. The pulvinar regulates information transmission between cortical areas based on attention demands. Science (New York, NY). 2012;337(6095):753-6.
661. Lauterbach EC, Price ST, Spears TE, Jackson JG, Kirsh AD. Serotonin responsive and nonresponsive diurnal depressive mood disorders and pathological affect in thalamic infarct associated with myoclonus and blepharospasm. Biological psychiatry. 1994;35(7):488-90.
662. de Vries BS, Rustemeijer LMM, van der Kooi AJ, Raaphorst J, Schröder CD, Nijboer TCW, et al. A case series of PLS patients with frontotemporal dementia and overview of the literature. Amyotrophic Lateral Sclerosis and Frontotemporal Degeneration. 2017;18(7-8):534-48.
663. Gamez J, Corbera-Bellalta M, Mila M, Lopez-Lisbona R, Boluda S, Ferrer I. Chorea-ballism associated with familial amyotrophic lateral sclerosis. A clinical, genetic, and neuropathological study. Mov Disord. 2008;23(3):434-8.

664. De Reuck JL, Deramecourt V, Auger F, Durieux N, Cordonnier C, Devos D, et al. Iron deposits in post-mortem brains of patients with neurodegenerative and cerebrovascular diseases: a semi-quantitative 7.0 T magnetic resonance imaging study. Eur J Neurol. 2014;21(7):1026-31.
665. O'Callaghan C, Bertoux M, Hornberger M. Beyond and below the cortex: the contribution of striatal dysfunction to cognition and behaviour in neurodegeneration. Journal of neurology, neurosurgery, and psychiatry. 2013.
666. Schuster C, Kasper E, Machts J, Bittner D, Kaufmann J, Benecke R, et al. Focal thinning of the motor cortex mirrors clinical features of amyotrophic lateral sclerosis and their phenotypes: a neuroimaging study. Journal of neurology. 2013;260(11):2856-64.
667. Bede P, Bokde A, Elamin M, Byrne S, McLaughlin RL, Jordan N, et al. Grey matter correlates of clinical variables in amyotrophic lateral sclerosis (ALS): a neuroimaging study of ALS motor phenotype heterogeneity and cortical focality. Journal of neurology, neurosurgery, and psychiatry. 2013;84(7):766-73.
668. Christidi F, Zalonis I, Kyriazi S, Rentzos M, Karavasilis E, Wilde EA, et al. Uncinate fasciculus microstructure and verbal episodic memory in amyotrophic lateral sclerosis: a diffusion tensor imaging and neuropsychological study. Brain imaging and behavior. 2014;8(4):497-505.
669. Christidi F, Karavasilis E, Rentzos M, Velonakis G, Zouvelou V, Xirou S, et al. Neuroimaging data indicate divergent mesial temporal lobe profiles in amyotrophic lateral sclerosis, Alzheimer's disease and healthy aging. Data in brief. 2020;28:104991.
670. Burke T, Elamin M, Bede P, Pinto-Grau M, Lonergan K, Hardiman O, et al. Discordant performance on the 'Reading the Mind in the Eyes' Test, based on disease onset in amyotrophic lateral sclerosis. Amyotrophic lateral sclerosis & frontotemporal degeneration. 2016:1-6.
671. Yokota O, Tsuchiya K, Noguchi Y, Akabane H, Ishizu H, Saito Y, et al. Coexistence of amyotrophic lateral sclerosis and argyrophilic grain disease: a non-demented autopsy case showing circumscribed temporal atrophy and involvement of the amygdala. Neuropathology : official journal of the Japanese Society of Neuropathology. 2007;27(6):539-50.
672. Neary D, Snowden JS, Mann DM, Northen B, Goulding PJ, Macdermott N. Frontal lobe dementia and motor neuron disease. Journal of neurology, neurosurgery, and psychiatry. 1990;53(1):23-32.
673. Kawashima T, Doh-ura K, Kikuchi H, Iwaki T. Cognitive dysfunction in patients with amyotrophic lateral sclerosis is associated with spherical or crescent-shaped ubiquitinated intraneuronal inclusions in the parahippocampal gyrus and amygdala, but not in the neostriatum. Acta neuropathologica. 2001;102(5):467-72.
674. Gorges M, Vercruysse P, Muller HP, Huppertz HJ, Rosenbohm A, Nagel G, et al. Hypothalamic atrophy is related to body mass index and age at onset in amyotrophic lateral sclerosis. Journal of neurology, neurosurgery, and psychiatry. 2017;88(12):1033-41.
675. Pinkhardt EH, van Elst LT, Ludolph AC, Kassubek J. Amygdala size in amyotrophic lateral sclerosis without dementia: an in vivo study using MRI volumetry. BMC neurology. 2006;6:48.
676. Passamonti L, Fera F, Tessitore A, Russo A, Cerasa A, Gioia CM, et al. Dysfunctions within limbic-motor networks in amyotrophic lateral sclerosis. Neurobiol Aging. 2013;34(11):2499-509.
677. Tsuchiya K, Takahashi M, Shiotsu H, Akiyama H, Haga C, Watabiki S, et al. Sporadic amyotrophic lateral sclerosis with circumscribed temporal atrophy: a report of an autopsy case without dementia and with ubiquitinated intraneuronal inclusions. Neuropathology : official journal of the Japanese Society of Neuropathology. 2002;22(4):308-16.
678. Ota S, Tsuchiya K, Akiyama H. "Forme fruste" of amyotrophic lateral sclerosis with dementia: a report of five autopsy cases without dementia and with ubiquitinated intraneuronal inclusions. Neuropathology : official journal of the Japanese Society of Neuropathology. 2005;25(4):326-35.

679. Saygin ZM, Kliemann D, Iglesias JE, van der Kouwe AJW, Boyd E, Reuter M, et al. High-resolution magnetic resonance imaging reveals nuclei of the human amygdala: manual segmentation to automatic atlas. NeuroImage. 2017;155:370-82.
680. Geser F, Hermle L, Egan P, Brettschneider J, Mitrovics T. Amyotrophic Lateral Sclerosis with Atrophy of the Amygdala. Practical Neurology. 2016;Jul/Aug.
681. Renard D, Collombier L, Castelnovo G, Fourcade G, Kotzki PO, LaBauge P. Brain FDG-PET changes in ALS and ALS-FTD. Acta neurologica Belgica. 2011;111(4):306-9.
682. Mitsumoto H, Brooks BR, Silani V. Clinical trials in amyotrophic lateral sclerosis: why so many negative trials and how can trials be improved? Lancet neurology. 2014;13(11):1127-38.
683. Kraemer M, Buerger M, Berlit P. Diagnostic problems and delay of diagnosis in amyotrophic lateral sclerosis. Clinical neurology and neurosurgery. 2010;112(2):103-5.
684. Yang Y, Wang JZ. From Structure to Behavior in Basolateral Amygdala-Hippocampus Circuits. Frontiers in neural circuits. 2017;11:86.
685. Amano T, Duvarci S, Popa D, Paré D. The fear circuit revisited: contributions of the basal amygdala nuclei to conditioned fear. J Neurosci. 2011;31(43):15481-9.
686. Adhikari A, Lerner TN, Finkelstein J, Pak S, Jennings JH, Davidson TJ, et al. Basomedial amygdala mediates top-down control of anxiety and fear. Nature. 2015;527(7577):179-85.
687. Kemppainen S, Jolkkonen E, Pitkanen A. Projections from the posterior cortical nucleus of the amygdala to the hippocampal formation and parahippocampal region in rat. Hippocampus. 2002;12(6):735-55.
688. Rytty R, Nikkinen J, Suhonen N, Moilanen V, Renton A, Traynor B, et al. Functional MRI in Patients with the C9ORF72 Expansion Associate Frontotemporal Dementia. Molecular Biology. 2014;3(1).
689. Sah P, Faber ES, Lopez De Armentia M, Power J. The amygdaloid complex: anatomy and physiology. Physiological reviews. 2003;83(3):803-34.
690. Maren S, Quirk GJ. Neuronal signalling of fear memory. Nature reviews Neuroscience. 2004;5(11):844-52.
691. Erlich JC, Bush DE, Ledoux JE. The role of the lateral amygdala in the retrieval and maintenance of fear-memories formed by repeated probabilistic reinforcement. Frontiers in behavioral neuroscience. 2012;6:16.
692. Kwon JT, Jhang J, Kim HS, Lee S, Han JH. Brain region-specific activity patterns after recent or remote memory retrieval of auditory conditioned fear. Learning & memory (Cold Spring Harbor, NY). 2012;19(10):487-94.
693. Schroeder BW, Shinnick-Gallagher P. Fear learning induces persistent facilitation of amygdala synaptic transmission. Eur J Neurosci. 2005;22(7):1775-83.
694. Manassero E, Renna A, Milano L, Sacchetti B. Lateral and Basal Amygdala Account for Opposite Behavioral Responses during the Long-Term Expression of Fearful Memories. Sci Rep. 2018;8(1):518.
695. Fudge JL, Tucker T. Amygdala projections to central amygdaloid nucleus subdivisions and transition zones in the primate. Neuroscience. 2009;159(2):819-41.
696. Floeter MK, Gendron TF. Biomarkers for Amyotrophic Lateral Sclerosis and Frontotemporal Dementia Associated With Hexanucleotide Expansion Mutations in C9orf72. Frontiers in neurology. 2018;9:1063.
697. Van Es M, De Vries B, Rustemijer L, Van Der Kooi A, Raaphorst J, Schroder C, et al. PLS-FTLD, expanding the spectrum of dementia in motor neuron disease. Journal of neurochemistry. 2016;138:360.
698. Butman JA, Floeter MK. Decreased thickness of primary motor cortex in primary lateral sclerosis. American Journal of Neuroradiology. 2007;28(1):87-91.
699. van der Graaff MM, Sage CA, Caan MW, Akkerman EM, Lavini C, Majoie CB, et al. Upper and extra-motoneuron involvement in early motoneuron disease: a diffusion tensor imaging study. Brain : a journal of neurology. 2011;134(Pt 4):1211-28.

700. Muller HP, Unrath A, Huppertz HJ, Ludolph AC, Kassubek J. Neuroanatomical patterns of cerebral white matter involvement in different motor neuron diseases as studied by diffusion tensor imaging analysis. Amyotrophic lateral sclerosis : official publication of the World Federation of Neurology Research Group on Motor Neuron Diseases. 2012;13(3):254-64.
701. Tzarouchi LC, Kyritsis AP, Giannopoulos S, Astrakas LG, Diakou M, Argyropoulou MI. Voxel-based diffusion tensor imaging detects pyramidal tract degeneration in primary lateral sclerosis. British Journal of Radiology. 2011;84(997):78-80.
702. Suh SI, Song IC, Koh SB. Primary lateral sclerosis with MR diffusion tensor image and tract tracking. American journal of physical medicine & rehabilitation. 2006;85(11):863-4.
703. Salameh JS, Patel N, Zheng S, Cauley KA. Focal absence of diffusion tensor tracts from primary motor cortex in primary lateral sclerosis. Eur J Neurol. 2013;20(4):e63-4.
704. Canu E, Agosta F, Galantucci S, Chio A, Riva N, Silani V, et al. Extramotor damage is associated with cognition in primary lateral sclerosis patients. PLoS ONE [Electronic Resource]. 2013;8(12):e82017.
705. Tanikawa S, Tanino M, Wang L, Ishikawa M, Miyazaki M, Tsuda M, et al. Autopsy findings in the early stage of amyotrophic lateral sclerosis with "dropped head" syndrome. Neuropathology : official journal of the Japanese Society of Neuropathology. 2019;39(5):374-7.
706. Kikuchi R, Ishihara K, Nagumo K, Sioda J, Kawamura M, Yoshida M. [An Autopsy Case of Amiotrophic Lateral Sclerosis Characterized by Upper Motor Neuron Degeneration and Progressive Pseudobulbar Palsy]. Brain and nerve = Shinkei kenkyu no shinpo. 2019;71(1):75-80.
707. Uchino A, Ogino M, Takahashi-Fujigasaki J, Oonuma S, Kanazawa N, Kajita S, et al. Pathological and immunoblot analysis of phosphorylated TDP-43 in sporadic amyotrophic lateral sclerosis with pallido-nigro-luysian degeneration. Neuropathology : official journal of the Japanese Society of Neuropathology. 2018;38(2):171-8.
708. Yamanami-Irioka A, Uchihara T, Endo T, Irioka T, Watanabe M, Kitagawa M, et al. Amnesia in frontotemporal dementia with amyotrophic lateral sclerosis, masquerading Alzheimer's disease. Case reports in neurology. 2011;3(3):242-7.
709. Iwasaki Y, Mori K, Ito M, Deguchi A, Yoshida M. [An autopsied case of senile onset frontotemporal lobar degeneration]. Rinsho shinkeigaku = Clinical neurology. 2011;51(6):426-9.
710. Piao YS, Tan CF, Iwanaga K, Kakita A, Takano H, Nishizawa M, et al. Sporadic four-repeat tauopathy with frontotemporal degeneration, parkinsonism and motor neuron disease. Acta neuropathologica. 2005;110(6):600-9.
711. Tsuchiya K, Ikeda K, Haga C, Kobayashi T, Morimatsu Y, Nakano I, et al. Atypical amyotrophic lateral sclerosis with dementia mimicking frontal Pick's disease: a report of an autopsy case with a clinical course of 15 years. Acta neuropathologica. 2001;101(6):625-30.
712. Yoshida M. Amyotrophic lateral sclerosis with dementia: the clinicopathological spectrum. Neuropathology : official journal of the Japanese Society of Neuropathology. 2004;24(1):87-102.
713. Konno H, Seki H, Chida K, Nomura H, Okita N, Takase S. [An autopsy case of motoneuron disease with dementia of long duration]. No to shinkei = Brain and nerve. 1999;51(11):963-7.
714. Bak TH, Chandran S. What wires together dies together: verbs, actions and neurodegeneration in motor neuron disease. Cortex. 2012;48(7):936-44.
715. Verstraete E, Veldink JH, van den Berg LH, van den Heuvel MP. Structural brain network imaging shows expanding disconnection of the motor system in amyotrophic lateral sclerosis. Hum Brain Mapp. 2013.
716. Meier JM, van der Burgh HK, Nitert AD, Bede P, de Lange SC, Hardiman O, et al. Connectome-Based Propagation Model in Amyotrophic Lateral Sclerosis. Annals of neurology. 2020;87(5):725-38.

717. Riku Y. Reappraisal of the anatomical spreading and propagation hypothesis about TDP-43 aggregation in amyotrophic lateral sclerosis and frontotemporal lobar degeneration. Neuropathology : official journal of the Japanese Society of Neuropathology. 2020.
718. Fisher CM. Pure spastic paralysis of corticospinal origin. Can J Neurol Sci. 1977;4(4):251-8.
719. Younger DS, Chou S, Hays AP, Lange DJ, Emerson R, Brin M, et al. Primary lateral sclerosis. A clinical diagnosis reemerges. Archives of Neurology. 1988;45(12):1304-7.
720. Pringle CE, Hudson AJ, Munoz DG, Kiernan JA, Brown WF, Ebers GC. Primary lateral sclerosis. Clinical features, neuropathology and diagnostic criteria. Brain : a journal of neurology. 1992;115 (Pt 2):495-520.
721. Tan CF, Kakita A, Piao YS, Kikugawa K, Endo K, Tanaka M, et al. Primary lateral sclerosis: a rare upper-motor-predominant form of amyotrophic lateral sclerosis often accompanied by frontotemporal lobar degeneration with ubiquitinated neuronal inclusions? Report of an autopsy case and a review of the literature. Acta neuropathologica. 2003;105(6):615-20.
722. Engel PA, Grunnet M. Atypical dementia and spastic paraplegia in a patient with primary lateral sclerosis and numerous necortical beta amyloid plaques: new disorder or Alzheimer's disease variant? Journal of Geriatric Psychiatry & Neurology. 2000;13(2):60-4.
723. Mochizuki A, Komatsuzaki Y, Iwamoto H, Shoji S. Frontotemporal dementia with ubiquitinated neuronal inclusions presenting with primary lateral sclerosis and parkinsonism: clinicopathological report of an autopsy case. Acta neuropathologica. 2004;107(4):377-80.
724. Mackenzie IR, Feldman H. Neurofilament inclusion body disease with early onset frontotemporal dementia and primary lateral sclerosis. Clinical Neuropathology. 2004;23(4):183-93.
725. Josephs K, Whitwell J, Murray M, Parisi J, Graff-Radford N, Knopman D, et al. Semantic dementia with primary lateral sclerosis (SD-PLS): A variant of FTLD-TDP type C pathology. Dementia and Geriatric Cognitive Disorders. 2012;34:37-8.
726. Kawakatsu S, Kobayashi R, Shibuya Y, Miura Y, Shibuya N, Nishida A, et al. A case of FTLD-TDP type a with primary lateral sclerosis presenting progressive nonfluent aphasia, anterior operculum syndrome and left pyramidal tract lesion on MRI. Neuropathology : official journal of the Japanese Society of Neuropathology. 2013;33(3):364.
727. Konagaya M, Sakai M, Iida M, Hashizume Y. [An autopsied case of dominantly affecting upper motor neuron with atrophy of the frontal and temporal lobes--with special reference to primary lateral sclerosis]. Rinsho shinkeigaku = Clinical neurology. 1995;35(4):384-90.
728. Bora E. Meta-analysis of social cognition in amyotrophic lateral sclerosis. Cortex. 2017;88:1-7.
729. Staios M, Fisher F, Lindell AK, Ong B, Howe J, Reardon K. Exploring sarcasm detection in amyotrophic lateral sclerosis using ecologically valid measures. Frontiers in human neuroscience. 2013;7:178.
730. Schmolck H, Mosnik D, Schulz P. Rating the approachability of faces in ALS. Neurology. 2007;69(24):2232-5.
731. Lule D, Diekmann V, Anders S, Kassubek J, Kubler A, Ludolph AC, et al. Brain responses to emotional stimuli in patients with amyotrophic lateral sclerosis (ALS). Journal of neurology. 2007;254(4):519-27.
732. Aho-Ozhan HE, Keller J, Heimrath J, Uttner I, Kassubek J, Birbaumer N, et al. Perception of Emotional Facial Expressions in Amyotrophic Lateral Sclerosis (ALS) at Behavioural and Brain Metabolic Level. PLoS One. 2016;11(10):e0164655.
733. Trojsi F, Di Nardo F, Santangelo G, Siciliano M, Femiano C, Passaniti C, et al. Resting state fMRI correlates of Theory of Mind impairment in amyotrophic lateral sclerosis. Cortex. 2017;97:1-16.
734. Siciliano M, Trojano L, Trojsi F, Monsurrò MR, Tedeschi G, Santangelo G. Assessing anxiety and its correlates in amyotrophic lateral sclerosis: The state-trait anxiety inventory. Muscle Nerve. 2019;60(1):47-55.

735. Olney RK, Murphy J, Forshew D, Garwood E, Miller BL, Langmore S, et al. The effects of executive and behavioral dysfunction on the course of ALS. Neurology. 2005;65(11):1774-7.
736. Burke T, Elamin M, Galvin M, Hardiman O, Pender N. Caregiver burden in amyotrophic lateral sclerosis: a cross-sectional investigation of predictors. Journal of neurology. 2015;262(6):1526-32.
737. Lule D, Pauli S, Altintas E, Singer U, Merk T, Uttner I, et al. Emotional adjustment in amyotrophic lateral sclerosis (ALS). Journal of neurology. 2012;259(2):334-41.
738. Piccione EA, Sletten DM, Staff NP, Low PA. Autonomic system and amyotrophic lateral sclerosis. Muscle Nerve. 2015;51(5):676-9.
739. Takeda T, Uchihara T, Kawamura S, Ohashi T. Olfactory dysfunction related to TDP-43 pathology in amyotrophic lateral sclerosis. Clin Neuropathol. 2014;33(1):65-7.
740. Turner MR, Swash M. The expanding syndrome of amyotrophic lateral sclerosis: a clinical and molecular odyssey. J Neurol Neurosurg Psychiatry. 2015;86(6):667-73.
741. Turner MR, Talbot K. Sweet food preference in amyotrophic lateral sclerosis. Pract Neurol. 2017;17(2):128-9.
742. Menzler K, Belke M, Wehrmann E, Krakow K, Lengler U, Jansen A, et al. Men and women are different: diffusion tensor imaging reveals sexual dimorphism in the microstructure of the thalamus, corpus callosum and cingulum. NeuroImage. 2011;54(4):2557-62.
743. Chen X, Sachdev PS, Wen W, Anstey KJ. Sex differences in regional gray matter in healthy individuals aged 44-48 years: a voxel-based morphometric study. NeuroImage. 2007;36(3):691-9.
744. Trojsi F, Siciliano M, Femiano C, Santangelo G, Lunetta C, Calvo A, et al. Comparative Analysis of C9orf72 and Sporadic Disease in a Large Multicenter ALS Population: The Effect of Male Sex on Survival of C9orf72 Positive Patients. Frontiers in neuroscience. 2019;13:485.
745. Caviness VS, Jr., Kennedy DN, Richelme C, Rademacher J, Filipek PA. The human brain age 7-11 years: a volumetric analysis based on magnetic resonance images. Cereb Cortex. 1996;6(5):726-36.
746. Goldstein JM, Seidman LJ, Horton NJ, Makris N, Kennedy DN, Caviness VS, Jr., et al. Normal sexual dimorphism of the adult human brain assessed by in vivo magnetic resonance imaging. Cereb Cortex. 2001;11(6):490-7.
747. Uematsu A, Matsui M, Tanaka C, Takahashi T, Noguchi K, Suzuki M, et al. Developmental trajectories of amygdala and hippocampus from infancy to early adulthood in healthy individuals. PLoS One. 2012;7(10):e46970.
748. Kogler L, Gur RC, Derntl B. Sex differences in cognitive regulation of psychosocial achievement stress: brain and behavior. Hum Brain Mapp. 2015;36(3):1028-42.
749. Chiò A, Moglia C, Canosa A, Manera U, D'Ovidio F, Vasta R, et al. ALS phenotype is influenced by age, sex, and genetics: A population-based study. Neurology. 2020;94(8):e802-e10.
750. Rooney J, Fogh I, Westeneng HJ, Vajda A, McLaughlin R, Heverin M, et al. C9orf72 expansion differentially affects males with spinal onset amyotrophic lateral sclerosis. Journal of neurology, neurosurgery, and psychiatry. 2017;88(4):281.
751. Kalra S. Magnetic Resonance Spectroscopy in ALS. Frontiers in neurology. 2019;10:482.